DESIGN, FABRICATION, ASSEMBLY, AND TEST OF A LIQUID HYDROGEN ACQUISITION SUBSYSTEM

MAY 1974

Prepared Under Contract NAS8-27571 by
McDonnell Douglas Astronautics Company
Huntington Beach, California 92647

for the

NATIONAL AERONAUTICS AND SPACE ADMINISTRATION
George C. Marshall Space Flight Center
Huntsville, Alabama 35812

MCDONNELL DOUGLAS

DESIGN, FABRICATION, ASSEMBLY, AND TEST OF A LIQUID HYDROGEN ACQUISITION SUBSYSTEM

PREPARED BY J. B. Blackmon
J. B. BLACKMON, Ph.D.
PROGRAM MANAGER

APPROVED BY
W. A. GAUBATZ, Ph.D.
CHIEF ADVANCED PROPULSION & MECHANICAL ENGINEER
PROPULSION & MECHANICAL DEPARTMENT

MAY 1974

Prepared Under Contract NAS 8-27571 by
McDonnell Douglas Astronautics Company
Huntington Beach, California 92647

for the

NATIONAL AERONAUTICS AND SPACE ADMINISTRATION
George C. Marshall Space Flight Center
Huntsville, Alabama 35812

FOREWORD

This document is submitted by the McDonnell Douglas Astronautics Company to the National Aeronautics and Space Administration, George C. Marshall Space Flight Center, in accordance with the requirements of contract NAS8-27571. Results are presented of a program involving the analysis, design, fabrication, and test of a multipurpose full-scale liquid hydrogen acquisition and thermal control system, termed the Interface Demonstration Unit (IDU). The IDU was developed for inclusion in a 105-in.-diameter liquid hydrogen tank as part of the NASA/MSFC auxiliary propulsion system breadboard.

This program was sponsored by the Fluid Mechanics and Dynamics Branch, Propulsion and Thermodynamic Division, Astronautics Laboratories, NASA/MSFC under the direction of Mr. George M. Young, III. The initial phase of this program was performed under the technical direction of Mr. Leon J. Hastings, NASA/MSFC.

This program was supported by the following personnel. J. N. Castle and P. Maruschak assisted in the system design and fabrication. D. W. Kendle and Professor Ivan Catton (Consultant) assisted in the analysis of the thermodynamic vent system. The computer codes were developed by D. W. Kendle. W. N. Geiger was instrumental in the fabrication of the IDU. Assembly and testing were performed under the direction of Roger Yeaman. The contributions and suggestions made by G. W. Burge, E. C. Cady, C. R. Easton, and C. E. Schroeder are appreciated. The support of Mr. Ralph Adams (NASA/MSFC Astrionics Laboratory) in the area of capacitance-level sensor evaluation is gratefully acknowledged.

CONTENTS

FIGURES

TABLES

NOMENCLATURE

a	Screen surface area-to-unit volume ratio
A	Area
b	Screen thickness
C_l	Specific heat of Liquid
D	Diameter
D_o	TVS tube spacing
g	Acceleration level
g_e	Gravitational constant
h	Heat transfer coefficient
h_{fg}	Heat of vaporization
K	Thermal conductivity
L	Length, insulation thickness, or screen thickness
m	Mass flowrate
Nu	Nusselt number
Pr	Prandtl number
ΔP	Pressure loss
q'	Heat flux per unit area
Q	Screen tortuosity factor (1.0 for square weave, 1.3 for Dutch weave)
Q	Volumetric flowrate of TVS
q, Q	Heat flux
Re	Reynolds number
Ra	Rayleigh number
t	Wall thickness
T	Temperature

ΔT	Temperature difference
V	Fluid approach velocity
α, β	Experimentally determined constants
β	Coefficient of volumetric expansion
ϵ	Screen void fraction
μ	Viscosity
ρ	Density
σ	Surface tension
X	Quality

Subscripts

a	Annulus
c	Channel
D	Dynamic
e	Evaporation
f	Free convection
F	Fluid
i	Inside
I	Insulation
L	Liquid
MAX	Maximum
r	Radiative
T	Tank, total
v	Vapor
w	Wall

Section 1
INTRODUCTION AND SUMMARY

Future space missions will require cryogenic fluid storage and expulsion subsystems capable of providing efficient long-term subcritical storage, reliable multiple low-g restarts, and low-g liquid expulsion for auxiliary propulsion, life support systems, and in-orbit propellant transfer. These requirements demand significant technology improvements in the areas of cryogenic propellant acquisition, venting, and thermal control relative to the concepts used in present operational vehicles. For most applications requiring low-g engine restarts, it is imperative that a passive propellant control system be used which supplies 100-percent liquid under a wide range of adverse acceleration levels at any point in the long-duration low-g coast. Use of present techniques for low-g engine restarts, such as auxiliary propulsion system (APS) propellant settling or idle-mode engine restart, involves high weight penalties and may not be sufficiently flexible to meet advanced mission requirements. Low-g thermal control techniques, involving the venting of ullage gas from a stratified cryogen and requiring either frequent or continuous propellant settling, also result in weight penalties and decreases in the overall mission time.

Presently, screen retention devices are considered prime contenders for cryogenic propellant acquisition, because of advantages of low weight, multicycle capability, reusability, long life, and simplicity. Efforts by the NASA and aerospace companies have resulted in a variety of screen retention device designs and an extensive background in terms of demonstration and development tests, and fabrication experience. However, cryogenic propellant screen retention devices can be subject to certain fluid dynamic and thermodynamic failure modes due to transient flow, pressure decay, or heat-transfer-induced "breakdown".* As a result, a concept termed the

*Loss of screen retention of liquid.

"integrated start tank" was conceived at McDonnell Douglas Astronautics Company (MDAC) in July 1968 (References 1, 2, and 3) which was designed to avoid problems associated with startup and shutdown transients and to isolate the propellant from tank pressure fluctuations and heat transfer.

The start-tank concept involves a screen retention device installed within a separately pressurized propellant tank located in the main tank. A line with a shutoff valve transmits LH_2 from the retention screen directly to the pump. A second line with a shutoff valve delivers propellant from the main tank to the internal tank. In low g, when liquid in the main tank is unsettled, cryogenic propellant is supplied to the pump from the acquisition device. When the liquid in the main tank is settled, following some period of relatively high positive vehicle acceleration, ($\geq 0.1\ g_e$) the retention device can be refilled by opening the internal tank refill valve and venting the ullage gas in this tank, yet maintaining constant pressure in the main tank. In this manner, the start tank can be refilled while a constant flow of propellant is maintained to the pump and engine.

Cryogenic screen acquisition devices subjected to heat transfer or tank pressure variations (such as pressure collapse below the saturation pressure of the retained liquid after engine shutdown) face potential failure modes due to bubble generation within the device and capillary "breakdown" due to screen drying. The start-tank concept minimizes these problems because the retained propellant is pressurized with cold helium, the tank is pressure isolated from main-tank pressure fluctuations, and the heat transfer into the start tank can be reduced by insulation, or eliminated by a wall-mounted thermodynamic vent system, which would intercept all heat flow into the start tank.

Retention failure ("breakdown"), due to startup or shutdown feedline pressure transients, is eliminated whenever the start tank is filled or the screen device itself is submerged within the propellant.

The IDU as designed, fabricated, and tested under this contract, incorporated the above features in terms of propellant acquisition and thermal control. In addition, it serves as a full-scale test article having a wide range of capabilities for investigating cryogenic propellant screen acquisition system operational modes. The IDU will also be part of planned NASA/MSFC liquid hydrogen APS breadboard tests, which will investigate the operation of a combined turbopump, accumulator, tankage, and acquisition system.

To meet these multiple objectives, the IDU was designed to supply liquid hydrogen to a turbopump system at flowrates up to 7.5 lb/sec for a period of approximately 5 seconds before refill. Refill is accomplished in less than 10 seconds, during which a constant flowrate can be maintained to the pumps.

The IDU shown in Figure 1-1 is comprised of a 10-ft^3 cylindrical tank, 29 inches in diameter and 35 inches in length, with three Parker submerged liquid hydrogen 2-inch ball valves, an externally mounted thermodynamic vent system with coolant flow control valves and orifices providing flowrates of at least 0.2 to 5 lb/hr, and an annular cylindrical screen device 24 inches in diameter and 24 inches in length, with 250 x 1370 fine mesh stainless steel screen within the tank. A bypass valve is provided to allow expulsion directly from the 105-inch diameter tank. Instrumentation provided includes seven carbon-point liquid-level sensors, three capacitance-point liquid-level sensors, a full-length capacitance liquid-level sensor, twenty platinum resistance temperature transducers, and four heat-flux gauges.

Subsystem acceptance and functional tests, including acquisition subsystem expulsion, pressurization, and refill, were performed in the MDAC cryogenic test facility. Additional tests were performed to investigate operational modes and possible limitations of surface tension screen-acquisition devices. These tests included: thermodynamic vent system operation, warm-gas pressurization effects, hydraulic pressure surge effects, screen device operational limitations, feedline vapor control, and two-phase refill. However, due to

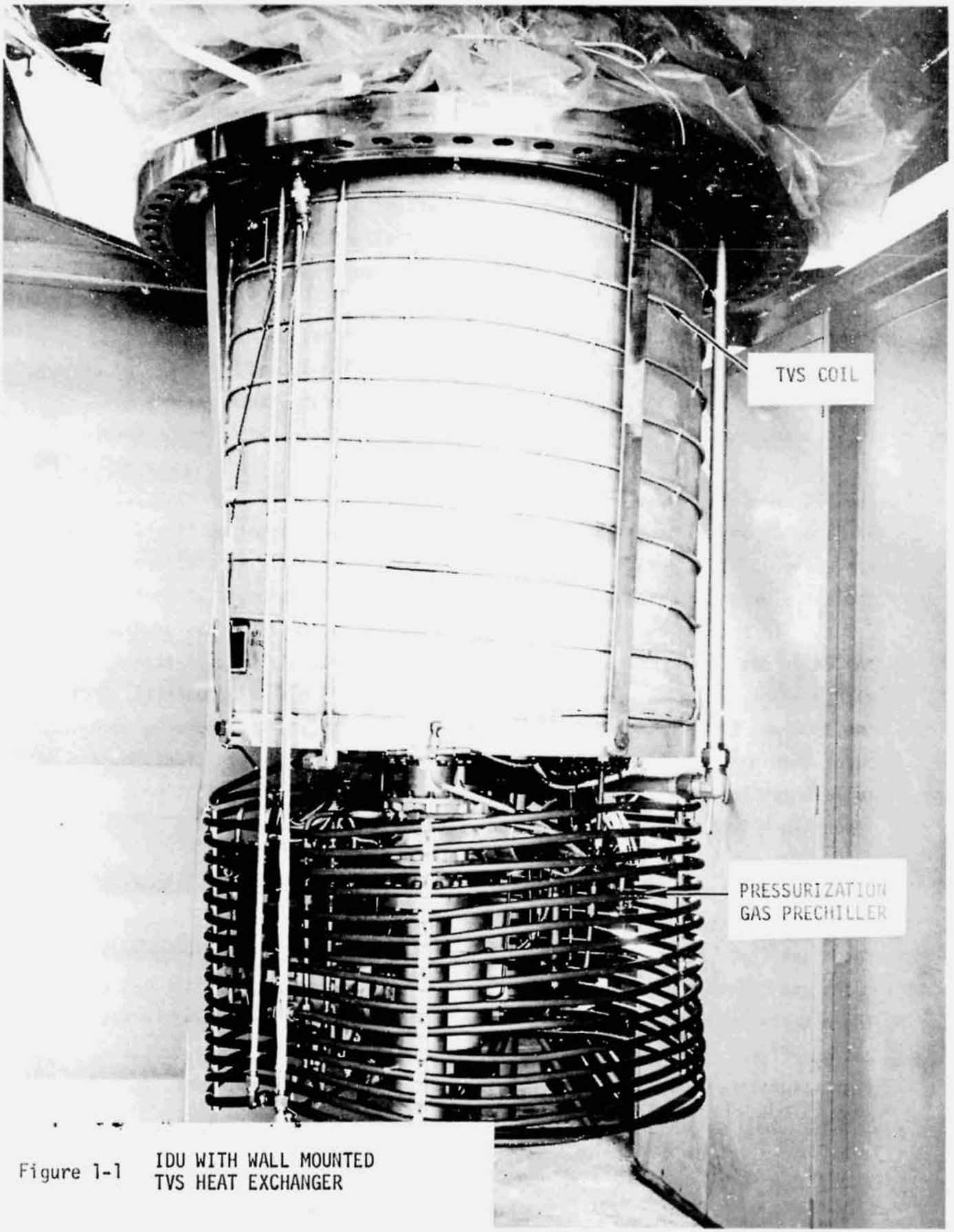

Figure 1-1 IDU WITH WALL MOUNTED TVS HEAT EXCHANGER

repeated malfunctions of the Parker submerged liquid hydrogen valves, test results were limited and certain other tests were not accomplished.

The tests achieved the following results:

- The screen device was shown to perform flawlessly for the cold-gas pressurization design condition with a higher "bubble point" or breakdown pressure difference than expected and with no indication of degradation throughout the test program.

- Both the overhead and submerged pressurization diffusers were used successfully.

- The data acquisition and instrumentation functioned properly.

- Flowrate control of the thermodynamic vent system was achieved over the entire range, and agreement between predicted and actual flowrates was good.

- Nc component failures were observed, although the 2-inch submerged liquid hydrogen ball valves malfunctioned, as discussed in detail in this report.

- The complete operational mode associated with a simulated low-g engine restart involving IDU outflow, followed by refill with simultaneous outflow was demonstrated.

- Breakdown data were obtained, showing a marked decrease in retention capability when warm hydrogen pressurant was used. Warm helium also decreased the retention capability causing premature breakdown, but the effect was not as great as with warm hydrogen.

- Use of a polyurethane adhesive to seal minor holes in the screen was successful; a conducting epoxy used to fill gaps in the TVS fillet on the IDU tank wall showed no adverse effect due to exposure to LH_2 and repeated thermal cycles.

- Finally, the integrity of the IDU subsystem in terms of operating pressures, flowrates, and soundness of welds, seals, and connections was demonstrated.

Analyses were performed of the liquid flow losses, autogenous (warm gaseous hydrogen) pressurization, and the thermodynamic vent system; a mathematical model of the thermodynamic vent system (TVS) was developed, programmed, utilized, and documented; and an existing MDAC tank-pressurization computer code was modified and used in assessing autogenous pressurization effects in the IDU.

Data obtained from the tests has been analyzed and the results correlated. However, because of feedline valve malfunctions, results in some tests are of marginal utility as discussed for each specific test in the following report. A corrective modification to the feedline valves has been recommended, based on a preliminary investigation of their operational factors of safety.*

An improvement to the basic start-tank concept was conceived but has not yet been reduced to practice. The principle of the "jet pump" can be used during start-tank refill to induce gas flow out of the start tank, with concurrent liquid inflow, while the main tank is pressurized and while a net flow to the turbopumps from the main tank through the start tank is sustained. This concept completely eliminates the need for overboard venting of start-tank ullage gas during refill, thereby decreasing the total system weight. The concept deserves additional consideration not only because of the improvements to the start-tank principle, but also because of possible additional applications to screen-device refill for both cryogenic and storable propellant systems. The external plumbing of the IDU pressurization system could be modified to incorporate a jet pump for refill witnout overboard venting.

An improved version of the cone screen housing, used for feedline vapor control, is described in Section 4, Test T; this version will ensure a liquid-filled feedline, thus diminishing the probability of vapor ingestion in the turbopump.

*Operational factor of safety is the ratio of applied actuation pressure to minimum actuation pressure.

This program was performed concurrently with another NASA/MSFC sponsored program, Contract NAS8-27685 (Reference 4) with MDAC; these two programs were complementary because: (1) fabrication experience gained on the IDU was beneficial in the fabrication of full-scale screen channel devices; (2) a screen device, developed and fabricated to simulate propellant retention for a cryogenic advanced space propulsion module (ASPM), is mounted inside the IDU for full-scale tests in the NASA/MSFC 105-inch tank; and (3) common, integrated feedline plumbing will be utilized between the IDU (with either the annular screen device or the ASPM device) and the full-scale screen channel for the NASA/MSFC APS breadboard tests. Finally, the IDU tests, verifying the operational aspects of the "start tank" concept, demonstrate the validity of the localized pressure isolated channel (LPIC) acquisition concept as well as the ASPM propellant acquisition concept selected in the system design study of Contract NAS8-27685.

Section 2 of this report encompasses a description of the IDU and TVS assembly and installation. Section 3 presents the supporting analyses. Section 4 is comprised of the test description and results; supporting annotated data from the tests is presented in a Supplemental Data Document. Conclusions are presented in Section 5. Appendices support the technical discussion.

Section 2
INTERFACE DEMONSTRATION UNIT DESIGN AND ASSEMBLY

2.1 DESIGN

This task included the design of the screen device, tank, and integrated system consisting of valves, components, instrumentation, line routing, and the thermodynamic vent system. Each of these elements is discussed in this subsection.

2.1.1 Screen Device Assembly

The basic requirements of the screen device assembly design are that it have an annular configuration and that it be capable of sustaining an outflow rate of 7.5 lb/sec of liquid hydrogen for approximately 5 seconds against 1 g before initiating refill.

Details of the screen assembly design were established using an MDAC computer code (Subsection 3.3) which determines, for specific configurations, screen breakdown level as a function of flowrate and includes all pertinent flow losses. Results showed that a 250 x 1370 stainless steel screen with a backup plate and coarse mesh standoff screen would meet the necessary requirements, and that the basic configuration should be a 24 inch outside diameter annular screen, 24 inches in height.

Detailed design specifications and drawings were submitted to NASA/MSFC by MDAC and, following approval, competitive bids were sought and a source selection made. The screen device, termed the Liquid Hydrogen Acquisition Device (LHAD), was subsequently fabricated by Western Filter Company; an assembly drawing is shown in Figure 2-1.

Additional detailed drawings have been submitted to NASA/MSFC.

2.1.2 Tank Design

The tank is comprised of a 6061 T6 aluminum cylindrical pressure shell 34.5 inches in length and 29 inches in diameter, a 2-inch-thick, 29-inch

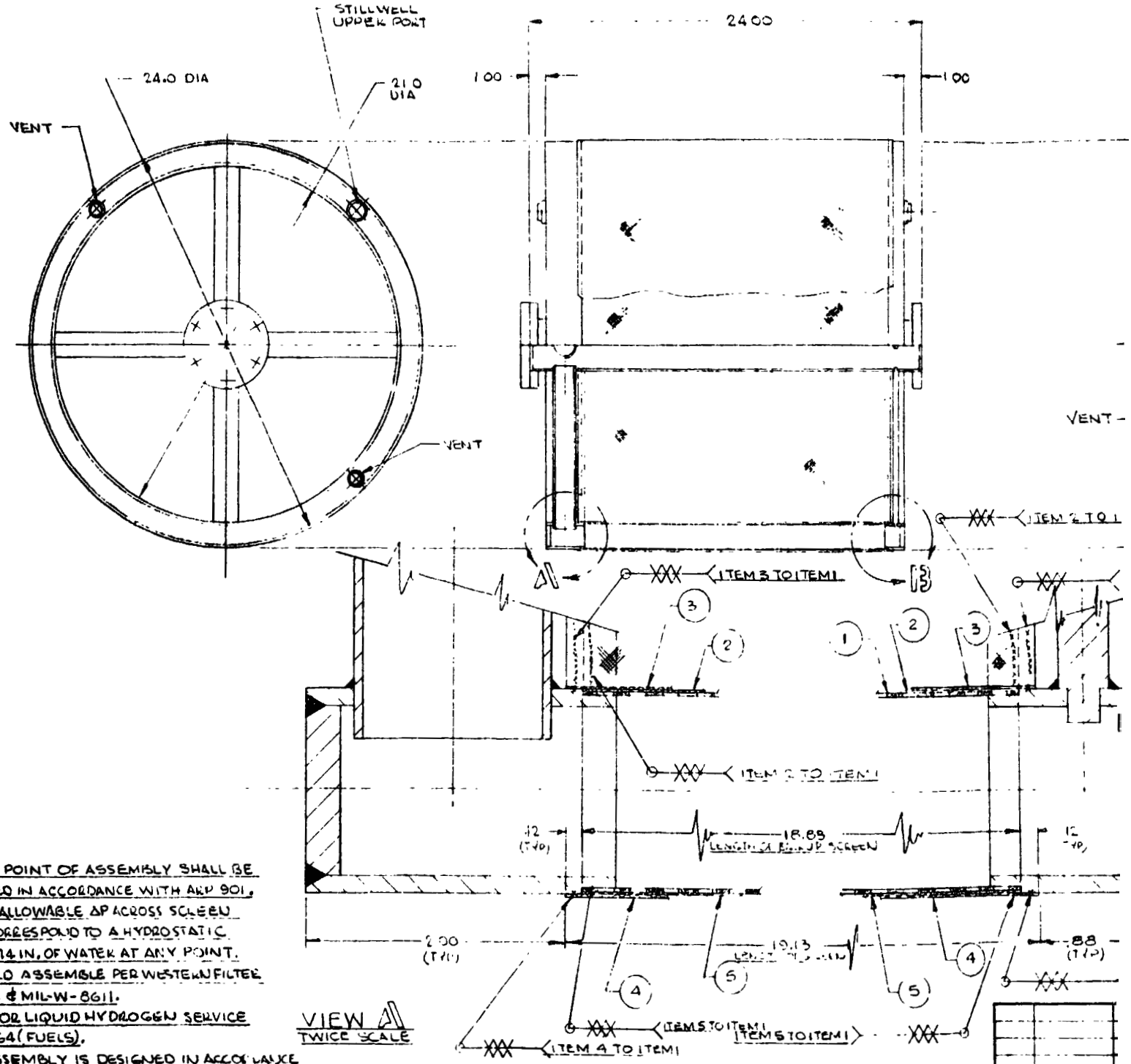

NOTE:

1. BUBBLE POINT OF ASSEMBLY SHALL BE MEASURED IN ACCORDANCE WITH ARP 901. THE MIN. ALLOWABLE ΔP ACROSS SCREEN SHALL CORRESPOND TO A HYDROSTATIC HEAD OF 14 IN. OF WATER AT ANY POINT.
2. TIG WELD ASSEMBLE PER WESTERN FILTER STD 204 & MIL-W-8611.
3. CLEAN FOR LIQUID HYDROGEN SERVICE MSFC 164 (FUELS).
4. THIS ASSEMBLY IS DESIGNED IN ACCORDANCE WITH MCDONNELL DOUGLAS ASTRO. DWG. 1T42607 N/C.

DASH NO	FINAL NEXT ASSY.

REVISIONS				
AUTHORITY	SYM	DESCRIPTION	DATE	APPROVED
		SEE REVISION NOTICE		

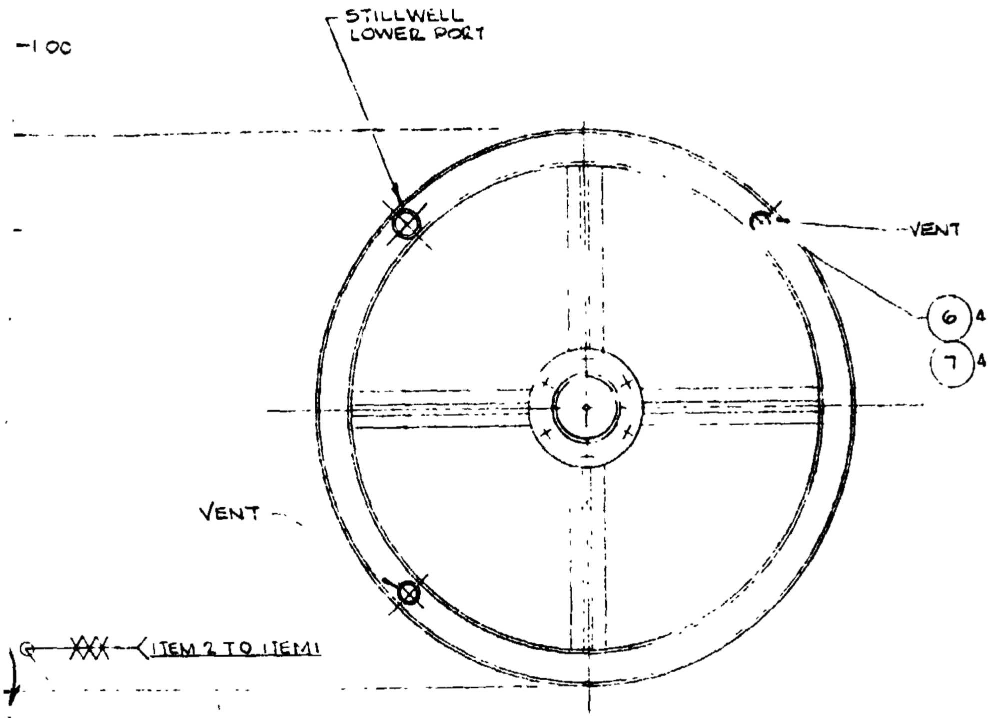

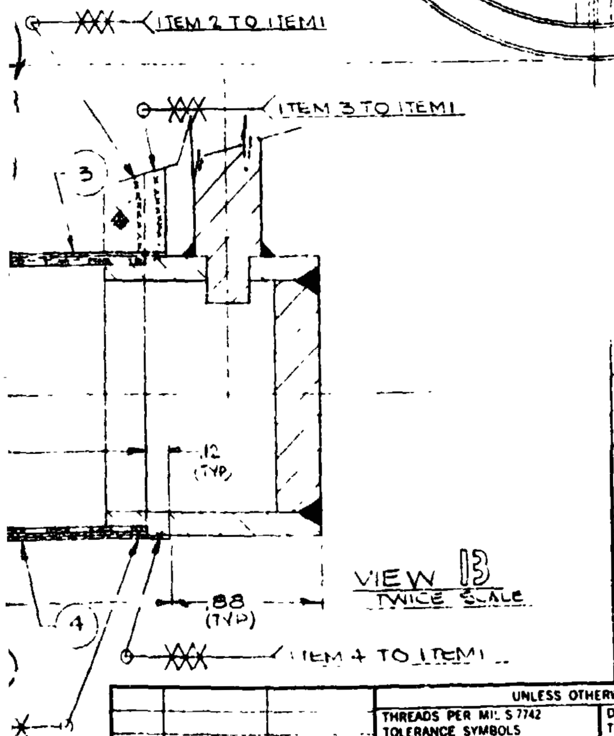

Figure 2-1

QTY REQ	PART NUMBER	CODE IDENT	NOMENCLATURE OR DESCRIPTION	SYM	MATERIAL OR NOTE	WT	MATERIAL SPECIFICATION OR PROCUREMENT DATA	ITEM
1	223227		PLUG W/ 1/8" NPT PORT					8
5	ARP5C8-908		O RING		TEFLON			
4	AN914-8K		PLUG & BLEEDER					6
			SCREEN BACKUP (OUTSIDE)		60X60 X.0045 (76 X 19) MATL 304L CRES			5
			SCREEN (OUTSIDE)		250 X 1370 SINTERED (76 X 19.5) MATL [illegible] CRES			4
			SCREEN (INSIDE)		250 X 1370 SINTERED (67 X 9.5) MATL 304L CRES			3
			SCREEN BACKUP (INSIDE)		60X60 X.0045 (67 X 19) MATL 304L CRES			2
1	[illegible]		MANIFOLD WELDMENT		304 L OR 316 CRES			1

LIST OF MATERIAL

DASH NO.	NEXT ASSY.	USED ON
	FINAL	

UNLESS OTHERWISE SPECIFIED

THREADS PER MIL S 7742
TOLERANCE SYMBOLS PER MIL-STD-8
REMOVE ALL BURRS
BREAK SHARP EDGES
MEET DIMS ~~BEFORE~~ AFTER FINISH
FINISH
HEAT TREAT
SIMILAR TO

DIMENSIONS ARE IN INCHES
TOLERANCES ON
FRACTIONS ± 1/32, DECIMALS .XX ±.01, ANGLES ± 1°

HOLE DIA	TOLERANCE
.0135 THRU .125	+ .004 — .001
.126 THRU .250	+ .005 — .001
.251 THRU .500	+ .007 — .001
.501 THRU .750	+ .008 — .001
.751 THRU 1.000	+ .010 — .001
1.001 THRU 2.000	+ .012 — .001

SURFACE ROUGHNESS PER MIL-STD-10
DIAMETERS ON SAME ℄ CONCENTRIC WITHIN — TIR

DRAFT, DESIGN, CHECK, ENGR, ENGR

WESTERN FILTER CO. INC.
8968 FULLBRIGHT AVENUE
CHATSWORTH, CALIFORNIA 91311

NOMENCLATURE
LIQUID HYDROGEN ACQUISITION DEVICE

CODE IDENT NO.	SIZE	DRAWING NO	REV
13520	D	423220	

SCALE AS NOTED | SHEET

423220

FOLDOUT [redacted] 2

diameter plate, and additional hardware as shown in Figure 2-2. The LHAD is bolted on the top of the plate. All tank penetrations for valves and ancillary plumbing are incorporated in the tank bottom plate. The cylindrical cover is equipped with a helical wall-mounted dip-brazed 0.25 inch outside diameter aluminum tube 70 feet in length. A summary of the design is presented below. Additional details are given in MDAC fabrication drawings submitted to NASA/MSFC.

2.1.3 Cover

The cylindrical pressure shell of the IDU is designed for 50 psid at ambient conditions. Crushing pressure is greater than 200 psid. Cryogenic allowables increase the cryogenic operating pressures by approximately 40 percent over the ambient conditions. Indium tin seals are used on the lip of the cover; these seals provide leakproof joints and are inexpensive and easily installed. There are no other seals, joints, or penetrations through the cover. The flange is internal to the cover to maximize tank volume within the envelope of 30 inch diameter.

2.1.4 Plate

The supporting plate contains all tank penetrations. The main feedline valve and cone screen housing were mounted on the plate along the tank centerline. The refill valve is mounted flush with the bottom. The total length of the hardware outside of the cover and plate is minimized. Bulkhead fittings are used for the diffusers and pressure sensing line and Borders/Physical Sciences cryogenic feed-throughs are used for wiring and coaxial cables.

2.1.5 Diffusers

The diffuser connections are composed of aluminum bulkhead flared tube fittings with K-seals. The overhead diffuser is a lateral multijet formed by two rows of ten 1/4-inch holes. The tube diameter is 1 1/4 inch outside diameter to allow sufficient vent outflow rate for tank refill within 10 seconds. The submerged helium diffuser is a horizontal circular tube, termed a ring-tube diffuser, with one row of forty 1/8-inch holes in the bottom. Locating the holes in the bottom of the ring-tube minimizes the possibility of having liquid fill the inside of the tube and affect gas outflow.

FOLDOUT FRAME /

117
116
115

TUBE 2 REQ'D

1T42536

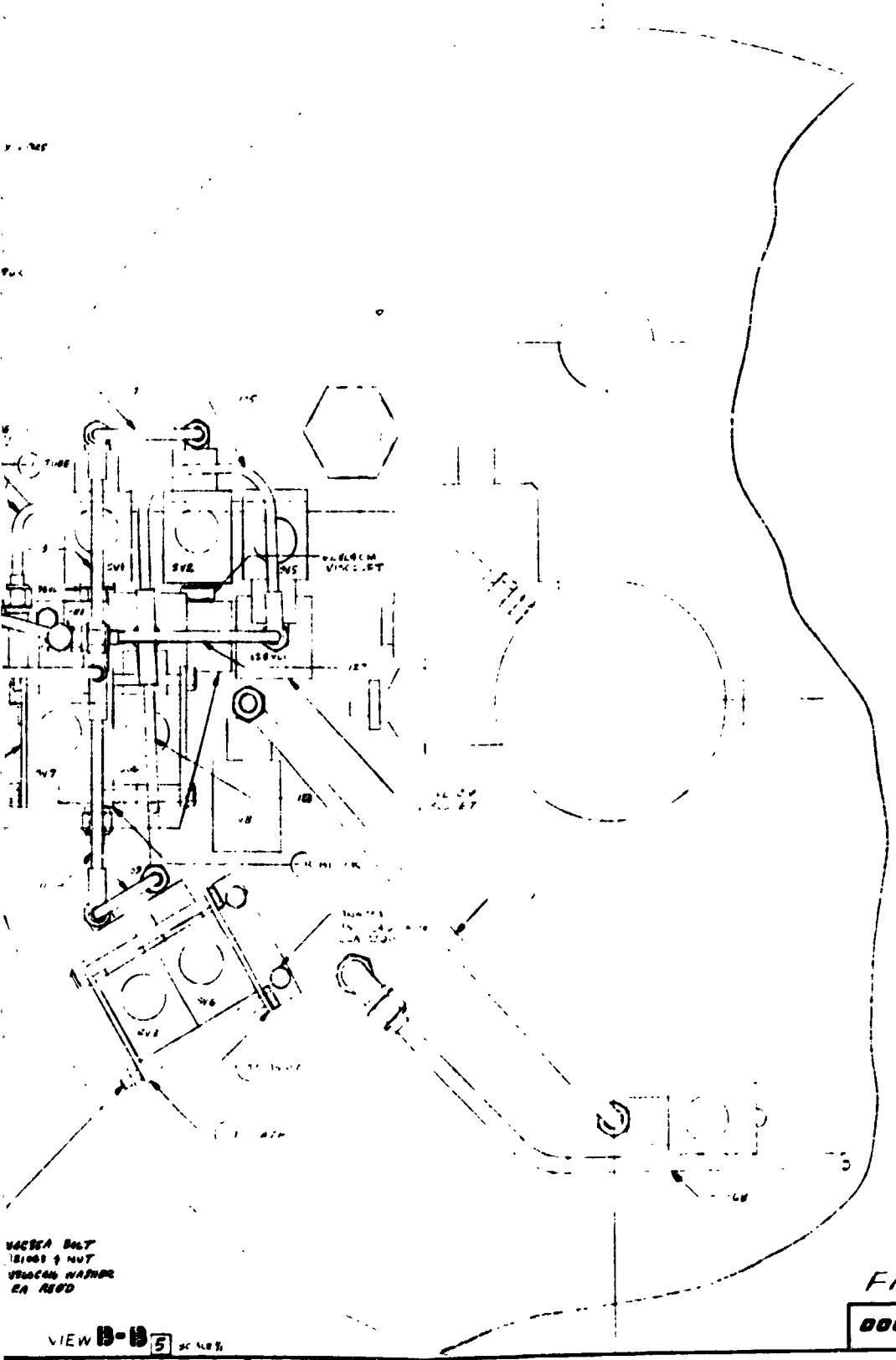

FIGURE 2-28

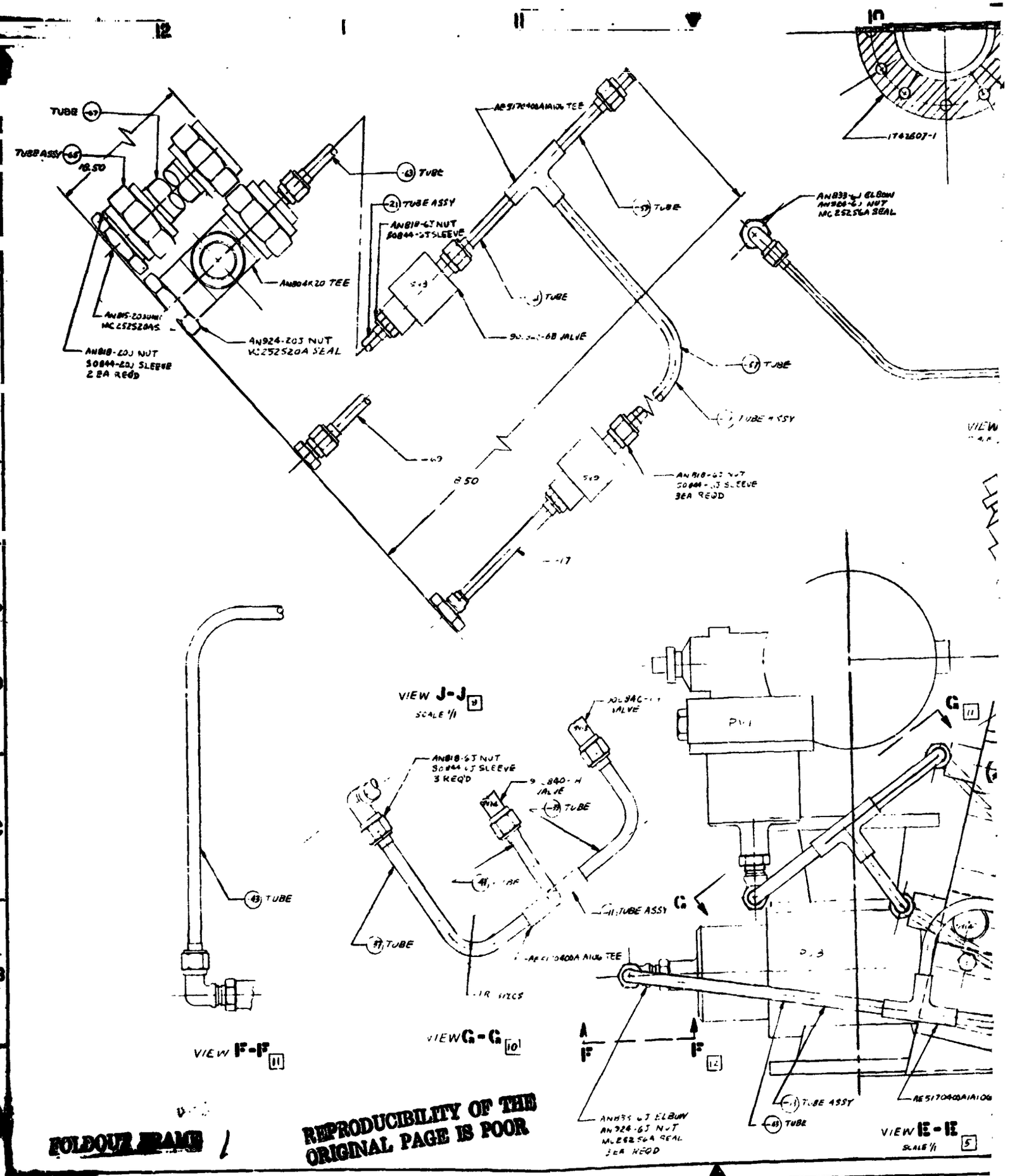

FOLDOUT FRAME 1

REPRODUCIBILITY OF THE ORIGINAL PAGE IS POOR

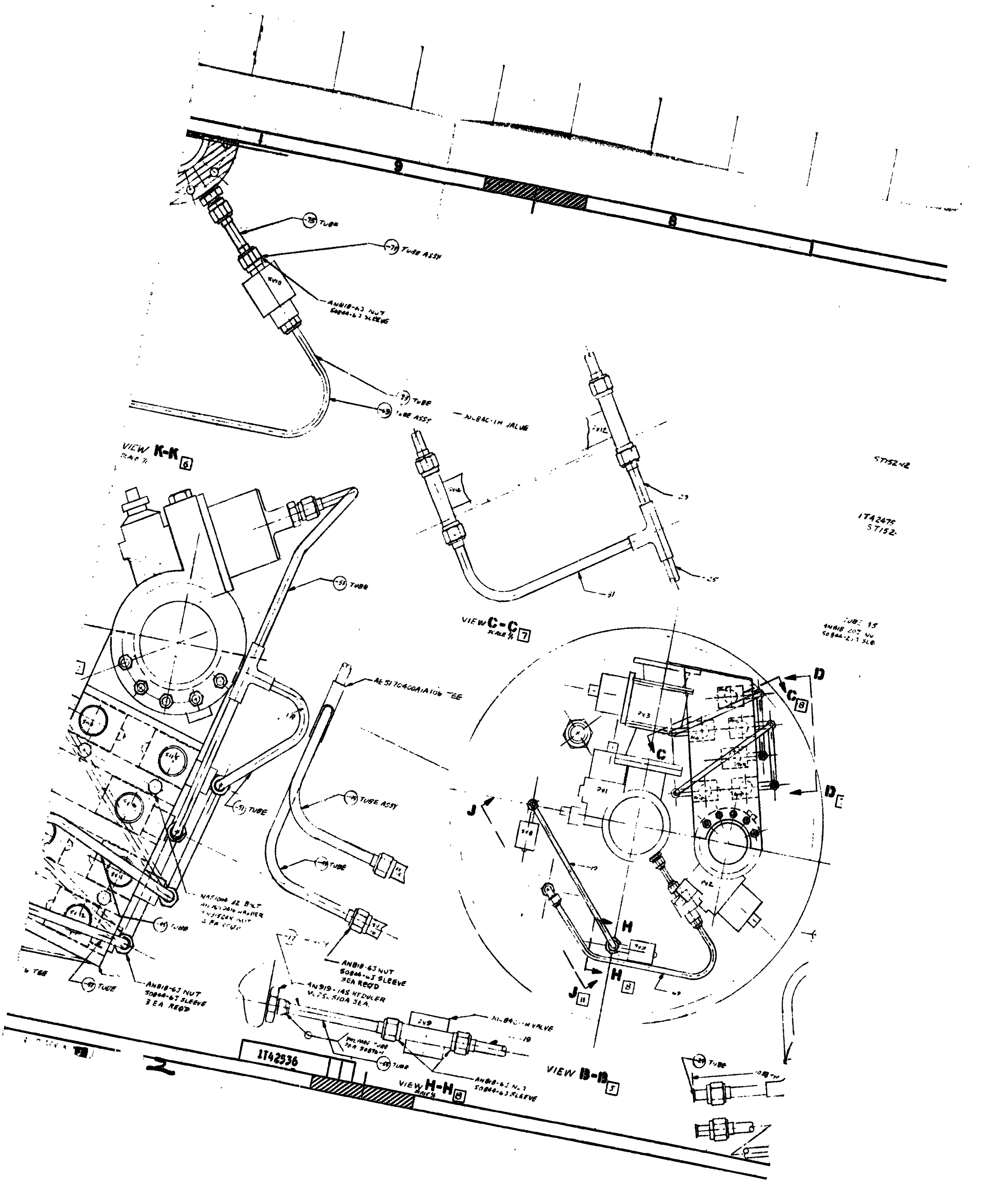
TUBE
TUBE ASSY
AN818-6J NUT
S0844-6J SLEEVE
TUBE
TUBE ASSY
VIEW K-K 6
ST152-12
1T42475
ST152-
VIEW C-C 7
AE51TC400A1A106 TEE
TUBE
TUBE ASSY
TUBE
NAS1004 BOLT
TUBE
AN818-6J NUT
S0844-6J SLEEVE
3 EA REQD
AN818-6J NUT
S0844-6J SLEEVE
3EA REQD
AN919-14S REDUCER
1T42936
VIEW H-H 8
VIEW B-B 5
AN818-6J NUT
S0844-6J SLEEVE
H
J
C
D
TUBE

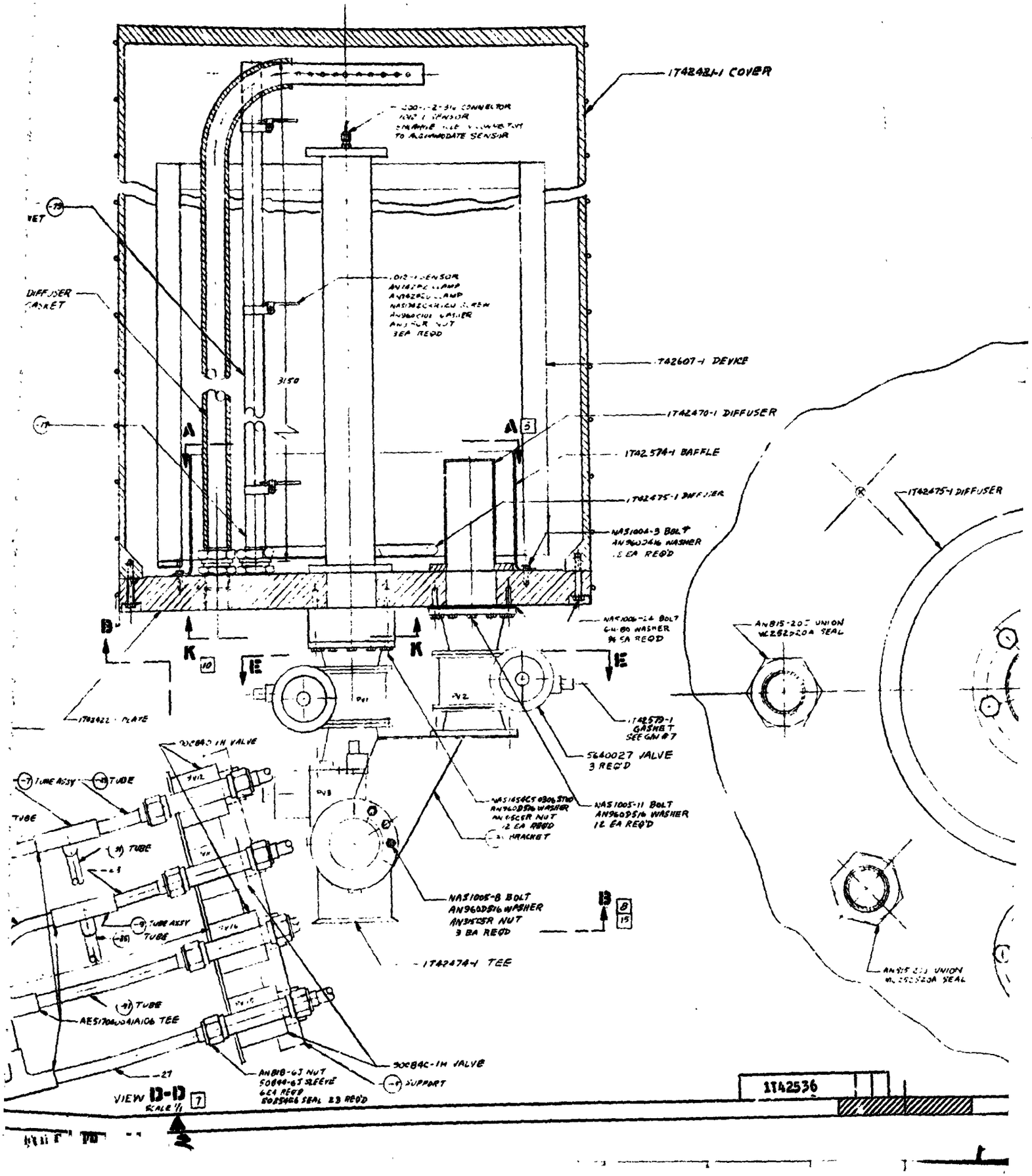
1T42421-1 COVER
DIFFUSER GASKET
1T42607-1 DEVICE
1T42470-1 DIFFUSER
1T42574-1 BAFFLE
1T42475-1 DIFFUSER
NAS1004-3 BOLT
AN960D416 WASHER
5 EA REQD
NAS1004-24 BOLT
AN960-416 WASHER
24 EA REQD
1T42422-1 PLATE
1T42579-1 GASKET
SEE GN #7
5640027 VALVE
3 REQ'D
NAS1005-11 BOLT
AN960D516 WASHER
12 EA REQ'D
NAS1005-8 BOLT
AN960D516 WASHER
AN315C8R NUT
3 EA REQD
1T42474-1 TEE
AN815-20J UNION
W/Z582Z20A SEAL
AN815-12J UNION
W/Z582Z12A SEAL
50CB4C-1H VALVE
AN818-6J NUT
50B44-6J SLEEVE
6 EA REQD
50B5446 SEAL 23 REQ'D
VIEW D-D
SCALE 1/1
1T42536

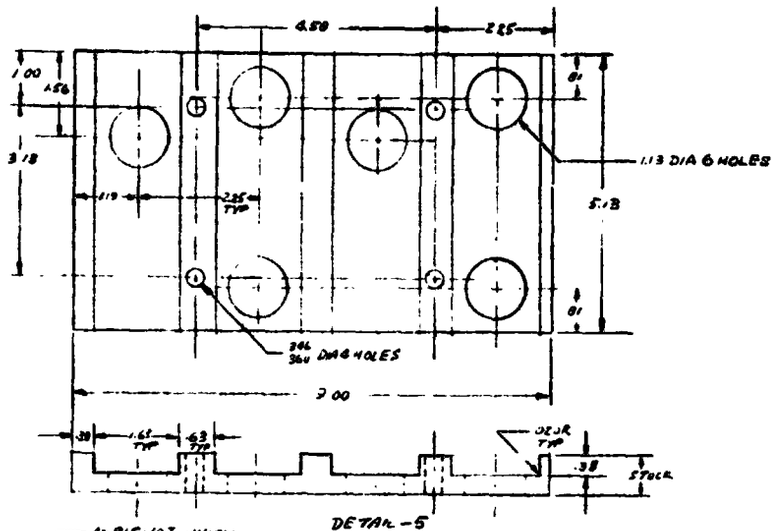

DETAIL -5

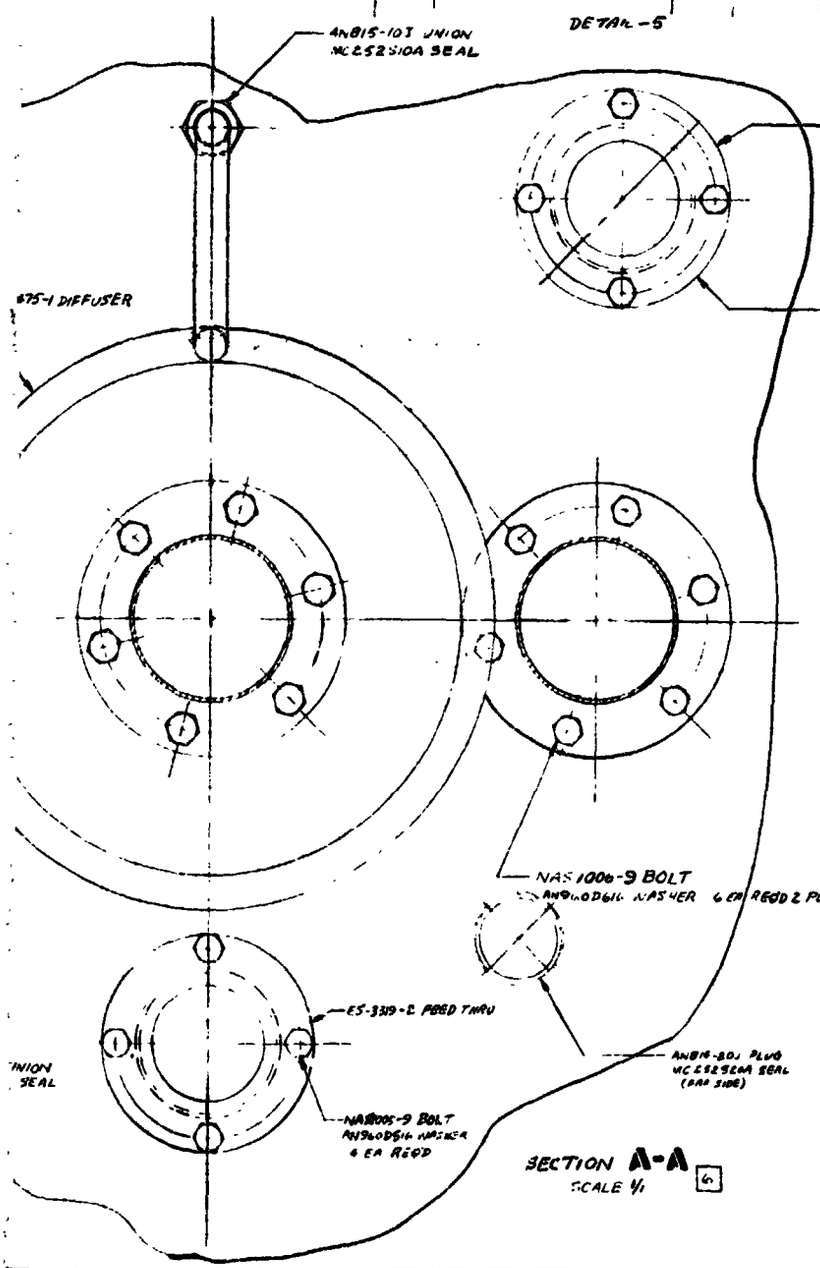

SECTION A-A
SCALE 1/1

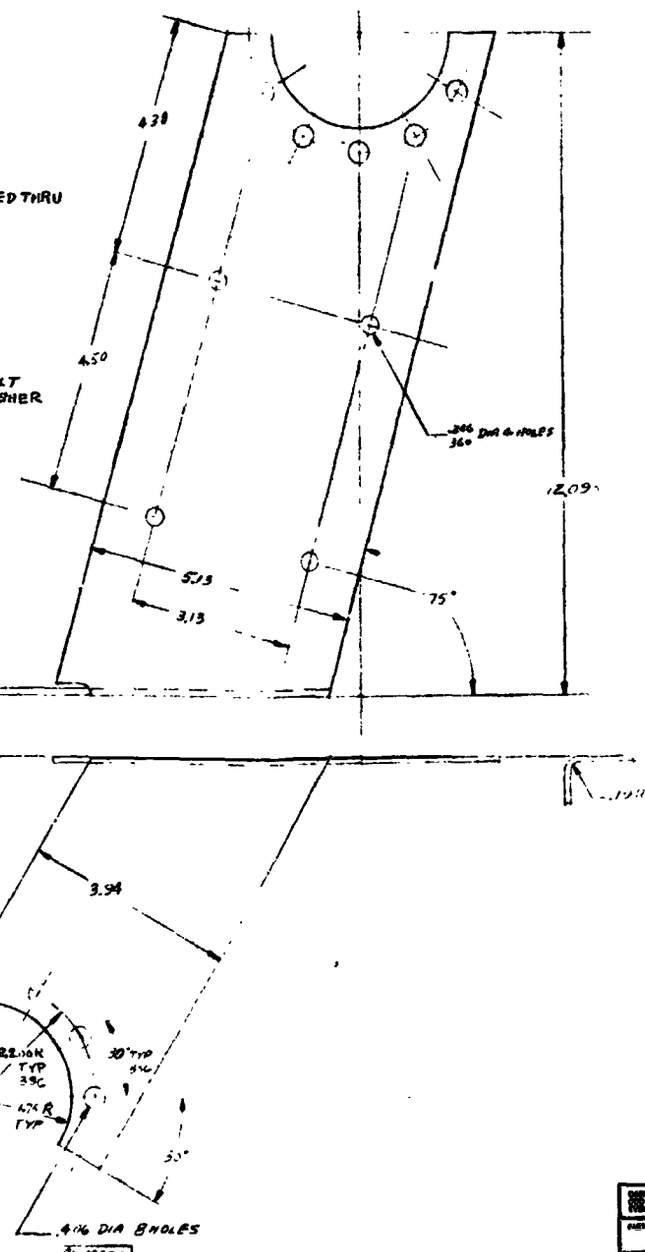

DETAIL -3

FOLDOUT FRAME

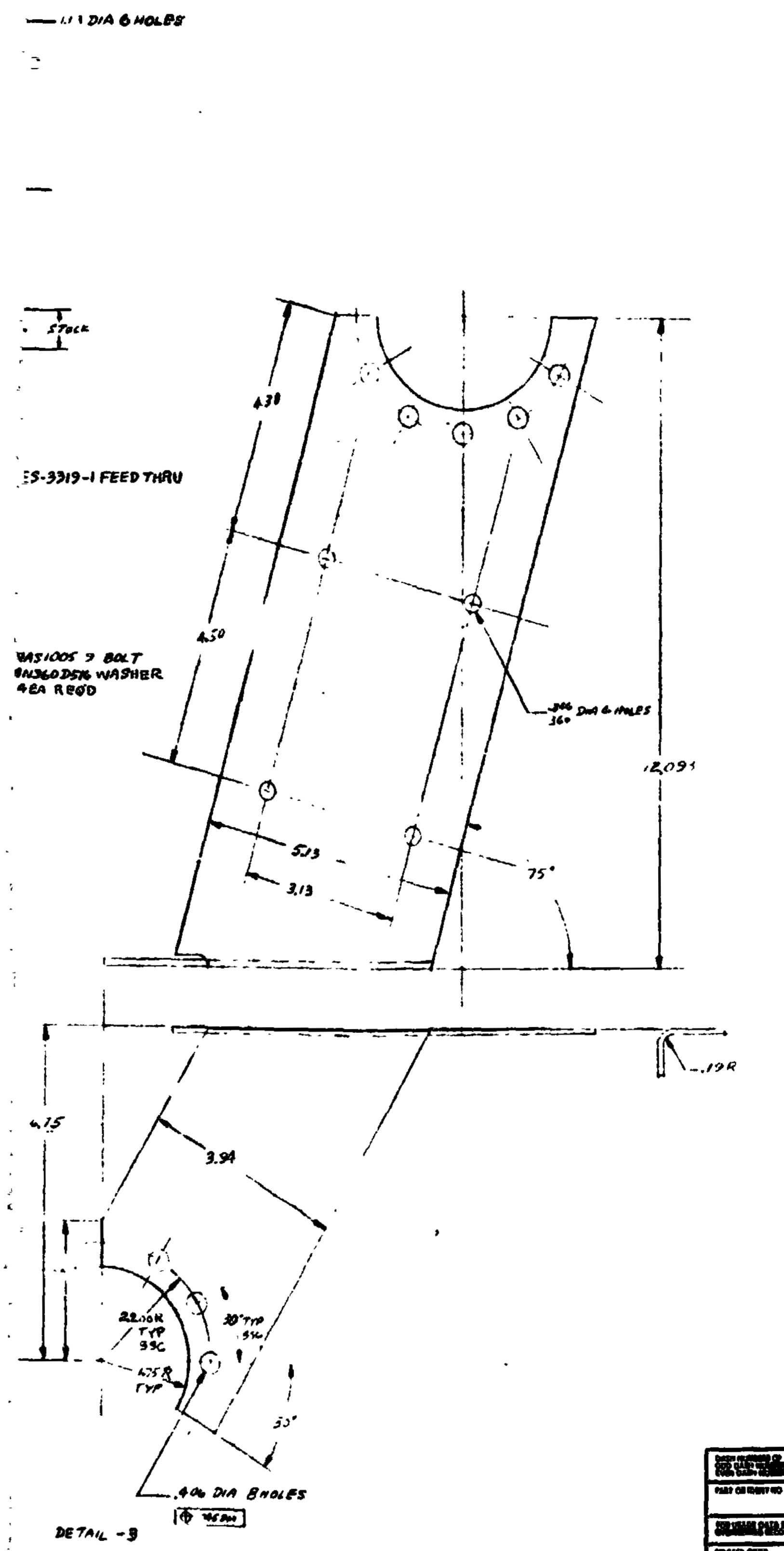

GENERAL NOTES:

UNLESS OTHERWISE SPECIFIED:

1. FUSION WELD PER MIL-W-8611. PENETRANT INSPECT PER MIL-I-6866, TYPE II. RADIOGRAPH WELDS 100% PER MIL-STD-453. INSPECT RADIOGRAPHS TO MIL-R-11468 STDS.
2. LEAK TEST [illegible] LINES TO 750 PSIG ± 20 PSIG WITH [illegible] BUREAU OF MINES, GRADE A [illegible] PARTICULATE CONTAMINATION OVER [illegible] MICRONS IN SIZE A MAXIMUM MOISTURE CONTENT OF 2 ± 3 PPM BY VOLUME AND A MAXIMUM NON-VOLATILE HYDROCARBON CONTENT OF 3 PPM [illegible] TER. IS OF OIL.
3. PREPARE TUBE ENDS PER STP0399-1
4. CLEAN PER STP0350-02 AND PACKAGE PER STP0589-04.
5. INDUCTION BRAZE PER MIL-B-7883 EXCEPT RADIOGRAPHIC INSPECT PER STP0398-01
6. LEAK TEST BRAZED JOINTS TO 1×10^{-6} SCCS.
7. FORM SEALS FROM .063 DIA INDIUM-TIN WIRE OVERLAP ENDS
8. PURGE BACKSIDE OF WELD WITH INERT GAS DURING WELDING.

FIGURE 2-2A

DATE	9 SEP 1977
TITLE	LH_2 ACQUISITION ASSEMBLY
SIZE	J
CODE IDENT NO.	18355
DRAWING NO.	1T42536

FOLDOUT FRAME 5

2.1.6 Tee

The bypass valve and main feedline valve are connected to the main outflow line through a tee connection. Several options were considered for the tee design since the 3-inch tank-outlet line must be expanded to the 4 inch outside diameter pump-inlet line. Use of a standard expansion joint (approximately 7 degrees total included angle) would increase the total connection length. Use of a standard tee and expansion flange increases the total pressure drop. As a compromise, a tee joint design which incorporates the flow expansion is used, as shown in MDAC Drawing 1T42474 (submitted to NASA/MSFC).

2.1.7 Integrated System

In the design of the tee, refill, overhead, and submerged helium diffusers, numerous flowrate and pressure drop calculations were made to assure practical operation. For hydrogen pressurization, a line diameter of at least 1/2 inch is required to meet the required volume flowrate of 1.7 ft^3/sec at 40°R with choked flow. In addition, the 3/8-inch Valcor solenoid valve must be bypassed to achieve the maximum vent rate. Therefore, a 1-1/4-inch-diameter bypass line is provided.

The refill diffuser has a pressure drop of 0.5 psid through 96 holes, each 1/2 inch in diameter. The corresponding impact pressure of the liquid hydrogen flowing into the tank and against the screen is difficult to determine analytically, but the inertial pressure ($P = \rho \frac{V^2}{2}$) is of the order of 1 psid even if the flow from the diffuser is assumed to expand to four times its outflow area; this pressure exceeds the screen bubble-point pressure. Therefore, a shield is used to stop possible bubble entrainment into the screen device.

The total pressure drop through the screen device is 0.06 psi. The loss through the valve is 0.17 psi at 7.5 lb/sec. The flow loss through the tee is approximately 0.5 psi.

Estimates of the overhead pressurization effects on the LH_2 interface were made, based on the results of visual pressurization tests reported in

Reference 5. No significant cavity will be formed due to incoming flow except for the liquid surface very close (~1 inch) to the diffuser.

2.1.8 Instrumentation

The complete instrumentation list is shown in Table 2-1.

2.1.9 Thermodynamic Vent System

The thermodynamic vent system (TVS) was added to the IDU after the design of the IDU had been completed, and the fabrication and assembly operations selected. Therefore, the TVS design was compromised to meet the existing design constraints. An external wall-mounted, helical-coil tube design was selected to be continuously dip brazed on the cylindrical portion of the IDU wall. Tubing was not placed on the top of the IDU since heat flux through the top would be relatively low in all cases and a separate brazing process would have added substantial costs. Furthermore, the wall-mounted TVS can be used with a slightly higher outflow rate and lower coolant temperature to remove the heat that enters the top plate of the IDU.

The mounting arrangement of the TVS offers several alternative flow paths. Two, 1/4 inch diameter tubes, 35 ft long, are helically wound on the outside of the IDU, and connected by a tee manifold at the top of the cover. Coolant flow on the IDU wall can be routed as follows:

A. A 70 ft continuous path is provided. Liquid enters at the bottom of the IDU, flows up through 35 ft of tubing to the top of the IDU, and then flows down through 35 ft of tubing to the bottom of the IDU. Coil separation is 3.5 inches on the IDU wall, with alternating uphill and downhill flow.

B. Flow can start at the top of the IDU and flow down through one 35 ft length of tubing (coil separation distance of 7 inches).

C. Flow can start at the bottom of the IDU, and flow up through one 35 ft length of tubing, exiting at the tee (coil separation distance of 7 inches).

D. Flow can enter at the top of the IDU through the tee and flow down both 35 ft tubes in parallel paths (coil separation distance of 3.5 inches).

Table 2-1 (Page 1 of 5)

INSTRUMENTATION LIST FOR MDAC FACILITY TEST - BASIC IDU CHECKOUT

Instrument/Type	Purpose	Number Applied	Manufacturer/ Part Number	Designation	Mounting Provision/Location/Wires	Calibration Range/ Output
Level sensor/ carbon resistance	Approx position for static breakdown	1	Ohmite "Little Devil"	RL1	Affixed to 1-1/4 in. IDU pressure sensing line - 5.5 in. above cover; 2 wires - IDU	1,000 ohms, 100 Mw
	Approx position for breakdown with $\dot{m}$ = 4.5 lb/sec	1	Ohmite "Little Devil"	RL2	Affixed to 1-1/4 in. IDU pressure sensing line - 10.5 in. above cover; 2 wires - IDU	1,000 ohms, 100 Mw
	Warning point for $\dot{m}$ = 4.5 lb/sec and approx position for breakdown with 7.5 lb/sec	1	Ohmite "Little Devil"	RL3	Affixed to 1-1/4 in. IDU pressure sensing line - 13.5 in. above cover; 2 wires - IDU	1,000 ohms, 100 Mw
	Warning point for $\dot{m}$ = 7.5 lb/sec	1	Ohmite "Little Devil"	RL4	Affixed to 1-1/4 in. IDU pressure sensing line - 18.5 in. above cover; 2 wires - IDU	1,000 ohms, 100 Mw
	Warning point for vent valve closure	1	Ohmite "Little Devil"	RL5	Affixed to 1-1/4 in. IDU pressure sensing line - 31.0 in. above cover; 2 wires - IDU	1,000 ohms, 100 Mw
	Maximum acceptable liquid level	1	Ohmite "Little Devil"	RL6	Affixed to 1-1/4 in. IDU pressure sensing line - 33.0 in. above cover; 2 wires - IDU (optional)	1,000 ohms, 100 Mw
	Phase sensor inside screen (requires oscillograph)	1	Ohmite "Little Devil"	RL7	Located in top port of screen device, beneath screen/annulus support weld connection/ 2 wires - IDU	1,000 ohms, 100 Mw
	Main tank level sensing	1	Ohmite "Little Devil"	RL8*	Near bottom of MDAC 260-gal main tank/ 2 wires - main tank	1,000 ohms, 100 Mw
	Main tank level sensing	1	Ohmite "Little Devil"	RL9*	Near mid-level of MDAC 260-gal main tank, at bottom of IDU 2 wires - main tank	1,000 ohms, 100 Mw
	Main tank level sensing	1	Ohmite "Little Devil"	RL10*	Near top of MDAC 260-gal main tank, at top of of IDU 2 wires - main tank	1,000 ohms, 100 Mw
Level sensor/ capacitance-point	Same as RL3 (oscillograph)	3	NASA-MSFC GFP	CL1	Same position as RL3/(coax) - 13.5 in.	
	Same as RL4 (oscillograph)		NASA-MSFC GFP	CL2	Same position as RL4/(coax) - 18.5 in.	
	Same as RL5 (oscillograph)		NASA-MSFC GFP	CL3	Same position as RL5/(coax) - 31 in.	
Level sensor/ capacitance	Continuous level sensing (oscillograph, digital volt meter)	1	NASA-MSFC-GFP	CL4	Attached to central IDU pipe (3 in. dia/(coax)	

*Denotes nondeliverable items used for MDAC facility test

Table 2-1 (Page 2 of 5)

INSTRUMENTATION LIST FOR MDAC FACILITY TEST - BASIC IDU CHECKOUT

Instrument/Type	Purpose	Number Applied	Manufacturer/ Part Number	Designation	Mounting Provision/Location/Wires	Calibration Range/ Output
Temperature sensor/ platinum resistance probe	Bulk liquid temperature	1	Thermal Systems/1012	T1	Affixed to 1-1/4 in. IDU pressure sensing line - 6 in. above cover; position as close to screen as practical; 4 wires - IDU	70° to -424° F/ 1,000 ± 5 ohms at 273.2° K
	Bulk liquid/interface region temperature	1	Thermal Systems/1012	T2	Affixed to 1-1/4 in. IDU pressure sensing line - 18.5 in. above cover; position as close to screen as practical; 4 wires - IDU	70° to -424° F/ 1,000 ± 5 ohms at 273.2 °K
	Ullage temperature	1	Thermal Systems/1012	T3	Affixed to 1-1/4 in. IDU pressure sensing line - 28.5 in. above cover; position as close to screen as practical; 4 wires - IDU	70° to -424° F/ 1,000 ± 5 ohms at
	Expelled liquid temperature temperature	1	Thermal Systems/1012	T4	Top of screen device central pipe/4 wires - IDU	-400° to -424° F/ 1,000 ± 5 ohms at 273.2° K
Temperature sensor/ platinum resistance probe	Inlet temperature	1	Thermal Systems/1012	T7	Tee connection at TVS inlet 4 wires - main tank	-400° to -450° F/ 1,000 ± 5 ohms at 273.2° K
Temperature sensor/ Platinum resistance probe	Outlet temperature	1	Thermal Systems/1012	T8	Tee connection at TVS outlet 4 wires - main tank	-400° to -450° F/ 1,000 ± 5 ohms at 273.2° K
	Fluid temperature	1	Thermal Systems 1012	T5*	Main tank - upper 4 wires - main tank	+70° to -424° F/ 1,000 ± 5 ohms at 273.2° K
	Fluid temperature	1	Thermal Systems 1012	T6*	Main tank - lower 4 wires - main tank	+70° to -424° F/ 1,000 ± 5 ohms at 273.2° K
Temperature sensor/ platinum resistance patch	IDU external tank temperature	1	Thermal Systems/ 5001-19	T9	Epoxy bonded to outside of cylindrical tank wall, near the top; 4 wires - main tank	+70° to -424° F 500 ohms at 273.2° K
Pressure transducers	Main tank pressure	1	TBD	P1*	Main tank pressure sensing line	0 to 75 psig
	IDU pressure	1	TBD	P2*	IDU pressure sensing line	0 to 75 psig
	TVS exit pressure	1	TBD	P3*	TVS exit line	0 to 200 in. mercury (ABS)

*Denotes nondeliverable items used for MDAC facility test

Table 2-1 (Page 3 of 5)

INSTRUMENTATION LIST FOR MDAC FACILITY TEST

Instrument/Type	Purpose	Number Applied	Manufacturer/ Part Number	Designation	Mounting Provision/Location/Wires	Calibration Range/ Output
Instrumentation List for MDAC Facility Test - Additional IDU Experiments						
Temperature sensor/ platinum resistance probe	VJ1 TVS expansion temperature	1	Thermal Systems/ 1012-1	T10	Tee, downstream of VJ1 in thermodynamic vent system; 4 wires - main tank	-400° to -450° F 1,000 ± 5 ohms at 273.2° K
	VJ2 TVS expansion temperature	1	Thermal Systems/ 1012-1	T11	Tee, downstream of VJ2 in thermodynamic vent system; 4 wires - main tank	-400° to -450° F 1,000 ± 5 ohms at 273.2° K
	VJ3 TVS expansion temperature	1	Thermal Systems/ 1012-1	T12	Tee, downstream of VJ3 in thermodynamic vent system; 4 wires - main tank	-400° to -450° F 1,000 ± 5 ohms at 273.2° K
	VJ4 TVS expansion temperature	1	Thermal Systems/ 1012-1	T13	Tee, downstream of VJ4 in thermodynamic vent system; 4 wires - main tank	-400° to -450° F 1,000 ± 5 ohms at 273.2° K
	VJ5 TVS expansion temperature	1	Thermal Systems/ 1012-1	T14	Tee, downstream of VJ5 in thermodynamic vent system; 4 wires - main tank	-400° to -450° F 1,000 ± 5 ohms at 273.2° K
	Temperature outside boundary layer at HF2-A	1	Thermal Systems/ 1012-1	T15	Probe support, connected to HF2-A plate 4 wires - IDU	70° to -424° F 1,000 ± 5 ohms at 273.2° K
	Temperature outside boundary layer at HF3-A	1	Thermal Systems/ 1012-1	T16	Probe support, connected to HF3-A plate 4 wires - IDU	70° to -424° F 1,000 ± 5 ohms at 273.2° K
	Temperature of overhead diffuser outlet gas	1	Thermal Systems/ 1012-1	T17	Swagelok fitting in end of overhead diffuser 4 wires - IDU	70° to -424° F 1,000 ± 5 ohms at 273.2° K
	Temperature near screen, below T17 or in ullage, for more accurate temperature distribution in ullage	1	Thermal Systems/ 1012-1	T18	Supported by pressure sensing line, and located approximately 1/4 in. from screen, 3 in. below weld seam of screen/annular support, or 18.5 in. above cover; 4 wires - IDU (optional)	70° to -424° F 1,000 ± 5 ohms 273.2° K
Temperature sensor/ platinum resistance patch	IDU outer wall temperature	1	Thermal Systems 5001-19	T19	Bonded to cylindrical IDU wall 4 wires - main tank	70° to -424° F 500 ohms at 273.2° K

Table 2-1 (Page 4 of 5)

INSTRUMENTATION LIST FOR MDAC FACILITY TEST

Instrument/Type	Purpose	Number Applied	Manufacturer/ Part Number	Designation	Mounting Provision/Location/Wires	Calibration Range/ Output
Temperature sensor/ platinum resistance	Screen device annular support	1	Thermal Systems 5001-19	T20	Bonded to top of annular support of screen device; 4 wires - IDU	-350° to -424° F 1,000 ± 5 ohms at 273.2° K
Heat flux meter/ thermopile	Heat flux into tank below liquid level in IDU	1	International Thermal Instrument Model-B (2 x 2 in.)	HF1-B	Bonded to outside of IDU, approximately 2.5 in. above datum line, between TVS coils; 2 wires - main tank	7 Btu/ft^{2}hr mv (3% accuracy)
Note: The output of the heat flux meters, HF2-A and HF3-A, can be read either separately or can be combined using a selector switch	Heat flux into tank above liquid level in IDU	1	International Thermal Instrument Model-A (4 x 4 in.)	HF2-A	Bonded to inside of IDU cylinder, approximately 15 in. above datum line, straddling one TVS coil 2 wires - IDU	7 Btu/ft^{2}hr mv (1% accuracy)
	Heat flux into tank above liquid level in IDU	1	International Thermal Instrument Model-A (4 x 4 in.)	HF3-A	Bonded to inside of IDU cylinder, approximately 30 in. above datum line, straddling one TVS coil 2 wires - IDU	7 Btu/ft^{2}hr mv (1% accuracy)
	Heat flux into tank above liquid level in IDU	1	International Thermal Instrument Model-B (2 x 2 in.)	HF4-B	Bonded to outside of IDU cylinder, approximately 30 in. above datum line, between TVS coils 2 wires - main tank	7 Btu/ft^{2}hr mv (3% accuracy)
Temperature sensor/ thermocouple	HF1-B surface temperature (needed for calibration)	1	International Thermal Instrument Model-B	T21	Bonded to HF1-B 2 wires - main tank	
	HF2-A surface temperature (needed for calibration)	1	International Thermal Instrument Model-A	T22	Bonded to HF2-A 2 wires - IDU	
	HF3-A surface temperature (needed for calibration)	1	International Thermal Instrument Model-A	T23	Bonded to HF3-A 2 wires - IDU	

Table 2-1 (Page 5 of 5)
INSTRUMENTATION LIST FOR MDAC FACILITY TEST

Instrument/Type	Purpose	Number Applied	Manufacturer/ Part Number	Designation	Mounting Provision/Location/Wires	Calibration Range/ OUtput
Temperature sensor/ thermocouple	HF4-A surface temperature (needed for calibration)	1	International Thermal Instrument Model-8	T24	Bonded to HF4-B 2 wires - main tank	
Position indicator switch/LH_2 Valve	Indicate valve position, PV1	1	---	PV1IS	Mounted on PV1, valve	
	Indicate valve position, PV2	1	---	PV2IS	Mounted on PV2, valve	
	Indicate valve position, PV3	1	---	PV3IS	Mounted on PV3, valve	
Total instrumentation wires from inside IDU = 52 to 58						
Total instrumentation wires from main tank = 56						
Hot-wire anemometer flowmeter	Measure TVS vapor flow rate	2	Thermal Systems	FM1*, and FM2*	Ambient location	0.003 to 0.3 scfm 0.3 to 30 scfm

These options allow pressure drop through the tube to be varied by varying tubing length, and tube separation distances of 7 inches or 3.5 inches can be tested. The latter flow configuration (D) was selected for these tests since cooling capacity was maximum and the pressure drop was minimum.

The flowrate control required for the TVS was 0.3 to 3 lb/hr of hydrogen. This was accomplished using five viscojets orifices, selected to provide flowrates of approximately 0.2, 0.4, 0.8, 1.4, 1.8 lb/hr of hydrogen with approximately 15-psi pressure difference across the viscojets. Increasing or decreasing the pressure difference, and selecting the appropriate combination of viscojets allowed the flowrates to be controlled within a band exceeding that required (i.e, 0.2 to 5 lb/hr).

2.2 ASSEMBLY

The sequence of operations leading to the final assembly of the IDU is presented in this subsection. Figure 2-3 gives a side view of the Liquid Hydrogen Acquisition Device (LHAD) after its completion by the subcontractor, Western Filter Company, Inc., Chatsworth, California.

A series of bubble-point tests were performed following fabrication of the LHAD. The film bubble-point test procedure was employed. The LHAD was partially submerged in ethyl alcohol and then a spray of alcohol was used to wet the inner and outer screens. Pressure was applied to the LHAD as it was rotated while partially submerged. Bubbles released from imperfection points on the screen were noted and marked for later sealing. This type of film bubble-point test procedure is necessary for screen devices of large size relative to the head of test liquid which can be supported, and the procedure used for the LHAD can be easily extended for testing of vehicle screen devices in-situ. In the first test, several small holes were located and sealed with Allstate 430 Cadmium-free solder. Although this particular solder has been used successfully with filter elements at liquid helium temperatures, the possibility of crystallization exists. Therefore, a special polyurethane adhesive (Spec-1P20075 DPS-32330) which has been used successfully in a number of cryogenic applications was applied over the solder spots as a precaution. The device was then shipped to Garwood Laboratories for final

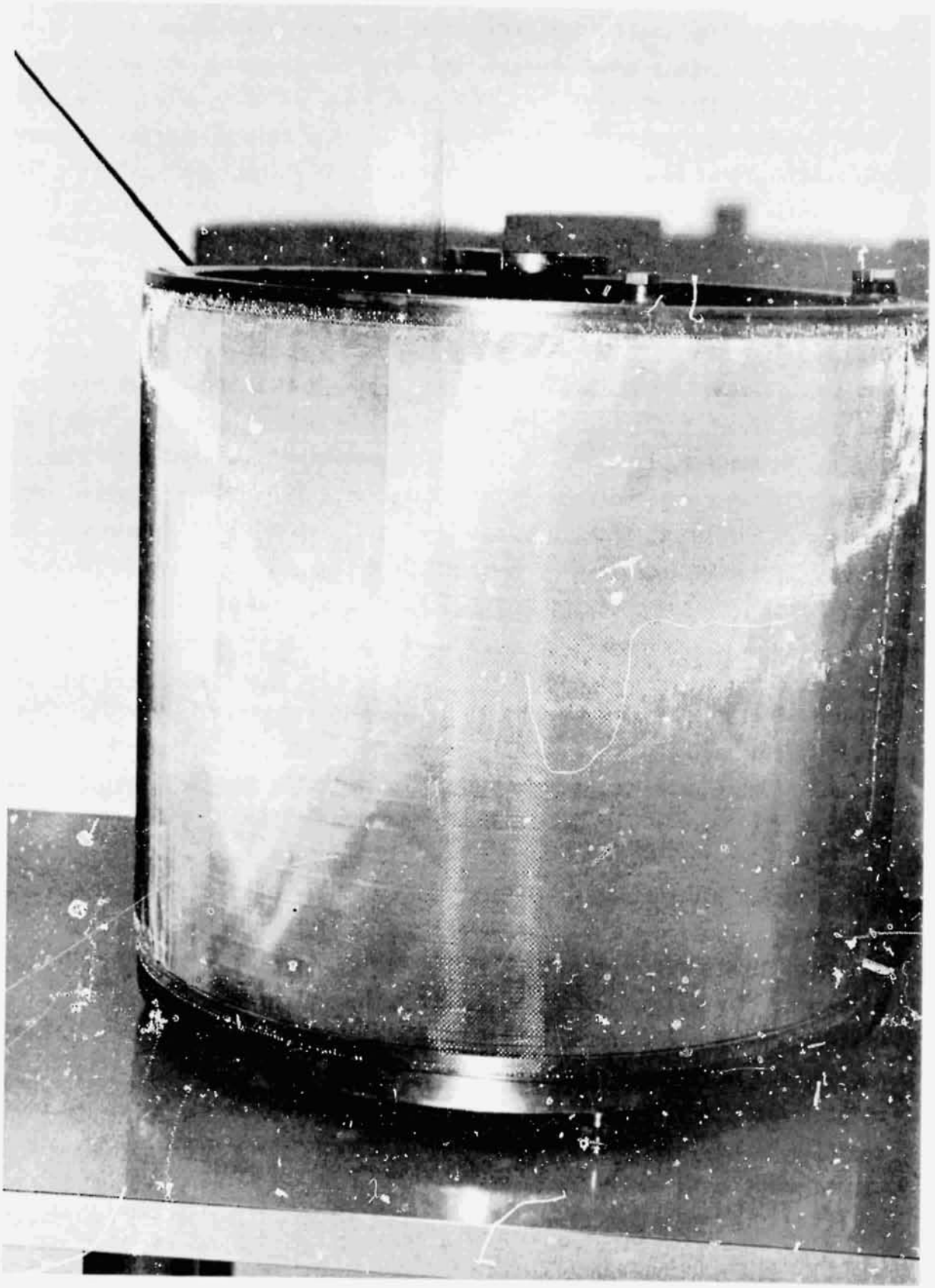

Figure 2-3 TDU LIQUID HYDROGEN ACQUISITION DEVICE

cleaning to NASA/MSFC Spec 164 and an acceptance bubble test, at which time approximately five small areas were sealed with the polyurethane adhesive to halt premature bubble breakthrough. The final bubble-point test was performed with isopropyl alcohol (68°F, σ = 21.8 dynes/cm, ρ = 0.785 g/cc). The bubble point pressure was approximately 14 inches of water column, whereas an immediate and total loss of retention did not occur until 16 inches water column. The cone screen device, used for feedline vapor control (see Test T), met a bubble-point pressure of 3.2 inches of water column, with isopropyl alcohol (68°F, σ = 21.8 dynes/cm, ρ = 0.785 g/cc).

Figure 2-4 shows the interior of the LHAD in an inverted position relative to its installation in the IDU. The protective layer of bolting cloth used on the outer layer of the LHAD is shown, as well as ports provided on both the top and bottom circular channels for instrumentation. A 3/4-inch AN plug (screen fitting) drilled through and covered with 250 x 1370 SS screen, (not shown), is located to facilitate refill of the LHAD following breakdown. This screen fitting was bubble-point tested.* A teflon plug was used in the top of the control pipe to eliminate ullage space and minimize heat transfer from the ullage space to temperature probe T4.

Figure 2-5 shows the tube routing during the early stages of assembly. The lines on the left are for pneumatic operation of the Parker Submerged LH_2 Ball Valves. Figure 2-6 shows the initial installation of the IDU internal hardware prior to the placement of the LHAD. The overhead diffuser is removed before positioning of the LHAD, but is shown in place for completeness. The submerged helium pressurization diffuser has 40 equally-spaced 1/8-inch holes underneath. Placing the holes underneath assures that no liquid remains entrapped in the diffuser. The NASA GFP continuous capacitance-level sensor is shown. The cylindrical baffle guards against direct impingement of two-phase, high-velocity flow against the screen. Installation of the LHAD and much of the instrumentation is shown in Figure 2-7. The NASA GFP capacitance point-level sensors are shown; two are mounted on the central pipe; the top capacitance-level sensor is mounted on the pressure sensing line. Backup carbon point-level sensors are shown. Punch marks were placed on the LHAD, refill baffle, and plate to assist in proper alignment for subsequent reassembly.

* Bubble point achieved was 22.4 inches of water column, using denatured ethyl alcohol (DPM 514) at 63.5°F, with σ = 22.6 dynes/cm.

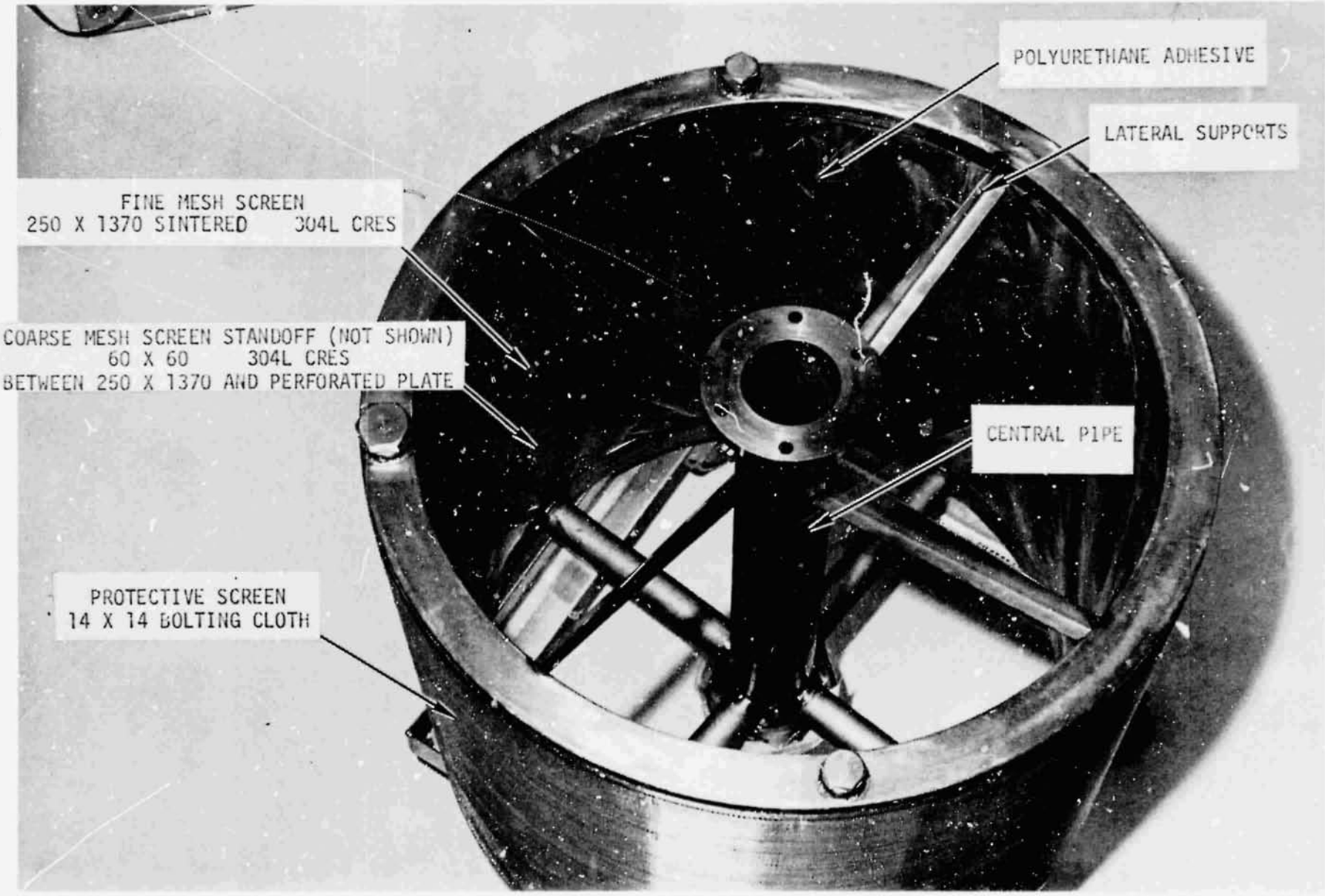

Figure 2-4 LIQUID HYDROGEN ACQUISITION DEVICE

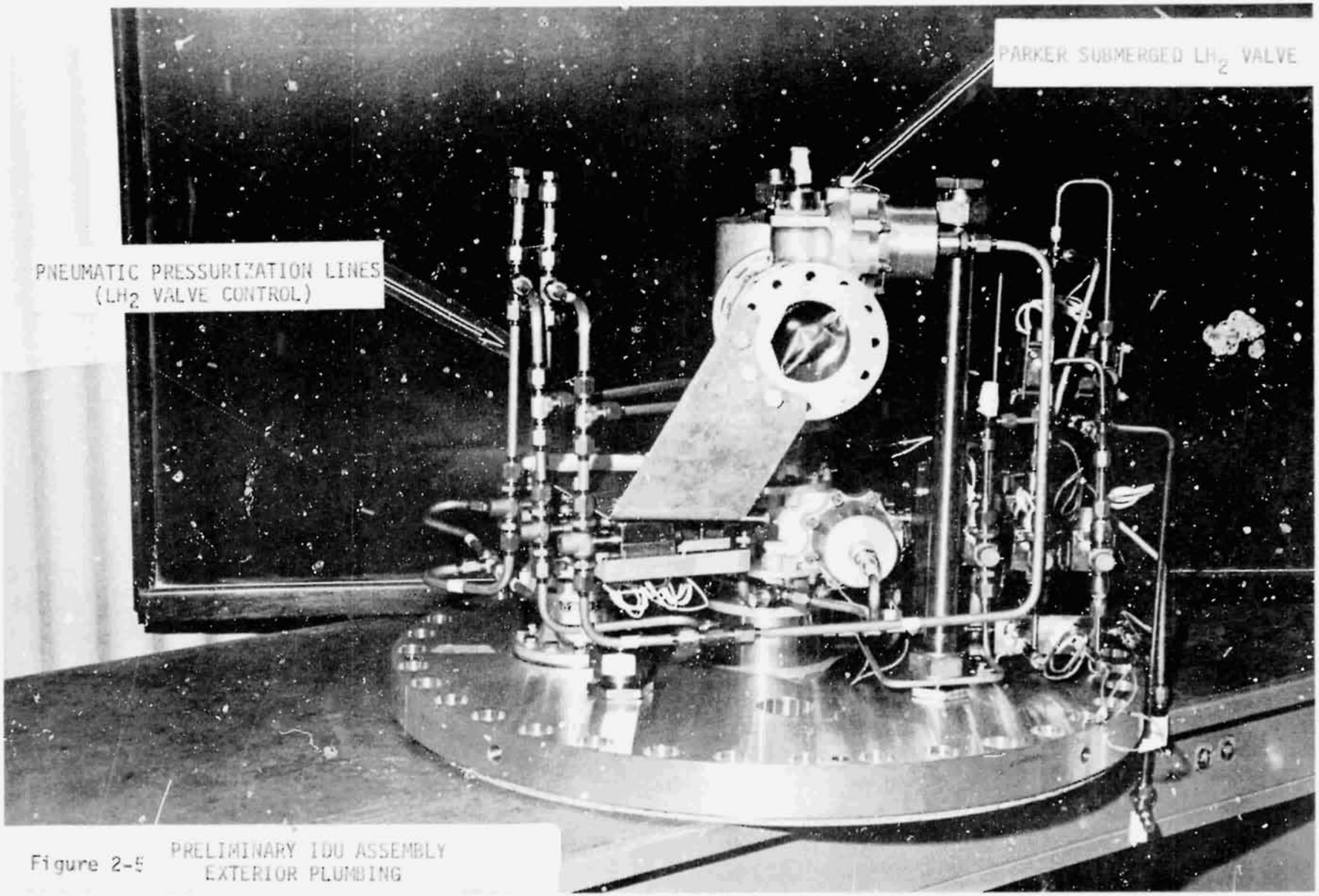

Figure 2-5 PRELIMINARY IDU ASSEMBLY
EXTERIOR PLUMBING

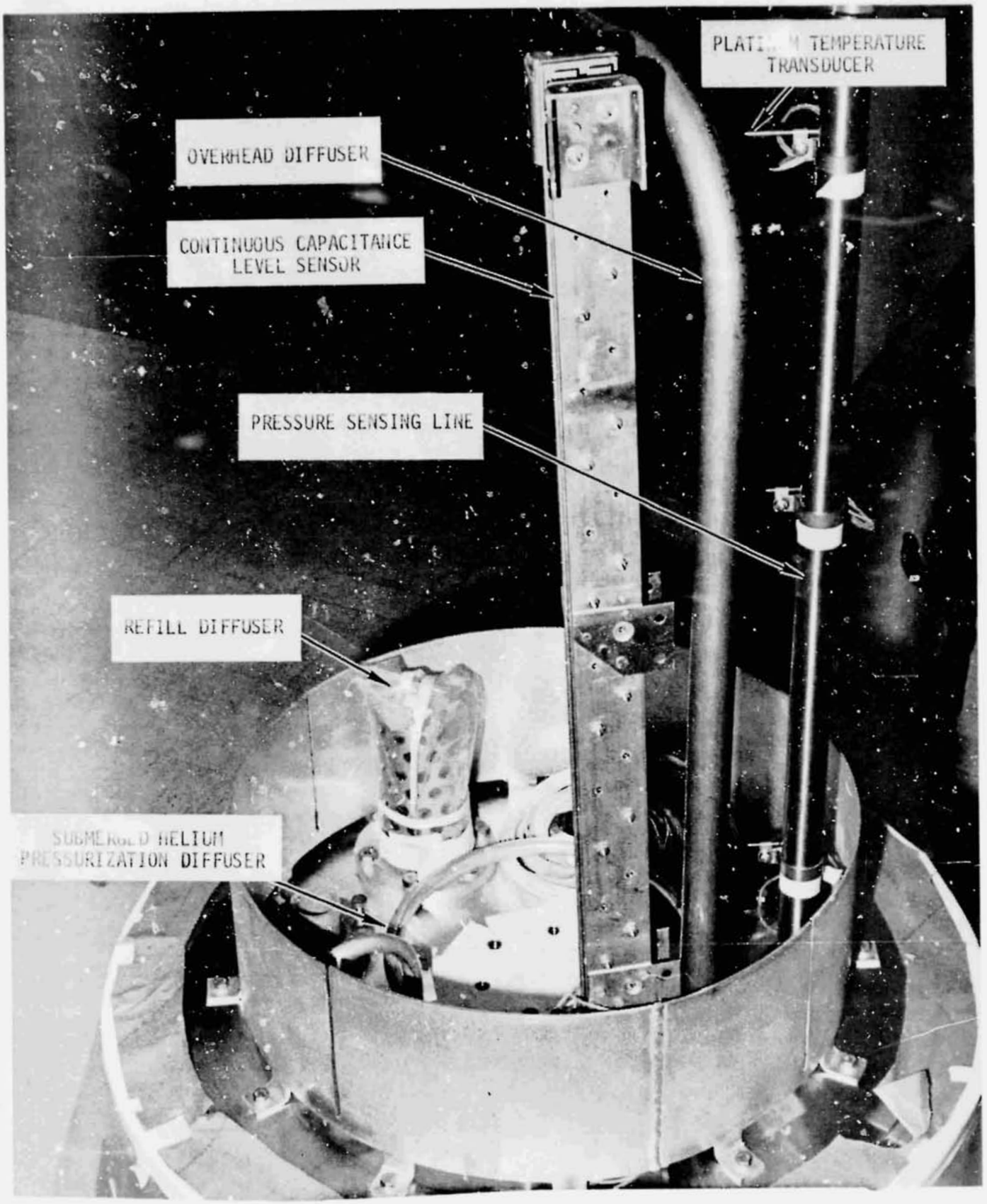

Figure 2-6 PRELIMINARY TDU ASSEMBLY-INTERIOR

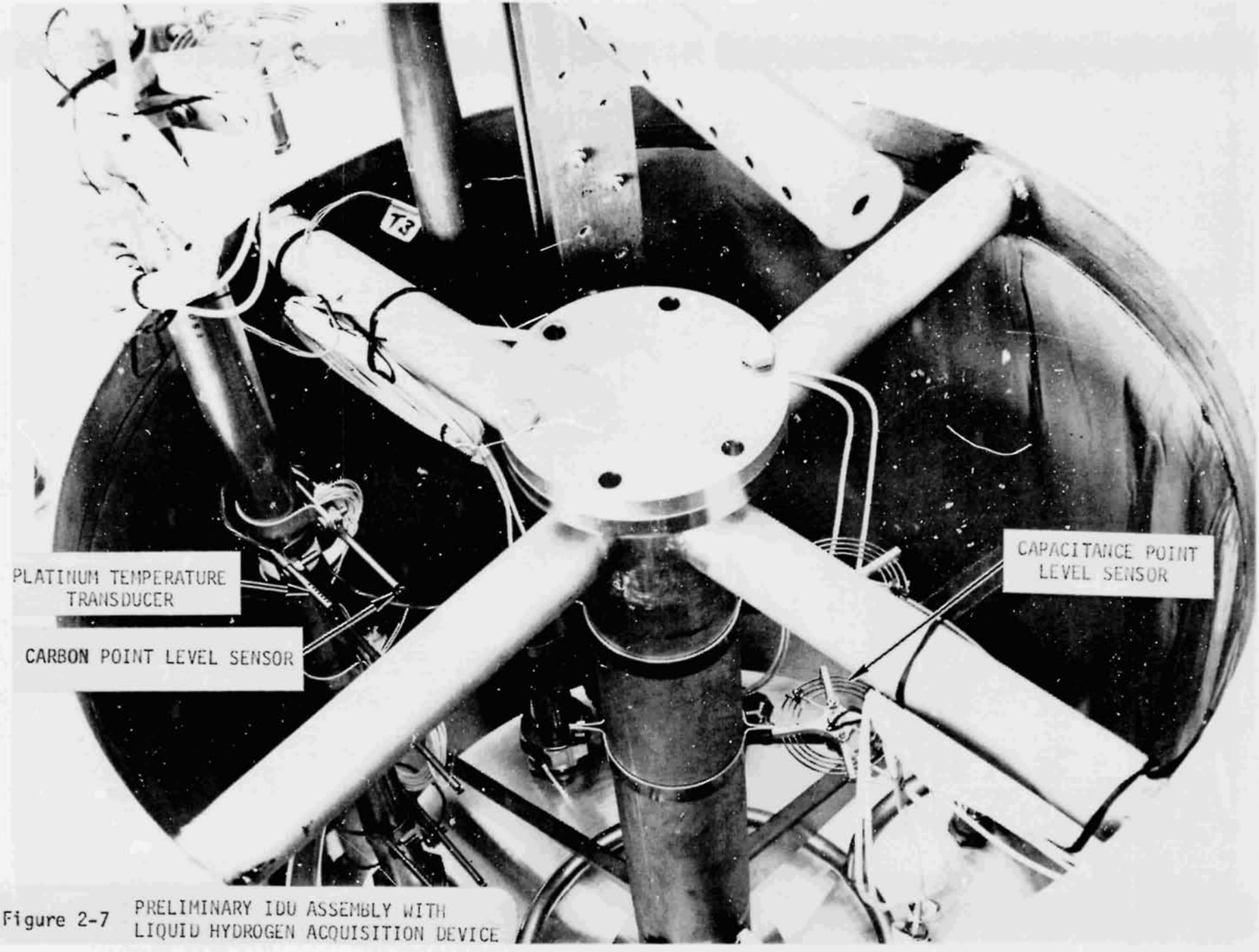

Figure 2-7 PRELIMINARY IDU ASSEMBLY WITH LIQUID HYDROGEN ACQUISITION DEVICE

Figure 2-8 shows the IDU before installation of the tank cover. Figure 2-9 shows various operatio , involved in tank closure. The top left-hand photograph shows the IDU ready for installation of the cover. The top right-hand photograph shows the cover suspended by a crane. The test engineer is shown installing guide rods which position the cover as it is lowered onto the IDU plate. The lower left-hand photograph shows the lowering of the cover onto the plate. The lower right-hand photograph shows the installation of the Indium tin seal.

Figure 2-10 shows the instrumentation wiring and heat flux gauges (4-inch by 4-inch area) mounted on the inside of the cover. Immediately before the lowering of the cover, an electrical technician connects the instrumentation wires from the heat-flux gauges to the wires passing out through the electrical feedthrough mounted on the IDU plate. All other instrumentation wires were previously connected to the feedthroughs. The cover is then lowered and bolted.

The IDU refill diffuser (1T42470) was tested on 2/1/73 to evaluate its effectiveness, prior to assembly. Water was used, with the setup shown in Figure 2-11. The test was run so that the degree of splashing could be observed over the range of fill depths. The maximum flowrate obtainable was 0.272 ft^3/sec. Figure 2-11 shows the diffuser installed upside down. Since the diffuser did not fill and allowed the water to flow out at approximately one half the height of the diffuser, the diffuser was only half as effective as it would have been in the proper orientation. This orientation appears to have maximized the degree of splashing, although the water flowrate was limited by the supply. Dynamic similarity conditions were only approximately achieved.

The degree of splashing and disruption of the interface should be governed predominantly by the Froude number, $Fr = V^2/2g$. With the IDU filled at the maximum LH_2 inflow rate (0.5 ft^3/sec), the Froude number is 0.38, assuming the entire refill diffuser hole area (96 hole, 1/2-inch diameter) is effectively diffusing the flow. The Froude number for the water test was 0.266. Consequently, the LH_2 inflow should be similar to that of the water test, even though the Froude numbers for the LH_2 and water are not equal.

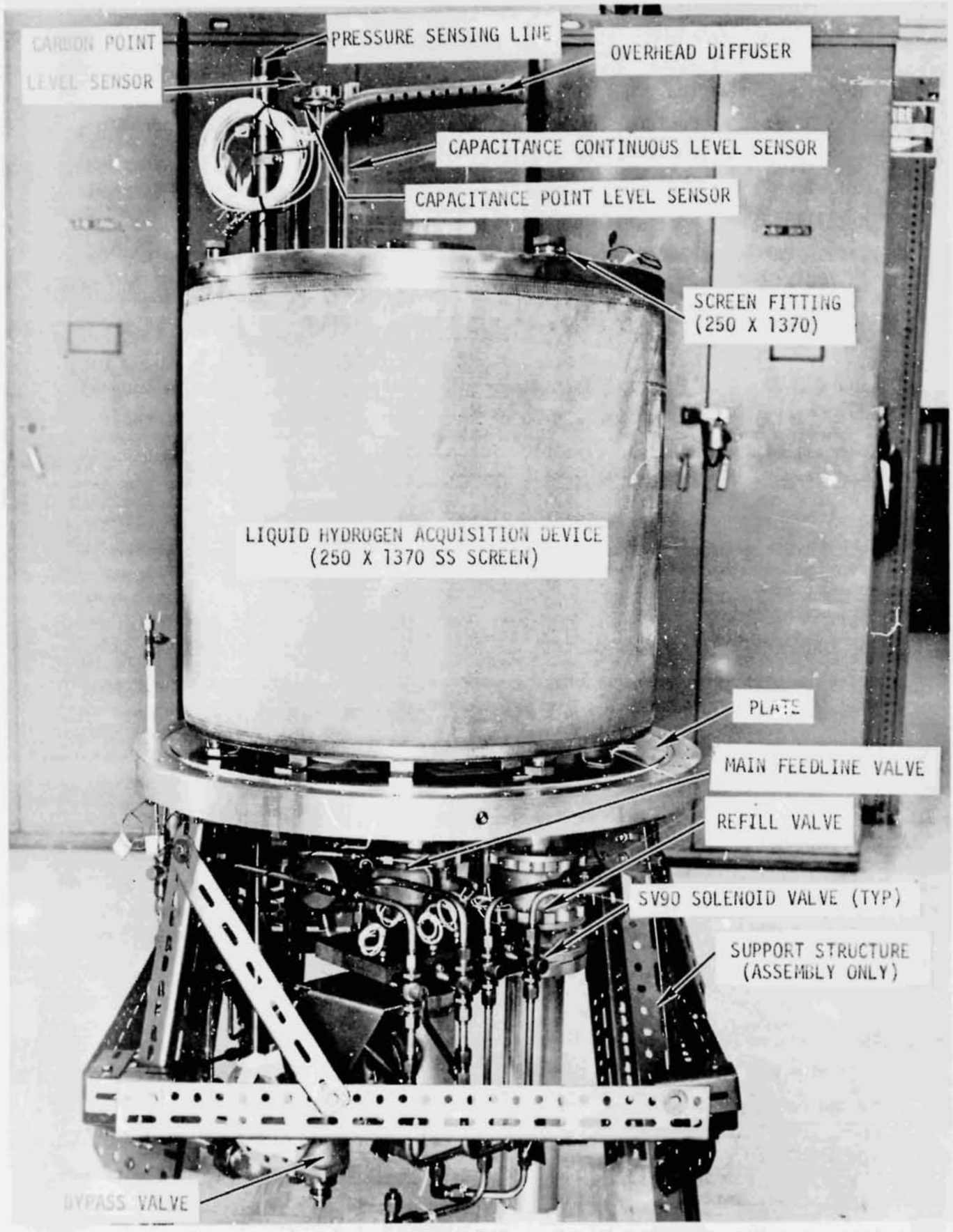

Figure 2-8 COMPLETED JDU PRIOR TO CLOSURE

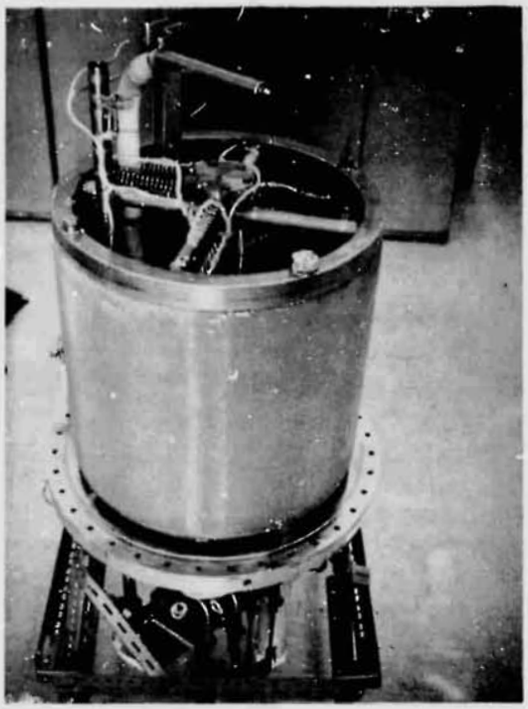

IDU PRIOR TO CLOSURE

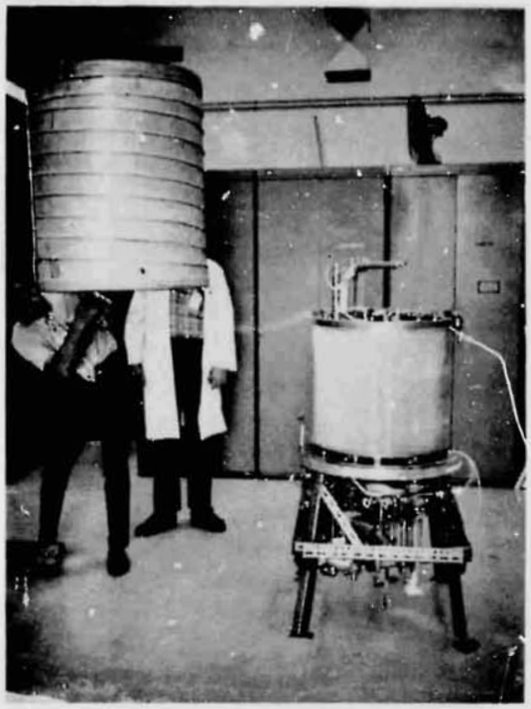

INSTALLATION OF GUIDE RODS

POSITIONING OF COVER

INSTALLATION OF INDIUM TIN SEAL

Figure 2-9 ASSEMBLY OF INTERFACE DEMONSTRATION UNIT

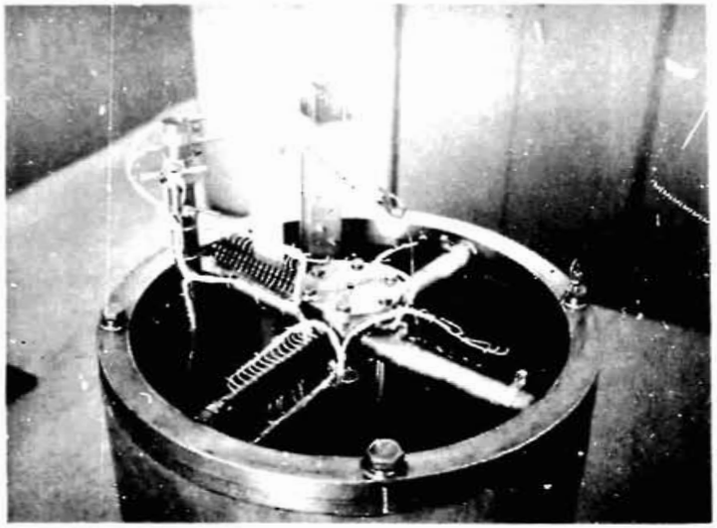

VIEW OF INSTRUMENTATION WIRING

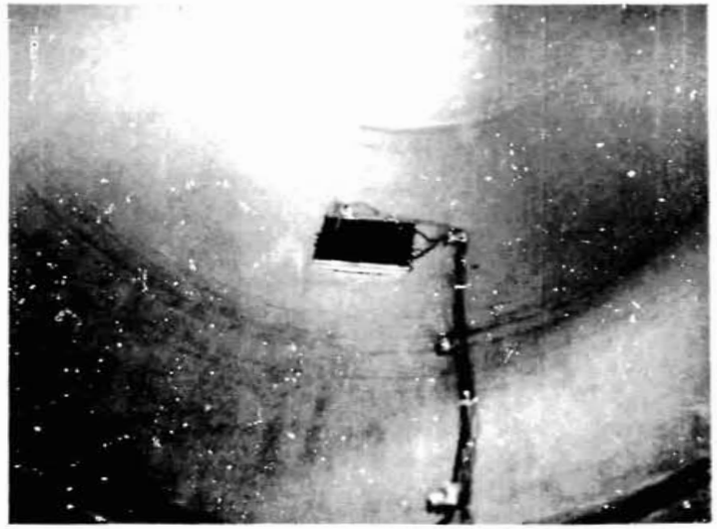

HEAT FLUX GAUGE (HF2) AND TEMPERATURE SENSOR

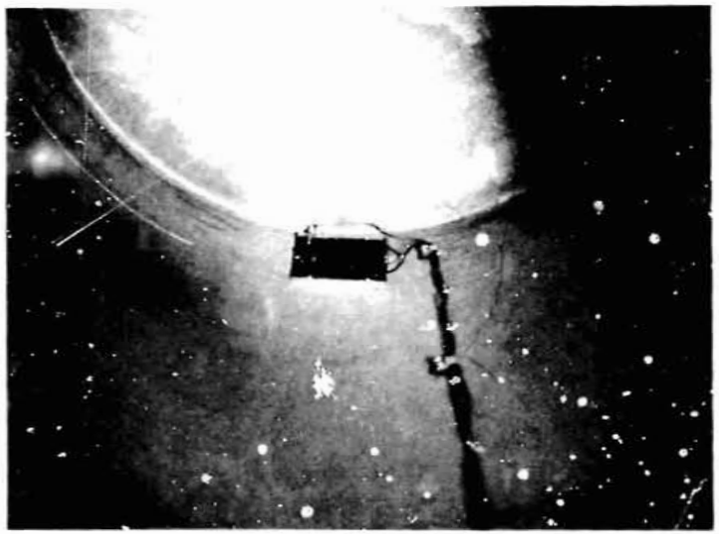

HEAT FLUX GAUGE (HF3) AND TEMPERATURE SENSOR

FINAL INTERIOR WIRING CONNECTION

Figure 2-10 IDU INTERIOR INSTRUMENTATION

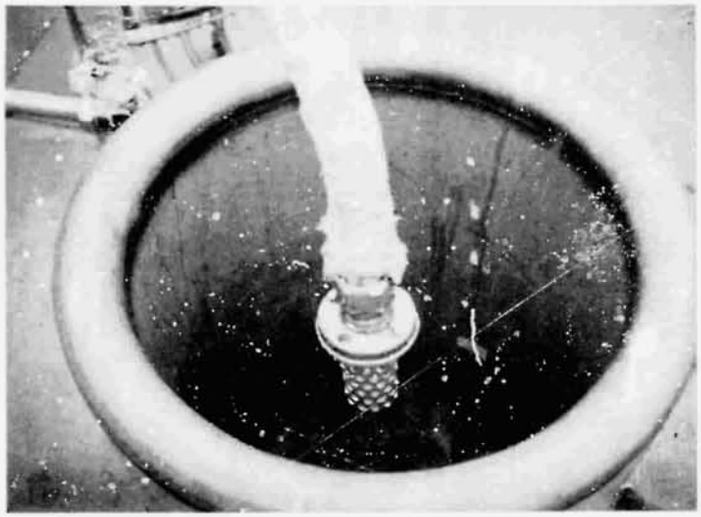

SET UP

MAXIMUM SPRAY

DIFFUSER PARTIALLY COVERED

SPRAY PRIOR TO QUIESCENCE

Figure 2-11 REFILL DIFFUSER WATER TEST

A principal observation of the test was that when the liquid level reaches the diffuser, the degree of splashing and surface disruption is greatly attenuated. When the diffuser was completely covered, there were only insignificant ripples on the surface. Since the IDU normally operates with the refill diffuser submerged, it was concluded that the diffuser design is satisfactory.

2.2.2 Thermodynamic Vent System (TVS) Assembly

The TVS coil is a 70 ft length of 1/4-inch outside diameter tubing wound in parallel helical paths along the cylindrical tank wall, with a spacing between tubes of 3.5 inches. The tubing was attached to the wall by supporting clips, spot welded to the wall, and then the tube was dip brazed. The supporting clips were spaced approximately 10 inches apart along the length of the tube to secure the tube during the dip braze operation. However, thermal expansion caused the tube to separate from the wall in certain areas, and portions of the tube were not brazed to the wall. These areas, ranging in length from 1 to 10 inches for a total length of approximately 10 feet out of 70 ft were filled with Wakefield Delta Bond which is a thermally conducting epoxy, and therefore, good thermal contact is maintained along the length of the tube.

The TVS was originally configured so that liquid would enter at the bottom, flow upwards through 35 ft of tubing, and then return via the remaining 35 ft to exit at the bottom.

However, calculations of the two-phase pressure drops for the maximum expected flowrate (5 lb/hr) indicated that for the 70 ft length path, the pressure drop could be as high as 12 to 15 psid. Moreover, there was some question regarding flow separation effects for the fluid flowing uphill through the 0.25 inch outside diameter TVS tube for the first 35 ft. By a slight modification of the routing, the inlet flow was brought directly up to the top of the IDU, where the flow splits and runs down in parallel paths. The running length is, therefore, 35 ft, rather than 70, and the maximum flowrate in each tube is 2.5 lb/hr; the maximum pressure drop is, therefore, reduced by a factor of eight, since pressure drop is directly proportional to length and proportional to the square of the mass flowrate.

Portions of the TVS line leading up to the TVS heat exchanger coil are not brazed to the IDU wall. These lengths were insulated with teflon tape to reduce extraneous heat transfer to the coolant fluid. However, this insulation is not a substitute for the foam insulation necessary to maximize the operating efficiency of the IDU/TVS, but is used to allow reasonable data to be obtained of the IDU/TVS operated under conditions of maximum heat flux.

2.2.3 Instrumentation

All instrumentation wiring in the IDU was checked to verify continuity. The heat-flux gauges were tested with an imposed heat flux to verify polarity and proper operation. The thermocouples were tested to verify operation. No problems were encountered.

2.3 INSTALLATION

The IDU is shown in Figure 2-12 immediately before installation in the 260-gallon tank. Figure 2-13 shows the tank suspended from the BEMCO vacuum chamber lid. Figure 2-14 shows the tank, wrapped with high performance insulation, immediately before installation in the BEMCO.

2.4 TEST HARDWARE LAYOUT, PLUMBING, AND INSTRUMENTATION

The schematic drawing of the IDU/TVS layout in the MDAC test facility is shown in Figure 2-15. The layout includes the IDU and associated plumbing and instrumentation. A heat exchanger composed of 130 ft of 1/2-inch outside diameter tubing is included in the IDU pressurization line for use when cold (40°R) pressurant is required. The TVS viscojet arrangement is shown. Both GH_2 and GHe pressurization can be supplied directly from storage tanks, and where necessary, a 1.5 ft^3 pressure bottle can be used so that the approximate gas inflow rate can be determined by measurement of the initial and final pressure and temperature of the bottle. The mass flowrate measurement system, consisting of two hot-wire anemometer devices, is included. IDU/TVS and facility fill, drain, vent, evacuation, and purge components are shown. A schematic of the cold traps added to the system to prevent any contaminants in the helium from reaching the 2 inch ball valves is shown in Figure 2-16.

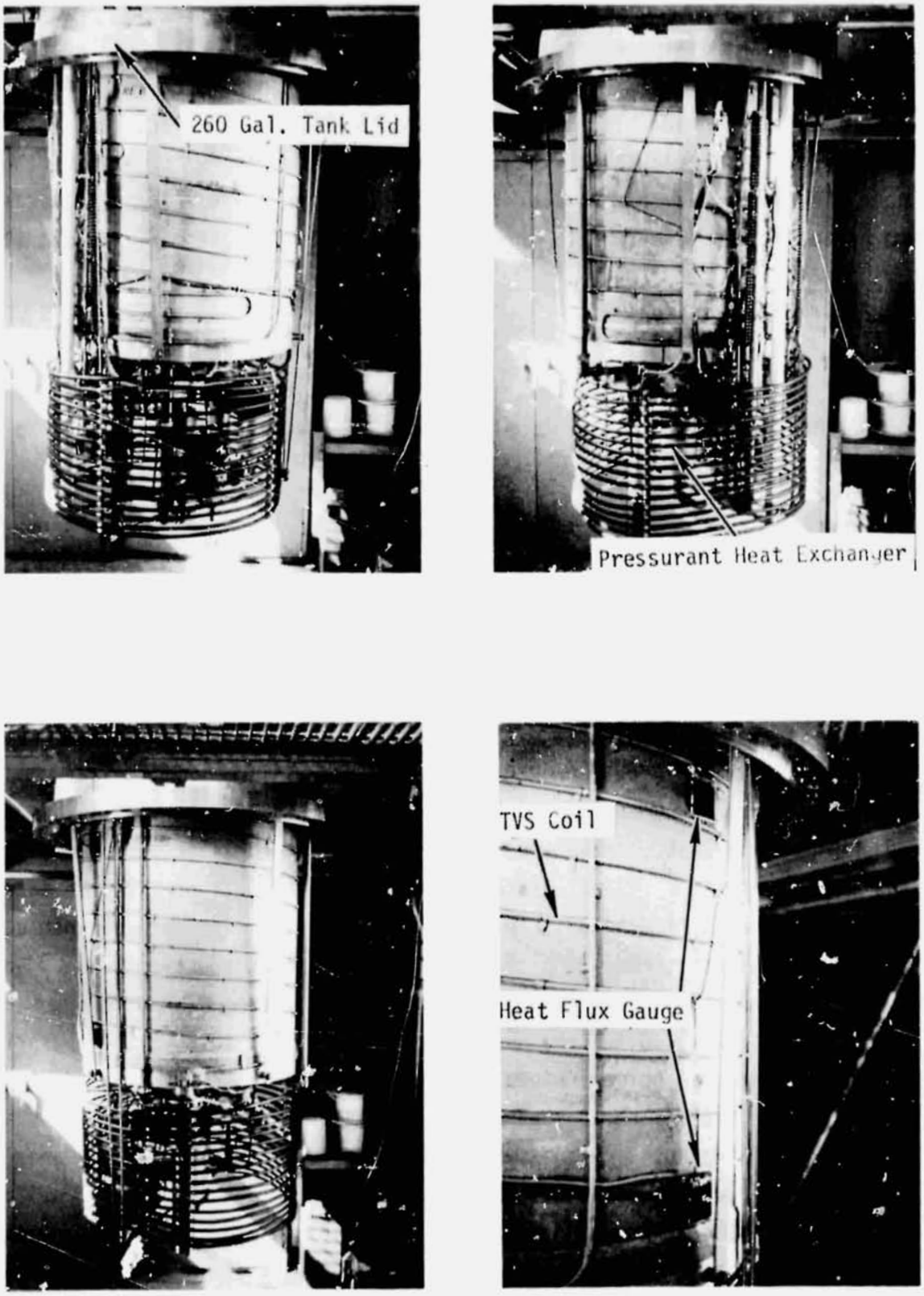

Figure 2-12 Views of IDU Prior to Installation in 260 Gallon Tank

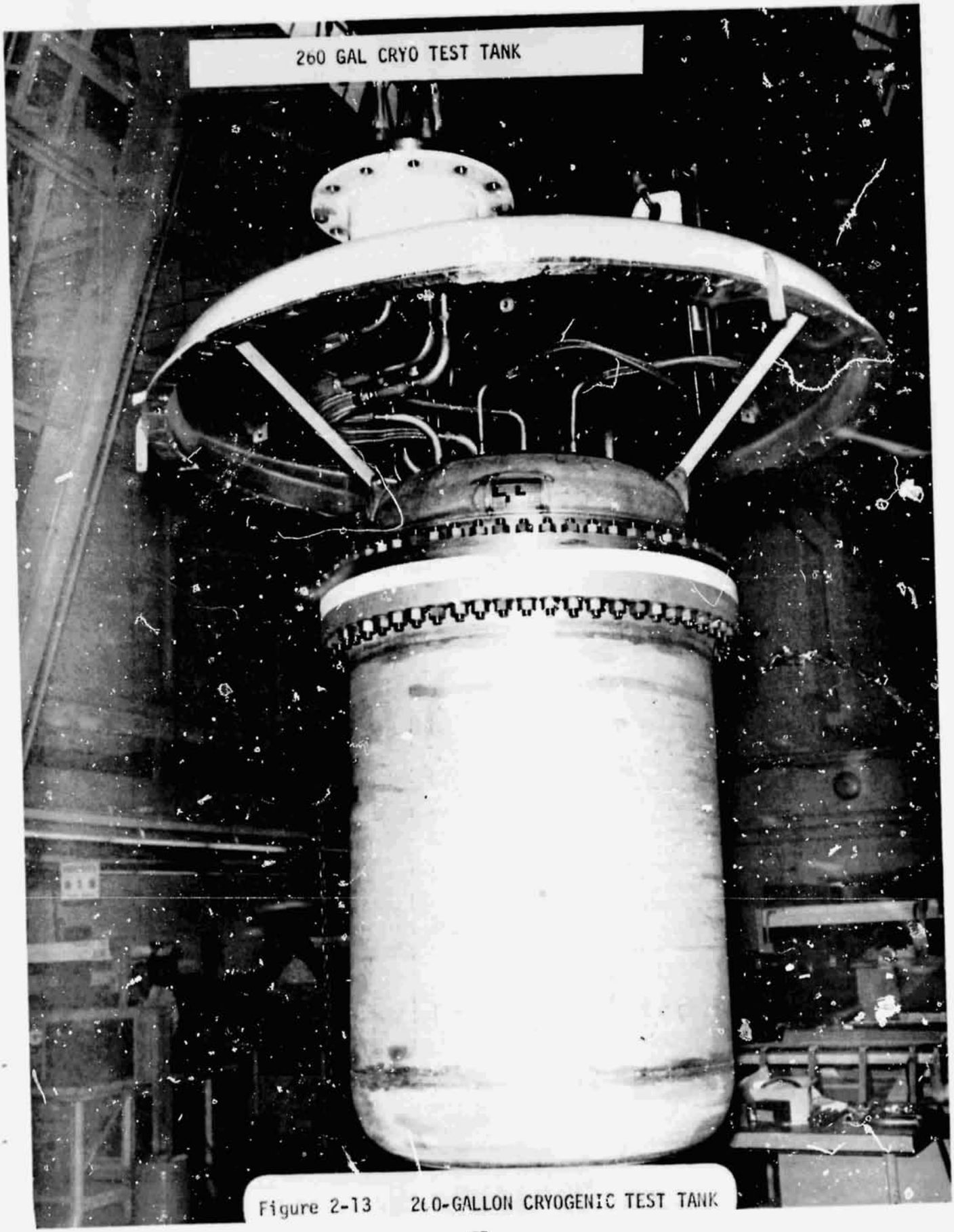

Figure 2-13 260-GALLON CRYOGENIC TEST TANK

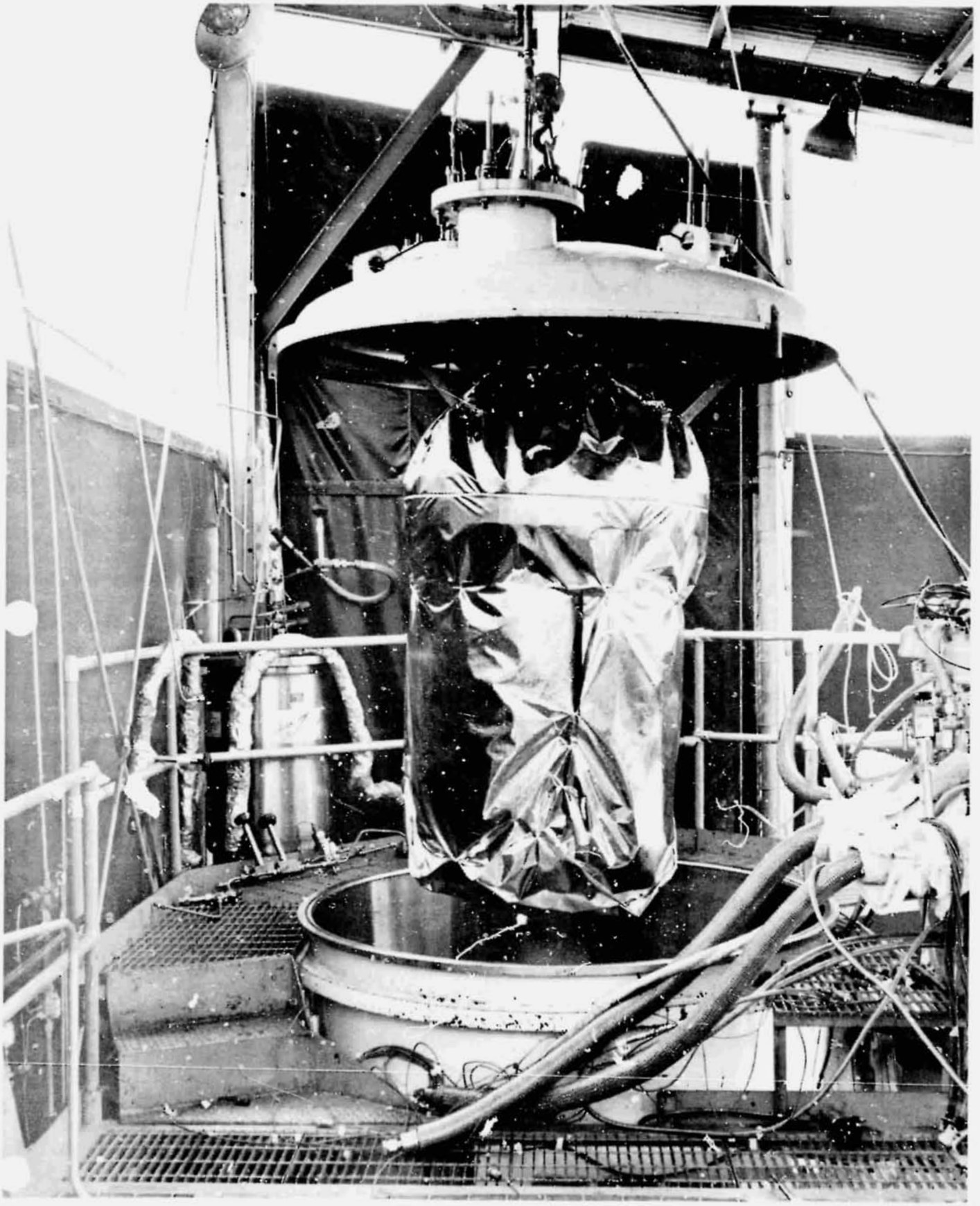

Figure 2-14 INSTALLATION OF INSULATED TEST TANK IN BEMCO

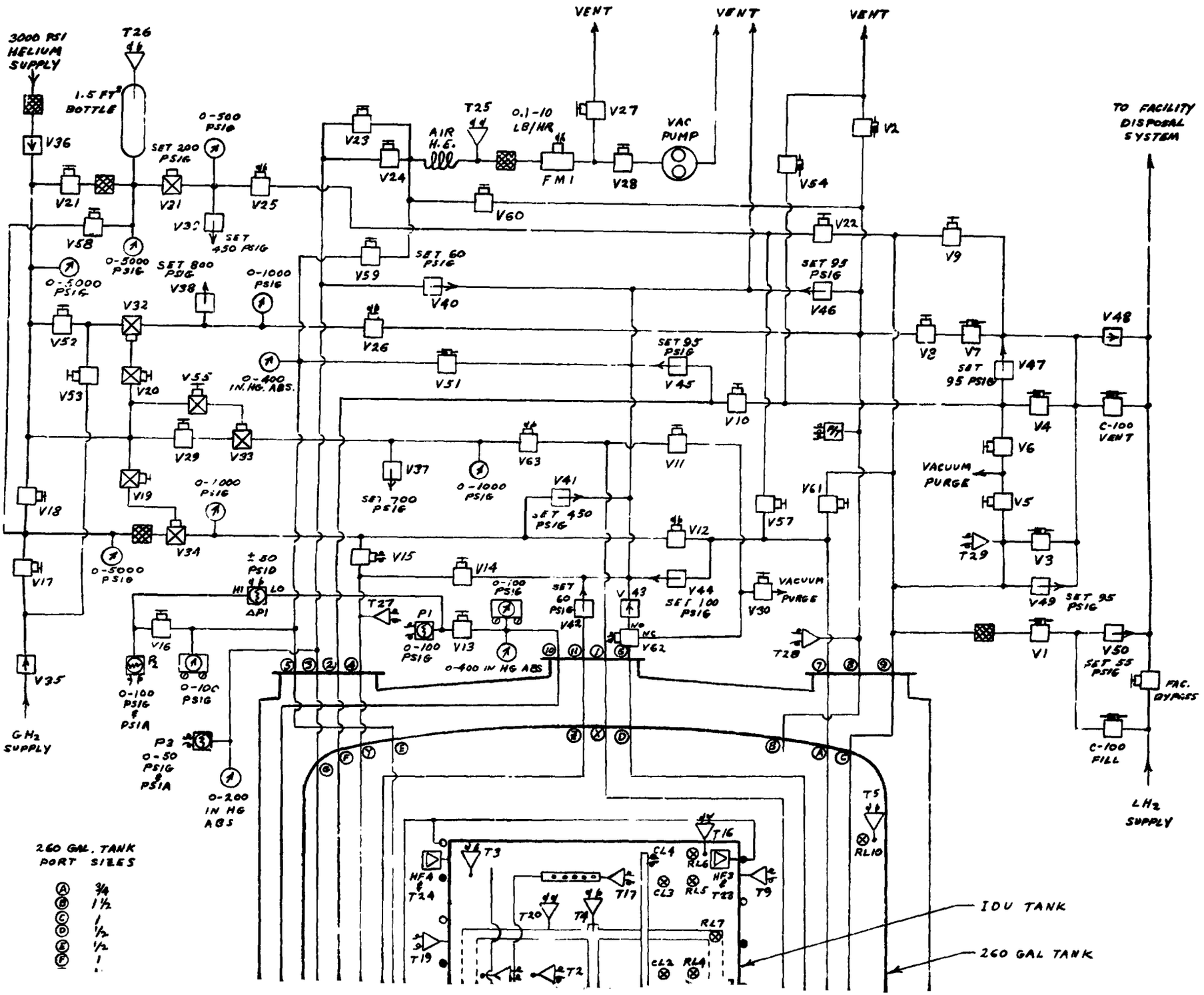

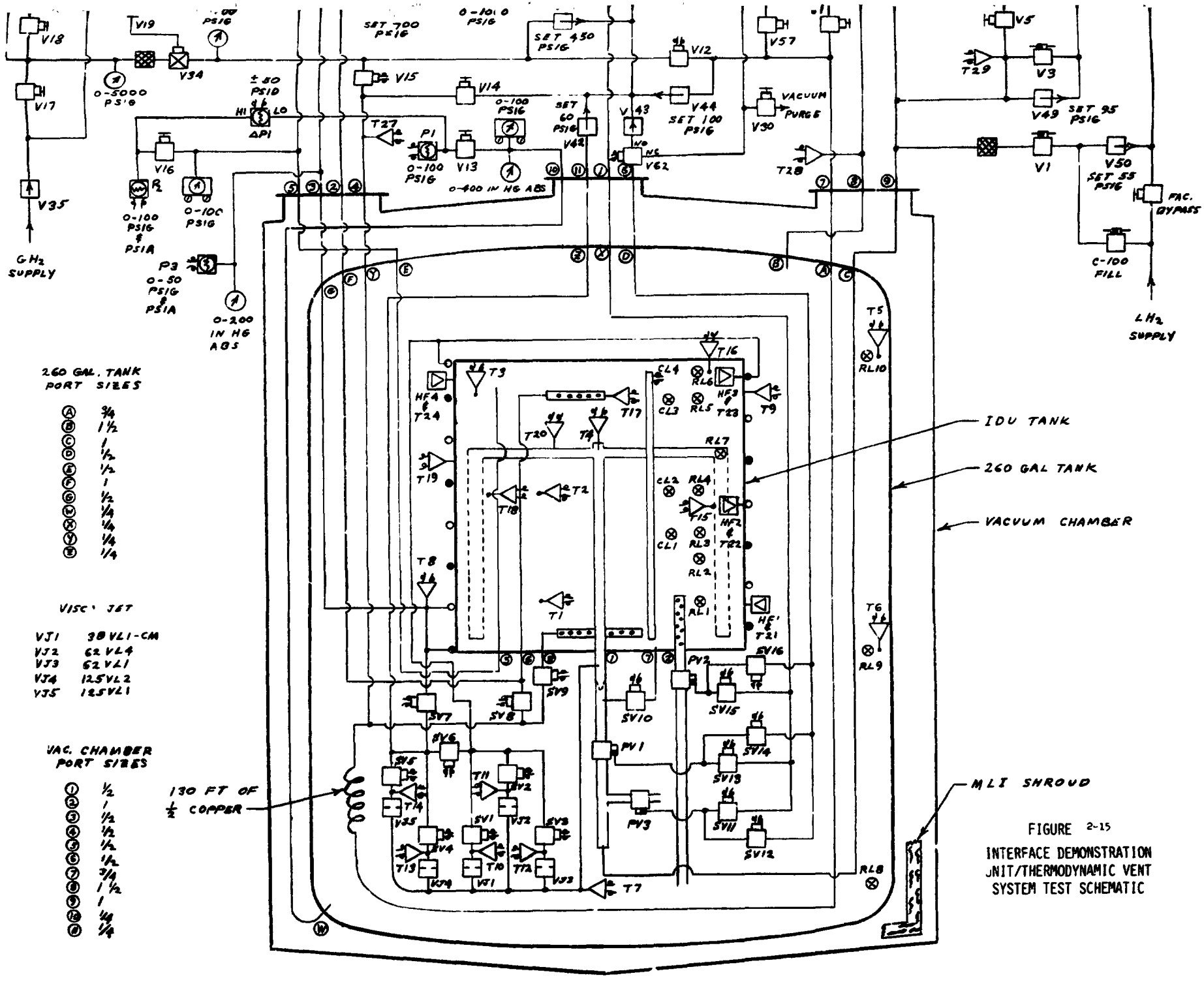

FIGURE 2-15
INTERFACE DEMONSTRATION UNIT/THERMODYNAMIC VENT SYSTEM TEST SCHEMATIC

FOLDOUT FRAME 2

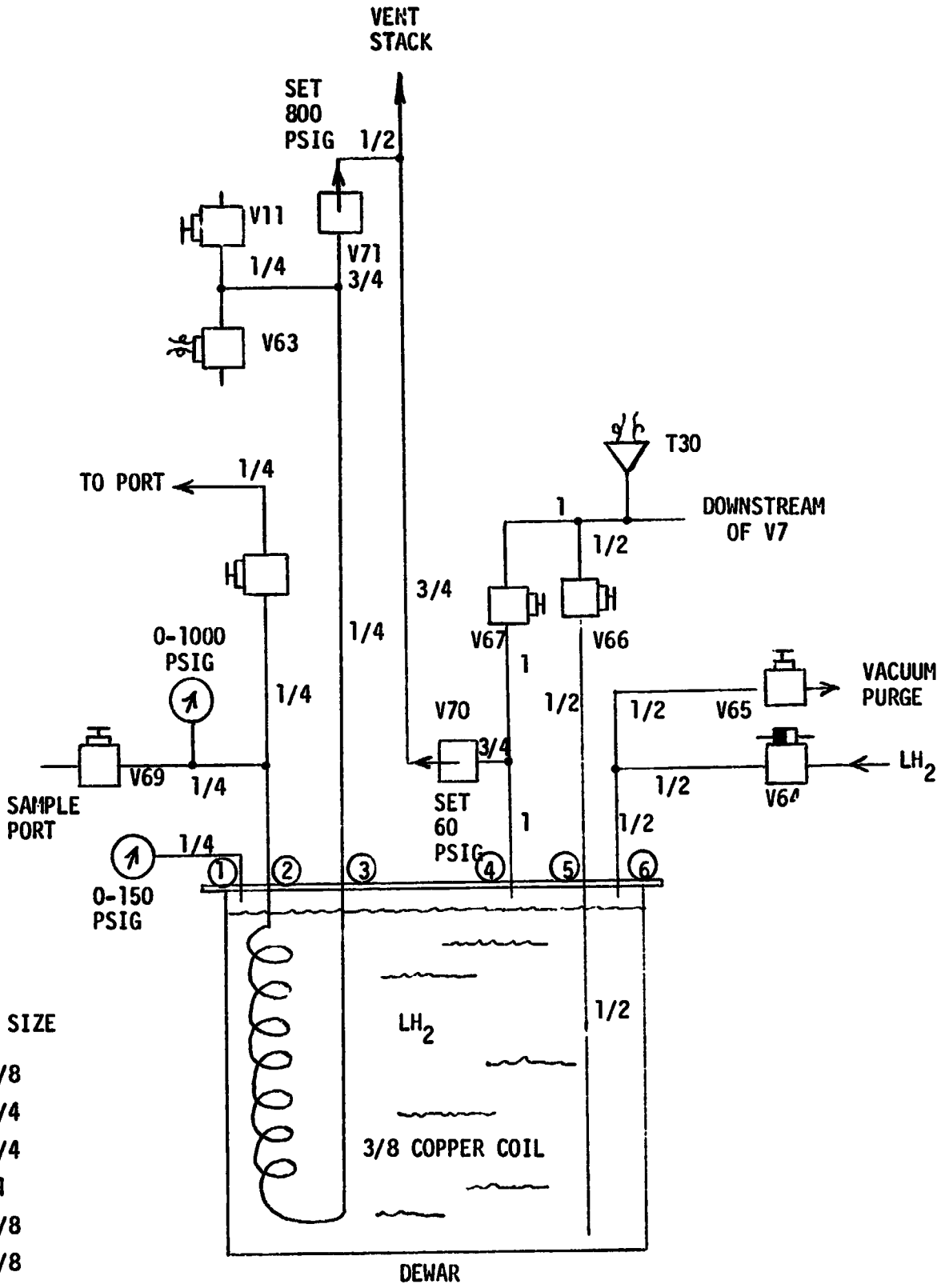

PORT	NPT SIZE
1	1/8
2	1/4
3	1/4
4	1
5	3/8
6	3/8

Figure 2-16 COLD TRAP SCHEMATIC

Section 3
ANALYSIS

The principle analyses performed for this study are presented in this section. An analysis of the IDU wall-mounted thermodynamic vent system (TVS) was performed and a computer program written and documented. An analysis was performed of the transient pressure, temperature, and heat transfer response of the IDU, with internal hardware, to warm GH_2 pressurization. The computer program used (H431) was a modified version of that in use at MDAC for several years. The analysis and computer code used in sizing the IDU screen device are presented.

3.1 ANALYSIS OF THE IDU WALL-MOUNTED THERMODYNAMIC VENT SYSTEM

3.1.1 Objectives

A TVS with a wall-mounted heat exchanger was incorporated in the IDU design to demonstrate the operation and control of this type of TVS. The specific objectives were to demonstrate (1) both steady-state and transient operation of the TVS, (2) control and predictability of the vented flowrate, (3) that the TVS could provide coolant flow for additional hardware such as feedlines and turbopumps, and (4) the fabricability of the wall-mounted heat exchanger subsystem.

To meet these objectives, the TVS was configured with a number of flow-control orifices (Viscojets®) in parallel, which gave a vent flowrate variable from 0.2 to 5 lb/hr. Bypass flow was also provided for turbopump or feedline cooling. The TVS heat exchanger coils on the IDU were configured to provide a number of alternate flow paths (as shown in Figure 2-15). Successful heat interception operation of the TVS required that the wall-mounted heat exchanger be insulated from the main tank fluid (to prevent condensation and loss of cooling capacity). However, funds were not available to provide the insulation,

and therefore, the performance tests of the TVS were made without insulation to determine flowrate as a function of applied pressure, and to verify flowrate control. Heat transfer/cooling tests showed that insulation would be required.

3.1.2 Operation

The theory of operation of the TVS has been discussed in the literature (References 6 to 10) and is straightforward. The process is shown in Figure 3-1. The vented liquid is expanded isenthalpically to a lower pressure and temperature (A to B) and becomes a two-phase fluid at a temperature below that of the tanked fluid. This two-phase mixture flows through a heat exchanger at an approximately constant pressure where it boils by absorbing heat from the warmer fluid in the IDU, and/or by intercepting heat from outside the IDU (B to C). Under steady-state conditions, a "design flowrate" will be just adequate to absorb all the heat entering the system, so that the vented fluid is completely boiled and exits the system as vapor. Additional heat transfer can increase the vapor temperature to equal or exceed the tanked liquid temperature, (C to D), which is equivalent to oriented vapor phase venting. This vented cold vapor can also be used to provide cooling of additional hardware, such as feedlines and turbopumps.

In addition to performance characterization during steady-state operation, the transient performance of the TVS, while achieving steady state from system start, was evaluated. The thermal performance of the TVS depends on convective/conductive heat transfer from the IDU fluid to the IDU tank wall, conduction along the tank wall to the heat exchanger tubing, and convection/boiling heat transfer inside the tube. Analysis of these heat transfer processes was necessary to evaluate the TVS performance.

3.1.3 TVS Analysis

The analysis of the wall-mounted TVS is presented in Appendix A for the case of a uniform heat-transfer coefficient between the heat-exchanger fluid and the inner TVS tube wall. Appendix B is an extension of this analysis which allows for the two heat-transfer coefficients encountered along the tube. In

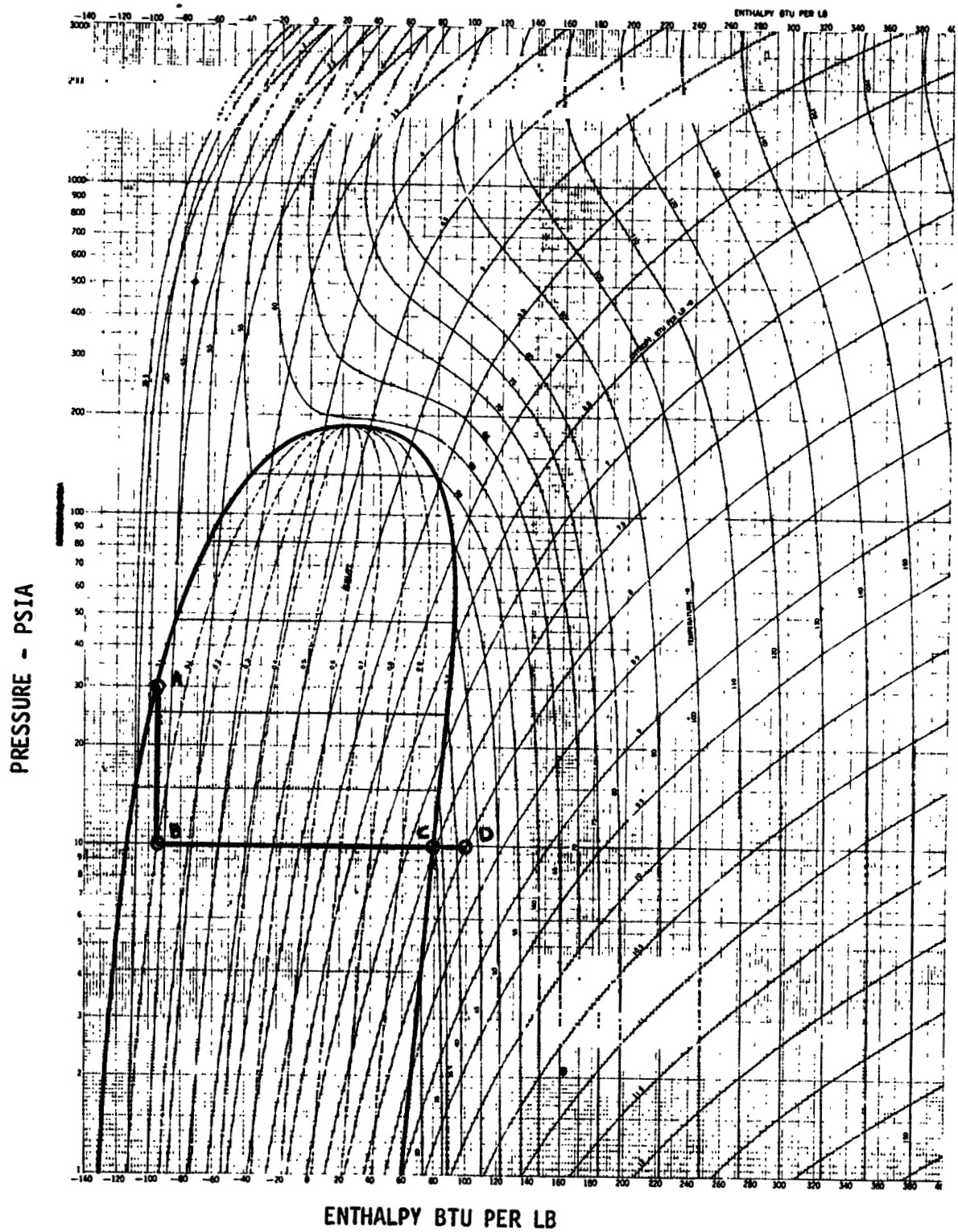

Figure 3-1 HYDROGEN PRESSURE - ENTHALPY DIAGRAM

the initial region, the heat-transfer mechanism is governed by annular flow with forced convection heat transfer and boiling in the liquid film and the Chen correlation is assumed for the heat transfer coefficients. At a critical quality, X_C, the heat transfer mechanism is transformed to forced convection of a two-phase "mist" flow. This second region is termed the liquid deficient regime.

The Dittus-Boelter heat transfer coefficient is used in this regime. Details of the heat transfer coefficients are given in Appendix C.

The principal unknown in the TVS analysis is the fluid quality at which transition from annular flow to liquid deficient flow occurs. Various reference data indicated that $X_{Critical}$ is of the order of 0.85 for hydrogen in 0.25-inch tubes and, therefore, this value is assumed. The IDU/TVS program was used to generate the required coolant flowrate for an uninsulated tank as a function of $X_{Critical}$, all other parameters being identical, and the results shown in Figure 3-2. It is seen that the total flowrate varies from 5.4 to 6.2 lb/hr for $X_{Critical}$ varying from 0.7 to 0.9, and therefore, the variation of

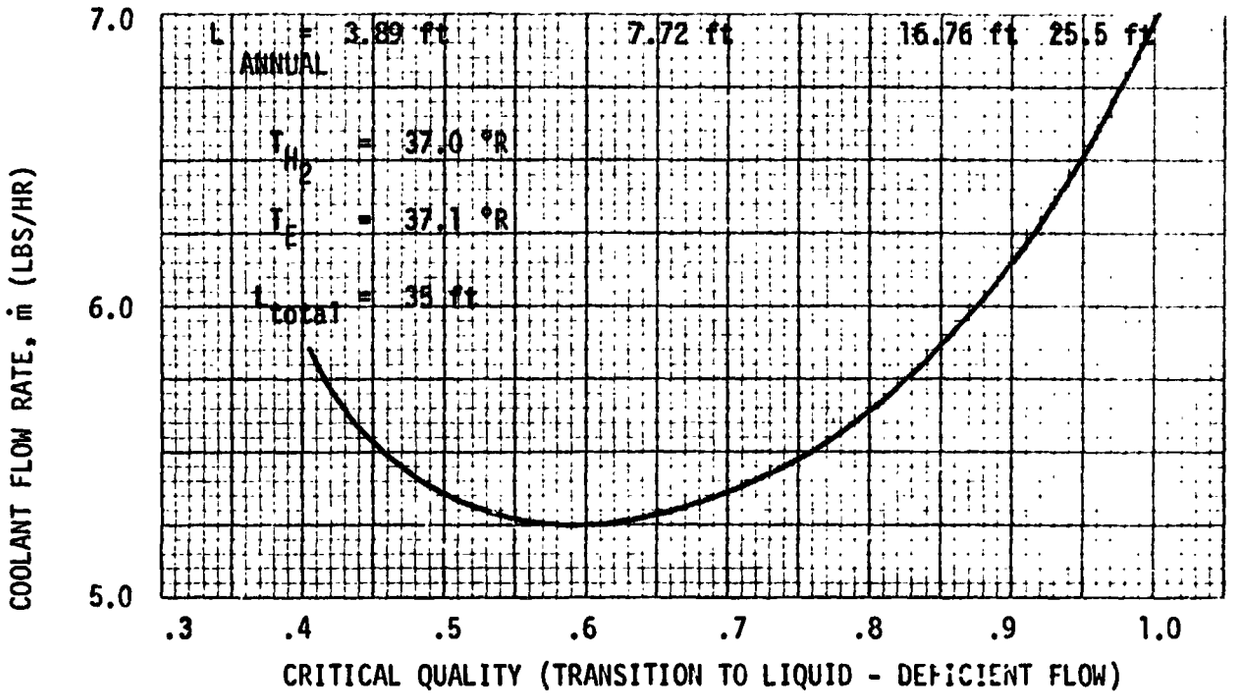

FIGURE 3-2. COOLANT FLOW RATE DEPENDENCE ON CRITICAL QUALITY, X

$X_{Critical}$ will not have a great effect on the coolant flowrate. However, there is a significant variation in the lengths of the annular and liquid deficient region. For example, at $X_C = 0.65$, the annular region is 7.72 ft (out of a total tube length of 35 ft) whereas, for $X_C = 0.85$, the annular region is 16.16 ft out of 35 ft. As a result, when the IDU is partially filled, the decreased heat transfer in the gaseous ullage region, coupled with a low critical quality, will lower the effective overall cooling capability of the TVS. This can occur in its present configuration, since the annular flow (high internal heat transfer coefficient) will occur in the upper part of the tank where the wall heat-transfer coefficient is decreased due to vapor. In addition, heat entering through the bottom portion of the tank, which is convected to the liquid interface, would not be removed efficiently if the TVS in that region has liquid deficient flow.

Two test conditions are analyzed using the IDU/TVS program. The first case corresponds to the IDU surrounded by GH_2 at a pressure greater than the saturation pressure of the IDU LH_2. The IDU is not insulated, and therefore, condensation occurs. The required coolant flowrate for two IDU LH_2 saturation pressures is plotted in Figure 3-3. Details of the results are given in Table 3-1. The second case is for free convection heat transfer from warm GH_2, surrounding the outer IDU wall. The coolant flowrate required to maintain the IDU liquid at a constant temperature is shown in Figure 3-4, and tabulated results are given in Table 3-2. Insulation conditions are shown for comparison.

Although the flowrates required of the TVS are of the order of 4 lb/hr, the system is capable of flowrates of the order of 10 lb/hr with a pressure drop of approximately 2 psi in the TVS line. However, the corresponding pressure drop through the viscojets would be approximately 70 psi. Details of the pressure drop versus mass flowrate are given in Appendix D.

Appendix E describes the computer code, and the listing is given in Appendix F.

Complete results generated by the IDU/TVS computer program are given in Appendix G for the IDU insulated with 0.25-inch and 0.5-inch of Saturn S-IVB type foam. These results are included so that comparisons can be made between

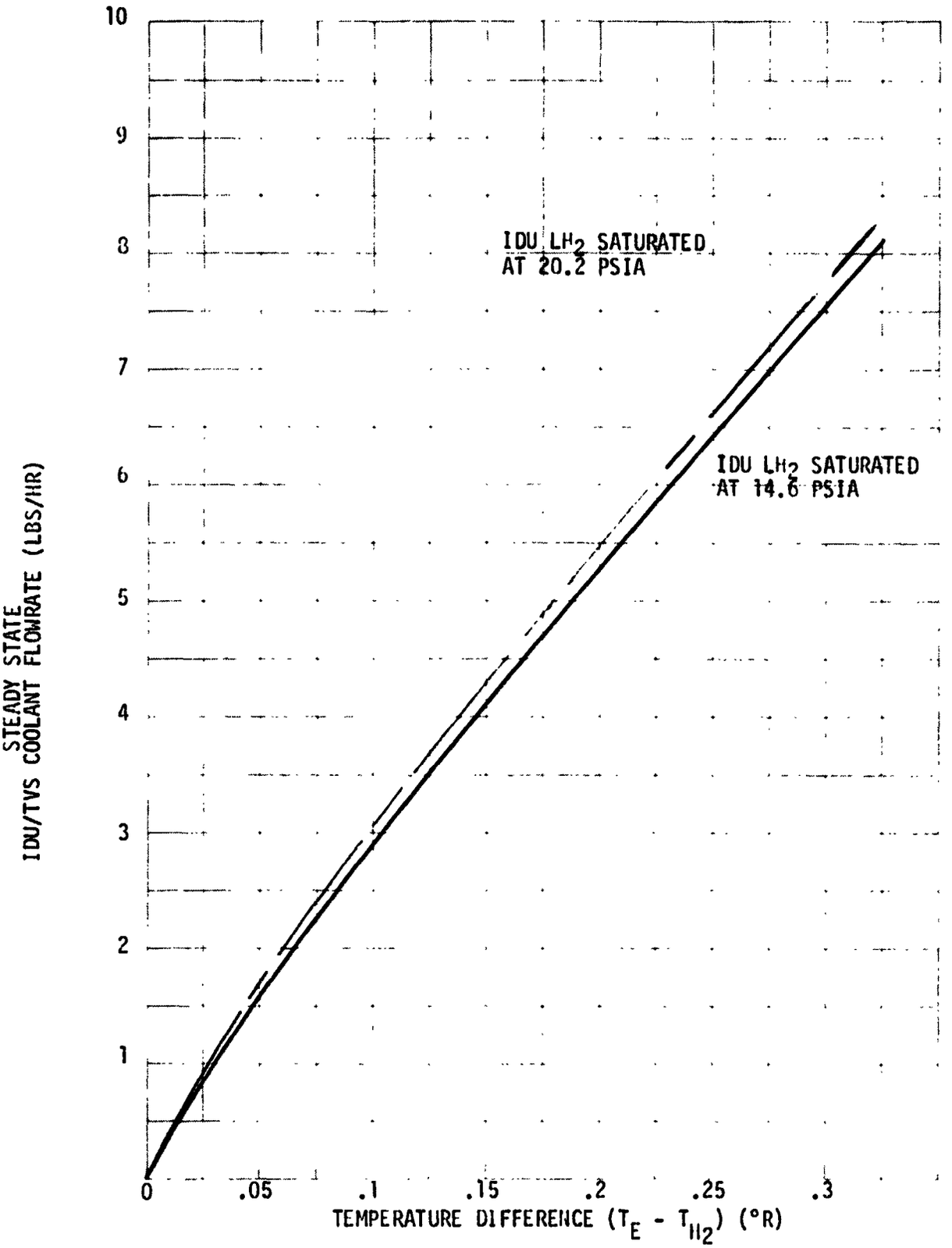

Figure 3-3 IDU/TVS COOLANT REQUIREMENTS - CONDENSATION ON IDU EXTERIOR - NO INSULATION

Table 3-1

PREDICTED OPERATIONAL REQUIREMENTS FOR IDU/TVS - CONDENSATION ON IDU EXTERIOR, NO INSULATION

Quality: $X_{Initial} = 0.05$, $X_{Critical} = 0.85$ STEADY-STATE CONDITIONS

P_{H_2} (psia)	T_{H_2} (°R)	P_E (psia)	T_E (°R)	ΔT	Inch Lb/hr	$Q_{Annular}$ (Btu/hr)	Q_{LD} (Btu/hr)	Q_{Total} (Btu/hr)	$Q_{Exchanged}$ (Btu/hr)	$Q_{Extraneous}$ (Btu/hr)	$L_{Annular}$ (ft)	$T_{HEX\ AVE}$	$P_{HEX\ AVE}$
14.6	36.5	14.72	36.55	0.05	1.5855	243.50	45.67	289.17	5.3079	0.0457	10.42	35.95	12.50
14.6	36.5	14.84	36.60	0.10	2.9185	448.26	84.05	532.31	10.7500	0.1153	12.98	35.83	12.34
14.6	36.5	14.96	36.65	0.15	4.1360	635.35	119.13	754.48	15.9460	0.1983	14.55	35.74	12.17
14.6	36.5	15.08	36.70	0.20	5.2785	810.9	152.04	962.94	20.9100	0.2916	15.67	35.68	12.00
20.2	38.5	20.36	38.55	0.05	1.6300	248.03	46.50	294.53	5.5400	0.0550	10.33	37.96	17.00
20.2	38.5	20.52	38.6	0.10	3.0200	458.9	86.04	544.94	11.1000	0.139	13.06	37.84	16.50
20.2	38.5	20.68	38.65	0.15	4.2900	651.57	122.17	773.74	16.3800	0.2399	14.72	37.76	16.20
20.2	38.5	20.84	38.70	0.20	5.4700	832.13	156.02	988.15	21.3400	0.3527	15.90	37.69	16.00

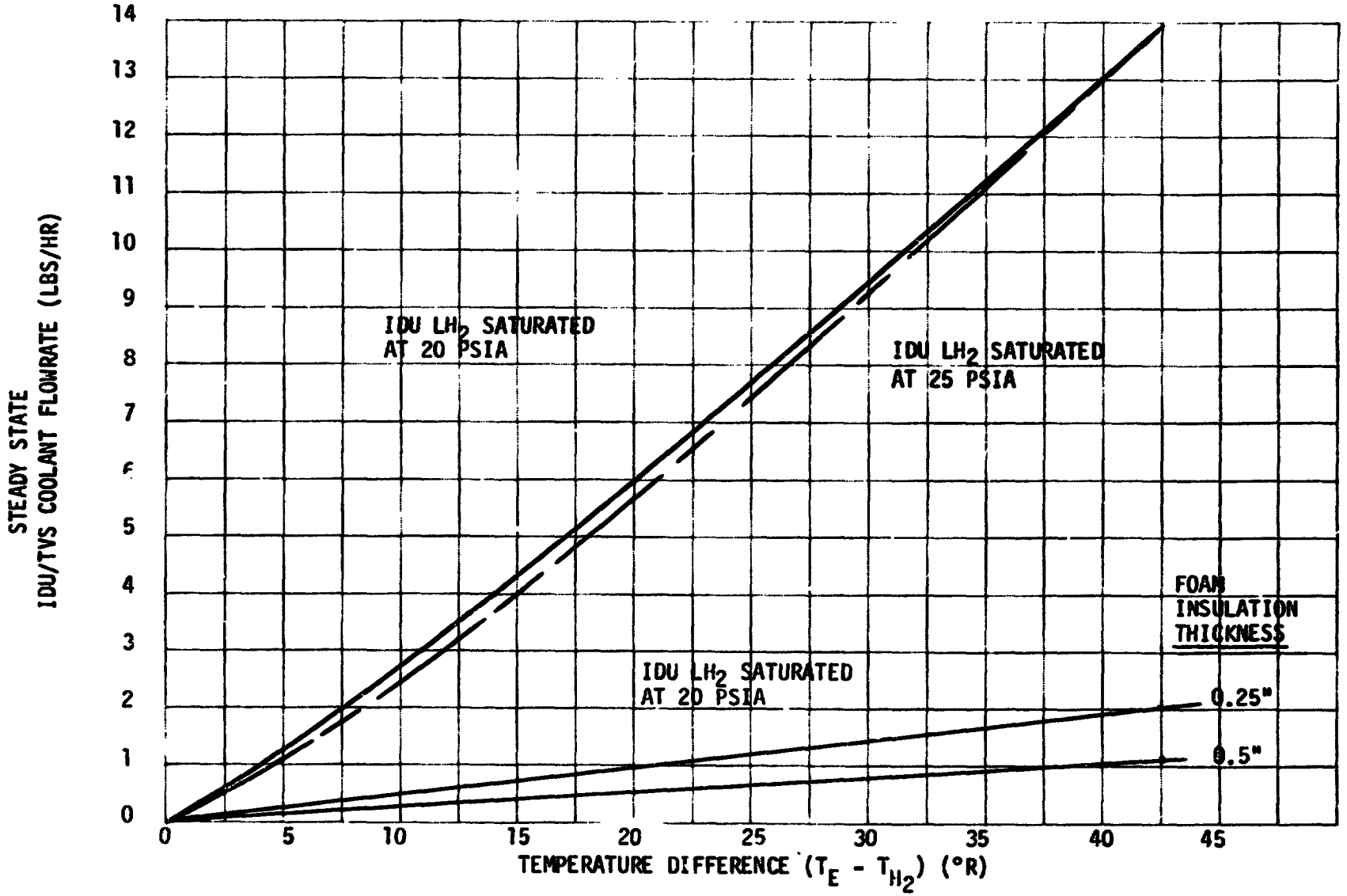

Figure 3-4 IDU/TVS COOLANT REQUIREMENTS - FREE CONVECTION ON IDU EXTERIOR

Table 3-2

PREDICTED OPERATIONAL REQUIREMENTS FOR IDU/TVS - FREE CONVECTION ON IDU EXTERIOR, NO INSULATION

Quality: $X_{Initial} = 0.05$, $X_{Critical} = 0.85$ STEADY-STATE CONDITIONS

P_{H_2}, SAT (psia)	T_{H_2}, SAT (°R)	P_E (psia)	T_E (°R)	ΔT (°R)	$\dot{m}$ (lb/hr)	$Q_{Annular}$ (Btu/hr)	Q_{LD} (Btu/hr)	Q_{Total} (Btu/hr)	$Q_{Exchanged}$ (Btu/hr)	$Q_{Extraneous}$ (Btu/hr)	$L_{Annular}$ (ft)	$T_{HEX\ AVE}$	$P_{HEX\ AVE}$
20	38.4375	15	40	1.6	0.25	37.6	7.0	44.6	15.15	4.8	13.45	38.10	17.4
20	38.4375	15	45	6.6	1.50	225.8	42.3	268.1	43.50	30.9	21.10	37.78	16.2
20	38.4375	15	50	11.6	2 96	451.4	84.6	536.0	59.3	62.7	23.40	37.56	16.0
20	38.4375	15	60	21.6	6.24	952.2	178.5	1,130.7	76.9	132.9	25.40	37.19	15.4
20	38.4375	15	70	31.6	9.74	1,490.0	279.0	1,769.0	86.6	206.9	26.30	36.88	14.7
20	38.4375	15	80	41.6	13.40	2,050.0	384.0	2,434.0	92.0	282.0	26.80	36.60	14.0
25	40.0000	15	45	5.0	1.07	160.6	30.1	190.7	35.9	23.0	19.90	39.44	22.0
25	40.0000	15	50	10.0	2.50	377.0	70.6	447.6	53.7	53.0	22.90	39.20	21.5
25	40.0000	15	60	20.0	5.76	868.9	162.9	1,031.8	72.6	127.9	25.20	38.82	20.0
25	40.0000	15	70	30.0	9.28	1,400.0	263.0	1,663.0	82.0	205.6	26.20	38.58	19.0
25	40.0000	15	80	40.0	12.96	1,960.0	368.0	2,328.0	87.1	284.9	26.80	38.21	18.0

the operating characteristics of the uninsulated and insulated IDU/TVS. The results of Appendix G clearly show the need for insulation, condensation heat transfer is eliminated, and the net thermal resistance is increased. Use of 1/4-in. foam thickness reduces the coolant flowrate to approximately one-fifth the values shown in Figure 3-4, and use of 1/2-in. foam thickness reduces the coolant flowrate to one-tenth the values of Figure 3-4. The IDU/TVS is capable of providing flowrates of the order of 5 lb/hr, whereas only approximately 1 lb/hr coolant flowrate is required for the IDU insulated with 1/2-in. of foam, and surrounded by 100°R gaseous hydrogen.

3.2 IDU AUTOGENOUS PRESSURIZATION

A versatile tank pressurization analysis computer code has been in regular use at MDAC for several years. This modular code was designed to facilitate modification and adaptation to specialized studies of heat and mass transfer which determine the course of propellant tank thermodynamics. Computer output includes the time-variable histories of the temperature distributions, heat and mass transfer rates, tank pressure, and pressurant flowrate.

3.2.1 Basic Tank Pressurization Computer Code

The analysis of tank pressurization performance is based on a one-dimensional model. Spatial variations in the system variables can occur only along the vertical tank axis; there are no radial or circumferential variations. Tank pressurization computer programs based on this type of model have been compared extensively with experimental data and found to be valid. Buoyancy tends to produce a stable thermal stratification in the gas and liquid, giving a temperature distribution which is essentially one-dimensional.

The thermal system for this analysis consists of the tank wall, internal hardware, propellant liquid, and ullage gas. Any size and configuration may be specified for the tankage. The ullage gas may be pure propellant vapor or a mixture with helium. Tabulated variable properties are used to describe the thermodynamic behavior of all materials.

The nomenclature and mathematical model for the code are delineated in Table 3-3.

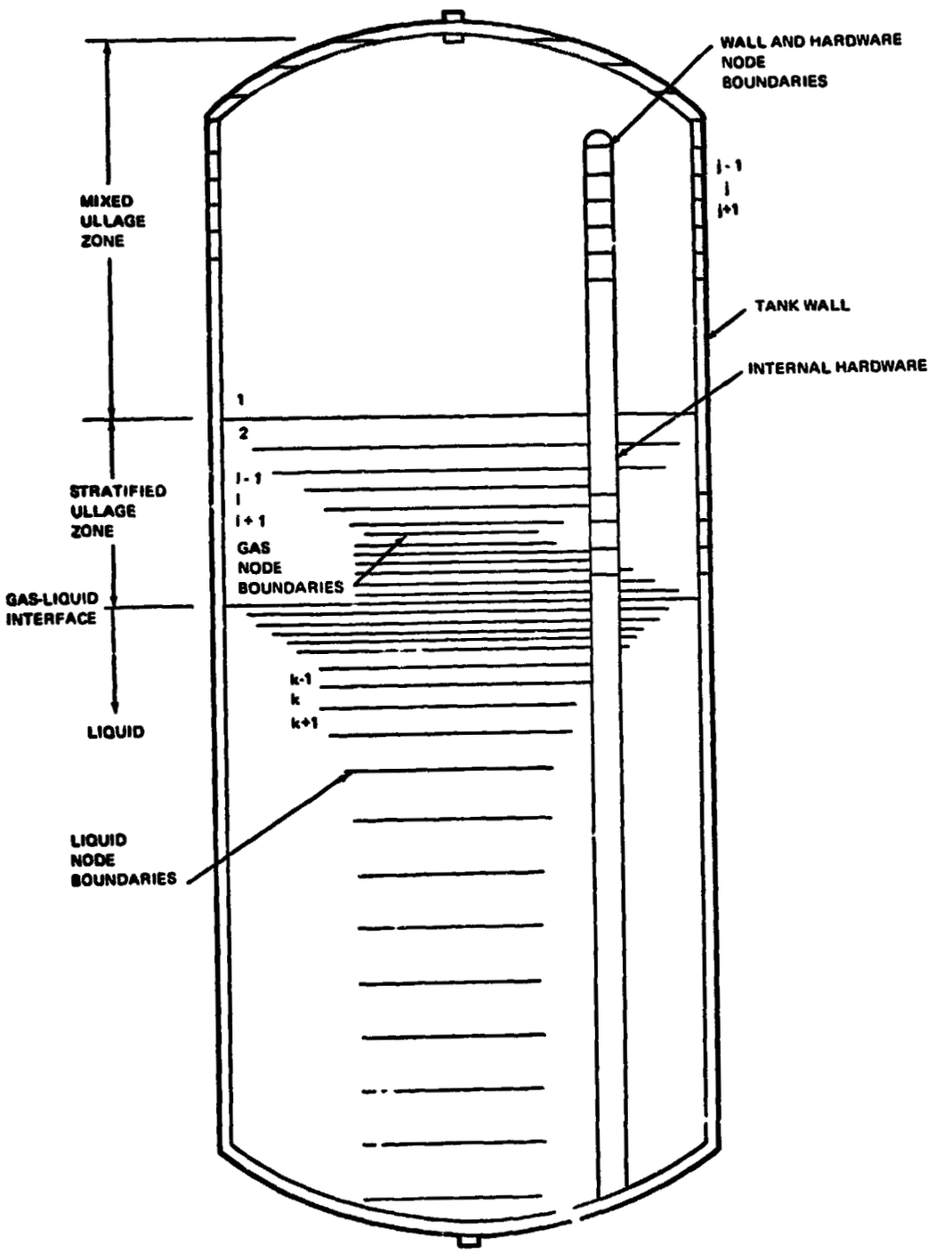

Table 3-3. TANK PRESSURIZATION COMPUTER CODE NOMENCLATURE

The computations are based on a finite-difference representation of the physical system. The tank wall, internal hardware, propellant, and ullage are each divided by horizontal planes into a number of nodes, the properties within each node being uniform. The gas and liquid are divided into nodes whose thickness and location can vary with time. The tank wall and hardware nodes are of equal axial thickness and are stationary. The size and number of these nodes is sufficient to give an adequate step function approximation to the continuous axial variation of the system variables. Gas and liquid nodes may be subdivided or combined as required to meet solution accuracy criteria.

The volume of each liquid and gas node is bounded by the top and bottom boundary planes and by the solid surface of the tank wall and the internal hardware. Heat transfer takes place between each gas node and the solid surfaces with which it is in contact. The physically simultaneous processes of heat transfer and pressure change are assumed to take place sequentially as isobaric heat transfer and isentropic pressure change. The numerical solution is obtained by calculating the change in the state of each node in the system during each successive time step throughout the total solution time. The state of each node is determined from equilibrium, conservation relationships.

Duty-cycle control data is input to the program in time-variable tables. These include propellant outflow rate, vehicle acceleration, pressurant inlet temperature and composition, tank pressure, and pressurant inflow rate. Heat-transfer coefficients may be input or calculated internally from free convection or other relationships. The solution may be computed in two modes: (1) either the tank pressure schedule is specified and the required pressurant flowrate is calculated or (2) the pressurant flowrate is specified and the pressure calculated. Initial conditions specified at the start of the duty cycle are the ullage fraction, tank pressure, and all temperature distributions.

3.2.2 Computer Code with Conduction

This basic computer code is available in various specialized versions with added capabilities. One such version analyzes the transient heat-transfer processes throughout the mission. Thermal conduction equations were added for one-dimensional heat transfer axially down the tank wall, the liquid and the ullage gas. The propellant remains settled. Heat is transferred between the gas and wall by free convection. Heat conducted down the wall to the liquid surface level is transferred directly to the surface liquid node.

The excess heat conducted from the gas to the liquid surface over that conducted from the liquid surface to the bulk liquid results in liquid vaporization. Conversely, a deficiency in this exchange will result in vapor condensation. Heat added to the liquid surface node by the wall conduction raises the liquid temperature. If the surface liquid node reaches saturation temperature, further heat addition causes vaporization.

With these assumptions, the tankage system is virtually always in a transient nonequilibrium state when prepressurization and propellant outflow events occur. The duty cycle can include continuous pressure control, giving pressurant requirements to maintain tank pressure, or pressure decay, giving the tank pressure history following the shutdown of the pressurization system.

3.2.3 Computer Code Modifications for IDU Analysis

The specialized version of the pressurization computer code used for the IDU analysis was further modified for this application. First, the code was simplified by removing components that were of no use to this study; this included the diffusion equations, applicable to a two-component ullage, and the associated interface heat and mass transfer model for use with helium. Then the available methods of numerical solution were reviewed to select the most efficient for this study. Both Gauss-Jordan and Gauss-Seidel methods had been adopted to this code. The simple Gauss-Seidel method was found to give identical results to the more reliable, but more expensive (in core storage and computing time) Gauss-Jordan method for typical test cases, so the former was adopted for this application.

The solid conduction routines were called to operate on the internal hardware as well as the tank wall. The various parts of the internal hardware (screen device) were lumped into a single component of equivalent mass and area. Different items of internal hardware could be treated individually with relatively simple modifications to the code, but this appeared to offer little advantage and would have greatly increased core storage and computing time.

The area and mass of the flat tank-top is accurately represented in the heat transfer calculations. However, the top must be treated as having a uniform temperature. Conduction between this mass and the cylindrical wall occurs according to the one-dimensional model with no provision for radial conduction analysis in the tank top.

Since the conditions of the IDU operation would permit portions of the wall and hardware to be at temperatures less than the saturation temperature of the vapor, it was necessary to add the computations for condensation heat transfer. Since condensation heat transfer rates are much greater than free convection rates, this led to an added complication. With the low specific heat of the metal at liquid hydrogen temperature, condensation heat transfer would give a rapid temperature rise during a single time step. The final temperature could greatly exceed the saturation temperature making the use of the condensation heat-transfer coefficient invalid for part of the computation.

To correct this inaccuracy, the final temperature of the wall or hardware node is checked at each time step when condensation occurs. If it exceeds the saturation temperature, the computation is repeated in two steps: first, the time required to reach the saturation temperature in the metal node is determined at the condensation heat transfer rate; then, the free convection heat-transfer coefficient is calculated and the metal node temperature increase, starting from the saturation value, is calculated for the remaining time of the time-step interval. This two-part computation removes the possibility of a significant error in the use of condensation heat-transfer rates.

When condensation occurs at any point on the wall or hardware, the condensed mass is removed from the gas at the point of condensation and is added to the surface liquid node. The manner in which the condensed liquid travels this distance is not treated.

When the screen device does not contain liquid, it is treated as internal hardware in the conventional manner; that is, its temperature distribution will change as heat and is transferred to it from the warmer gas. To simulate the liquid-filled screen device, it is treated as a constant-temperature heat sink. This "constant" temperature may be either the initial temperature distribution or a uniform saturation temperature. In the former case, condensation will occur at any point that is below the saturation temperature; in the latter case, condensation will not occur, but the temperature itself will change to follow any tank pressure changes.

3.2.4 IDU Autogenous Pressurization Results

The MDAC H431 tank pressurization computer code, modified to model the IDU, has been used to generate results for two warm GH_2 tank prepressurization cases. In Figure 3-5, the GH_2 pressurant inflow rate and ullage temperature at the top of the tank are plotted versus time. A 5-second prepressurization rise from 15 to 40 psia is assumed. The temperature profile results of Figure 3-6 show that the initial ullage is compressed by the incoming pressurant and undergoes a temperature increase of 10°R. After approximately 400 seconds, the tank temperature gradient varies slowly, and the incoming pressurant mass flowrate is less than 10^{-3} lb/sec.

Results shown in Figures 3-5 and 3-6 are for an adiabatic tank corresponding to the IDU with insulation. Figures 3-7 and 3-8 correspond to the conditions for a noninsulated tank with free-convection heat transfer from the outer tank wall to 37°R GH_2. (Heat transfer to the LH_2 through the tank wall from the surrounding GH_2 is neglected, since it has little effect on ullage conditions.) The characteristic time for the ullage temperature profile and incoming gas to reach a steady-state condition is somewhat longer than for the adiabatic tank wall case.

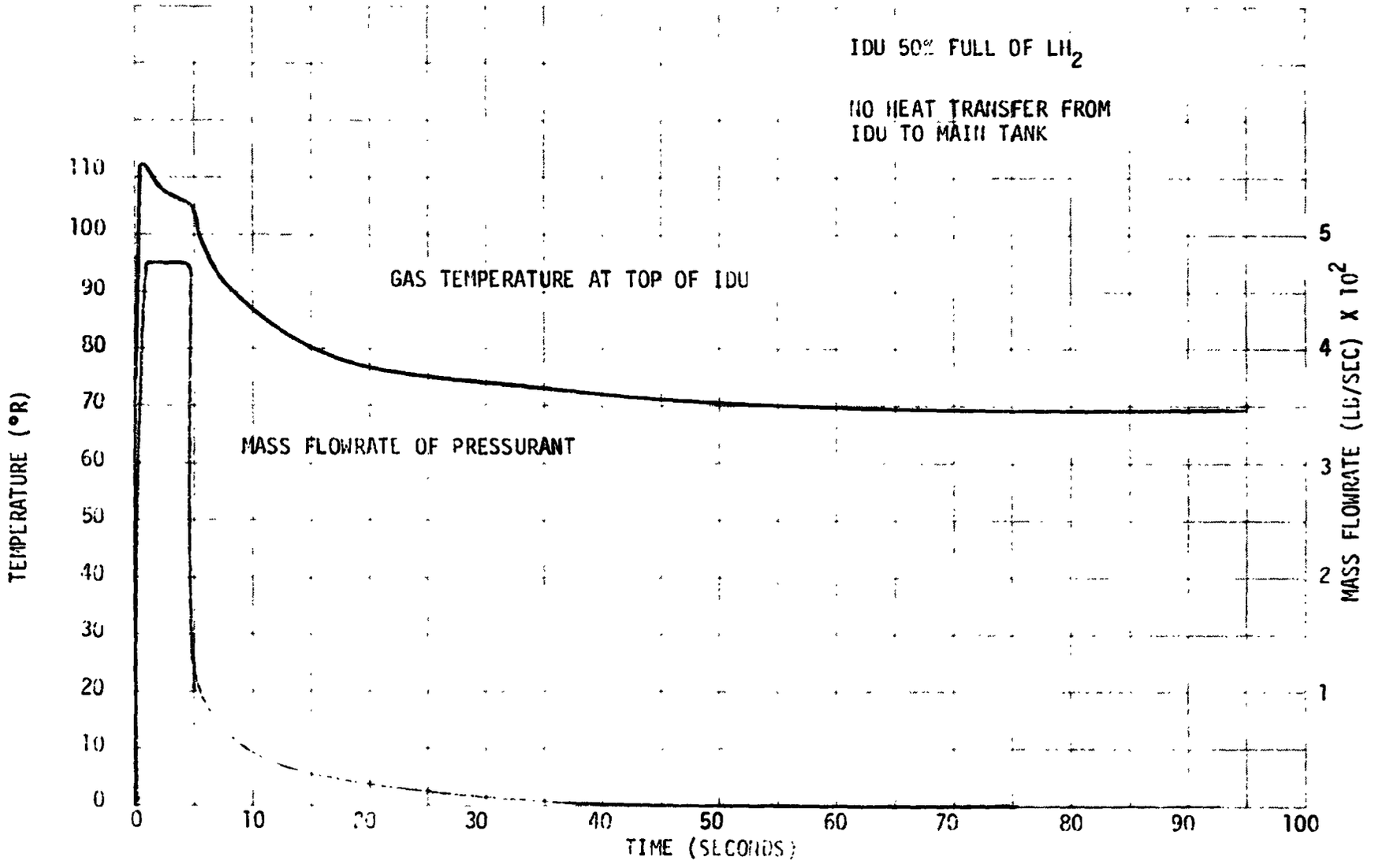

Figure 3-5 TRANSIENT PRESSURIZATION CONDITIONS IN IDU

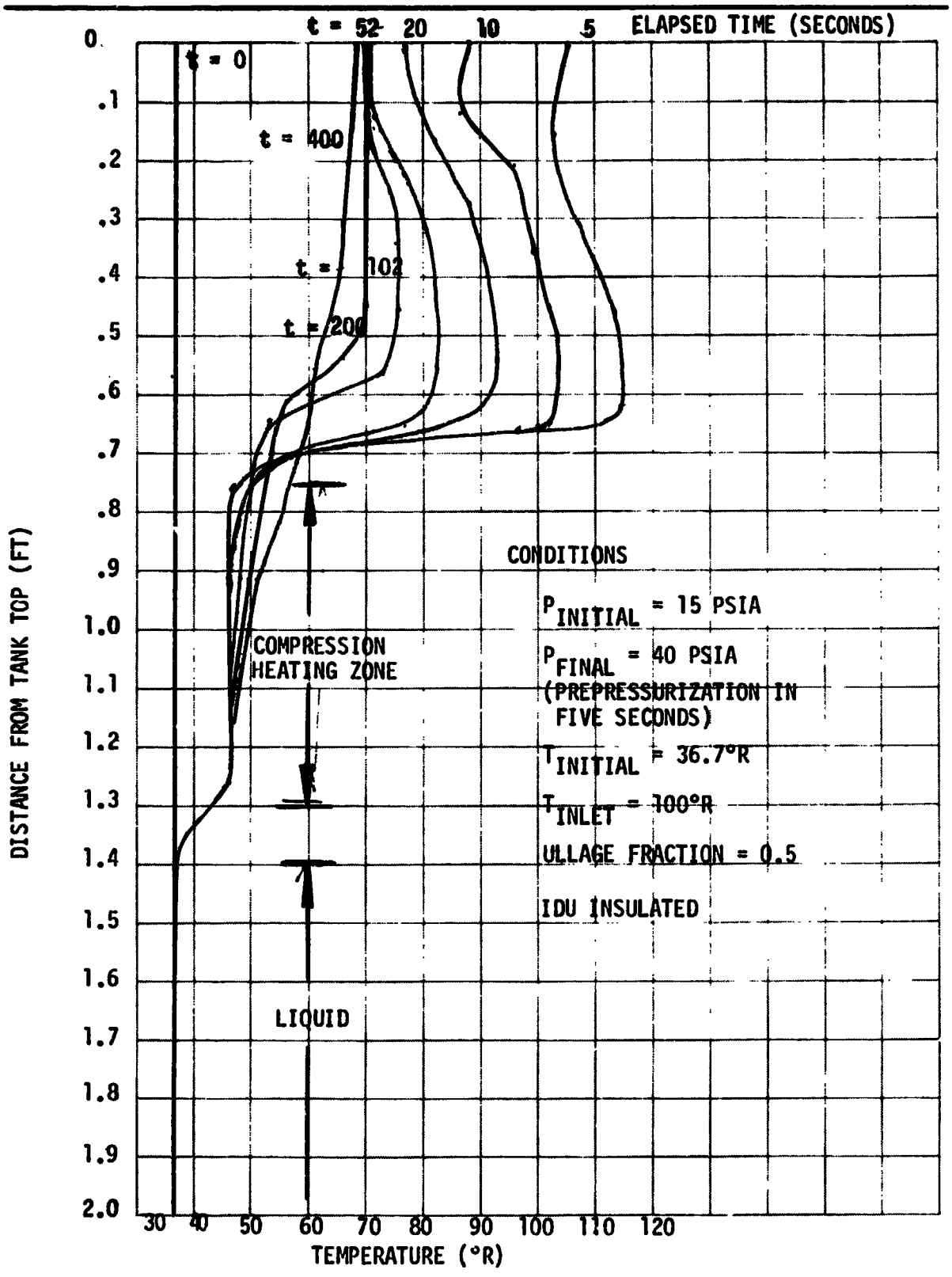

Figure 3-6 PREDICTED TEMPERATURE DISTRIBUTION FOR IDU PREPRESSURIZATION

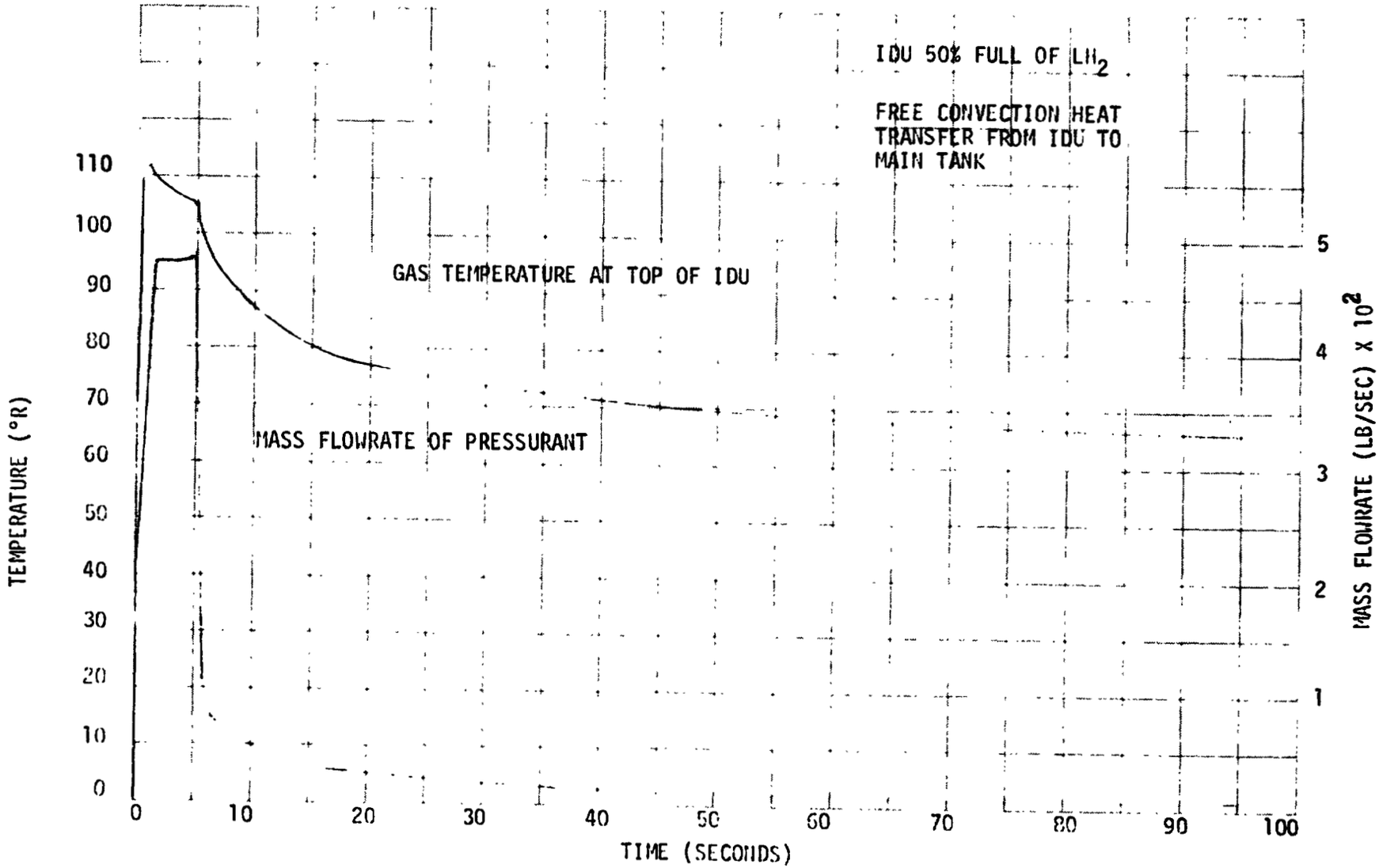

Figure 3-7 TRANSIENT PRESSURIZATION CONDITIONS IN IDU

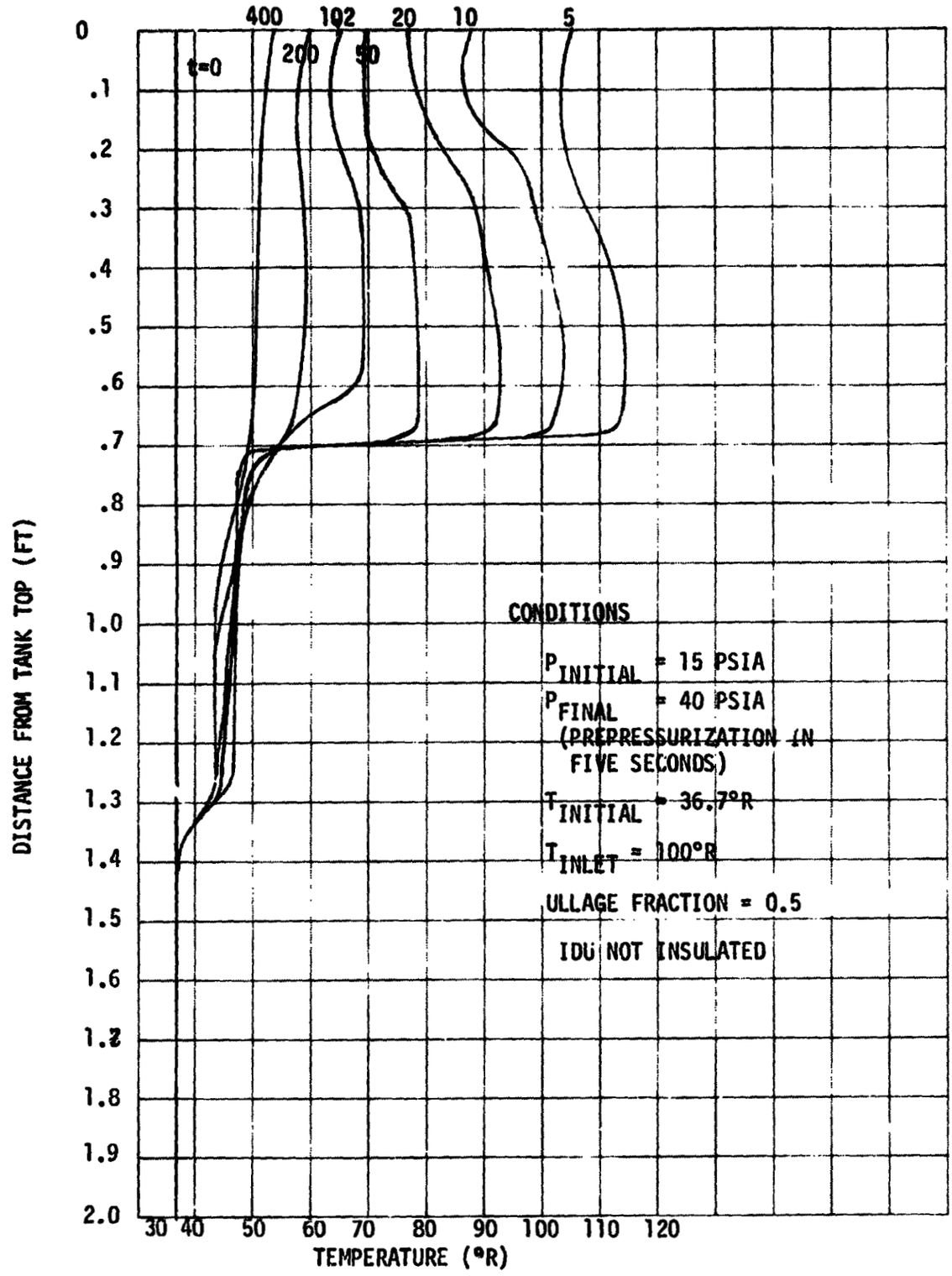

Figure 3-8 PREDICTED TEMPERATURE DISTRIBUTION FOR IDU PREPRESSURIZATION

3.3 SCREEN SIZING COMPUTER PROGRAM

The expulsion characteristics of an annular screen acquisition device are predicted by the computer program in Appendix F. The total ΔP across the screen in steady-state operation is the sum of several contributing factors evaluated by the program: (1) flow loss accompanying the movement of liquid through the screen into the annular outflow passage, (2) hydrostatic head loss as the liquid moves upward away from the bulk liquid pool, (3) viscous flow losses within the annular passage, and (4) dynamic pressure loss ($1/2\ \rho v^2$) due to fluid motion at the most critical point in the passage. Liquid expulsion can continue only as long as these flow losses do not depress the pressure within the outflow passage to the point where pressurant gas can break into the passage.

One of two experimental correlations can be used to determine the pressure loss for flow through the screen. If the screen mesh forming the walls of the passage is 200 x 1400 mesh or coarser, flow correlations established for cryogenic fluids in Reference 11 are used:

$$\Delta P = \frac{A_1 L}{D^2}\ \mu V + \frac{A_2 L}{D}\ \rho V^2 \qquad (3\text{-}1)$$

where

V = average flow velocity through screen
D = average screen pore diameter
L = screen thickness
$A_1 A_2$ = empirical constants

If a finer mesh screen is present (or if a comparison is made between fine and coarse mesh screen performance), the correlation developed in Reference 12 is used. Ambient temperature fluids were used to establish this correlations.

$$\Delta P = \frac{1.3\ L\rho V^2}{\varepsilon^2 D}\ \left(C_1\ \frac{\nu a^2 D}{V} + C_2\right) \qquad (3\text{-}2)$$

where

ϵ = screen volume void fraction

a = surface area to unit volume ratio

$C_1 C_2$ = empirical constants

Backup material to this screen (such as perforated plate) can be introduced into the mathematical model described by the computer program.

The computer program requires as input the acquisition device dimensions, outflow rate, and screen characteristics. It then computes the most critical pressure differential across the screen liquid-gas interface as a function of the liquid level within the tank containing the acquisition device. At each step this critical ΔP is compared with the bubble-point pressure of the screen to determine whether breakdown has occurred.

Section 4
TESTING

The objectives of this phase of the program were to: (1) perform a component and overall system checkout of the IDU/TVS and (2) explore certain fluid dynamic and thermodynamic phenomena associated with screen device propellant acquisition. The basic checkout tests included component functional tests, tank-leakage and proof-pressure tests, determinations of the LHAD screen retention breakdown ("bubble point") condition as a function of flowrate, TVS flowrate control, and a thorough demonstration of the operational characteristics of the "start tank" principles, including outflow and refill with simultaneous outflow.

Additional tests were performed to evaluate the IDU/TVS thermal control, transient thermal response, effects of warm hydrogen and helium pressurization on breakdown, effectiveness of the cone screen for feedline vapor control, two-phase refill, and hydraulic pressure transients due to valve actuation/deactuation.

As detailed in Test G and Appendix J, problems were encountered with the three Parker LH_2 ball valves which impaired the capability to meet the test goals. Extensive effort was made to correct this situation, and a solution is proposed which involves relatively minor modification to the valve pressurization system. The valve problem caused severe test schedule problems, directly affected test operation, and eliminated two tests (Tests R and W). However, useful data were obtained in the major areas investigated, and the successful operation of the IDU/TVS was demonstrated in all other respects.

Detailed, annotated data are presented in a separate document, the Supplemental Data Document (SDD), which has been submitted to NASA/MSFC. This section discusses the test results and outlines the data available. More detailed evaluation of individual tests is provided in the SDD.

4.1 TEST A - SOLENOID ACTUATION

The solenoid valves were actuated under ambient conditions, and current and voltage recorded. All valves drew 0.8 to 0.85 amperes at actuation, with 28 VDC applied.

4.2 TEST B - BALL VALVE ACTUATION - AMBIENT

The three Parker submerged LH_2 ball valves were actuated five times to verify their operation, using 500 psig GHe. The output of the position indicators was verified using ohm meters. The valves deactuated properly without back pressure. On 11 December 1973, the minimum pressure to actuate the valves was determined for ambient conditions. No line pressure was applied, and therefore, the initial deactuation pressure was approximately the same as the actuation pressure supplied. The minimum actuation pressures were 150 psi for PV1 and 175 psi for PV2 and PV3.

4.3 TEST C - PROOF PRESSURE TEST - AMBIENT

The IDU tank was proof tested at 75 psig with GHe for five minutes and inspected. There were no indications of deformation.

4.4 TEST D - LEAK TEST - AMBIENT

The IDU was pressurized with GHe to 40 psig and all joints sniffed with a mass spectrometer. Leaks at the tee connections used for the platinum temperature transducers were corrected by tightening the fittings until the mass spectrometer revealed no leakage. The sensitivity of the mass spectrometer was shown to be 5.8×10^{-8} sccs.

Two leaks were detected. A very low leak (10^{-5} sccs) was found at the K-Seal on the bottom of the plate, at the overhead diffuser fitting. A second leak was detected at the cone screen housing which bolts to the plate and forms

a portion of the main IDU feedline. Upon further testing, it was found that the -7 port of the housing had a small crack in the weldment. This was rewelded, the Indium tin seals changed, and the housing reassembled. Subsequent leak tests revealed no indication of leakage anywhere in the system, except for the K-Seal. This low leakage rate is small compared to the nominal, unavoidable leakage through the Parker valves, and therefore, no attempt was made to correct this leak.

4.5 TEST E - CONDITION LEVEL SENSORS (PRIOR TO ASSEMBLY)

The carbon-resistor, point-level sensors were conditioned by dunking in LH_2 and examined for damage. No damage was detected

4.6 TEST F - SOLENOID ACTUATION - CRYOGENIC

All solenoid valves were actuated at cryogenic temperatures during the test series. A variable voltage power supply was used to control the current to the solenoid valves to assure that the current to each solenoid was approximately 1 ampere. At ambient conditions, the solenoid valves (Valcor SV 90) use 28 volts at 0.8 ampere. At reduced temperatures, the decrease in resistance allows a larger current to be supplied, thus increasing the magnetic force, while maintaining the same rate of electrical energy dissipation, I^2R. At -420°F, current of 0.8 ampere corresponded to a supply voltage of 2 volts. In practice, 1 to 2 amperes at approximately 3 to 5 volts was normally supplied to the pairs of solenoid pilot valves to actuate the Parker submerged liquid hydrogen valves. At pressures above 500 psi, and at temperature of the order of -420°F, the solenoid pilot valves opened sluggishly, and at 750 psi would often fail to open.

4.7 TEST G - BALL VALVE ACTUATION

On 13 November 1973, tests were initiated and the 260-gallon main tank was filled. Following a wait period of several hours, the Parker submerged LH_2 ball valves (PV1, PV2, and PV3) were actuated, but did not respond properly. Numerous attempts to actuate these valves were made, until the vent check valve (V43) froze shut due to cold helium being expelled from PV1, PV2, and PV3. With V43 frozen shut, the Parker valves could not be vented. Check

valve V43 was freed by blowing air over it, and additional attempts were made to actuate the valve. The valve signals ("talk back") indicated the valves could not be closed completely. During a main-tank fill operation, liquid entered the IDU, proving that either PV1 and PV3, and/or PV2 were at least partially open. Anticipating that the problem lay with the pilot valves (SV11, 12, 13, 14, 15, and 16) not opening properly, a solenoid valve was installed upstream of V43 (see Figure 2-15), this valve was used to apply pressure to PV1, PV2, and PV3 simultaneously. Again, the PV valves could not be made to operate properly; actuation pressures were increased to 750 and then to 1000 psi, but to no avail. On 14 November, the PV valves again did not actuate, and therefore the tests involving the PV valves were postponed and the thermodynamic vent system (TVS) tests were initiated. On 15 November, the system was shutdown and, when the temperature reached -110°F on 19 November, the valves were actuated properly.

During consultation with George Young and Haschal Hyde of NASA/MSFC on 20 November, it was determined that extremely pure helium was required to actuate the valves, and it was agreed that samples of helium would be tested.

Proper operation at -110°F was an indication that ice was probably not present in the valves; although thermal expansion could have caused affected parts to break loose of ice, this was not considered likely. Subsequent mass spectrograph analysis of the helium disclosed no measurable amounts of water vapor. The failure of the PV valves to operate when the pilot valves were not actuated but the external solenoid valve upstream of V43 was used, indicated that the problem lay with the PV valves. Although it was possible that the pilot valves had failed, subsequent testing confirmed that the solenoid pilot valves (SV11, 12, 13, 14, 15, and 16) were operating properly with 500 psi helium.

It was agreed that a long-duration vacuum purge coupled with numerous valve operations with clean helium would be performed to remove any contaminants in the valves and lines.

A helium sample was taken near the PV valve pressurant line inlet to the vacuum chamber lid on 20 November, and on 21 November the IDU system was pumped down for the entire day. The helium sample results were received on 26 November; the mass spectrograph analysis indicated the presence of 0.7-percent N_2 and 0.2-percent O_2, which indicated that the helium supply system was contaminated with air.

A second sample was taken within the helium supply system, which indicated 0.3-percent N_2 and 0.03-percent O_2. Two additional samples were taken of the helium in the high-pressure bottles of the supply trailer. These samples indicated (a) 0.04-percent N_2, 0-percent O_2, and (b) 0.1-percent N_2, 0.02-percent O_2. Since the samples from the helium trailer indicated contaminant levels within the experimental accuracy of the mass spectrograph analysis and sampling technique, it was assumed that the helium in the trailer was sufficiently pure. A helium pressurization line was run directly from the helium to the Parker valve pressurization system.

On 29 November 1973, it was noted that a leak somewhere in the 500-psi PV valve pressurization system was causing a loss of 3.15 SCFM of helium when the lines were pressurized to 500 psi. It was decided to continue testing, but to minimize the helium loss wherever practical by decreasing the line pressure after actuating the PV valves. It was later determined that a silver soldered 1/4-inch outside diameter joint at the top of the 260-gallon tank was the leak site.

Tests were initiated on 5 December, following a full day of vacuum purging and valve operations. At -125°F, during the tank chilldown and loading, the PV valves were actuated but responded sluggishly, which may have been due to differential of thermal expansion problems, caused by not having reached a steady-state temperature in the valves. Both the external and internal pilot valves were used, but the PV valve response was the same. After approximately one hour at -420°F, the valves were again actuated, but would only open part way, followed by erroenous "closed" signals with pressure applied. However, following another hour of thermal adjustment, the valves were actuated with

both the internal (pilot) solenoid valves and the external valve. Six successful PV actuations were recorded. Following a 45-minute period, testing was initiated on the IDU fill and drain, but the valves began to behave erratically. One slow expulsion was obtained through the refill valve (PV2) since the main feedline valve, PV1, would not open. Following this, none of the valves could be made to operate, even at 750 psi. However, test data were obtained for calibration of the level sensors, even though PV1 was frozen closed and PV2 and PV3 were frozen open. Testing was halted on 5 December.

By 7 December, the IDU temperature had reached -250°F. The PV valves were actuated several times and the signals indicated proper operation. However, when the IDU was vented or pressurized, the main-tank pressure remained equal to the IDU pressure, which either indicated a severe leak or the PV valves were not completely closed. Subsequent testing proved that there were no leak paths between the IDU and main tank, other than the PV valves. On 10 December, the IDU temperature was above 32°F. All valve signals indicated that the valves were closed. Both the IDU and main tanks had 10 psig. The IDU was vented, and again the main tank pressure followed along. The valves were actuated several times, and both tanks pressurized to 10 psig. The IDU was then vented, but the main tank pressure did not decrease. Therefore, the microswitches were apparently not properly adjusted to indicate complete closure of the PV valves, or are inherently unreliable at liquid hydrogen temperatures.*

A liquid hydrogen cold trap was then installed to freeze out any trace impurities in the helium supply, and the separate line connected directly with the helium supply trailer used as the source. The IDU was vacuum purged for a full day, with intermittent valve actuation (at least 10 valve actuations for each valve), for a total of five complete vacuum purges.

---

*C.E. Schroeder, MDAC Saturn Propulsion, has investigated microswitch performance for valve position indications at liquid hydrogen temperatures, and has found them to be unreliable. Microswitches have indicated valves open, when they were closed, and vice-versa, and have failed to close when the valves were partially open or completely open or closed, giving an open circuit indication. Similar observations were made of the Parker valves.

On the next test day, 12 December, the cold trap was first filled with LH_2; helium was then passed through the heat exchanger to freeze out any foreign gases, and the Parker valves actuated 10 times with the purified helium. This operation served to clean out the Parker valves to an additional level, before filling the 260-gallon tank with LH_2.

During the main-tank fill, when T6 indicated -387°F, PV3 was closed per the test procedure. This was required to ensure that the decreased pressure in the valve pressurization line below the check valve, V43, would be minimized, and therefore, decrease the probability of air flow through the check valve, V43, in the event it was leaking. PV3 was then commanded open with 200 psi line pressure, but did not actuate. The line pressure was increased to 500 psi and the valve opened upon command. All subsequent operations to diminish the line pressure decrease were performed by opening and closing V11, to pressurize the line up to V62 with 500-psi helium. V62 was then opened so that the helium trapped upstream would flow into the cold line, but would not cause the Parker valves to open. This operation assured that no air could leak past V43 into the helium pressurization line to the Parker valves.

During the IDU leak test of 12 December, valve V63 was closed because the leak in the high pressure helium line (inside the main tank) to the Parker 2-inch ball valves was causing an excessive loss of helium. PV3, which had been maintained open, did not close completely, but could be completely opened. It was left in the partially closed condition with V63 closed to conserve helium.

The erratic behavior of the PV valves outlined above continued throughout the tests. Significant valve failures are discussed in conjunction with each test in the following sections. Numerous attempts were made to induce the valves to operate properly, including increasing the supply pressure to 750 psi, decreasing it to 250 psi, increasing the current to the solenoid pilot valves to cause more rapid opening and closing, and frequent valve cycling as well as valve cycling with long periods in between. None of these attempts were successful. As discussed in the following sections, the valves would sometimes fail to open, or would fail to open all the way, and at no point did PV2 and PV1 or PV3 close completely, thus pressure isolating the IDU from the main tank.

The reasons for the problems encountered with the Parker valves have not been fully ascertained. A number of factors have been identified which are potential sources or contributory sources of the erratic valve behavior observed, as listed below.

- Parker baked the valves at 165°F for two hours to remove moisture before their qualification tests. This was not done with the valves before assembly into the IDU.
- Tube routing was performed in a shop area, rather than in a clean room. Pressurant tubing was cleaned before assembly but assembly progressed in several stages, with modifications which required the removal and replacement of tubing. Contaminants, therefore, could have been introduced into the high-pressure helium pressurization lines.
- The facility helium supply was evidently contaminated and appeared to be a major cause of the initial problems encountered. However, subsequent purging and use of helium directly from the trailers with a LH_2 cold trap did not solve the problem.
- Each Parker valve was pressurized and vented by a pair of two-way solenoid valves, since a LH_2 submersible three-way solenoid valve was not available. The valve closure required that residual pressure and spring force close the valve, with both of these forces diminishing as the valve approached the closed position. In principle, the valves can be operated to use supply pressure (500 to 750 psi) for both opening and closing (dual pressurization and venting) but this would have required the use of additional solenoid valves and cables. An analysis showing the comparative operational factors of safety is given in Appendix J, which shows that dual pressurization and venting significantly increases the net actuation/deactuation forces.
- The solenoid pilot valves selected were rated for 1,000 psi but would sometimes fail to open or would open slowly at pressures of 750 psi. In principle, the use of higher actuating pressures should have helped in the 2-in. ball valve operation. However, we found no improvement throughout the test program as a result of the frequent use of 750-psi actuation pressure, rather than 500-psi pressure.

- All three valves were observed not to operate after a 1-hour thermal soak period at -420°F, but in the one case appeared to actuate properly for a total of six times following a 2-hour soak period. (However, the position indicators may have been giving erroneous readings.) Thermal transients and differential coefficients of expansion could, therefore, have been a contributing factor to the observed failures. During the testing, it was necessary to sometimes drop the main-tank liquid level beneath the valves, exposing them to the main-tank ullage gas. However, the temperature differences were small (usually of the order of 10°F to 50°F), and the effect would be expected to be minor.
- The piston seal effectiveness under cryogenic conditions is not known. Defective seals would cause more rapid pressure equalization across the piston, which decreases the net actuation force.

4.7.1 Conclusions

The valve behavior may be due to: (1) peculiarities of the valves (i.e., history of usage or design, (2) contamination, or (3) use of contaminated helium. However, the analysis of operational factors of safety, given in Appendix J, indicates that modifying the valve pressurization system to pressurize the actuator during opening and closing should increase the net actuation forces by at least a factor of two; this modification appears to present the greatest probability of solving the valve malfunction problem, and is therefore, the recommended "least cost" approach.

4.8 TEST H - LEVEL SENSOR EVALUATION

A number of tests were performed to compare the response of the carbon point-level sensors, capacitance point-level sensors, and the capacitance continuous-level sensor. A calibrated curve of the liquid-level versus continuous-level sensor signal voltage and corresponding level indications from the carbon point-level sensors is given in Figure 4-1. The capacitance continuous-level output (CL4) is linear above the 6-inch level and the carbon point-level sensors, RL1, RL2, RL3, RL4, RL5, and capacitance point-level sensors, CL1, CL2, CL3, accurately indicate liquid level, as shown by comparison with CL4. Below the 6-inch level, there is an apparent nonlinearity. In addition, the

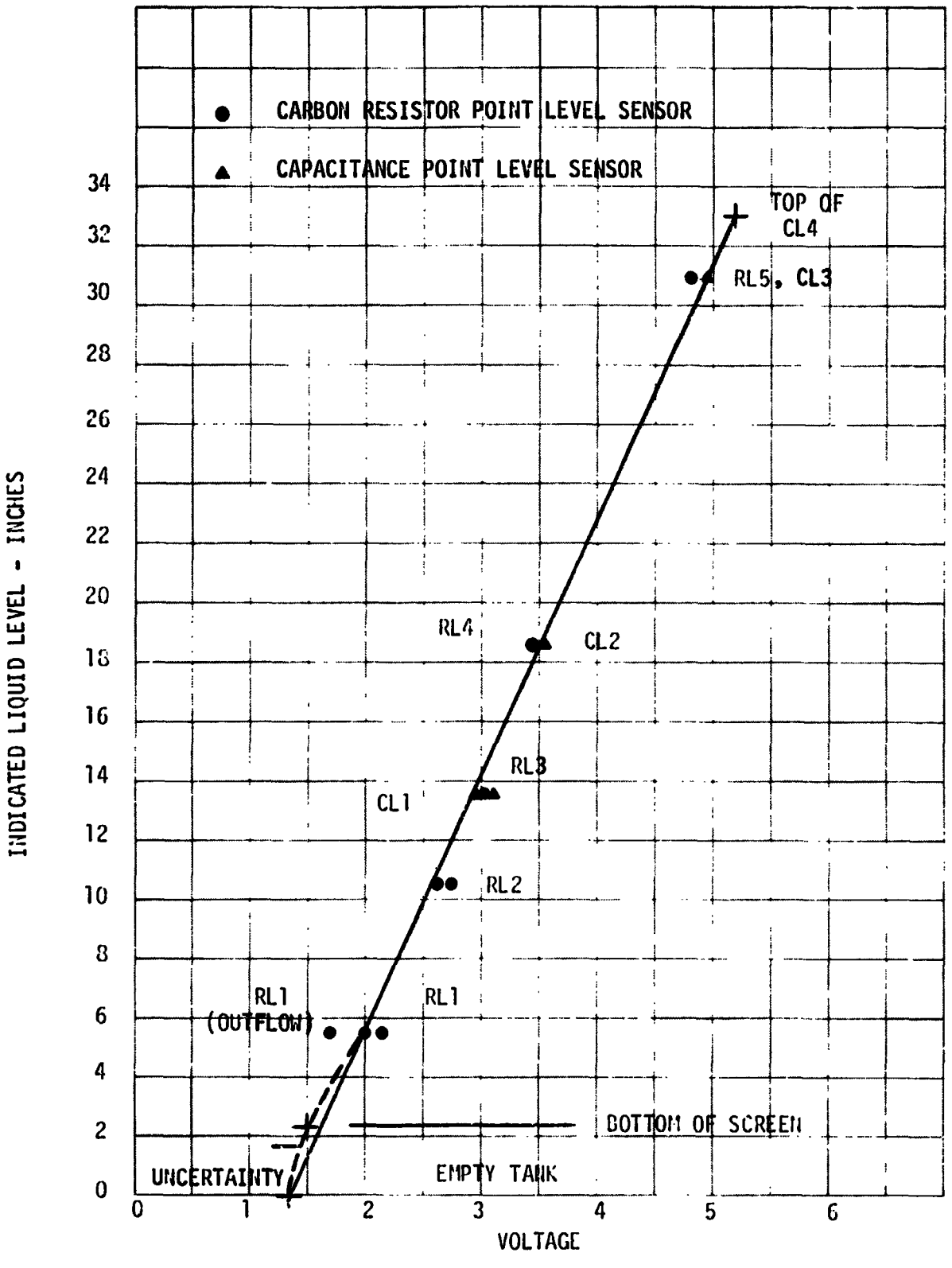

Figure 4-1 CALIBRATION CURVE OF LEVEL SENSORS

voltage output and capacitance are nonlinear, as shown in Figure 4-2, but since the level range is in the linear portion, this effect should not have caused the nonlinear voltage versus height portion of the CL4 curve. Since the voltage reading with no liquid in the tank is 1.38 volts, and the voltage reading when static breakdown occurs is 1.4 volts, at a level 2.25-inches above the tank bottom, there is an unexplained nonlinearity in this region. Unfortunately, there are no level sensors below 5.5 inches, and therefore, no independent measurements can be made.

However, the calibration curve in this region can be inferred. Since liquid dropout occurs at breakdown, the liquid held in the annular screen region of the LHAD (above the free liquid surface), flows out, increasing the height of liquid measured by the probe a known amount. In most cases with liquid hydrogen saturated at 15 psia, the measured voltage at breakdown increases from 1.5 to 1.9-2.0 volts, which corresponds to the dropout of liquid in the LHAD. The volume of liquid depends on the degree to which the uppermost region of the LHAD is full, and this is indeterminent. However, the approximate amount of liquid corresponds to that in the annulus, above a height of 2.25 to 2.5 inches from the bottom of the IDU, where breakdown occurred in most cases. The annulus volume is 1.26 ft^3 and the height increase after dropout is 3.6 inches. Therefore, the cases for which breakdown as measured by CL4 occurs at 1.5 volts, followed by an increase to 1.9 to 2.0 volts due to liquid dropout, correspond to breakdown at 2.25 inches (the bottom of the screen) followed by the dropout height increase to 5.85 to 6.1 inches. The calibration curve thus exhibits the nonlinearity shown in Figure 4-1.

The carbon point-level sensors responded rapidly to liquid level during fill, indicating a liquid level which corresponded closely to both the capacitance point-level sensors and the capacitance continuous-level sensor. However, during expulsion, the carbon point-level sensors sometimes gave late indications of exposure to ullage gas, probably due to a film of droplets of liquid hydrogen being retained on the resistor element. Examples of the response of RL1, RL2, RL3, RL4, and RL5 are shown in Figure 4-1.

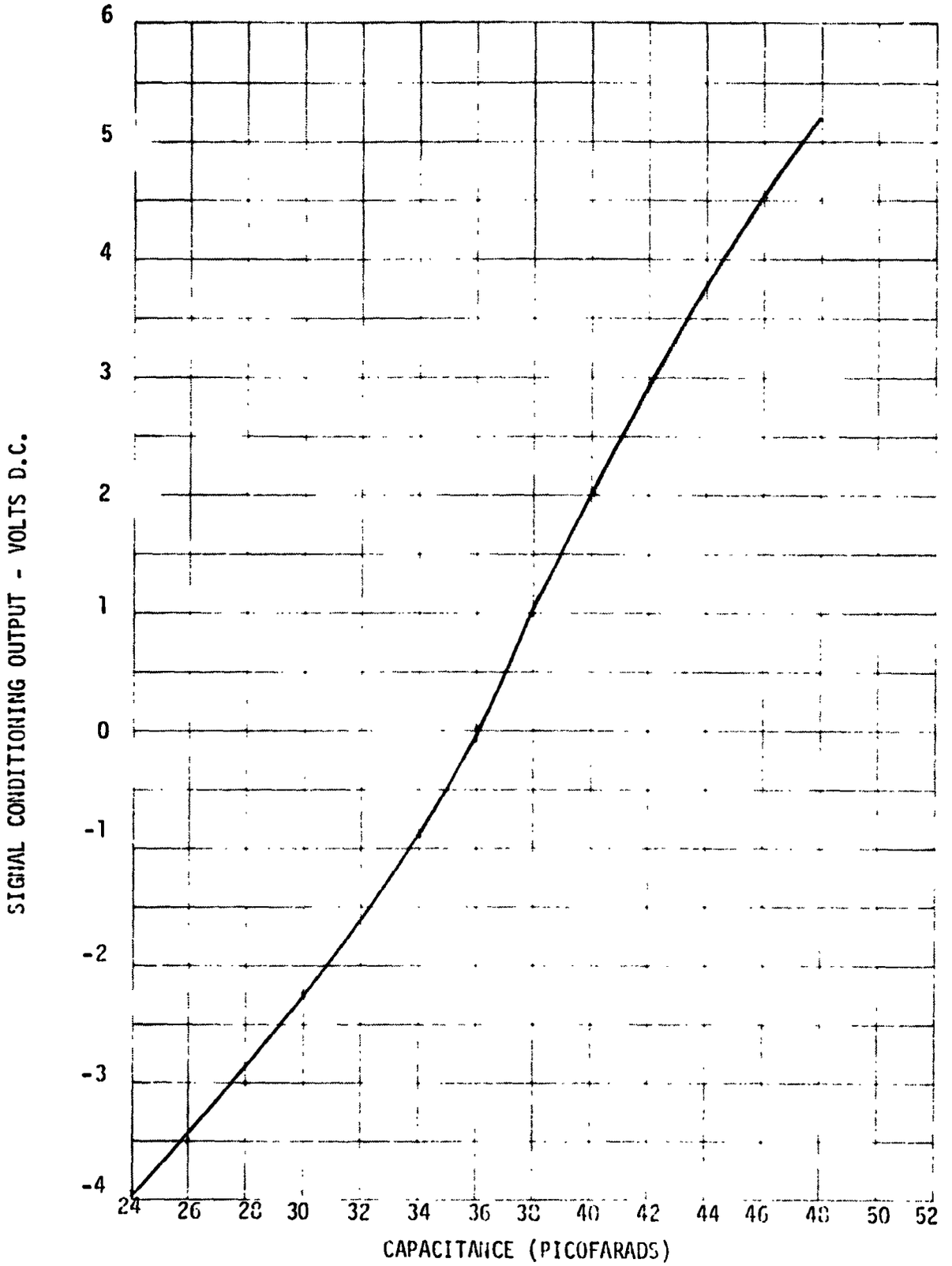

Figure 4-2 CALIBRATION CURVE FOR CONTINUOUS LEVEL SENSOR

Test experience indicates that CL1, CL2, CL3, and CL4 provide fast response, accurate measurements of liquid level during fill or expulsion. Submerged helium pressurization causes a very slight (±0.5 inch) variation in indicated liquid level due to the bubble and surface disturbances of the liquid hydrogen.

4.9 TEST I - TANK LEAKAGE - CRYOGENIC

The leak test of the IDU was first performed on 13 November by pressurizing the IDU to 52 psig, with the main tank vented to atmosphere. The main tank was partially filled with liquid hydrogen. Figure 4-3 shows the pressure decay starting approximately five minutes after the IDU was pressurized. The temperature of the IDU and main tank near the top of the IDU was approximately 90°R, and constant during the test; the temperature beneath the IDU was approximately 40°R. The pressure decay was, therefore, due primarily to leakage.

The loss corresponded to 0.3 lb of helium in 2,500 sec, for a loss rate of 1.2×10^{-4} lb/sec at approximately 40°R, or 0.6 SCFM. This leakage is much higher than would be expected with the fittings used in the IDU lines and the nominal leakage of the PV valves would be expected to be 10 SCIM according to Parker data. Further, the mass spectrometer tests showed no significant leakage of any of the connections. Therefore it was concluded that the leakage is through the Parker valves which could not be completely closed.

On 12 December 1973, the second IDU leak test was initiated. The IDU was initially empty of liquid and purged with helium. The PV1 and PV2 valves were closed at ambient conditions and remained closed during the test. Following the main-tank fill to a level above the IDU (indicated by RL10), the main-tank pressure was increased to 50 psig and controlled at this level. The IDU was locked up at 3 psig and the pressure monitored for any increase. Temperatures inside the IDU were monitored to assure steady-state conditions were maintained. The pressure increased to 3.65 psig in 30 minutes, for a rate of approximately 3.51×10^{-4} psi/sec. The top temperature (T3) indicated an increase from 45.5 to 56°R, whereas the bottom temperatures were maintained

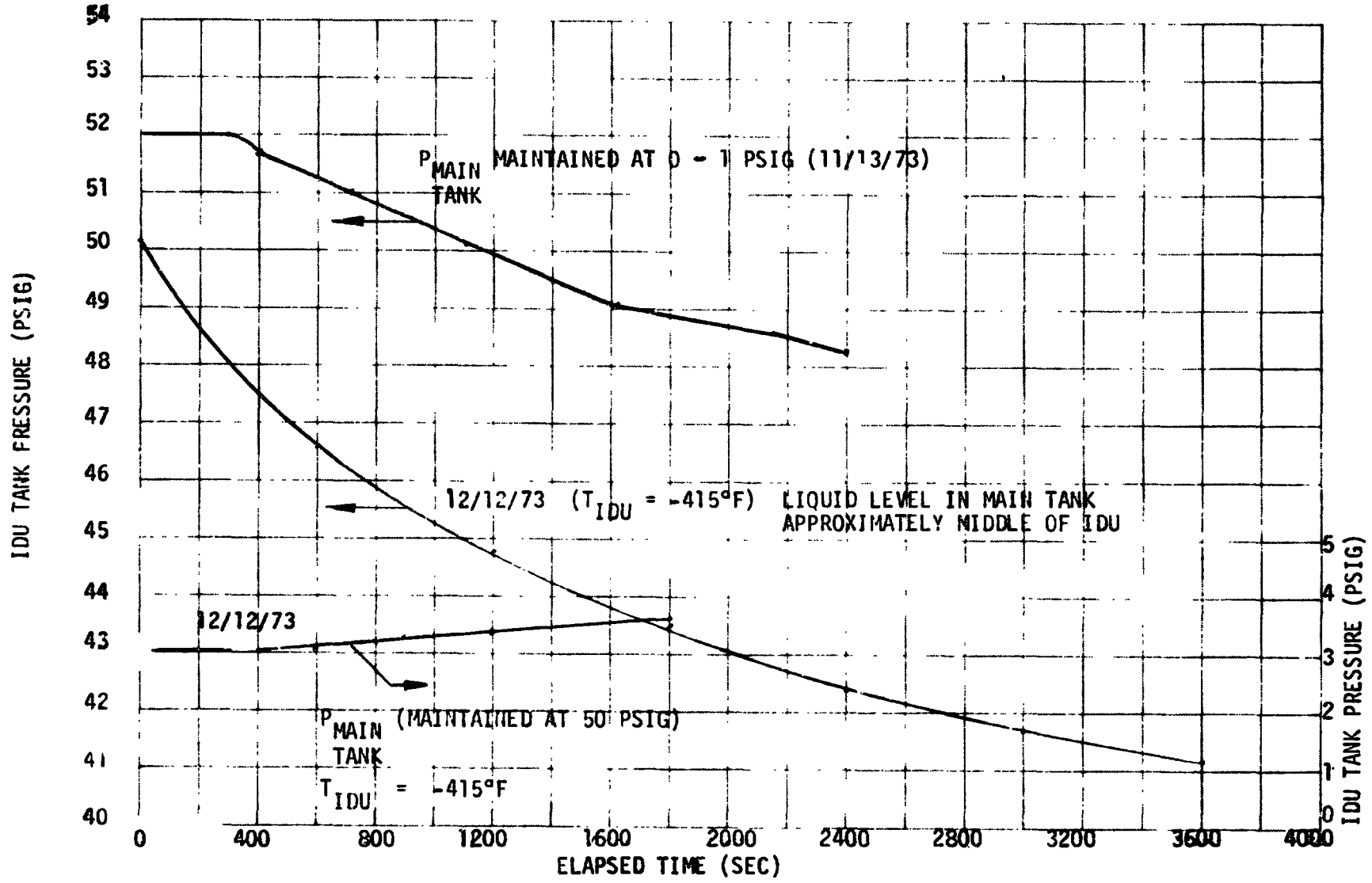

Figure 4-3 TEST I - TANK LEAKAGE - CRYOGENIC

at approximately 40°R. The effective pressure increase due to temperature increase in the top portion of the IDU would be of the order of 2.8 psi, assuming a linear temperature increase from the bottom of the tank to the top. The actual temperature profile for a typical stratified ullage would not be linear over the IDU tank length since liquid in the main tank is above the bottom of the IDU; however, the level is indeterminate. It can only be concluded that the pressure increase is probably due primarily to the temperature increase in the top region of the IDU, which is the result of a lowering of the main-tank liquid level from boiloff. Neglecting the temperature increase effect, the observed pressure increase of 0.65 psi would correspond to approximately 0.035 lb of hydrogen gas in 1,800 sec, for a rate of 2×10^{-5} lb/sec or 0.2 SCFM of hydrogen, which indicates that the observed pressure increase is due to heat flux into the IDU, since valve closure was complete under ambient conditions. Also, the leakage based on the 10 SCIM nominal rate at 40°R, as well as the ambient leak test data, are much lower than the 0.2 SCFM required to produce the observed pressure increase.

The IDU was then pressurized to 50.2 psig and the main tank vented to atmosphere and the pressure decay rate of the IDU observed. Results are shown in Figure 4-3. Temperature readings were not obtained during the first 30 minutes of the test due to a faulty connection in the vacuum chamber, but subsequent temperature readings indicated steady-state conditions were obtained. The pressure decay rate during the period from 12:13 to 12:33 indicated a loss rate approximately the same as that observed during the 13 November tests.

4.10 TEST J - SCREEN BREAKDOWN, PRESSURIZATION, AND IDU REFILL

The objective of this series of tests was to determine the breakdown point of the IDU liquid hydrogen acquisition device (LHAD) for various flowrates, including "static breakdown" conditions, for both cold helium submerged and overhead pressurization, as well as cold and ambient overhead hydrogen pressurization. A series of tests at a maximum flowrate of 7.5 lb/sec was scheduled. Because of the difficulties encountered with the Parker submerged liquid hydrogen valve, the test plan was modified, and high flowrate tests

could not be performed. However, except for the problems encountered with sporadic valve opening and closing malfunctions, the basic response of the system was as expected. IDU outflow and breakdown levels indicated that the screen device static bubble point was not adversely affected by the tests, successful screen devices (LHAD) refill was accomplished following breakdown, and, with one exception, all instrumentation functioned properly. A carbon point-level sensor (RL7) (located inside the LHAD annulus at the top of the device, between two of the 1-inch diameter tubes from the central pipe) did not properly indicate breakdown in some cases, apparently because of liquid "hang up." However, breakdown readings were obtained in all cases because of a characteristic hump in the capacitance continuous-level sensor curve as well as measurements of temperature increases within the LHAD.

Details of each outflow test are summarized in Table 4-1 and discussed below. Detailed annotated data are presented in the Supplemental Data Document and examples of test data are presented in Appendix H. Selected data for breakdown level at various outflow rates are compared in Figure 4-4 with the analytical predictions obtained from the flow-loss computer program of Appendix F. It should be noted that the screen device performs better than predicted in the majority of tests with the cold pressurant, as shown, for example by Test J-19. The use of warm pressurant, however, resulted in premature breakdown.

Certain tests were not performed due to the valve malfunctions, and data on flowrate versus pressure drop across the valves is of little use since the valves would not open fully. Another difficulty encountered which limited the rate of outflow from the IDU was the limitation on the rate of venting the main tank. The main-tank vent (Port B of Figure 2-15) was used as a conduit for the electrical wires, and the reduction in flow area limited the rate at which the main tank could be vented. As a result, the initial outflow rate from the IDU to the main tank was higher than the final rate before breakdown, for the high flowrate cases. For example, the initial outflow rate for Test J-25 was 1.5 lb/sec, whereas the final outflow rate was 0.73 lb/sec.

Table 4-1
TEST J - OUTFLOW

Test No.	Final Outflow Rate prior to Breakdown (lb/sec)	Breakdown Height (in.)	Pressurant	Diffuser	Approximate Pressurization Gas Temperature in IDU, T4 (°R)	Liquid Hydrogen Saturation Pressure (psia)	IDU Pressure (psia)	Main Tank Pressure (psia)	Approximate Pressure Difference (psi)	Remarks
J-3	0.250	2.85	Helium	Overhead	40	15	25	25		
J-5A	0.0	2.25	GH_2	Overhead	40	15	25	25		Depleted GH_2 supply; main tank vented to obtain expulsion from IDU to main tank. Negligible GH_2 pressurant used
J-5B	0.108	4.20	GH_2	Overhead	40	15	25	25	0 to 0.4	
J-5C	0.236	6.00	GH_2	Overhead	56	15	25	25		
J-7	0.540	15.00	GH_2	Overhead	100	15	25	25	0 to 2.0	Warm GH_2 causes premature breakdown. RL7 indicates breakdown in 5 sec
J-11	0.313	2.25	Helium	Overhead	40	15	25	24	1.0	
J-19	0.554	2.85	Helium	Overhead	40	15	25	25		
J-21	0.440	10.00	GH_2	Overhead	46	15	26	26		Warm GH_2 causes premature breakdown
J-25A	0.726	2.50	Helium	Submerged	40	15	25	25	4.2	
J-25B	0.554	2.5 to 6	Helium	Submerged	40	15	25	25		Apparent "breakdown" at h_B = 6 in. followed by expulsion may have been due to spurious liquid level indication, due to helium bubbles
J-27A	0.200	2.25	Helium	Overhead	40	15	27	27		
J-27B	0.783	2.95	Helium	Overhead	40	15	25	25	0.1	
J-29	0.163	2.25	GH_2	Overhead	40 to 56	15	27	27		No premature breakdown
J-31	1.300	14.70	GH_2	Overhead	>100	15	35	35	0.1	Premature breakdown
J-33A	0.750	2.25	Helium	Submerged	40	15	25	25	0.1	
J-33B	0.650	2.85	Helium	Submerged	40	15	37	33	4.0	
J-35A	0.893	6.40	Helium	Overhead	73 to >100	15	35	35	0.1	Premature breakdown due to warm helium
J-35B	0.517	2.55	Helium	Overhead	45 to 60	15	35	30	2 to 5.0	Premature breakdown due to warm helium
J-35C	0.761	2.85	Helium	Overhead	40 to 59	15	35	≈20 to 35	0 to 12.0	Premature breakdown due to warm helium
J-39	0.36	14.70	GH_2	Overhead	60 to >100	15	24	16	8.0	Premature breakdown due to warm GH_2

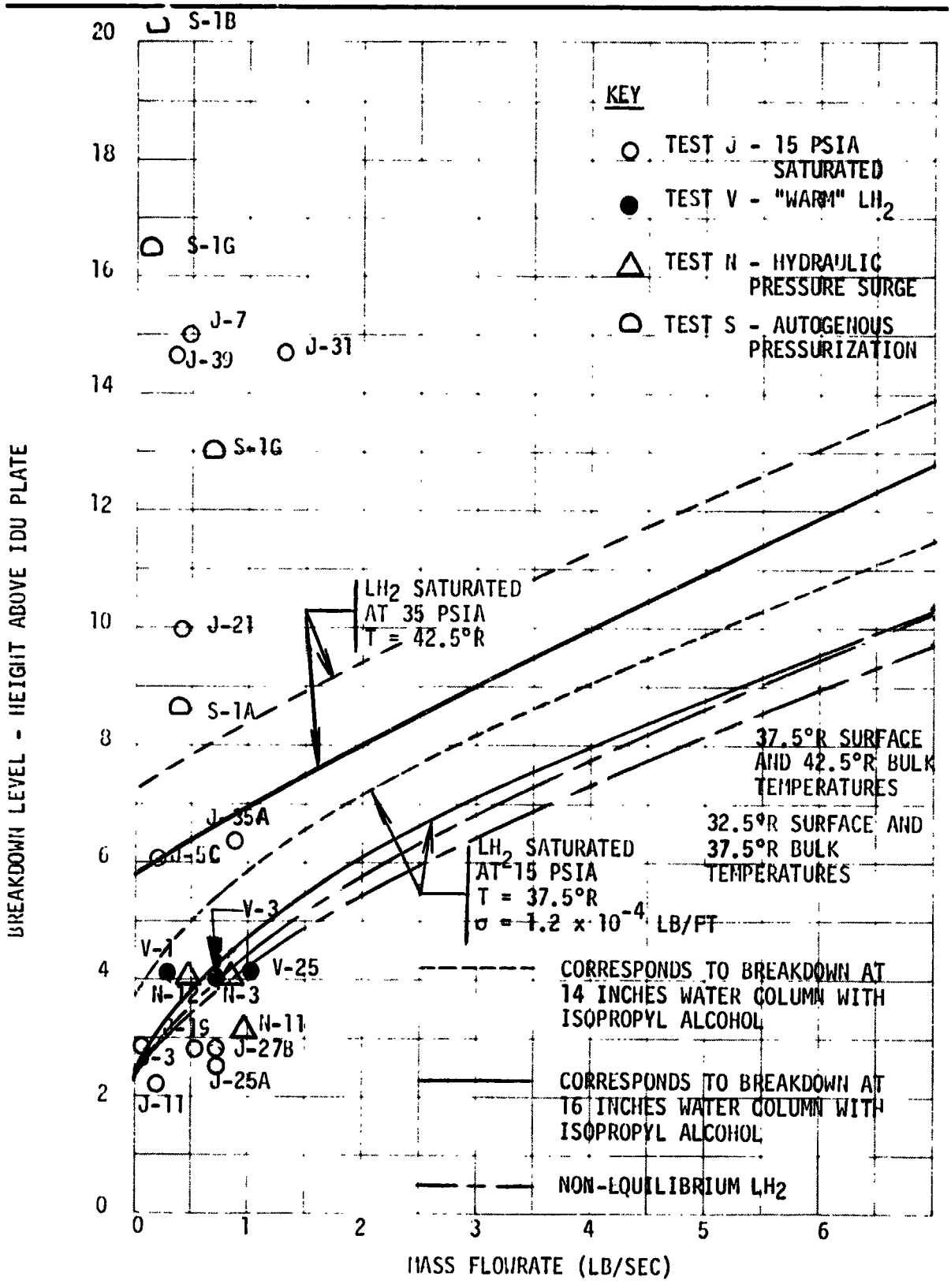

Figure 4-4 IDU BREAKDOWN LEVEL AND OUTFLOW RATE

C-2

Different methods of IDU pressurization were used to evaluate the effects on screen device performance. The methods used for IDU pressurization were:

- Cold submerged helium
- Cold overhead helium
- Warm overhead helium
- Cold overhead hydrogen
- Warm overhead hydrogen

Tests J-25A, J-25B, J-33A, and J-33B showed that breakdown occurred near the bottom of the LHAD (2.25 to 2.85 inches above the bottom of the tank) with a submerged screen depth no greater than 0.5 inch, for flowrates from 0.5 to 0.73 lb/sec. The helium was passed through the pressurization gas heat exchanger located below the IDU, and additional cooling was achieved by the gas bubbling up through the LH_2 in the IDU. Heat transfer effects on breakdown were of negligible importance in these cases. Since the flowrates obtained were relatively low, viscous and dynamic pressure losses were low, and hence breakdown occurred very close to the bottom of the LHAD screen. Test J-25B shows a spurious indication of breakdown at 6 inches, as determined by the "hump" in the capacitance probe liquid height versus time curve, but this is probably not an actual breakdown since expulsion continues to the 2.5-inch level.

Tests J-3, J-11, J-19, J-27A, J-27B, J-35B, and J-35C also showed that breakdown occurred near the bottom of the IDU, for flowrates ranging from 0.25 to 0.78 lb/sec. Tests J-35B and J-35C showed that helium temperatures of the order of 60°R, as measured by temperature probe T4 inside the LHAD (at the top of central column), did not cause an observable degradation in breakdown level of the LHAD. Since T4 is inside the LHAD, its measured gas temperature would be less than the gas temperature surrounding the LHAD. The outflow periods were of the order of one minute; it is not clear what the effects on the screen device would have been with longer periods of exposure of the LHAD to the 50 to 60°R warm gas.

The data obtained for the overhead and submerged cold helium pressurization indicates that either of these is satisfactory for LH_2 outflow. However, at higher outflow rates, the higher mass flow of helium entering the IDU through the submerged diffuser would increase the voltage fluctuation or "noise" obtained from the continuous capacitance level sensor, as well as distorting the readings from the capacitance point-level sensors. Therefore, use of the overhead diffuser is recommended, with cold helium.

Tests with both warm gaseous hydrogen and warm helium pressurant showed a marked decrease in effective screen bubble point. As expected, the heat flux caused screen drying and premature breakdown. The warm gaseous hydrogen (autogenous) pressurization caused a greater reduction in effective screen bubble point than warm helium. This may be due to the higher heat-transfer coefficient for hydrogen condensing on the upper solid portions of the LHAD compared with the lower free convection heat-transfer coefficient for the helium near the top of the LHAD.

Test J-35A, with helium temperatures ranging from approximately 70° to over 100°R, showed breakdown at a liquid level of 6.4 inches above the bottom of the IDU. By contrast, Test J-5C, with 56°R gaseous hydrogen, showed breakdown at 6 inches; Tests J-7, J-31, and J-39, with approximately 100°R gaseous hydrogen, showed breakdown at approximately 15 inches.

These tests do not prove that warm pressurant cannot be used with screen devices since the LHAD has a relatively large area of exposed stainless steel annular channel to which the 250 x 1370 screen is welded. Heat transfer through this region could cause boiling and screen dryout that could perhaps be avoided by a design which had a minimum of exposed sheet metal surface. The LHAD was originally intended to supply liquid hydrogen, using cold helium pressurant, hence heat transfer effects were not an important consideration in its design. Consequently, the LHAD was designed to minimize fabrication costs rather than to optimize its performance with warm pressurant.

IDU refill test data are summarized in Table 4-2, and the annotated data from the strip chart presented in the Supplemental Data Document. The maximum inflow rate obtained was 8.35 lb/sec (Test J-26A) which was obtained with V4 (see Figure 2-15) wide open.

Two types of refill were demonstrated: (1) refill through PV2, which is the procedure for "start tank" refill, and (2) refill through PV1 and PV3. The latter procedure "backfilled" the IDU by flowing liquid up the control IDU column, through the four communication tubes to the annulus. Refill directly through PV2 brought liquid into the IDU through the refill diffuser. Both methods refilled the IDU completely, as determined by RL7 and T4 data. In both cases, the screen port (see Figure 2-6) appears to have allowed gas inside the LHAD to pass out of the annular region until the liquid level, both inside and outside the annular region, covered the screen port, wetting and sealing it. If the LHAD had not refilled completely, T4 and/or RL7 would have indicated the presence of the gas, at least in some cases. Neither indication was observed, and therefore, it appears that either refill method can be used successfully. The preferred procedure is to refill through PV2. Refill through PV1 and PV3 results in flow out of the screen device, which places an

Table 4-2
TEST J - IDU REFILL

Test No.	IDU Initial Liquid Height (in.)	IDU Final Liquid Height (in.)	Refill Time (sec)	Refill Rate (lb/sec)
J-2	18.5	31.5	42	0.47
J-6A	4.2	31.5	38	1.1
J-6B	4	31.5	24	1.76
J-10	6.2	31.5	75	0.52
J-18	16	31.5	12	3.24
J-24	10	31.5	28	1.18
J-26A	20.5	31	2	8.35
J-26B	5.8	31	28	1.38
J-28	14.4	31	17	1.5
J-32	2.6	22.8	16	1.94
J-34A	5.8	31	26	1.5
J-34B	9.6	30.2	25	1.27
J-38	14.4	31	23	1.11

outward pressure on the inner cylindrical screen, which is not supported. Therefore, continued refills in this manner at high rates could conceivably cause failure of the screen weldment to the supporting annulus, or bubble-point degradation. Further, refill through PV1 and PV3 can introduce gas into the LHAD, which is minimized by refill through PV2. It was necessary in our tests to both verify the refill procedure using PV1 and PV3 and to use this technique when PV2 would not open (and vice-versa). Refill through PV2 is a proven and preferred technique and should be used in general.

The response of the continuous-level sensor to IDU refill was satisfactory in all cases. Refill through PV1 and PV3 resulted in a smoother output voltage versus time curve than for refill through PV2. Refill through PV2, even with the refill diffuser, results in surface sloshing, as shown in the water tests of Figure 4-2. As the liquid level in the IDU rises, the surface disturbance decreases. In the worst case (Test J-18), a voltage fluctuation of ±0.1 volts was observed, which corresponds to a measured liquid-level variation of ±0.75 inch. Most of the data showed a liquid-level variation of less than ±0.5 inch.

4.11 TEST K - EXPULSION/REFILL

The objective of this test was to demonstrate the complete IDU sequence of operations involved in the start tank procedure for engine start, refill, and continued expulsion. The maximum expulsion outflow rate obtainable through the relatively small (1 in.) port of the main tank (with the additional flow losses associated with the liquid hydrogen vent system) was 0.75 lb/sec. The complete outflow and refill procedure was demonstrated, as shown by the data of Test K-2 of the Supplemental Data Document. Outflow through PV1 was initiated with the IDU full; it continued to a liquid level of 5.8 inches, where PV2 was opened and refill, along with outflow, continued until the main tank was depleted of liquid hydrogen. The IDU was refilled to a level of 24 inches. Breakdown did not occur during this test.

4.12 TEST L - VALVE SEQUENCING BY OPERATOR

The objective of this test was to determine whether the test conductor could manually actuate the PV valves during IDU expulsion before breakdown for refill or for halting expulsion. Because of the difficulties with the PV valves, this test could not be performed as planned. Experience at the flow rates of approximately 1 to 2.5 lb/sec (e.g., Tests N-1 and N-12) revealed no difficulty with manual flow control, and it is expected that manual control could be used for flow rates of the order of 4.5 lb/sec.

4.13 TEST M - THERMODYNAMIC VENT SYSTEM FLOWRATE VERSUS PRESSURE

The objective of this test was to determine the TVS mass flowrate as a function of pressure for the various combinations of viscojet flow control orifices, and to compare the results with analytical predictions. These tests were performed with a TVS line pressure of approximately one atmosphere, and an IDU pressure of approximately two atmospheres.

Tests were performed on 14 November 1973. The IDU and main tank were partially full of LH_2; the IDU was pressurized with cold helium through the overhead diffuser. The TVS flow control valves, SV1, SV2, ..., SV6, shown in Figure 2-15, were opened in a sequence that allowed the mass flowrate to increase with each step, except in three cases. In all cases in which the successive opening of a valve led to an expected flowrate increase, the flowrate agreed well with predicted results. However, in those cases where certain valves were opened and closed to decrease the flowrate, the measured outflow rate would stabilize at a higher value than expected and in the case of Test M-27, not reach a steady flowrate for periods in excess of 20 minutes. This inconsistency was not noted during Tests M6 and M7 since the flowrates appeared to represent steady-state values for periods of 5 to 10 minutes. In restrospect, it is seen that the flowrates in these cases were high due to the presence of additional liquid in the TVS tube which was evaporating, and contributing to the total flowrate almost as if additional flow control valves were open. The time to reach equilibrium would be shorter if the heat flux to the TVS were higher. In these tests, heat flux to the TVS was quite low since the IDU was submerged in LH_2 over most of its height. However, heat-flux data was not taken during these tests.

Data are compiled in Tables 4-3 and 4-4 and test results are shown in Figure 4-5 where the analytical results are given for comparison.

Using data from Reference 10, the correlation of flowrate and pressure drop for saturated (x>0) versus subcooled hydrogen (x=0) in the viscojet was found to be improved if the effective density of the two-phase fluid was used instead of the liquid density. The average effective density of the two-phase fluid in the viscojet is given by

$$\rho_{TPF} = (1 - \frac{x}{2}) \rho_{LH_2} + \frac{x}{2} \rho_{LH_2} \qquad (4\text{-}1)$$

where x is the vapor quantity at the viscojet exit. Figure 4-6 shows data for the VJ-1 viscojet (P/N 38VL1-CM) which was used in earlier MDAC IRAD tests. Agreement between the subcooled and saturated conditions (inside the viscojet) are seen to compare well. Over the range of conditions tested with the IDU/TVS, data were found to correlate adequately using pressure drop times liquid density versus flowrate, since the quality was less than 0.1 in all cases.

As discussed in Appendix D, the flow resistance of the viscojets is given in terms of LOHMS, with

$$L\ (LOHMS) = \frac{1270\ f}{\dot{m}_L} \sqrt{\Delta P\ \rho_L}\ , \quad \rho_L \text{ corresponds to single phase, subcooled fluids} \qquad (4\text{-}2)$$

where LOHM is a flow resistance unit corresponding to the flow of 100 gallons/minute of 80°F water with a pressure drop of 25 psi. The factor f is required for specific fluids. Previous tests (Reference 13) showed this value to be f = 0.823 for liquid hydrogen.

The data confirmed the expectation that total flowrate for multiple parallel paths is given by,

$$\dot{m} = 1{,}270\ f\ \sqrt{\Delta P \rho_{TPF}} \left[\sum_{i=1}^{n} \frac{1}{L_i} \right] \qquad (4\text{-}3)$$

since the flowrates from viscojets in parallel are additive.

Table 4-3

THERMODYNAMIC VENT SYSTEM FLOWRATE VS PRESSURE
(IDU pressure = 29.7 psig)

Test No.	Valves Opened	Flowrate Measured (lb/hr)	IDU Line Pressure (in. hg)	(psia)	LH_2 Inlet Temperature (°F)	Remarks
M-1	SV1	0.312	30.3	14.87	- 420.5	
M-2	SV2	0.439	30.6	15.02	- 420.5	
M-3	SV3	0.936	31.2	15.32	- 420.0	
M-4	SV4, SV7	1.151	31.5	15.46	- 420.5	
M-5	SV5, SV7	1.58	32.6	16.00	- 420.5	
M-6	SV1, SV3	1.432	31.5	15.46	- 420.0	Flowrates are high, probably due to steady-state condition not being reached
M-7	SV2, SV3	1.432	31.8	15.61	- 420.0	
M-8	SV1, SV4, SV6	1.432	31.9	15.66	- 421.0	
M-9	SV2, SV4, SV6	1.50	32.2	15.81	- 421.0	
M-10	SV1, SV5, SV6	1.94	32.8	16.10	- 421.0	
M-11	SV2, SV5, SV6	2.18	33.1	16.25	- 421.5	
M-12	SV1, SV2, SV5, SV6	2.31	33.4	16.4	- 421.5	
M-13	SV3, SV5, SV6	2.62	34.0	16.69	- 421.5	
M-14	SV1, SV3, SV5, SV6	2.81	34.3	16.84	- 421.5	
M-15	SV4, SV5, SV7	3.0	35.0	17.19	- 421.5	
M-16	SV1, SV4, SV5, SV6	3.07	35 4	17.38	- 421.5	
M-17	SV2, SV4, SV5, SV6	3.25	35.5	17.43	- 422.0	
M-18	SV3, SV4, SV5, SV6	3.32	35.8	17.58	- 422.0	
M-19	SV1, SV3, SV4, SV5, SV6	3.56	36.2	17.78	- 422.0	
M-20	SV2, SV3, SV4, SV5, SV6	3.72	38.2	18.76	- 421.5	
M-21	SV1, SV2, SV3, SV4, SV5, SV6	3.97	36.1	17.73	- 421.5	

Table 4-4

THERMODYNAMIC VENT SYSTEM FLOWRATE VS IDU AND TVS PRESSURE

Test No.	Valves Opened	Flowrate Measured (lb/hr)	IDU Pressure (psia)	TVS Line Pressure (psia)	TVS Inlet Temperature (°F)	Remarks
M-22	SV1	0.312	50.4	15.2	-422	
M-23	SV2	0.720	50.4	15.2	-422	
M-24	SV3	1.37	50.4	15.7	-422	
M-25	SV4,SV7	1.75	50.4	16	-422	
M-26	SV5,SV7	2.88	49.5	17	-422	
M-27	SV2,SV3	-	-	-	-	Spurious reading due to slow boil-off of liquid remaining in tube from previous flow. Test halted
M-28	SV2,SV5,SV6	3.15	49.9	17.7	-416	
M-29	SV1,SV2,SV5,SV6	3.34	49.7	17.7	-416	
M-30	SV4,SV5,SV7	3.93	49.7	18.7	-420	
M-31	SV1,SV3,SV4,SV5, SV6	4.68	50.8	19.2	-420	
M-32	SV1,SV2,SV3,SV4, SV5,SV6					No data since all liquid drained from IDU

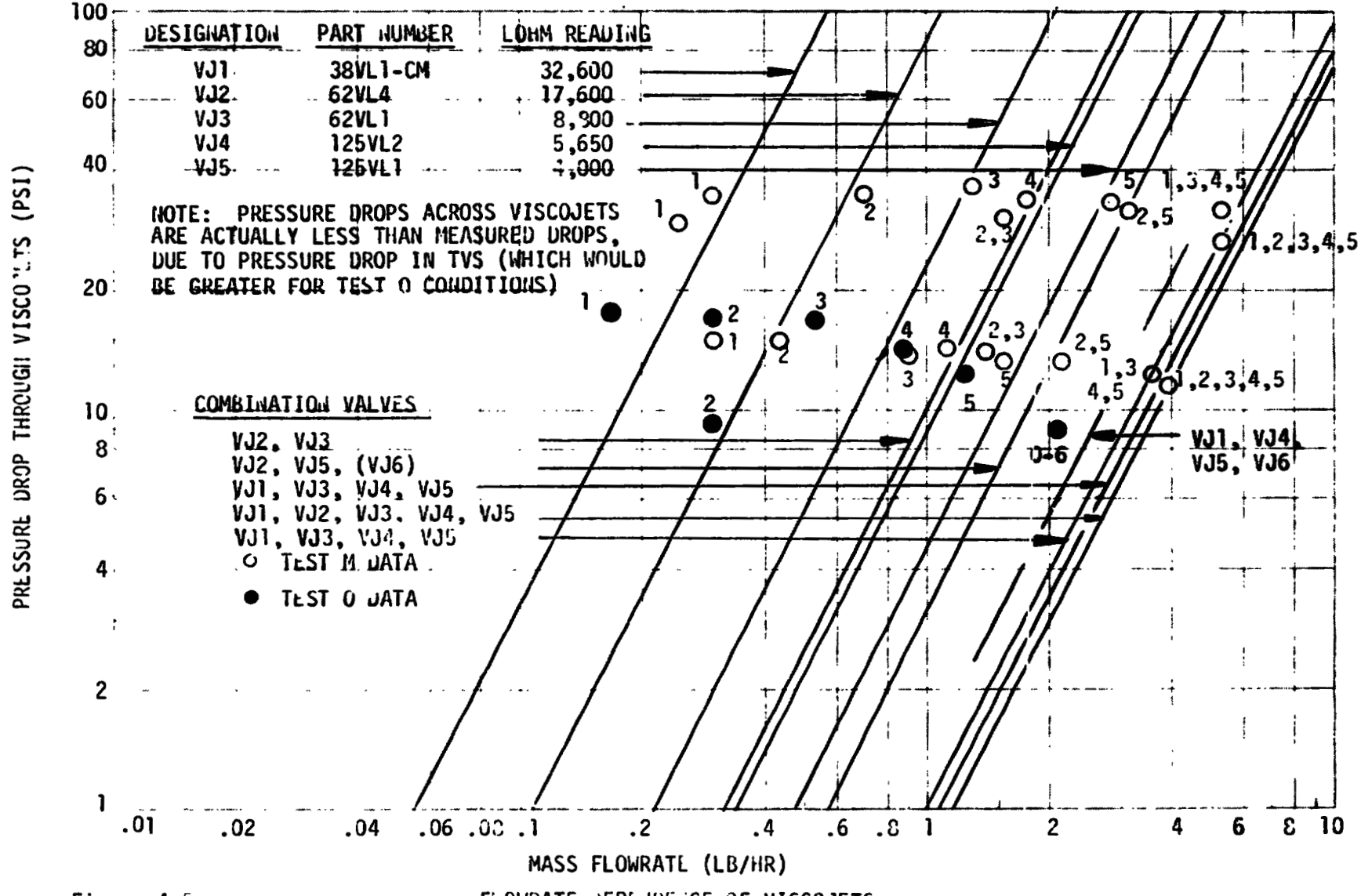

Figure 4-5 FLOWRATE DEPENDENCE OF VISCOJETS

DATA FROM MDAC REPORT MDC G3092,
JUNE 1972
VISCOJET - 38 VL1-Cm

$$\rho_{TPF} = \left(1 - \frac{X}{2}\right) \rho_{LH_2} + \frac{X}{2} \rho_{GH_2}$$

- ○ SUBCOOLED HYDROGEN, X = 0
- △ SATURATED HYDROGEN, X ≠ 0
- ⬭ IDU/TVS DATA

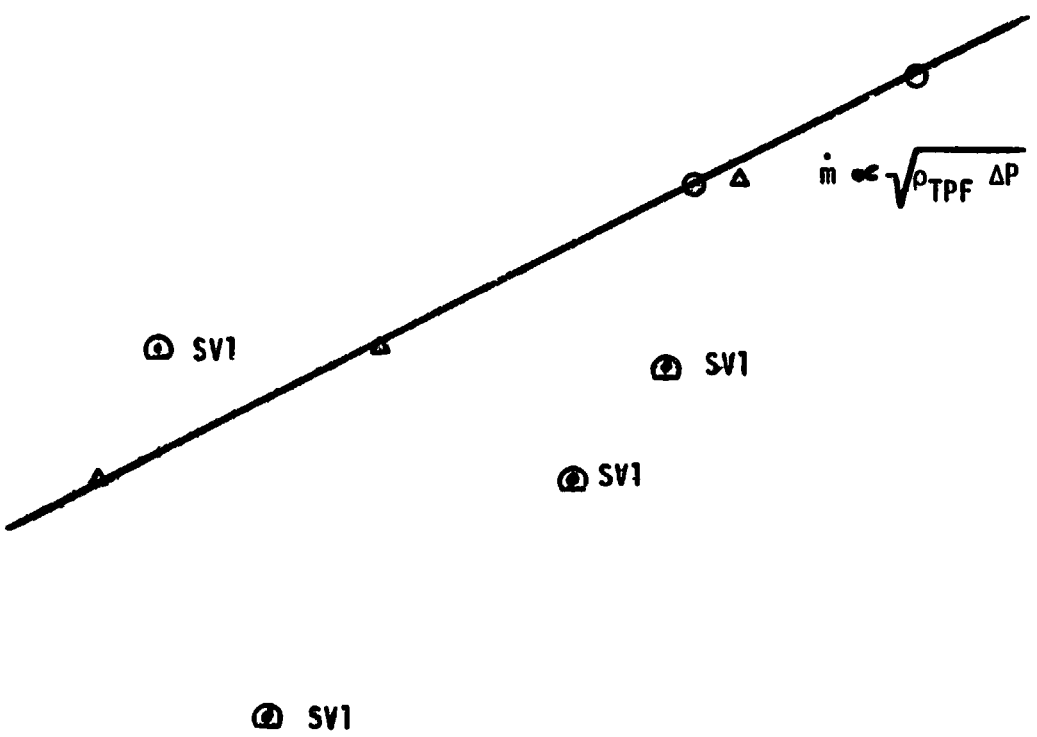

$\dot{m}$, VISCOJET MASS FLOWRATE, LB/HR

10 20 30 40 50 60 70 80 90 100

MODIFIED PRESSURE DIFFERENCE, $[P_{TANK} - P_{TVS_{INLET}}] \frac{\rho_{TPF}}{\rho_{LH_2}}$

Figure 4-6 FLOWRATE CORRELATION

Where ρ_{TPF} is a more general correlation parameter than ρ_L. Equation 4-3 is recommended for predicting flowrate as a function of quality, x, and pressure drop across the viscojet. In the analysis of Appendix I, the pressure drop across the viscojet is shown to be two orders of magnitude greater than the pressure drop along the TVS tube (see Figure D-1), and therefore, the pressure difference between the IDU ullage and the TVS exit should adequately represent the pressure drop across the viscojets. However, no measurements were made of the pressure drop in the TVS line, and therefore the measured total pressure drop may exceed the actual pressure drop across the viscojets alone. This may explain the fact that some of the data show a smaller than expected maximum flow rate for the measured pressure drops.

4.14 TEST N - HYDRAULIC PRESSURE SURGE

Exploratory tests were performed to determine the effects of pressure transients induced by valve opening/closing on screen device retention capability. Five tests were performed in which valve opening/closing was partially successful. Numerous tests were attempted, without success, due to valve malfunction. In particular, PV1 failed to open in the majority of cases. Because of the relatively low flow rates (1 lb/sec), the pressure surges encountered at the screen were relatively low. The expected pressure surge level was analyzed as a part of the parallel effort of NAS8-27685, Reference 1. The MDAC Liquid Propulsion Feed System Dynamic Analysis Program, H572, was used to determine pressure and flow conditions caused by valve opening and closing. The program uses a nonlinear description of components at discrete junctions with solutions to the flow between junctions obtained by the method of characteristics. Using a mathematical model of the IDU, results were obtained for pressure transients of both a rigid and compliant annular screen device. For a steady-state flow rate of 6.5 lb/sec, the pressure excursion at the top of the screen device was found to vary from 1 psi above the ullage pressure to 2 psi below the ullage pressure assuming a valve opening time of 100 Ms. However, the maximum flow rates obtained during the test was 1 lb/sec, and since the pressure surge is proportional to the steady-state velocity of the flowing fluid, the maximum pressure surges at the screen would be expected

to be of the order of 0.15 to 0.3 psi. Attenuation of the pressure transient due to screen compliance would be expected to further reduce the pressure surge. The critical condition for screen device retention capability is the valve-opening induced rarefaction wave effect, rather than the valve closing induced compression wave effect since the resulting pressure drop inside the screen device can cause gas ingestion through the screen (Reference 14). The total flowrate out of the IDU was not necessarily through the screen device and PV1. Since the refill valve often gave indications of incomplete closure, some of the outflow was undoubtedly through PV2. Therefore, the pressure decrease due to PV1 opening would be less than if PV2 were not leaking. In spite of these difficulties and low flowrates, there were three cases in which opening of PV1 was followed by an apparent premature breakdown. Oscillograph data for the tests are given in the Supplemental Data Document. Results are summarized in Table 4-5 Tests N-1, N-2, and N-3A show breakdown occurring 0.5 second after PV1 is opened, but the liquid level cannot be determined accurately near the bottom of the tank, because of the nonlinearity in voltage versus liquid level in this region. Therefore the results are questionable.

Opening and closing PV1 with the IDU liquid level 8 to 20 inches above the plate never resulted in breakdown at the flowrates obtainable, and in test. N-11 breakdown did not occur on opening PV1 with the liquid level at 13.5 inches and an apparent outflow rate of 1.04 lb/sec. This flowrate is sufficiently high to cause an unattenuated pressure decrease of the order of 0.3 $lb/in.^2$, which could cause noticeable premature breakdown. The absence of pressure transient induced breakdown significantly preceding the nominal breakdown level could be explained by (1) valve closure is sluggish, thus decreasing the pressure transient (2) the vapor region in the top of the LHAD attenuates the wave, or (3) the actual feedline outflow rate was less than the apparent outflow rate due to leakage from the IDU to the main tank through PV2. Structural compliance could not contribute significantly to the wave attenuation since the wave travels through the relatively ridig feedline, central IDU pipe, across the four arms of the IDU, and to the top of the screen device where breakdown occurs.

Table 4-5

HYDRAULIC PRESSURE SURGE TESTS

Test No.	Flowrate (lb/sec)	Breakdown Level (height above IDU plate, in.)	Breakdown Time after Valve Opening (sec)	Remarks
N-1	0.665	4.25	0.5	PVI would not open until last attempt, followed by breakdown
N-2	0.61	3.0	0.5	Five opening/closing cycles of PVI observed. Apparent leakage out of IDU through PVI and/or PV2
N-3A	0.49	4	0.5	Three opening/closing cycles of PVI observed. Leakage observed when PV3 opened, indicating partial closure of PVI
N-11	1.04	4	10.5	PVI reopened with liquid level 13.5 in. above IDU plate. No breakdown occurred due to pressure transient
N-12	0.48	4	15	PVI reopened with liquid level 9.5 in. above IDU plate. No breakdown occurred due to pressure transient. Leakage observed while PVI closed

4.15 TEST O - TVS FLOWRATE WITH VARIABLE TVS LINE PRESSURE

Based on the analysis of TVS flowrate versus pressure difference, it would not be expected that TVS line pressure would have a first-order effect on flowrate for a given pressure difference. Tests were performed to confirm this expectation; the TVS line pressure was controlled at values ranging from 5 to 15 psia, and flowrates measured and compared with theory. Originally, these tests were to be performed at 5 psia only, but two considerations led to varying the TVS line pressure over the stated range. First, for steady-state thermal isolation (i.e., heat interception), the TVS is required to maintain both a given flowrate and a given temperature inside the TVS line. Maintaining a given temperature of the coolant implies that a given, constant pressure be maintained. Based on the analytical results shown in Appendix G, in most applications of the IDU this pressure will be of the order of 10 psia, and a valve downstream of the TVS coil will be required to throttle the flow to the required TVS line pressure.

A second consideration was that the vacuum pumps available for the tests could not maintain 5 psia in the TVS at the higher flowrates, and therefore, some variation in TVS line pressure was unavoidable.

The TVS schematic drawing of Figure 2-15 shows that line pressure is controlled by needle valves V23 and V24. These were adjusted, as necessary, to vary the line pressure, and hence partially control flowrate for selected viscojets and a constant IDU pressure.

Data obtained from the tests is shown in Table 4-6 and plotted in Figure 4-5. The dependence of flowrates on the square root of pressure difference times the effective two-phase fluid density is partially confirmed within the range of conditions tested, but the flowrate obtained for a given total pressure drop (including the TVS line pressure drop), is lower than predicted. This may be due to the two-phase pressure drop through the TVS being higher than predicted by the analysis of Appendix D. It would be expected that the pressure drop through the TVS would be greater with the lower line pressure and hence higher

Table 4-6

THERMODYNAMIC VENT SYSTEM FLOWRATE VS IDU AND TVS PRESSURE

Test No.	Valves Opened	Flowrate Measured (lb/hr)	IDU Pressure (psia)	TVS Line Pressure (psia)	TVS Inlet Temperature (°F)	Remarks
0 to 1	SV1	0.173	22.6	5	-420	
0 to 2	SV2	0.312	22.7	5	-420	
0 to 3	SV3	0.5	22.7	5.9	-420	
0 to 4	SV4,SV7	0.875	22.6	7.9	-420	
0 to 5	SV5,SV7	1.25	22.6	9.8	-420	
0 to 6	SV1,SV4, SV5,SV6	2.06	22.24	13.2	-420	
0 to 7						No data. Boiling in line prior to viscojet occurred. Increased P_{IDU}
0 to 8	SV2	0.296	20.0	10.2	-422	
0 to 9						No data. Boiling in line prior to viscojet occurred. Increased P_{IDU}
0 to 10	SV4,SV7	0.89	21.1	8.0	-423	

quality obtained in Test 0. Since there were no provisions for measuring TVS line pressure at the viscojet exit, this could not be confirmed. The TVS line was bypassed in Tests 0-4, 0-5, and 0-10 in an attempt to evaluate pressure drops directly through the viscojets. Flow proceeded directly to the overboard vent, as shown in Figure 2-15, through a 1/2-inch outside diameter line. The flowrate in these cases was also low compared to the analytical value. Further, no comparison test was performed, using the same viscojet (e.g., VJ4, or VJ5) and flowing through the TVS line, and therefore, an approximation to the TVS line pressure drop cannot be made.

The test data obtained are sufficient to empirically determine flowrate vs. pressure, and the analytical prediction for viscojet flowrate/pressure dependence still appears to be valid, although the actual pressure drop across the viscojets is not known. It is therefore recommended that at least one additional pressure pick-off point be included immediately down stream of the viscojets in any future tests.

The data obtained is particularly useful since the TVS line pressures corresponds to values required for steady state thermal control of the IDU.

4.16 TEST P - STEADY-STATE THERMAL CONTROL OF IDU

Thermal control of the IDU, or any type of similar tank with a wall mounted TVS heat exchanger, can be accomplished by one of two basic methods: (1) steady-state operation in which the total heat entering the propellant is zero at all times, or (2) transient operation in which the tank pressure is maintained within certain limits by intermittent flow through the TVS. Steady-state operation offers the advantage of minimum transient heat transfer and thermal control problems. (In principal, heat-flux meters can be used to monitor heat flux into the tank. Maintaining TVS outflow so that the overall net heat flux is zero allows rapid response to changing heat flux.) The thermal stratification in the fluid is minimized and the total mass vented is always equal to the amount required to intercept the heat into the tank. The pertinent boundary condition is that the total surface integral of the heat transfer, taken at the inner walls of the tank, be zero. This condition

implies that the maximum temperature between the TVS coils not be equal to desired steady-state temperature of the liquid in the tank. Rather, the maximum temperature is somewhat higher than the tank liquid. Thus, some heat enters the liquid in the vicinity of the midpoint between coils, whereas an equal amount of heat is absorbed from the tank liquid near the coils so that no net heat enters the propellant. This procedure implies that the maximum temperature of the tank liquid approaches the maximum temperature between the coils. The further implication is that boiling will occur unless the total pressure in the tank exceeds the vapor pressure associated with the maximum temperature between the coils. Therefore, the coil separation distance will be governed by the maximum acceptable wall temperature (for a given heat flux). This condition on T_{max} between the coils allows the total TVS tube length and spacing to be determined. Otherwise, a wide variety of combinations of tube length, spacing, and coolant temperatures are possible.

The IDU has been designed so that the steady-state operation can be demonstrated with two coil separation distances. This test flexibility is obtained by the addition of a "Tee" connection in the IDU line, resulting in two spiral loops covering the tank length of 35 ft and 70 ft. In the current test plan, the two 35-ft loops are used in parallel. Additional capability can be obtained by the addition of an SV-90 solenoid valve and an extra TVS outlet line; it is recommended as a desirable addition for any subsequent tests.

The main objective of this test was to demonstrate steady-state thermal control by flowing sufficient coolant, at the required TVS line pressure (and hence coolant temperature) to maintain complete heat interception. Heat flux from the main tank was to be sustained by maintaining a gaseous hydrogen ullage pressure slightly higher than the saturation pressure of the liquid in the IDU, with the result that condensation heat transfer would occur on the IDU tank wall and coils. It must be emphasized that the IDU/TVS is designed so that an external foam should be applied to the tank wall to alleviate condensation heat transfer, but that the foam could not be applied until after these

initial tests. The presence of a relatively cold TVS coil with a surface temperature several degrees below the saturation temperature of the main tank GH_2 results in a relatively high, localized condensation heat-transfer coefficient; this results in high overall heat flux to the coolant, which tends to diminish the effectiveness. Insulation, however, would alleviate condensation and the TVS would then be able to maintain a steady-state thermal condition without the additional complexity of local, high-heat flux to the TVS tube itself.

In these tests, it was originally intended that the IDU be filled with liquid, the PV valves closed, and the proper TVS coolant flowrate and temperature adjusted to maintain a steady-state temperature and pressure inside the IDU. However, the PV valves could not be closed completely, in spite of repeated attempts, and hydrogen continuously leaked from the IDU to the main tank. As a partial demonstration of thermal control, it was decided that the main-tank liquid level would be set at the bottom of the IDU, and the main-tank pressure controlled to approximately 0.2 to 0.3 psi above the IDU pressure. The IDU pressure would be vented periodically to maintain the pressure difference. The net result, it was hoped, would be that liquid in the main tank would tend to flow into the IDU, maintaining a full tank during the test, while the higher external GH_2 pressure would result in heat transfer to the IDU. The TVS coolant flowrate would be adjusted to maintain steady state.

The test was performed as described for over 1 hour, and an overall thermal steady state was demonstrated. The measured heat fluxes showed a higher heat flux into the tank near the top of the IDU, and an approximately zero net heat flux into the IDU near the bottom of the IDU. The results are shown in the data plots, taken directly from the DYMEC Data System, in Figures 4-7 to 4-9. Due to leakage of liquid into and out of the IDU, as well as the IDU venting, the total liquid lost exceeded the expected liquid loss based on the measured flowrate and total test duration. Table 4-7 compares the measured and expected liquid levels.

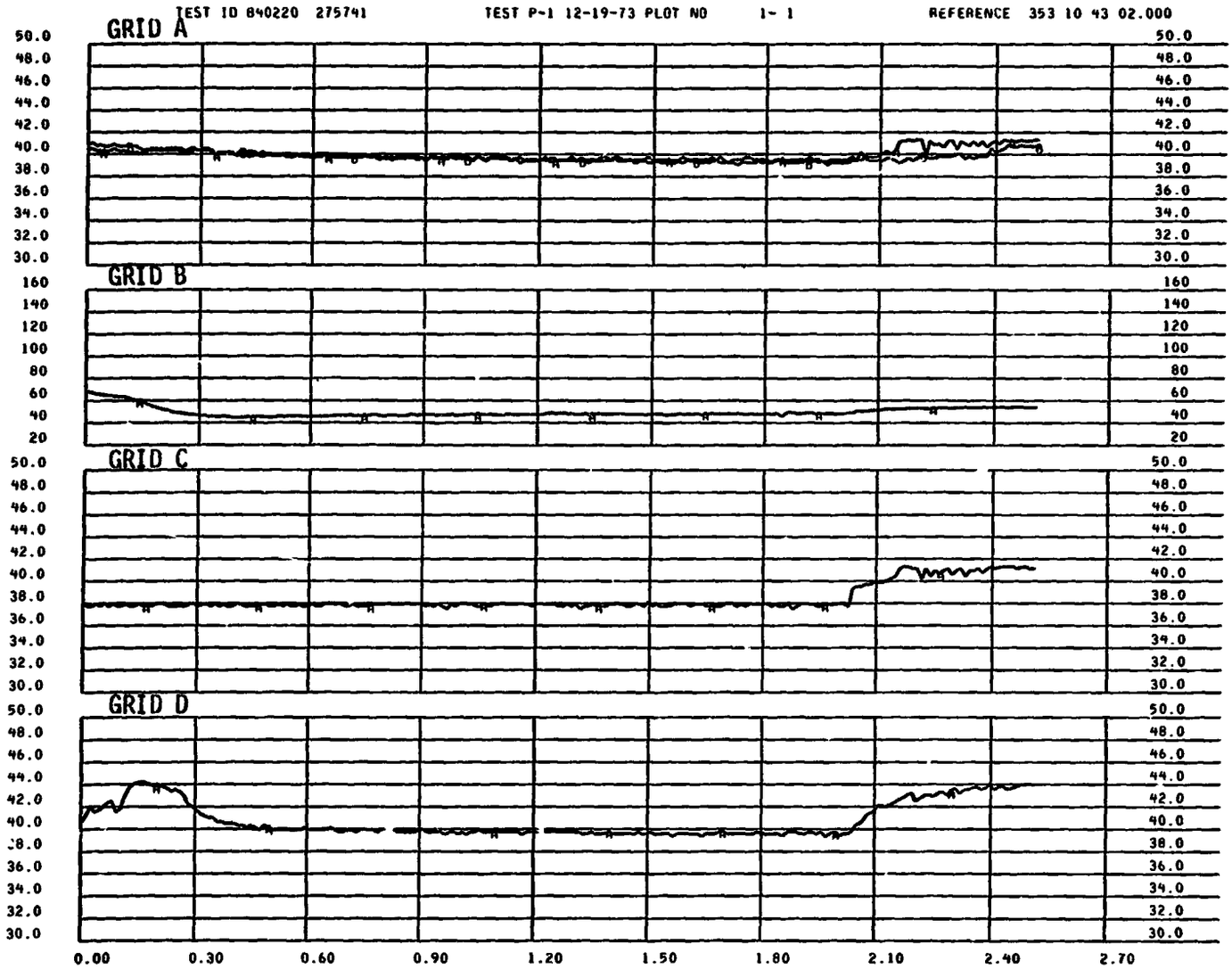

MEAS. NUMBER	CHANNEL ASGN.	TITLE	RANGE	UNITS	GRID-SYM
* T7	7	TVS INLET TEMPERATURE	30.0 TO 50.0	DEGREE R	AA
* T8	8	TVS OUTLET TEMPERATURE	30.0 TO 50.0	DEGREE R	AB
* T9	9	IDU EXTERNAL TANK TEMP AT TOP	20 TO 160	DEGREE R	BA
* T14	14	VJ5 TVS EXPANSION TEMPERATURE	30.0 TO 50.0	DEGREE R	CA
* T15	15	TEMP OUT BOUNDARY LAYER AT HF2	30.0 TO 50.0	DEGREE R	DA

Figure 4-7 – TEST P-1, PLOT NO. 1-1

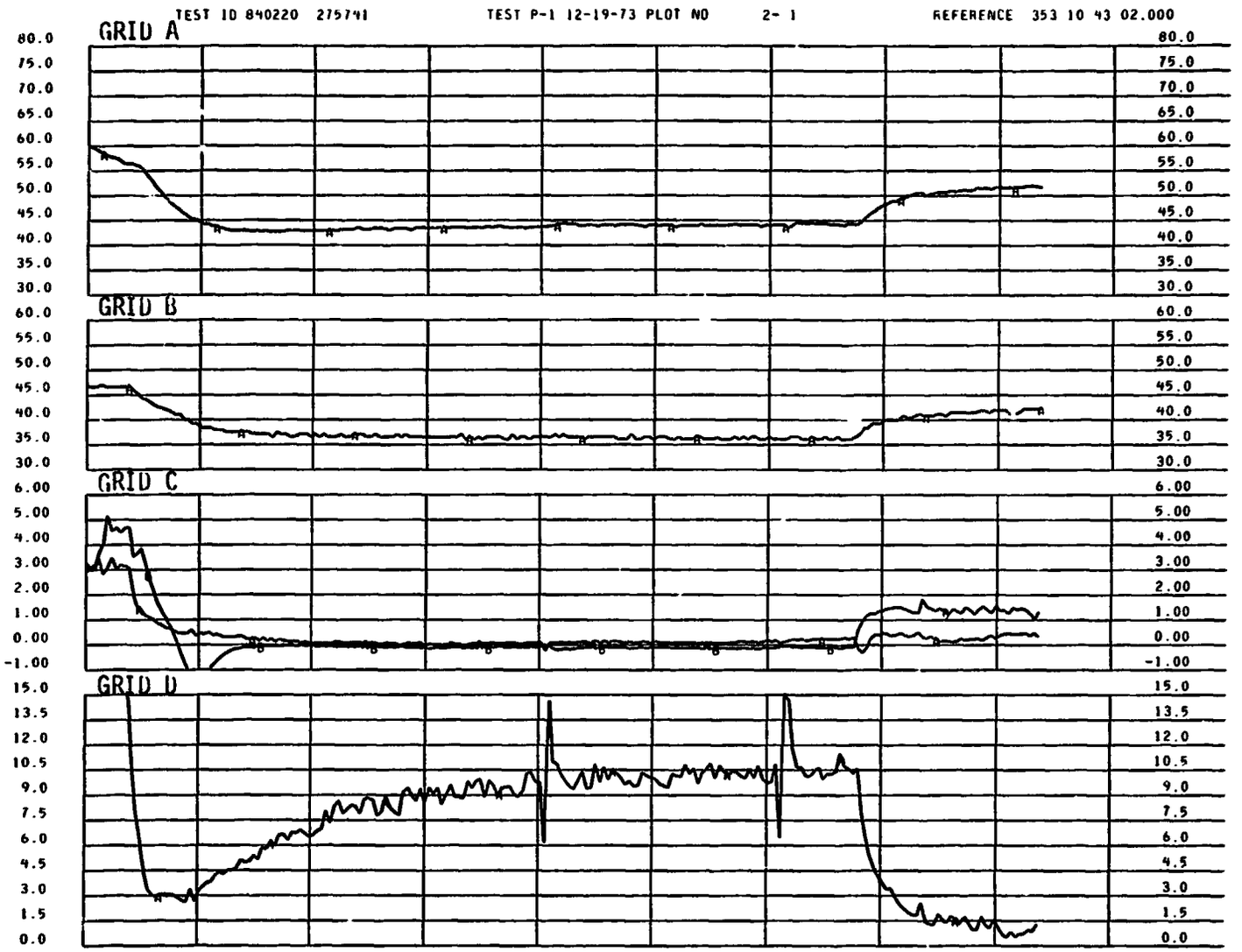

MEAS. NUMBER	CHANNEL ASGN.	TITLE	RANGE	UNITS	GRID-SYM
$ T16	16	TEMP OUT BOUNDARY LAYER AT HF3	30.0 TO 80.0	DEGREE R	AA
$ T19	19	IDU OUTER WALL TEMPERATURE	30.0 TO 60.0	DEGREE R	BA
HF1-B	30	HEAT FLUX NEAR BOTTOM OF IDU,E,(	-1.00 TO 1.00	BTU/HRF2	CA
HF2-A	31	HEAT FLUX NEAR MIDDLE OF IDU,I (	-1.00 TO 1.00	BTU/HRF2	CB
HF3-A	32	HEAT FLUX NEAR TOP OF IDU, INT	0.00 TO 5.00	BTU/HRF2	DA

Figure 4-8 - TEST P-1, PLOT NO. 2-1

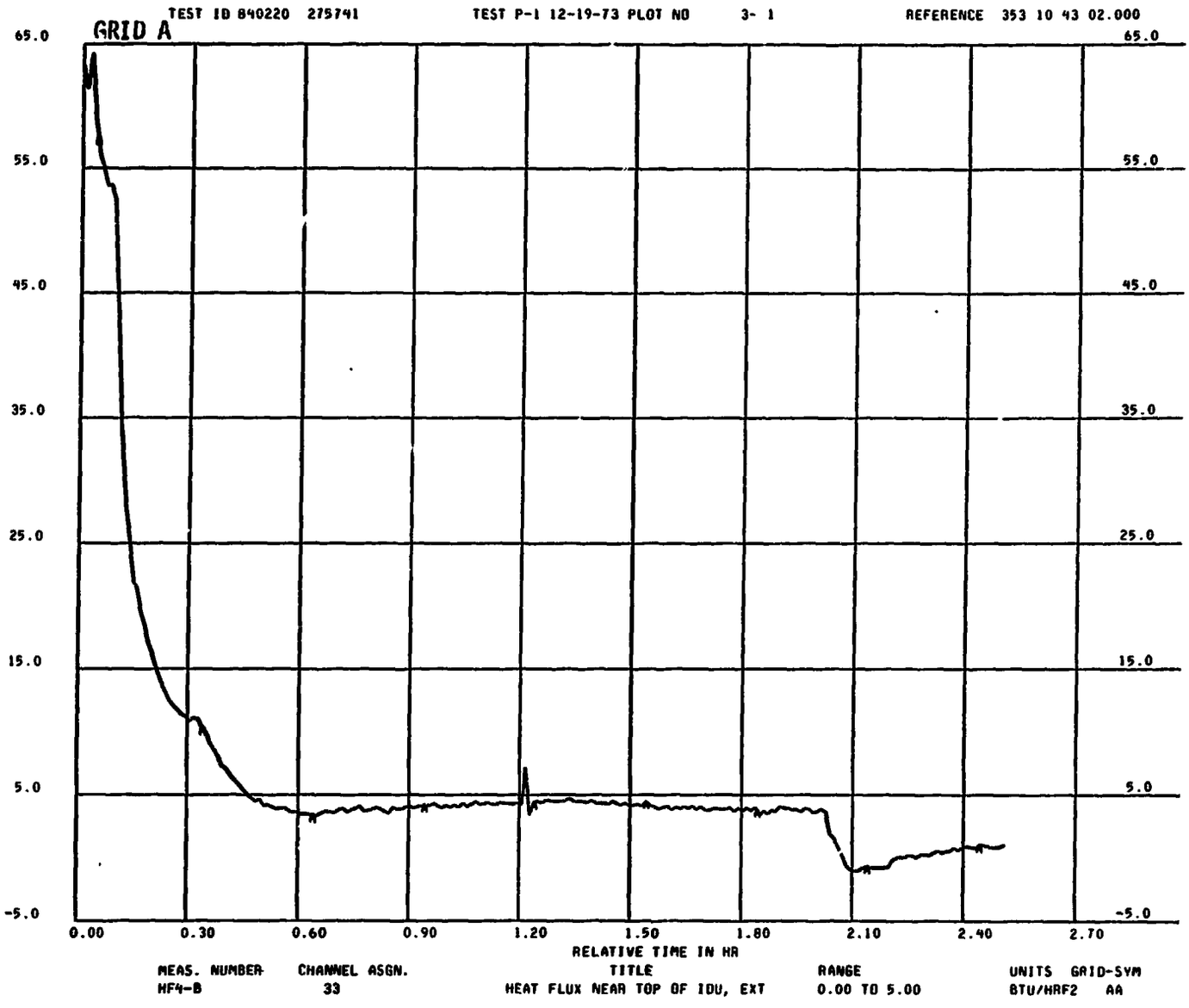

Figure 4-9 -TEST P-1, PLOT NO. 3-1

Table 4-7

TEST P-1 (12/19/73)
TVS OUTFLOW/IDU LIQUID LEVEL CORRELATION

Time	TVS Flowrate (lb/hr)	Total LH_2 Coolant Mass Expelled at Time Shown (lbs)	Expected Liquid Level Above IDU Plate (in.)	Measured Liquid Level (in.)
10:45	2.3	0	22.6	22.6
10:53	2.3	0.306	22.35	19.0
11:13	2.5	1.106	21.77	18.5
12:20	2.5	3.906	19.55	18.0
12:40	2.5	4.739	18.9	16.5

It is recognized that these test results are of limited value from a heat transfer standpoint. However, a steady-state coolant outflow rate was demonstrated, a relatively steady-state heat flow was observed, and all IDU/TVS instrumentation was observed to function properly.

4.17 TEST Q - EFFECTS OF DOWNSTREAM FLOW CONTROL

A basic question concerning the operation of the TVS is the method by which coolant flowrate and temperature can be varied to meet the thermal control requirements and the TVS response. A variable downstream orifice can be used to control the TVS line pressure and hence coolant temperature, while flowrate can be controlled by varying the selected orifice and the IDU pressure with respect to the TVS line pressure. When steady-state conditions are not maintained, transient flow effects occur. The objective of this test was to demonstrate some of the transient phenomena resulting from (1) closing the downstream flow control valve, V24, thus halting the outflow, (2) achieving a steady state, and then (3) reopening the valve. Immediately after Test P, V24 was closed, but the solenoid valves used to provide a controlled flowrate of 2.5 lb/hr were left open. The IDU and TVS conditions were then observed until a steady state was reached. The steady state was observed for approximately 1 hour, and then the TVS flow was reinitiated and conditions monitored. Throughout this period, the main tank and IDU pressures were maintained at 25 psia. The IDU liquid level was approximately 16 inches.

Referring to the selected data of Figures 4-10 to 4-16, the phenomena observed are described below in chronological order. At 12:45:00, valve V24 (see Figure 4-10) was closed, halting all TVS outflow, and entrapping some subcooled liquid in the TVS tube. For a period of approximately 10 to 15 minutes, the coolant in the upper part of the TVS coil was vaporized by heat flux from the main tank ullage, and the vapor and liquid forced back into the IDU.

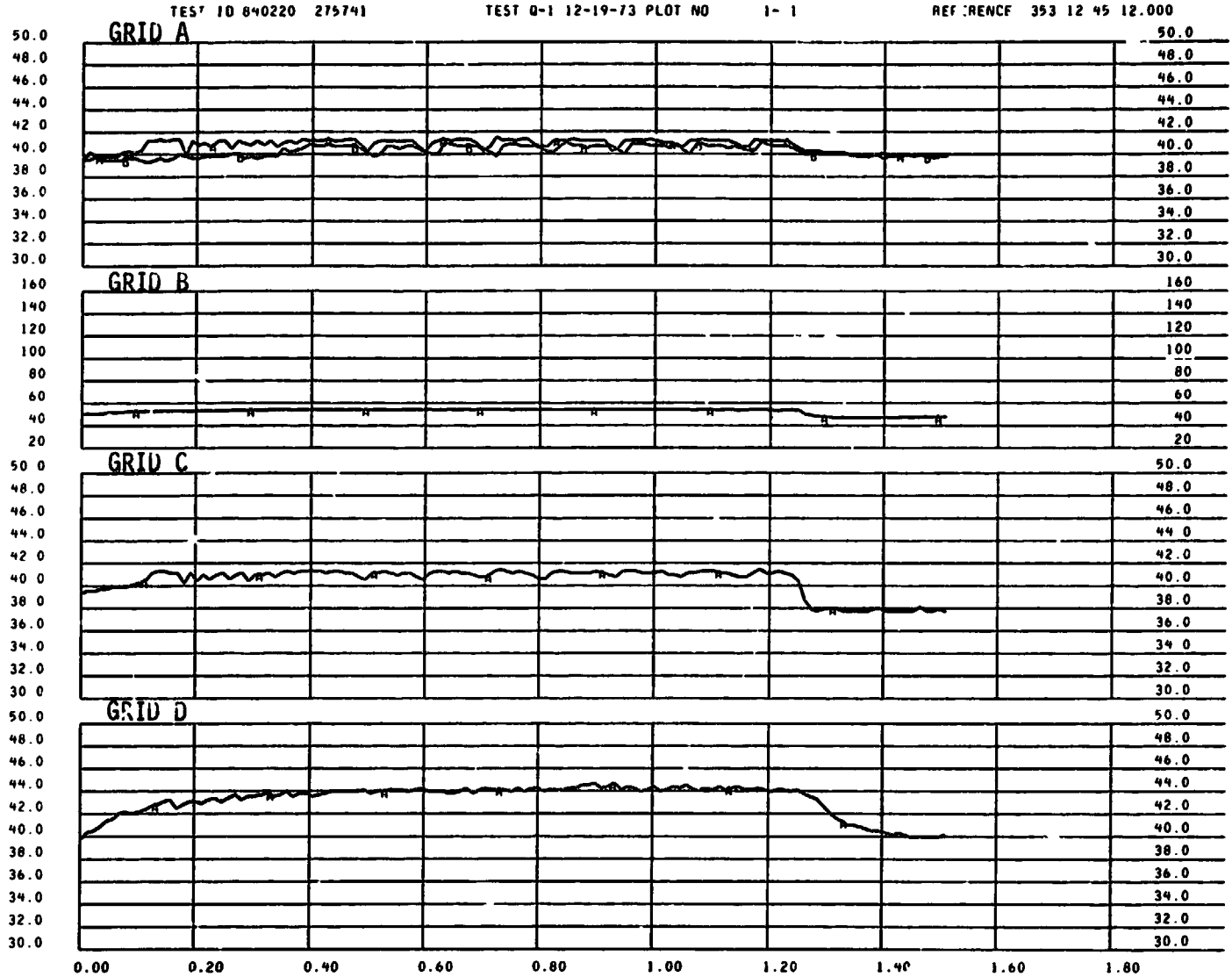

MEAS. NUMBER	CHANNEL ASGN.	TITLE	RANGE	UNITS	GRID-SYM
* T7	7	TVS INLET TEMPERATURE	30.0 TO 50.0	DEGREE R	AA
* T8	8	TVS OUTLET TEMPERATURE	30.0 TO 50.0	DEGREE R	AB
* T9	9	IDU EXTERNAL TANK TEMP AT TOP	20 TO 160	DEGREE R	BA
* T14	14	VJ5 TVS EXPANSION TEMPERATURE	30.0 TO 50.0	DEGREE R	CA
* T15	15	TEMP OUT BOUNDARY LAYER AT HF2	30.0 TO 50.0	DEGREE R	DA

Figure 4-10 – TEST A-1, PLOT NO. 1-1

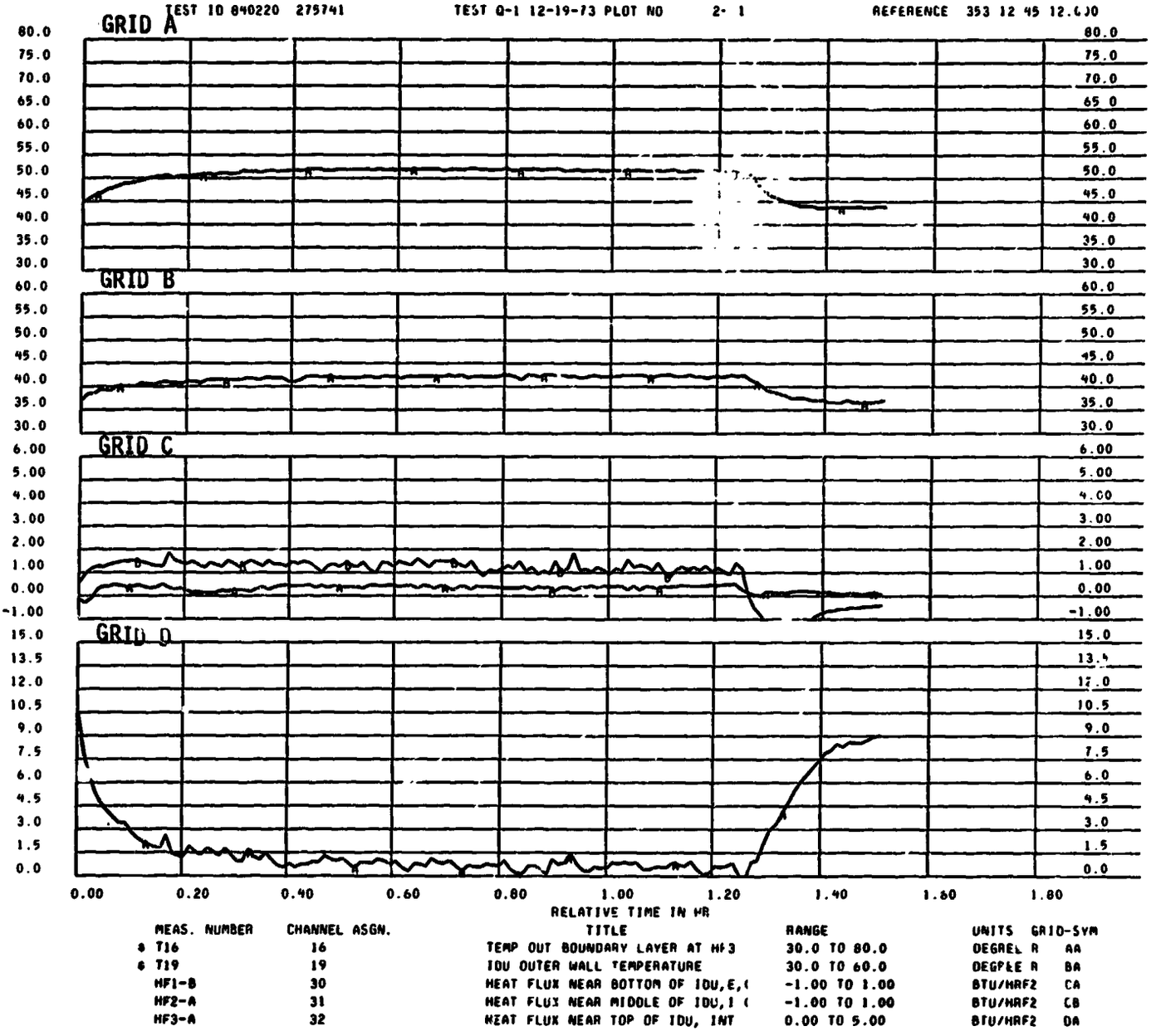

MEAS. NUMBER	CHANNEL ASGN.	TITLE	RANGE	UNITS	GRID-SYM
* T16	16	TEMP OUT BOUNDARY LAYER AT HF3	30.0 TO 80.0	DEGREE R	AA
* T19	19	IDU OUTER WALL TEMPERATURE	30.0 TO 60.0	DEGREE R	BA
HF1-B	30	HEAT FLUX NEAR BOTTOM OF IDU,E,(	-1.00 TO 1.00	BTU/HRF2	CA
HF2-A	31	HEAT FLUX NEAR MIDDLE OF IDU,I (	-1.00 TO 1.00	BTU/HRF2	CB
HF3-A	32	HEAT FLUX NEAR TOP OF IDU, INT	0.00 TO 5.00	BTU/HRF2	DA

Figure 4-11 - TEST Q-1, PLOT NO. 2-1

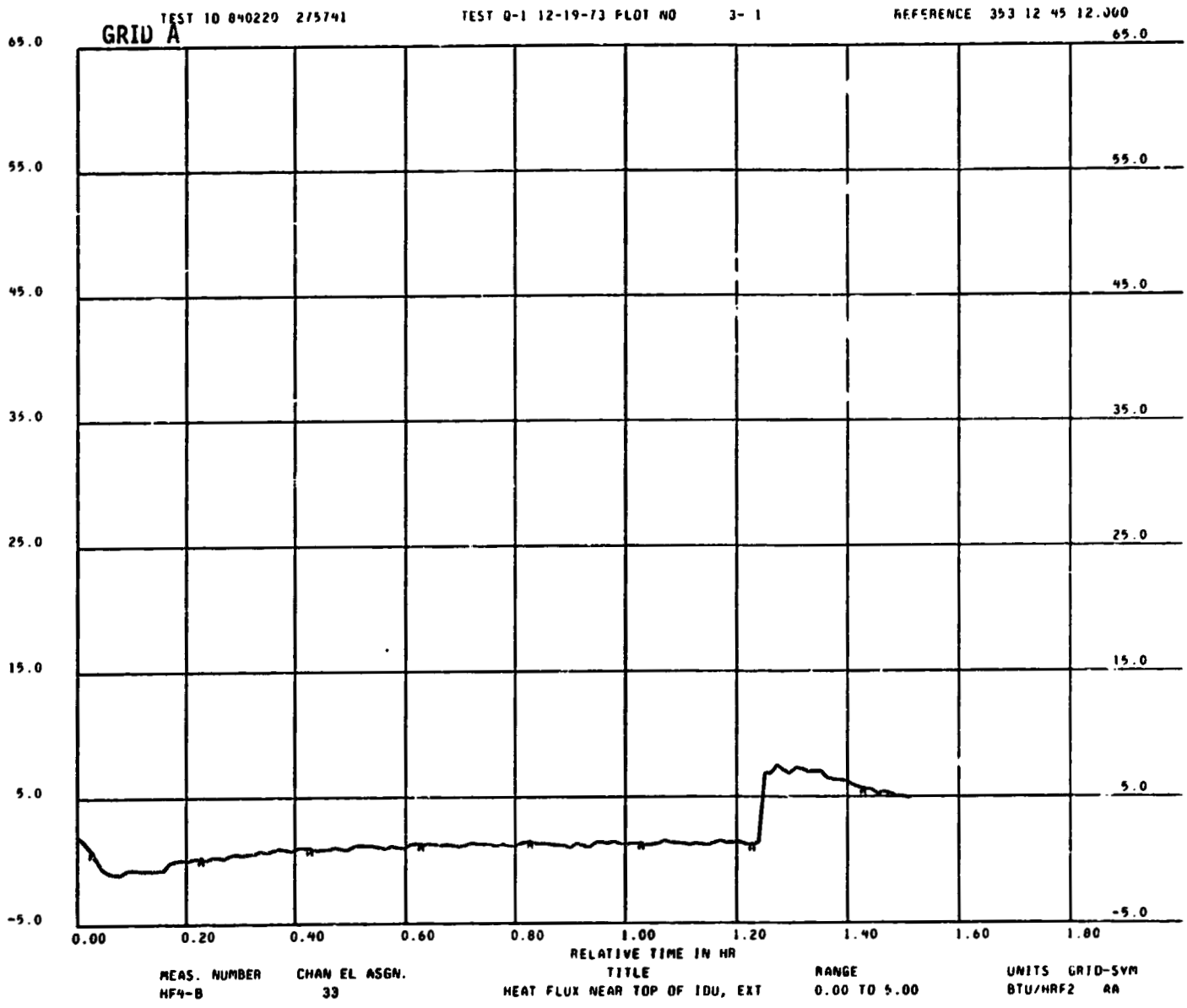

Figure 4-12 - TEST Q-1, PLOT NO. 3-1

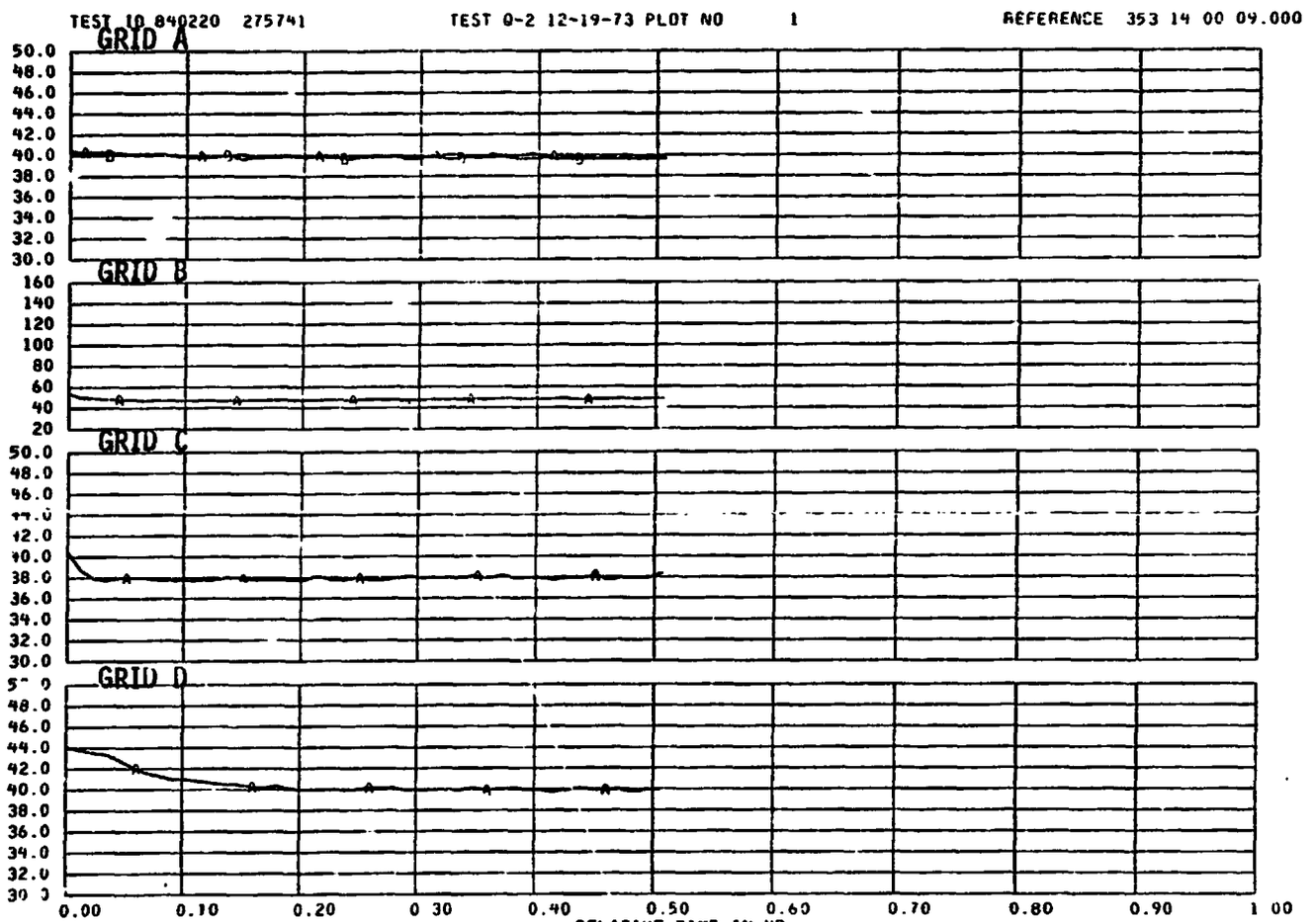

	MEAS. NUMBER	CHANNEL ASGN.	TITLE	RANGE	UNITS	GRID-SYM
*	T7	7	TVS INLET TEMPERATURE	30.0 TO 50.0	DEGREE R	AA
*	T8	8	TVS OUTLET TEMPERATURE	30.0 TO 50.0	DEGREE R	AB
*	T9	9	IDU EXTERNAL TANK TEMP AT TOP	20 TO 160	DEGREE R	BA
*	T14	14	VJ5 TVS EXPANSION TEMPERATURE	30.0 TO 50.0	DEGREE R	CA
*	T15	15	TEMP OUT BOUNDARY LAYER AT HF2	30.0 TO 50.0	DEGREE R	DA

Figure 4-13 - TEST Q-2 - PLOT No. 1

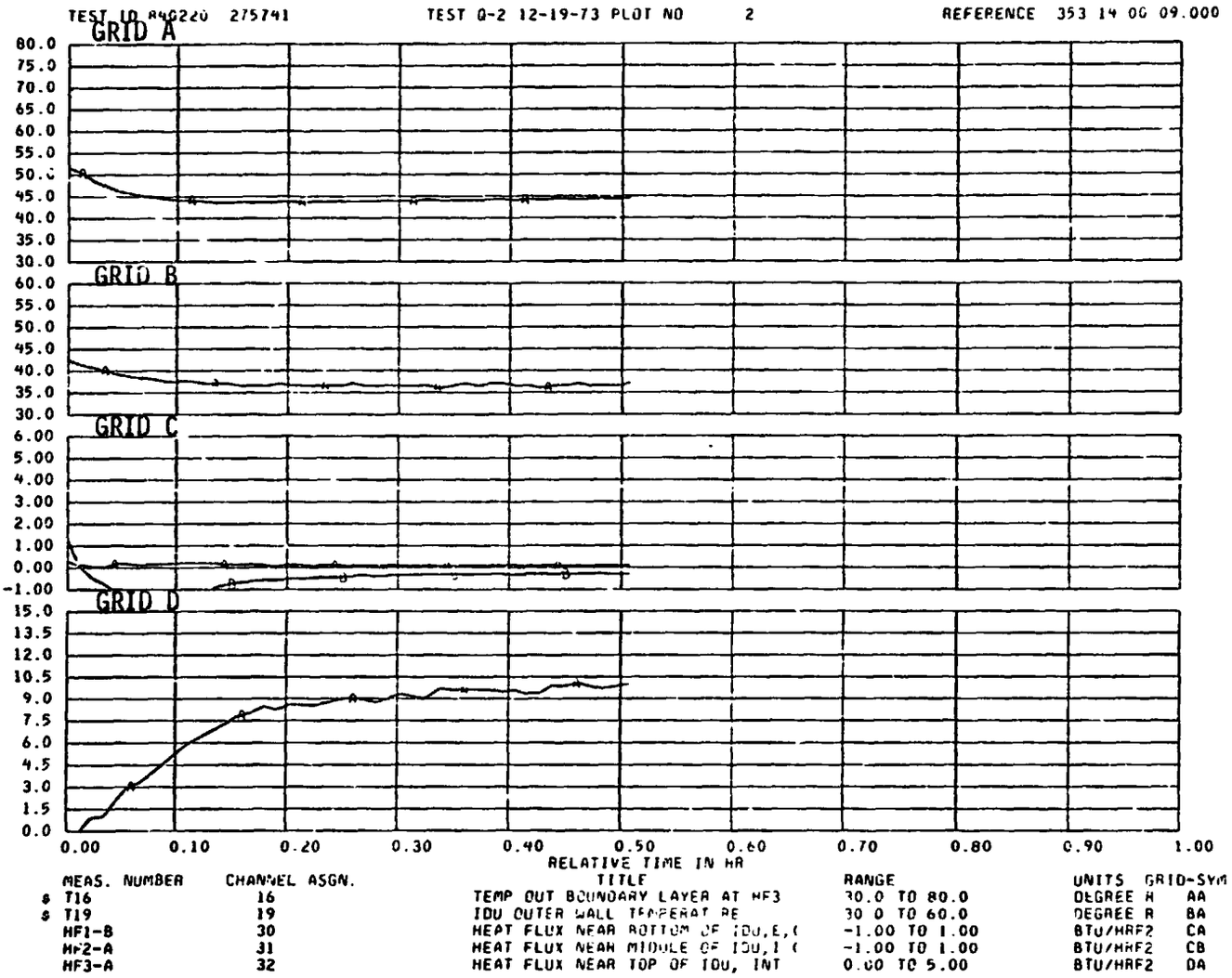

Figure 4-14 - TEST Q-2, PLOT NO. 2

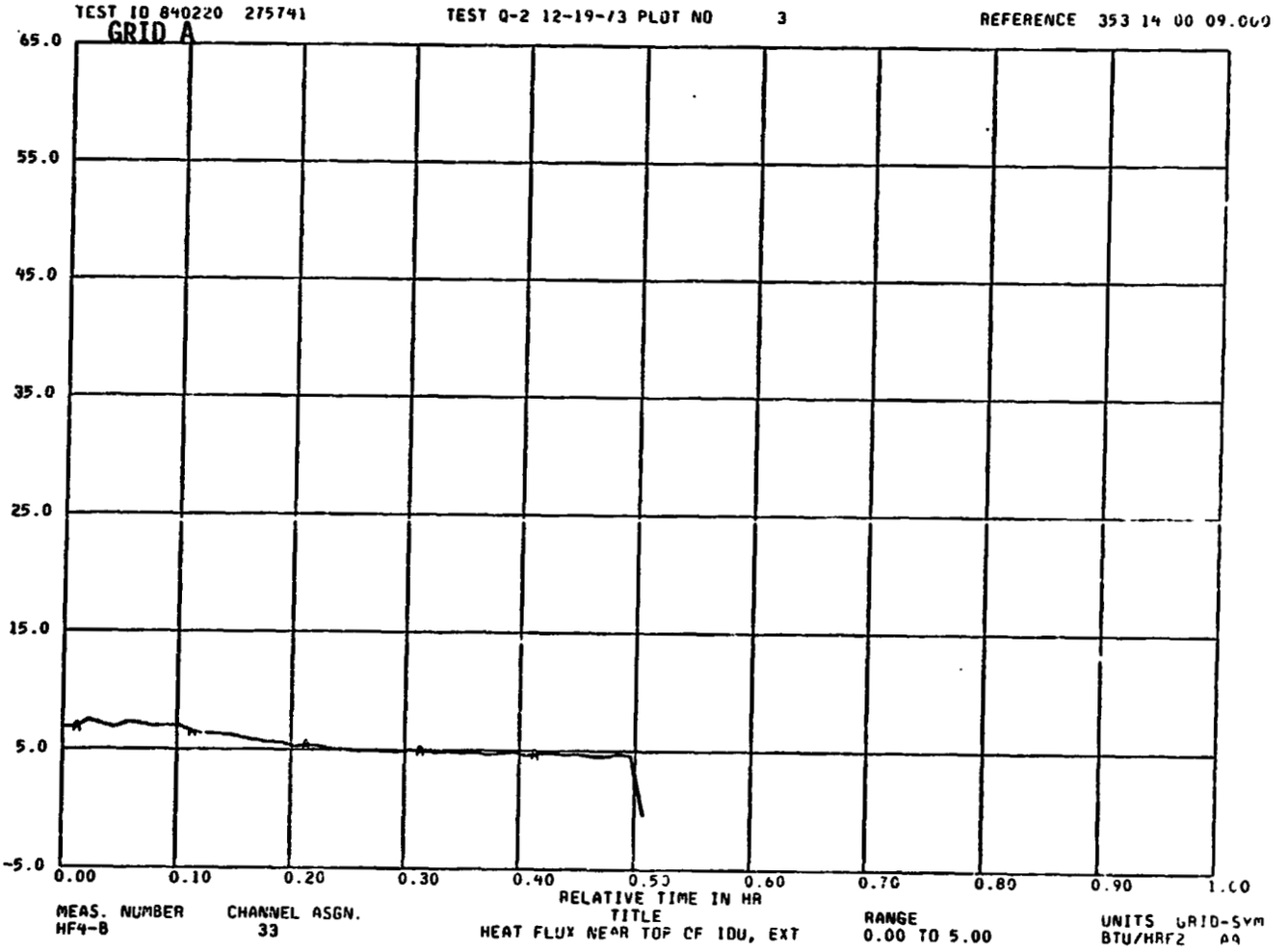

Figure 4-15 - TEST Q-2, PLOT No. 3

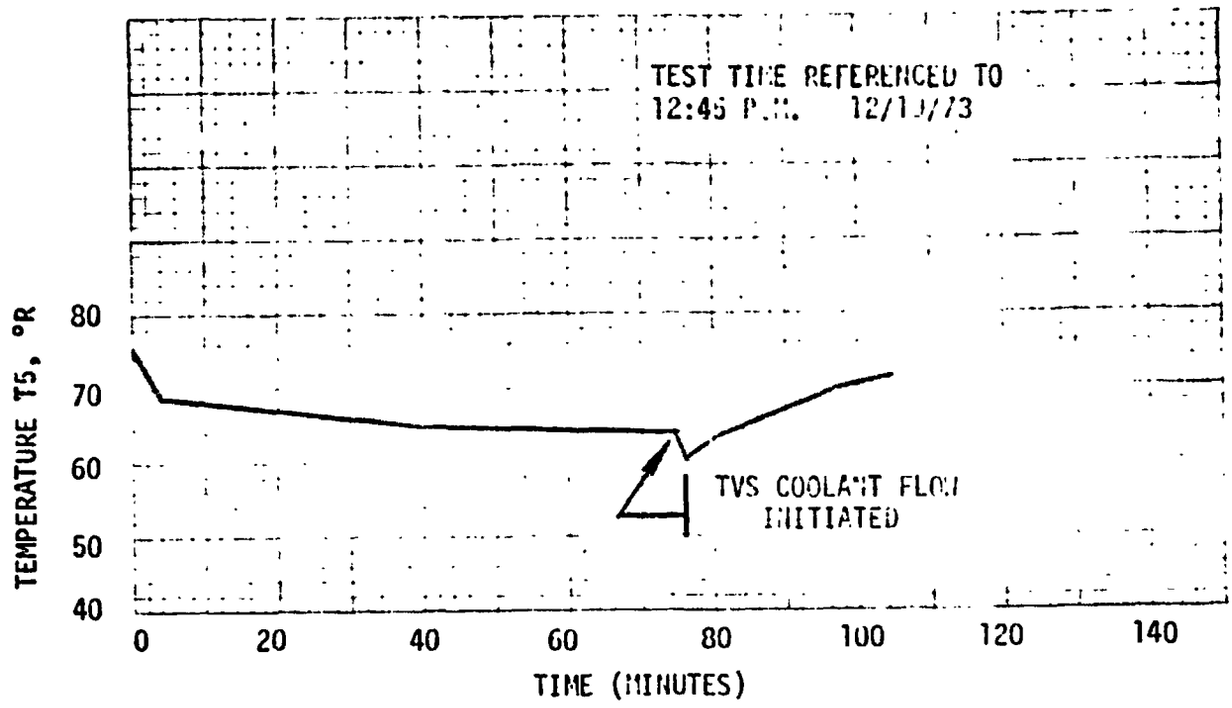

Figure 4-16 MAIN TANK TEMPERATURE, T5, DURING TESTS Q-1 AND Q-2

During the first 4 minutes, the TVS inlet temperature, T7, increased from 40°R to 41.0°R, and remained approximately constant (±0 5°R) during the entire steady-state period. The TVS outlet temperature also remained constant, at approximately 41.0 ± 0.5°R for the 1.2 hour steady-state period. The temperature, T14, immediately downstream of viscojet orifice FJ5 increased in the first six minutes from 29° to 41.5°R, and remained approximately constant the the 1.2 hour period. Thus, the TVS equilibrated in approximately 5 to 6 minutes. The IDU ullage temperature (T15) measured at HF2-A required approximately 20 minutes to reach a steady-state condition, increasing from 40°R to an approximately constant 44°R. The IDU ullage temperature (T16) measured near the top (HF3-A location) was warmer, increasing in approximately 15 minutes from 45° to 52°R (Figure 4-11). The IDU outer-wall temperature near the top also warmed slightly, from 36° to 41°R in approximately 10 minutes. During this initial period, the heat flux into the IDU near the bottom (HF1-B) was approximately zero, since both sides of the IDU wall were immersed in liquid. The heat flux near the middle of the IDU was measured by the interior heat-flux gauge, HF2-A, was approximately 1.5 Btu/ft^2 hr, and was relatively

constant. The heat flux near the top of the IDU, as measured by the interior heat-flux meter, HF3-A, showed a rapid decrease from 10 to 15 Btu/ft^2 hr to approximately 1.0 ± 0.5 Btu/ft^2 in approximately 15 minutes. Recall that this heat-flux meter is positioned to straddle the position of a TVS coil located on the exterior of the IDU cover. Positive heat flux is directed from the IDU to the TVS coil, and therefore, the cold TVS fluid, located at the top of the IDU, was cooling the interior of the IDU as it vaporized and flowed back into the IDU through the VJ5 orifice. The heat flux measured by HF4-B, located between the TVS coils on the outside of the IDU cover, showed a relatively low heat flux during both the initial and steady-state periods.

After the steady-state period had been observed for over 1 hour, the TVS downstream valve (V24) was reopened, and within 1 minute a steady outflow rate of 2.5 lb/hr was incurred. Within approximately 6 minutes, all IDU temperature measurements showed a marked decrease to steady-state values, which were maintained for approximately 30 minutes, as shown by Figures 4-13 and 4-14, for Test Q-2.

Figure 4-14 shows that the heat flux near the top of the IDU, measured by HF3-A, climbs rapidly from approximately 1.0 ± 0.5 Btu/ft^2 hr to 9 Btu/ft^2 hr. This is, of course, due to the TVS cooling the IDU interior. Similarly, in Figure 4-15, HF4-B shows that the heat flux from the main tank to the top of the IDU cover (as measured by the exterior heat-flux gauge located between the TVS coils) increases from approximately 1 to 2 Btu/ft^2 hr to approximately 8 to 9 Btu/ft^2 hr. Again, the TVS coolant, having lowered the IDU wall temperature, has caused a significant increase in heat flux to the coil from both sides of the IDU. Figure 4-16 shows that the main tank ullage temperature momentarily decreased immediately after TVS flow is reinitiated, but the incoming warm GH_2 soon brought the ullage temperataure back up to 70°R. As predicted by the TVS analysis, the uninsulated IDU/TVS causes an increase in the overall heat flux by increasing the temperature difference between the main tank and the IDU, but more importantly, by causing condensation heat transfer to occur, rather than free-convection heat transfer. Tests Q-1 and Q-2, therefore, demonstrate the need for insulation on the IDU exterior if the TVS heat interception capability is to be fully exploited.

4.18 TEST R - TVS TRANSIENT OPERATION

The principle of transient TVS operation is that heat entering the propellant tank is allowed to induce stratification until the total tank pressure exceeds a predetermined value, at which time coolant flow is initiated. An immediate concern is the response of the ullage pressure to the initiation of chilldown flow. This test was to demonstrate the response rate for an external heating condition similar to that demonstrated with Test P with the IDU approximately filled with liquid. IDU pressure would be allowed to increase until a facility pressure switch exceeds a set value (e.g., 28 psia). At this time, the TVS valve for maximum flowrate would be opened, and flow maintained until IDU pressure decreases to a previously determined lower value (e.g., 20 psia). However, tank leakage due to partial closing of the PV valves could not be alleviated, and therefore, this test was scrubbed following repeated unsuccessful attempts to induce complete valve closure.

4.19 TEST S - AUTOGENOUS PRESSURIZATION

The original objective of Test S was to evaluate the response of the IDU to warm gaseous hydrogen prepressurization, without outflow, and to determine the pressurization collapse factors for two cases: (1) the screen device (LHAD) full of liquid, and (2) the LHAD empty. Heat transfer out of the IDU was to be minimized by evacuating the main tank. However, because of the Parker valve malfunctions, this test was modified to further determine the effect of warm gaseous hydrogen pressurization on screen retention.

The tests were run in the same manner as Test J, with warm hydrogen pressurant exclusively. Outflow from the IDU to the main tank occurred in every case, due to incomplete closure of PV1 and/or PV2. The IDU was pressurized to 40 psia in all tests.

Table 4-8 summarizes the results. The data of Tests S-1A and S-1B show that vapor is formed inside the LHAD before breakdown, due to exposure of the upper part of the LHAD to the warm pressurant. Note that the initial liquid level in Test S-1A was 14 inches, thus initially exposing the upper portion of the LHAD to warm pressurant. In Test S-1B, the LHAD is submerged in liquid

Table 4-8

TEST S

Note: $P_{IDU} = P_{main\ tank} = 40$ psia

Test No.	LH_2 Outflow Rate (lb/sec)	Initial Liquid Level (in.)	Breakdown Level (in.)	Breakdown Indicator			LHAD Exposure Time to Warm GH_2 (sec)	Maximum T4 Reading Following Breakdown °R	Remarks
				CL4	T4	RL7			
S-1A	0.43	14	8.6	X	X	-	55	81	T4 indicated vapor 40 sec prior to breakdown
S-1B	0.22	24	20.5	X	X	X	80	76	T4 and RL7 indicated vapor 18 sec prior to breakdown
S-1D	0.74	31	21.0	X	X	X	5	61	T4 and RL7 indicated vapor 1 to 2 sec after CL4 breakdown indication
S-1F	0.74	31	13.0	X	X	X	22	86	T4 and RL7 indicated vapor approximately 5 sec after CL4 indication
S-1G	0.18	31	16.5	X	X	X	38	70	T4 indicated vapor 1 to 2 sec prior to CL4 indication. RL7 indicated vapor simultaneously with CL4 indication

initially, and vapor formation occurs 20 sec before breakdown, as compared to 40 sec for Test S-1A. In Test S-1A, breakdown does not occur until the liquid level is 8.6 inches. This is significantly above the breakdown level expected with cold pressurant, but shows significantly higher retention capability than Test S-1B, with breakdown occurring at a liquid level of 20.5 inches, which is immediately below the top part of the screen device. Test S-1D gives results similar to S-1B; breakdown occurs at a level of approximately 21 inches, but in this case the IDU was initially filled and therefore the time the LHAD was exposed to warm ullage before breakdown was only 5 seconds. This extremely rapid, and unusual, breakdown response is not seen in other tests; it can be surmised that the LHAD was not completely filled with liquid initially, and the presence of vapor in the top region led to immediate breakdown. Tests S-1F and S-1G again show premature breakdown, due to warm gaseous hydrogen, but no vapor is indicated inside the IDU by either T4 or RL7.

In Tests S-1A and S-1B, breakdown is explainable as being due to heat flux through the solid central pipe, communications ducts, and cylindrical channel to which the screen is attached. The heat flux would be expected to vaporize the LH_2, filling the upper region with vapor, and thus causing breakdown by exposing the screen. However, in Test S-1F, there is no indication of vapor forming in the LHAD before breakdown; in fact, T4 indicates vapor 5 seconds after breakdown. In Test S-1G, T4 indicates vapor only 1 to 2 seconds before the CL4 indication (i.e., no further outflow and liquid dropout from the LHAD). These two tests and especially Test S-1F, appear to represent a degradation in screen retention capability due to heat flux to the wetted screen.

In all cases, however, the use of warm gaseous hydrogen pressurization caused a very pronounced premature loss of liquid retention which appears to be due to heat flux. A discussion of a possible model explaining the loss of retention for a column of liquid hydrogen supported by a screen exposed to heat flux is given in Reference 1, and will not be repeated here. The model does present a possible reason for screen device retention failure, independent of the vapor formation mechanism due to heat flux directly through solid metal walls, such as the top of LHAD, above the screen weldment.

4.20 TEST T - FEEDLINE VAPOR CONTROL

The interface between the main tank or a start tank and the feedline poses a potential problem with screen devices due to vapor generated in the feedline, (above the feedline valve) passing into the screen device iteself. A feedline vapor barrier screen has been included in the IDU design (see Figure 4-17) which alleviates this problem by allowing vapor to bypass the screen barrier into the IDU, thus maintaining liquid above the screen.

The operation of the feedline vapor barrier screen as currently incorporated in the IDU is described below. This screen is used to keep gas from passing up into the screen device with vaporization in the feedline above the feedline valve. In principle, it would keep the vaporized hydrogen from breaking through the screen even if the feedline were completely dry (i.e., all feedline liquid boiled off).

Consider the vapor barrier screen and bypass line shown in Figure 4-18A. When gas is being forced out through the elbow, but the vertical portion is full of liquid, then the pressure at the elbow is

$$P_L = P_T + \rho g \, [h_{LIQ} + H_{OUT} + h_{ELBOW}]$$

which is approximately equal to the feedline pressure, for the low flowrates involved.

A pressure immediately above the screen is

$$P_{SCREEN} = P_T + \rho g \, h_{LIQ}$$

The liquid remains above the screen, and no gas breaks through, if the bubble of pressure is,

$$\Delta P_{BP} \geq P_L - P_{SCREEN} \geq \rho g \, (h_{OUT} + h_{ELBOW})$$

Thus, h_{ELBOW} must be minimized, which has been accomplished in the tube routing of the IDU. To test this device, GHe was introduced into the feedline up to the screen by backflow through the feedline from a 1.5 ft^3 helium supply bottle.

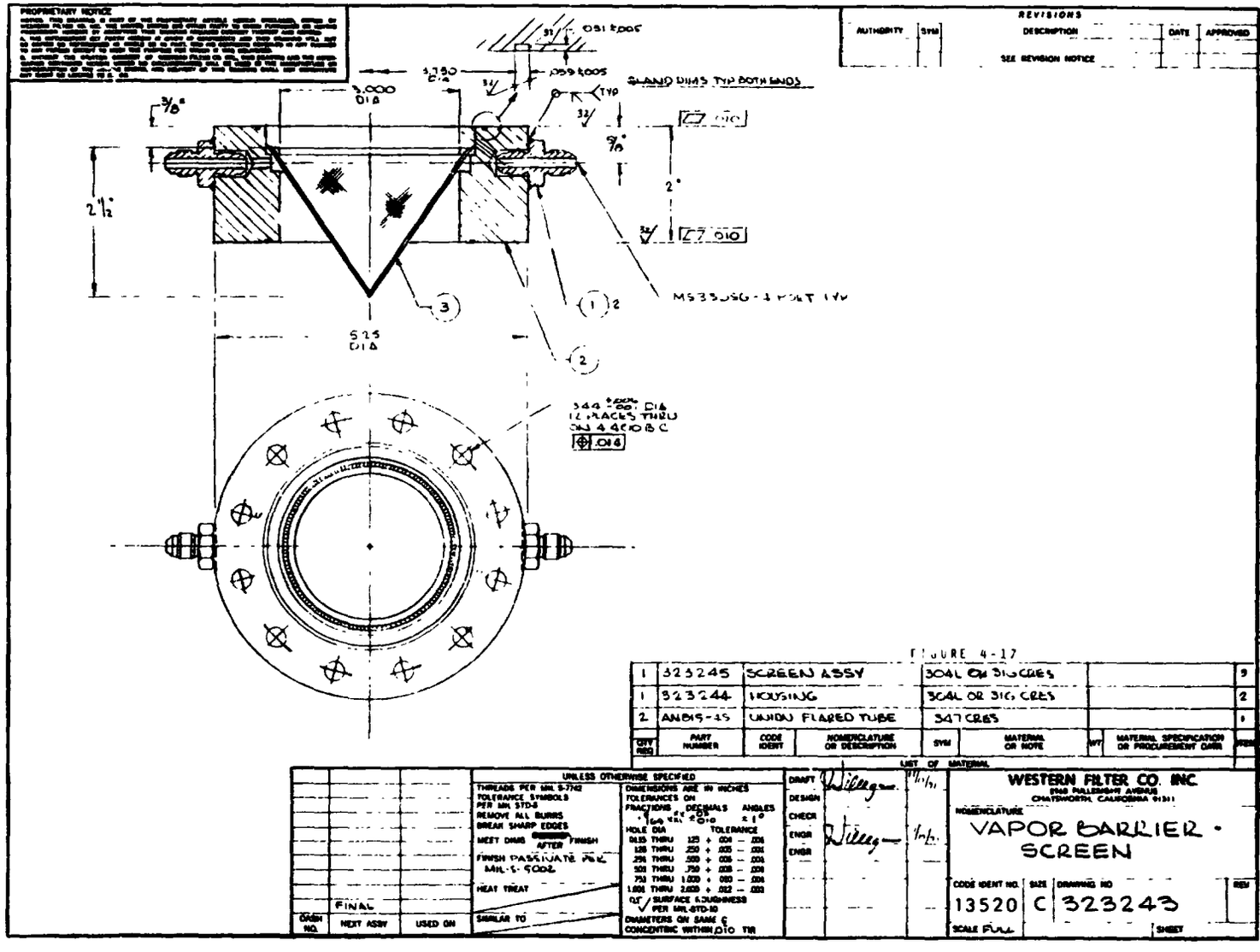

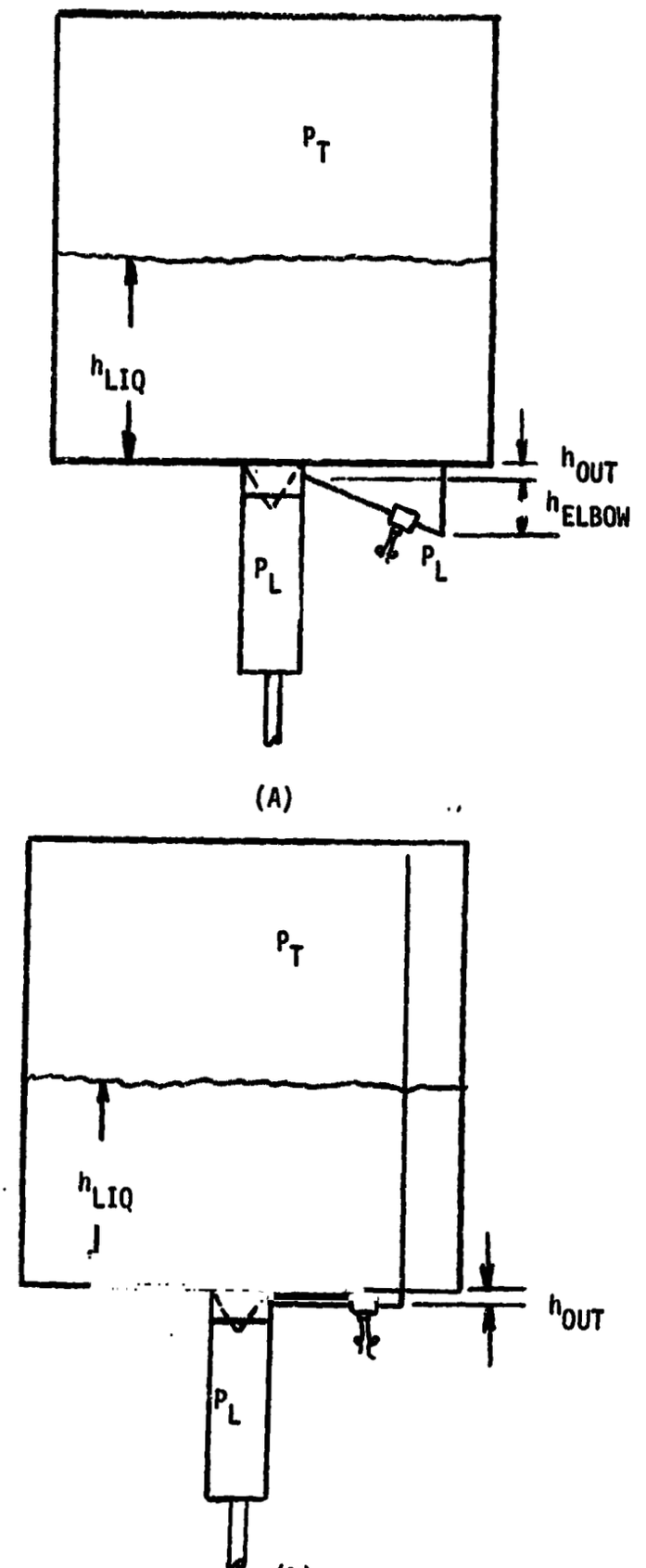

Figure 4-18 - FEEDLINE VAPOR BARRIER SCREEN

The GHe flow was bypassed through the solenoid valve, SV10, between the cone screen housing and the bottom of the IDU (see Figure 2-15). Approximate flowrates were measured by noting the 1.5 ft^3 bottle temperature and pressure as a function of time.

A flowrate of 0.004 lb/sec was observed to have no effect on screen retention, nor was there any indication of vapor passing through the cone screen into the LHAD. The flowrate used corresponds to extremely high equivalent heat transfer rates into a feedline, assuming all the heat input causes boiloff. For a 10-ft section of feedline, 4 inches in diameter, a flowrate of hydrogen gas of 0.004 lb/sec corresponds to a heat flux of 275 Btu/ft^2 hr, which far exceeds the values easily obtained with foam or HPI-insulated feedlines. Even helium purged HPI under ground-hold conditions has heat-transfer rates of the order of 200 to 300 Btu/ft^2 hr, and therefore, the screen cone device appears to be a feasible approach to vapor control under the most severe conditions.

A useful modification to the IDU has been conceived which could be incorporated if considered necessary. This modification ensures that the IDU feedline would be full of liquid before feedline valve opening and flow to the turbopumps. If a separate line were attached to the inlet which allowed gas to pass directly into the ullage, conditions would be different, as shown in Figure 4-18B.

Considering Figure 4-18B, the pressure above the screen is,

$$P_{SCREEN} = P_T + \rho g\, h_{LIQ}$$

The pressure beneath the screen is P_T. Thus,

$$P_{SCREEN} - P_T = \rho g\, h_{LIQ}, \text{ which is positive,}$$

and liquid flows down through the screen, keeping the feedline full of liquid. This alternate design may serve as a useful addition to the IDU, since vapor filling the feedline would normally pass through the pumps, possibly causing

damage. As a precautionary measure, the feedline vapor bypass valve could be opened momentarily, before initiation of flow. Thus, any vapor in the feedline would be displaced by liquid. This modification to the IDU would require either:

A. An extension line to the inlet, as shown in Figure 4-18B, which would then eliminate the capability for maintaining a nonwetted feedline, or
B. An additional solenoid valve and extension line, so that the feedline could be maintained full of gas or liquid, depending on the desired conditions.

4.21 TEST U - TWO-PHASE REFILL

Two-phase refill with high gas volume percentages was simulated to assess any limitations of the LHAD. In particular, it was necessary to determine whether or not the gas inflowing with the liquid caused the capacitance probe to give spurious liquid-level measurements, and whether or not liquid would be lost through the vent due to the bubbles rising in the bulk liquid. The tests demonstrated that complete settling and displacement of all gas bubbles from the bottom of the main tank is not necessary before refill of a start tank since no adverse effects were observed. Thus, decreased propellant settling times can be used, which decreases the required start tank size and weight, and allows a constant, relatively short duration settling time to be used with variable propellant percentages in a given tank, rather than settling times programmed to the specific settling conditions encountered.

Two refill tests were performed, U-1 and U-2, and data are shown in the Supplemental Data Document. In both tests, refill was initiated through PV2, with simultaneous helium flow through the submerged diffuser to simulate two-phase flow into the IDU. In Test U-1, the refill rate was a relatively constant 0.66 lb/sec, and in Test U-2, the refill rate was 0.805 lb/sec. The helium inflow rate was approximately 1 ft^3/sec, which had no deleterious effect on refill. The capacitance point-level sensor showed maximum voltage fluctuations of approximately 0.1 to 0.2 volts, corresponding to disruptions

of the liquid interface of approximately 0.8 to 1.6 inches. These maximum fluctuations appeared only at the initiation of refill. and were strongly attenuated for liquid levels above approximately 20 inches from the IDU bottom.

4.22 TEST V - RETENTION WITH WARM LH_2

The objective of this test was to determine the screen retention capability with a bulk liquid hydrogen temperature higher than that investigated in Test J. Since surface tension decreases with temperature, the tests were expected to result in a decrease in retention capability, which was indeed observed.

The original test plan called for a series of tests with various flowrates and bulk liquid temperatures, and both gaseous hydrogen and helium pressurization. However, due to the 2-inch (PV) ball valves malfunctioning, only five tests could be performed, all with cold helium pressurization (both overhead and submerged); results are summarized in Table 4-9. In Test V-25, the actual flowrate through the LHAD and PV1 is suspected to be less than the value calculated from the continuous level sensor data since PV2 may not have closed completely, thus allowing LH_2 to leak directly from the IDU to the main tank.

The bulk liquid temperature of the hydrogen was controlled by the fill operation. A constant IDU/Main Tank vent pressure was maintained during initial fill from the liquid hydrogen storage tanks in order to achieve the desired bulk liquid temperature. This procedure was far more rapid and practical than waiting for the tanked liquid to warm up from, say 37°R to 42°R, and it assured a well mixed, destratified propellant rather than a stratified propellant.

The breakdown tests were performed as in the Test J cases, and the data are shown in Figure 4-4. The improvement, in terms of retention capability for the Test V cases is again seen, relative to the expected performance. The bulk liquid hydrogen was saturated at 35 psia (42.5°R) and, for example, a breakdown height of 7.6 inches above the IDU cover was expected at a flowrate of 0.8 lb/sec, whereas in Test V-3, breakdown did not occur until the liquid level reached 4.2 inches, which is a significant improvement. Part of this improvement may have been due to the cooling of the screen interface as

Table 4-9

TEST V - OUTFLOW

Test No.	Outflow Rate (lb/sec)	Breakdown Height (inches)	Pressurant	Diffuser	Approximate Pressurant Gas Temperature In IDU (°R)	Liquid Hydrogen Saturation Pressure (psia)
V-1	0.277	4.2	Helium	Overhead	42.5	35
V-3A	0.515	4.2	Helium	Overhead	42.5	35
V-3B	0.816	4.2	Helium	Overhead	42.5	.
V-25	1.05	4.0	Helium	Submerged	42.5	35
V-39	0.39	4.2	Helium	Overhead	42.5	35

hydrogen was vaporized from the free surface of the liquid wetting the screen as the screen was suddenly exposed to the ullage gas. Part of this improvement was apparently due to the screen breakdown point pressure difference being higher than the bubble point pressure difference; i.e., a "catastrophic" breakdown as opposed to single bubble breakthrough. Therefore, Figure 4-4 shows both of the curves corresponding to the expected breakdown points based on the isopropyl alcohol bubble point of 14 inches of water column pressure head and the isopropyl breakdown point of 16 inches of water column pressure head. Part of this improvement may also have been due to the actual flowrate through the LHAD being less than the total flowrate as measured by the capacitance probe. However, even if the viscous and dynamic pressure losses were negligible (corresponding to a negligible flowrate through the LHAD) the hydrostatic head alone should have caused failure at 5.8 to 7.2 inches. Therefore, the observed retention improvement had to be caused, at least in part, by effects other than leakage flow through PV2 decreasing the viscous and dynamic pressure losses.

With helium as the pressurant, there is apparently a significant mass transfer effect taking place at the suddenly exposed liquid surface as the liquid drains out of the IDU. As this hydrogen is vaporized and transported into the ullage region by diffusion and convection, the free surface temperature would tend to drop below the initial bulk liquid temperature, assuming heat transfer into the IDU and screen device is low (as was the case for these tests). This effect was apparently present in the corresponding Test J conditions (i.e. cold helium pressurization) except that the liquid bulk temperature was lower

The surface tension is determined by the temperature at the free surface, rather than the bulk temperature, and for the cold helium pressurization/expulsion cases, equilibrium conditions were, of course, not met (i.e., the partial pressure of the hydrogen was not constant and equal to the vapor pressure corresponding to a bulk liquid temperature). Since this vaporization would tend to cool the free surface, the surface tension would increase, thus improving the screen retention performance. Conversely, use of saturated hydrogen pressurant at a pressure exceeding the saturation pressure of the bulk liquid would result in condensation of a relatively warm liquid film, or condensate, which would have a reduced surface tension and, therefore, result in decreased screen retention performance.

Comparison of breakdown le· ; of Test V-3 and Tests J-25A and J-27B provides some insight into the surface temperature decrease due to vaporization. These three tests were performed at approximately the same apparent flowrate, but the bulk liquid temperatures were different.

An estimate as to the surface temperature cooling effect can be inferred by interpolating between the appropirate curves shown in Figure 4-4. For example, the Test V-3 breakdown point lies between the expected breakdown point for (1) the curve corresponding to breakdown with a 16 inch water column bubble point in isopropyl alcohol, with LH_2 properties for both the surface and bulk corresponding to 42.5°R, and (2) the curve for breakdown assuming a 16 inch water column bubble point and the viscosity and density of the liquid hydrogen evaluated at 42.5°R, but the surface tension evaluated at a surface temperature of 37.5°R. Linear interpolation gives an expected temperature at the surface of 39.2°R, or an apparent cooling due to evaporation of 3.3°R. Even if the flow through the LHAD is assumed to be zero (i.e., all outflow is through PV2) then the apparent cooling is estimated to be 2.6°. (In this case, it is assumed that V-3 breakdown was due to hydrostatic head alone, and Fig. e 4-4 shows that the expected breakdown would be 5.8 inches above the IDU bottom not the observed 4.2 inches.)

In the Test J cases, it is difficult to use the same limiting flowrate reasoning, since the assumption of all outflow taking place through PV2 (i.e., breakdown assumed to be due to hydrostatic head alone) places the appropriate Test J data so close to the expected breakdown level of approximately 2.5 inches above the IDU bottom that the deviation falls within experimental accuracy. This deviation is further obscured by the inaccuracy of the liquid level calibration curve very near the bottom of the IDU. However, it is unlikely that PV1 failed to open at all, and PV2 failed to close completely, in cases J-11, J-19, J-25A, and J-27B, for example. Since even a decrease by a factor of two in the actual flowrate through the LHAD for the above cases still demonstrates an improvement in the breakdown height, the occurrence of a surface cooling effect significantly affecting the bubble point in the cold helium pressurization cases of Test J as well as Test V is plausible.

These results indicate, but by no means prove, that with cold helium pressurization an improvement in screen retention performance can be expected with non-equilibrium conditions (i.e., outflow). This would be fortuitous from an acquisition design standpoint since the worst case conditions are normally encountered when outflow losses are combined with the hydrostatic level. Additional non-equilibrium outflow cases with rapid outflow rates are required to further assess this potential free surface temperature decrease and resultant retention performance improvement. Further, this type of testing should be performed under "bench test" conditions, for which higher accuracies and better control can be obrained, as opposed to large scale, hardware development testing, such as with the IDU.

One other comparison of the Test V and related Test J data is given in Figure 4-19, which shows the breakdown level for the two bulk temperatures. As expected, all of the related case data shows a tendency for breakdown to occur more readily with warmer bulk liquid. The question raised by the closer examination of the results is whether or not vaporization induced cooling can significantly improve retention performance.

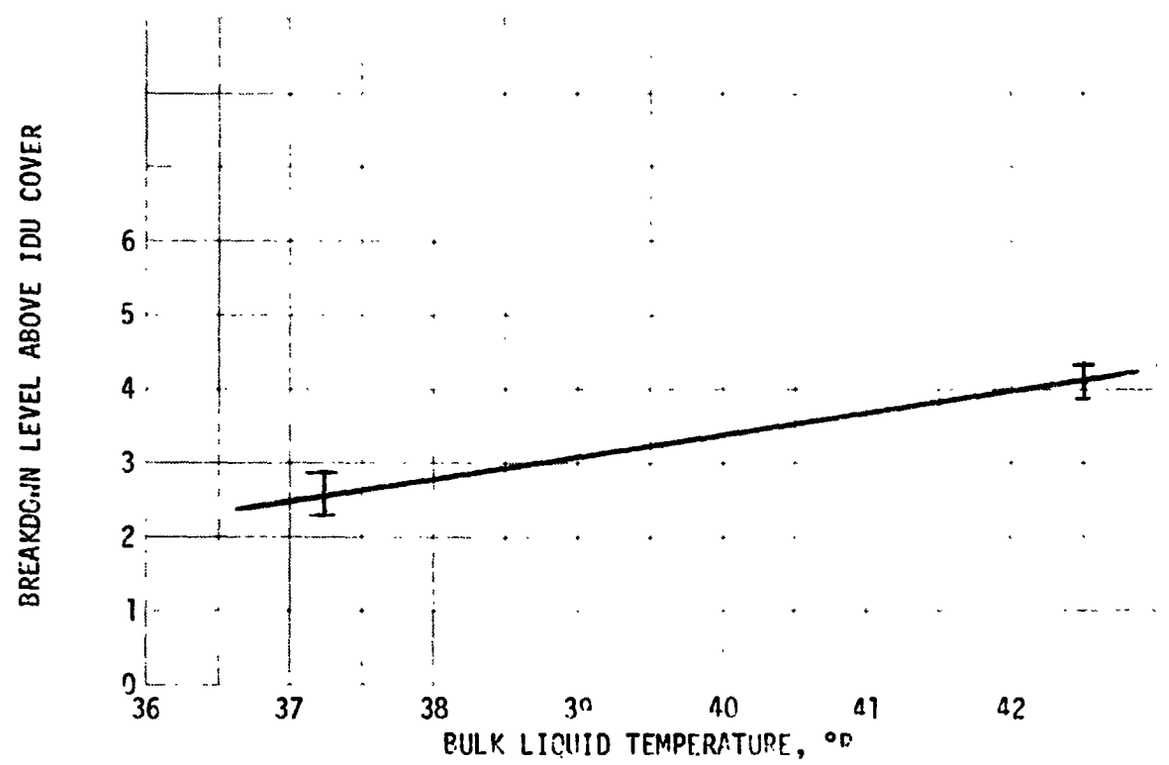

Figure 4-19 OBSERVED RETENTION PERFORMANCE DECREASE WITH TEMPERATURE

4.23 TEST W - VACUUM VENT/REFILL

The objective of this test was to demonstrate start-tank refill following a vacuum vent. This test had been performed successfully in MDAC IRAD tests of the 10-gallon start tank. In principle, the start tank is first emptied of liquid by flowing back into the main tank. The start tank is then vented to vacuum, the vent valve closed, and the refill valve opened to allow inflow. Complete refill was demonstrated in the MDAC IRAD tests. However, due to the Parker valve malfunctions, the IDU could not be evacuated with liquid hydrogen in the main tank, and therefore, this test was not attempted.

Section 5
CONCLUSIONS

The design, fabrication, assembly, and test of the Interface Demonstration Unit has demonstrated that the integrated start tank is a viable candidate for the solution of certain crucial thermodynamic and hydrodynamic problems associated with multiple restart cryogenic vehicles. In addition, the IDU itself serves as a flexible test bed, capable of extensive modification and/or easy replacement of components, subassemblies, and instrumentation. As such, it should be a useful tool in the continuing development of reliable, lightweight cryogenic propellent acquisition devices.

Specific objectives, results, and conclusions associated with the development and test of the IDU are summarized in Table 5-1. Recommendations for the further improvement of the IDU, and its use in extending the technology of cryogenic acquisition systems, are delineated in Table 5-2.

Table 5-1

PROGRAM RESULTS

Task/Item	Description/Objective	Results/Remarks
Interface Demonstration Unit Design and Fabrication		
*Screen device (liquid hydrogen acquisition device - LHAD)	Simulates conditions comparable to full-scale cryogenic vehicles. Designed for inclusion in full-scale NASA-MSFC auxiliary propulsion system (APS) breadboard. Bubble point tested. Screen standoff used to minimize flow-through loss. Special screen fitting allows LHAD to be completely filled with LH_2.	Rolled spot-welded screen verified. Overall design and retention performance exceeded requirements. LHAD can be positioned in four ways to test various configurations. Bubble point sealing with polyurethane and/or solder demonstrated. Screen fitting verified.
*Interface Demonstration Unit tank	Contains 10 ft^3 of LH_2. Readily modifiable for additional devices. Sized to accommodate outflow, refill, and start tank simultaneous outflow/refill operation. No tank wall insulation.	Additional screen acquisition device, designed and fabricated under companion program, NAS 8-27685, fits into IDU tank. Resulting system is full-scale version of candidate cryogenic space tug start tank concept. Insulation required on IDU tank to fully test thermodynamic conditions.
*Pressurization and feed system	Full-scale hardware used, including 2-inch submerged LH_2 ball valves. Overhead and submerged pressurization diffusers, including coiled heat exchanger to cool pressurant. Vent bypass included to maximize vent rate (and hence refill). Features bypass tee, cone screen for feedline vapor control, screen baffle, insulated pressurant lines, and refill diffuser. System is assembled with flared tube fittings to facilitate modification.	All pressurization and feed system components performed satisfactorily, except for 2-inch ball valve malfunctions; cause identified and correction recommended.

Table 5-1 (Sheet 2 of 7)

PROGRAM RESULTS

Task/Item	Description/Objective	Results/Remarks
*Thermodynamic vent system	Two 35-ft., 1/4" aluminum tubes dip-brazed to IDU tank. Provides four different flow paths. Viscojets and valves provide 0.2 to 5 lb/hr flow rate, and bypass capability for pump and feedline cooling. Flowpath selection results in various pressure drop conditions.	TVS fabrication fully verified. Dip-brazing techniques perfected. Use of Wakefield Delta bond-conducting epoxy demonstrated successfully. Flow path selection maximizes TVS test capability. Viscojets guard against clogging since flow area is approximately 5-10 times greater than equivalent orifice.
*Instrumentation	Consists of seven carbon point level sensors, three capacitance point level sensors, one capacitance continuous level sensor, sixteen platinum probe temperature transducers, two platinum resistance patch temperature transducers, four heat flux gauges with four thermocouples, and three ball valve position indicators.	Instrumentation designed to provide backup capability for expulsion and refill control and thermodynamic surveillance. Capacitance probes demonstrated to be reliable, accurate, with fast response. All instrumentation performed satisfactorily, with exception of 2-inch ball valve microswitches, which gave spurious readings.
Interface Demonstration Unit Assembly and Installation Procedure	Procedure fully documented, including annotated photographs and detailed assembly drawings.	Future disassembly and modification facilitated.
Interface Demonstration Unit Supporting Analysis		
*Wall-mounted thermodynamic vent system analysis	Numerical program with steady-state conditions met by determining coolant outflow conditions so that surface integral of wall heat flux is zero.	Output results obtained for insulated and noninsulated tank, with free convection and/or condensation. Program includes pressure drop equations so

Table 5-1 (Sheet 3 of 7)

PROGRAM RESULTS

Task/Item	Description/Objective	Results/Remarks
	Tube internal heat transfer coefficients governed by two-phase flow with two regimes and transition at critical quality. Extensive variations available for heat transfer coefficients for liquid and/or vapor.	that coolant flow rate, tube pressure, and IDU pressure are specified. Program fully checked-out and operational.
*IDU autogenous pressurization analysis	Time-dependent, finite-difference numerical program solving for pre-pressurization conditions, pressurant flow rate, pressure decay, condensation/evaporation, and temperature distribution. Incorporates variable duty cycle (acceleration, expulsion, etc.). Uses tabulated real variable properties. Flexible heat transfer coefficients, with corrective procedure at each time step to verify proper use of free convection or condensation values. IDU internal hardware modeled. Screen device can be treated as full or empty. Thorough simulation of IDU ullage gas heat and mass transfer phenomena with gaseous hydrogen pressurization. Specifically designed for comparison of results with IDU test data, so that improved heat transfer coefficients can be ascertained for use in design of full-scale start tanks or equivalent systems.	Program used to determine pre-pressurization and pressure decay phenomena taking place in the IDU with and without wall insulation. Characteristic ullage temperature distribution variations determined. Fully checked out and operational. Results could not be compared directly with test S data since ball valves leaked and constant pressures both inside and outside IDU could not be maintained.

Table 5-1 (Sheet 4 of 7)

PROGRAM RESULTS

Task/Item	Description/Objective	Results/Remarks
*Screen sizing computer program	Forerunner of extensive MDAC screen device design program. This version incorporates principal pressure losses, LHAD geometry, pressure loss correlations for flow-through screens based on GDA or Armour and Cannon data. Incorporates multiple, pleated, and/or backup screens. Programmed on terminal to maximize ease of screen device design, comparison and selection.	Used to size screen LHAD, select screen, and compare breakdown conditions with test results. Fully operational. Improved versions with non-uniform flow, complex geometries, improved flow loss correlations, etc., now available at MDAC.
Interface Demonstration Unit Checkout		
*Component, subassembly, checkout (Tests A, B, C, D, E, F, G, H, I)	Verify operation of all critical components, including solenoid valves, submerged LH_2 2-inch ball valves, level sensors. Verify structural capability.	Tests verified proper operation of all components. Level sensor calibration curve obtained for all sensors. Proof-pressure and leak tests performed (ambient and cryogenic). Ball valves malfunctioned; corrective procedure recommended.
System Checkout Tests		
*Test J — Screen breakdown, pressurization, and IDU refill	Determine breakdown point vs. flow rate, verify pressurization modes. Verify refill following breakdown (to completely refill LHAD) and start tank refill.	All objectives met except outflow rates limited to less than 1-2 lb/sec in spite of repeated ball valve malfunctions. Data compared with screen sizing program predicted behavior. Start tank operation demonstrated. Warm pressurant caused premature breakdown, especially use of warm GH_2 (> 50° R).

Table 5-1 (Sheet 5 of 7)

PROGRAM RESULTS

Task/Item	Description/Objective	Results/Remarks
*Tests K and L – Expulsion/refill and valve sequencing by operator	Demonstrate complete start tank operation and manual control.	Successful refill accomplished during simultaneous expulsion, without breakdown. High refill rates tested, but ball valve malfunctions constrained expulsion rates to 2 lb/sec or less, rather than design condition of 4.5 lb/sec.
*Test M – Thermodynamic vent system flow rate vs. pressure	Determine TVS mass flow rate vs. pressure for various viscojet combinations. Compare results with analysis. TVS line pressures of 15 psia tested.	Results obtained and compared. Improved correlation for viscojet pressure drop obtained, based on equivalent two-phase density. Some results show mass flow rates smaller than expected; probably due to TVS line pressure drop inaccuracies. Additional pressure pickoff points recommended.
*Test N – Hydraulic pressure surge	Determine effects of pressure transients on screen device retention capability.	Inconclusive results due to ball valve malfunctions.
*Test O – TVS flow rate control with variable TVS line pressure	Determine TVS flow rate for line pressures less than 15 psia.	Results obtained tend to verify correlation based on equivalent two-phase density. Results particularly applicable to coolant conditions required for IDU steady-state thermal control, since line pressures and corresponding coolant temperatures are close to required conditions for IDU.

Table 5-1 (Sheet 6 of 7)

PROGRAM RESULTS

Task/Item	Description/Objective	Results/Remarks
*Test P – Steady-state control of IDU	Demonstrate steady-state thermal control by maintaining constant flow rate at proper conditions, so as to maintain complete heat flux interception. Verify heat flux gauges.	Tests were modified due to ball valve leakage, but steady-state temperature control was demonstrated. All instrumentation, including heat flux gauges, performed satisfactorily.
*Test Q – Effects of downstream flow control	Investigate transient effect of closing and opening downstream TVS valve.	Tests demonstrated TVS line boiling characteristic time, characteristic time for TVS startup, and heat flux and temperature variations. Tests demonstrated need for IDU insulation when wall-mounted TVS is employed.
*Test R – TVS transient operation	Demonstrate ullage pressure control by use of transient TVS chilldown flow.	IDU leakage through partially closed ball valves caused test to be scrubbed. Tests should be performed to provide comparison with steady-state thermal control operation.
*Test S – Autogenous Pressurization	Evaluate response of IDU and LHAD to warm gaseous hydrogen prepressurization, with LHAD full and with LHAD empty.	Due to ball valve leakage, this test was modified to provide data on retention capability with warm gaseous hydrogen pressurization. Premature breakdown observed is attributed to use of warm hydrogen.

Table 5-1 (Sheet 7 of 7)

PROGRAM RESULTS

Task/Item	Description/Objective	Results/Remarks
*Test T — Feedline vapor control	Verify and demonstrate feedline vapor control provided by cone screen and bypass valve.	Simulated boiling in feedline above PV1 was shown not to cause gas passage into LHAD, because vapor was bypassed into IDU, outside of LHAD. A new vapor control technique which provides for a wet feedline was conceived. This modification is recommended for the NASA-MSFC APS tests.
*Test U — Two-phase refill	Demonstrate effect of two-phase refill on start tank operation.	Tests demonstrated that complete propellant settling (i.e., bubbles displaced from liquid) need not be accomplished prior to IDU refill, which allows for additional operational safety margin, or decreased start tank size and weight.
*Test V	Determine screen retention capability with a bulk liquid hydrogen temperature higher than that investigated in Test J.	Tests performed with helium pressurization alone. Results indicate but do not prove, that surface cooling takes place, resulting in high surface tension and retention performance.
*Test W — Vacuum vent/ refill	Demonstrate the vacuum vent refill procedure.	Test could not be performed due to ball valve leakage.

Table 5-2

RECOMMENDATIONS

* Modify ball valve pressurization system for dual mode pressurization

* Incorporate jet pump diffuser for IDU/start tank refill without overboard ullage venting.

* Perform additional tests with TVS system to provide further data on two-phase flow phenomena.

* Incorporate additional TVS pressure pickoff points, especially immediately downstream of viscojets.

* Incorporate new feedline vapor cotrol system.

* Incorporate Saturn SIVB-type foam on IDU exterior.

* Modify positions of level sensors to increase accuracy of calibration curve for capacitance continuous level sensor near bottom of IDU.

* Extend TVS numerical program to include more representative geometries for wall-mounted systems.

* Improve heat transfer coefficients with empirical results obtained by extended steady-state tests with TVS.

* Include diffusion equations in current autogenous pressurization computer program for application to more general case (i.e., helium pressurization).

* Perform hydraulic pressure surge tests to evaluate valve opening/closing on LHAD retention performance.

* Incorporate redundant phase sensors inside LHAD to provide more complete instrumentation on breakdown phenomena.

* Perform test program in IDU with acquisition system designed and fabricated under companion program (NAS 8-27685).

Section 6
REFERENCES

1. Advance Maneuvering Propulsion Technology Study. Mid-Term Report. MDAC Report DAC 58160, July 1968 (CONFIDENTIAL)

2. J. B. Blackmon. An Integrated Start Tank for Cryogenic Propellant Control. Presented at 12th CPIA Propulsion Conference, Las Vegas, Nevada, November 1970. Published in conference proceedings.

3. G. W. Burge, J. B. Blackmon, and J. N. Castle. Design of Propellant Acquisition Systems for Advanced Cryogenic Space Propulsion Systems. AIAA Paper No. 73-1287. Presented at AIAA/SAE 9th Propulsion Conference, Las Vegas, Nevada. November 5-7, 1973.

4. G. W. Burge and J. B. Blackmon. Study and Design of Cryogenic Propellant Acquisition Systems. McDonnell Douglas Report MDC G5038, May 1974. Final Report for NASA Marshall Space Flight Center Contract NAS8-27685.

5. J. B. Blackmon. Pressurization Gas Flow Effects on Liquid Interface Stability. Douglas Aircraft Report No. DAC-60711, July 1967.

6. H. M. Kavanagh and P. L. Rice. Development of Subcritical Oxygen and Hydrogen Storage and Supply Systems. Contract NAS9-1065, Airesearch Manufacturing Company, Division of the Garrett Corporation, September 1964.

7. W. H. Sterbentz. Liquid Propellant Thermal Conditioning System. NASA CR-72113, Contract NAS3-7942, Lockheed Missiles and Space Company.

8. J. A. Stark, et. al. Cryogenic Zero Gravity Prototype Vent System. Contract NAS8-20146, General Dynamics, Convair Division, October 1967.

9. W. H. Sterbentz. Liquid Propellant Thermal Conditioning System. Contract NAS CR-72375, Lockheed Missile and Space Company, August 1968.

10. E. C. Cady. A Comparison of Low-G Thermodynamic Venting Systems. McDonnell Douglas Report MDAC-G3174, April 1969.

11. General Dynamics. Low Gravity Propellant Control Using Capillary Devices in Large Scale Cryogenic Vehicles - Related IRAD Studies. General Dynamics Report GDC-DDB70-009, August 1970.

12. J. C. Armour and J. N. Cannon. Fluid Flow Through Woven Screens. AIChE Journal, Vol. 14, No. 3, May 1962, p 415-420.

13. J. N. Castle and E. C. Cady. Performance Testing of An Integrated Liquid Hydrogen Storage, Acquisition, and Vent System. McDonnell Douglas Astronautics Co. Report MDC G3092, June 1972.

14. D. F. Gluck. Transient Flow in Capillary Systems. Rockwell International Report SD 73-SA-0041, NASA/MSFC Contract NAS7-200, 27 March 1973.

Appendix A

THERMAL ANALYSIS OF THE INTERFACE DEMONSTRATION UNIT (IDU) THERMODYNAMIC VENT SYSTEM (TVS)

The derivation of the governing equations for an LH_2 tank equipped with thermodynamic vent system (TVS) cooling coils is given below. The tank is cylindrical with a helical TVS coil and optional external insulation. Heat is transferred to the tank by convection, condensation, and/or radiation. Steady-state conditions are assumed. Equations are first obtained for the case of uniform heat transfer coefficient between the heat exchange fluid and the tube wall over the tube length. The analysis is then extended to the case of two regions of different tube wall heat transfer coefficients in Appendix B.

A.1 DERIVATION OF GOVERNING EQUATIONS

For steady-state one-dimensional heat flow with the finned tube model shown in Figure A-1, the heat balance is (see Figure A-1):

$$Q_o|_x = Q_i|_{x + dx} + (Q_r + Q_e + Q_f)|_{dx} \tag{A-1}$$

The conductive heat flux out is:

$$Q_o|_x = K_T A \frac{dT}{dx} \tag{A-2}$$

The conductive heat flux in is:

$$Q_i|_{x + dx} = K_T A \frac{dT}{dx} + \frac{d}{dx}\left(K_T A \frac{dT}{dx}\right) dx \tag{A-3}$$

The external net radiative heat flux out is assumed to be constant, independent of the wall temperature, since the wall temperatures are of the order of 40° to 50°R. The radiative heat flux is, therefore, decoupled from the heat transfer analysis for the tank, which greatly simplifies this problem. The radiative heat flux is given by

$$Q_r|_{dx} = q_r L\, dx \tag{A-4}$$

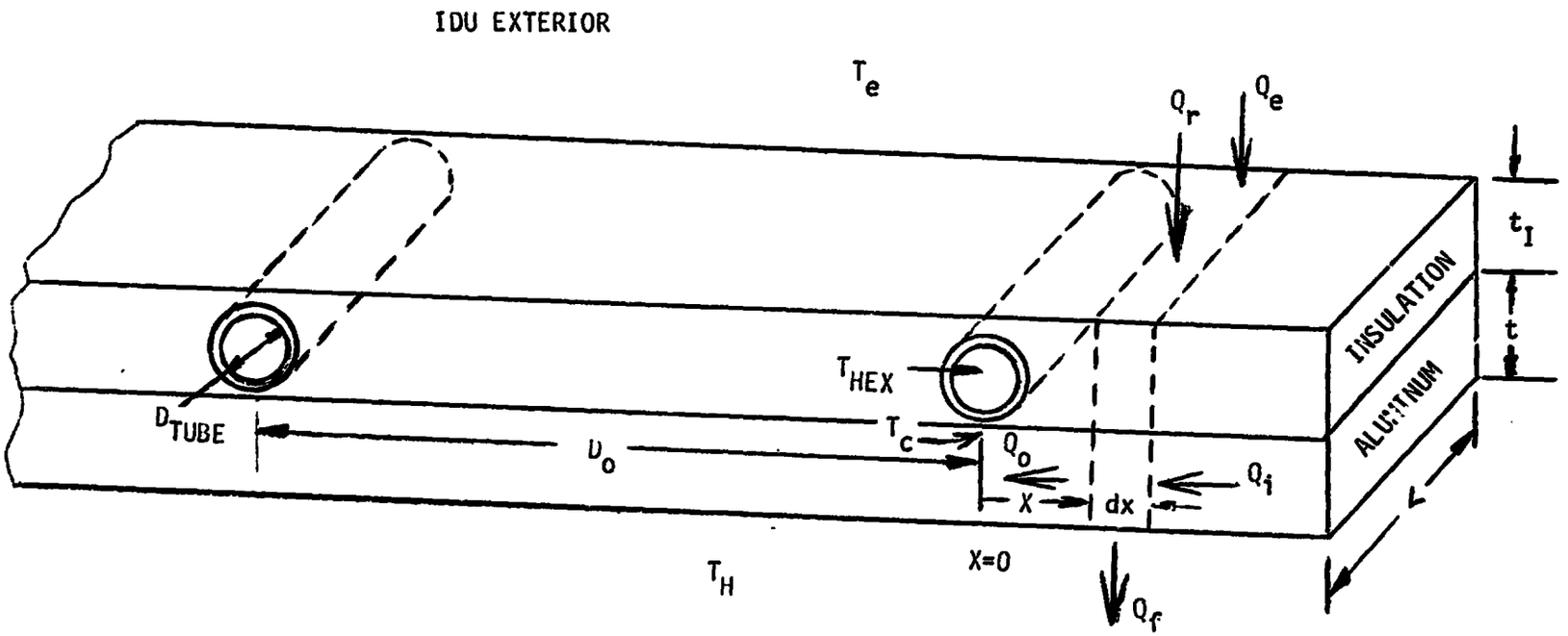

Figure A-1 - IDU/TVS CONFIGURATION

The external heat flux reaching the metal wall due to convection or condensation, and including the effect of the thermal resistance of the insulation is

$$Q_e\Big|_{dx} = U\ L\ dx\ (T_e - T), \tag{A-5}$$

where U, the overall heat transfer coefficient is given by

$$\frac{1}{U} = \frac{1}{h_e} + \frac{t_I}{K_I}\ . \tag{A-6}$$

(If condensation occurs, radiation heat flux will be neglected.)

Allowing for the presence of liquid and vapor in the IDU tank requires that the heat balance be obtained for these two separate regions. The TVS tube length adjacent to the liquid is LH_L/H_T and for the vapor, the length is $L(1 - H_L/H_T)$, where H_L is the height of the liquid in the tank. The tank height is H_T.

The internal convective heat transfer from the liquid to the wall is

$$Q_f\Big|_{dx,L} = h_{f_L}\ L\ dx\ (T_{H_L} - T)\ \frac{H_L}{H_T}\ , \tag{A-7}$$

where it is assumed that the bulk liquid temperature T_{H_L} outside the thermal boundary layer is constant in the liquid; that is, there is no thermal stratification in the liquid. This assumption is necessary for this one-dimensional analysis.

The internal convective or condensation heat transfer from the vapor to the wall is

$$Q_f\Big|_{dx,V} = h_{f_V}\ L\ dx\ (T_{H_V} - T)\ \left(1 - \frac{H_L}{H_T}\right) \tag{A-7a}$$

The governing differential equation for the liquid region is obtained by substituting Equations (A-2) to (A-5) and (A-7a) into Equation (A-1), assuming the tube length is $L\ H_L/H_T$, which gives

$$K_T \frac{L\ H_L}{H_T}\ t\ \frac{d^2T}{dx^2} = -\ q_r \frac{H_L}{H_T} - h_{f_L} \frac{H_L}{H_T} (T_{H_L} - T) - U \frac{L\ H_L}{H_T} (T_e - T) \qquad \text{(A-8)}$$

or, upon simplification and rearranging,

$$\frac{d^2T}{dx^2} = -\ \frac{(h_{f_L} + U)}{K_T t} (T_{a_L} - T) \qquad \text{(A-9)}$$

where

$$T_{a_L} = \frac{q_r + h_{f_L}\ T_{H_L} + UT_e}{h_{f_L} + U} \qquad \text{(A-10)}$$

Similarly, the differential equation for the vapor region is

$$\frac{d^2T}{dx^2} = -\ \frac{(h_{f_v} + U)}{K_T t} (T_{a_v} - T) \qquad \text{(A-11)}$$

where

$$T_{a_V} = \frac{q_r + h_{f_v}\ T_{H_v} + UT_e}{h_{f_v} + U} \qquad \text{(A-12)}$$

The boundary conditions for Equation (A-9) are

$$T = T_{C_L} \text{ at } X = 0 \qquad \text{(A-13a)}$$

$$\frac{dT}{dx} = 0 \text{ at } X = D_o/2 \qquad \text{(A-13b)}$$

and for Equation (A-11),

$$T = T_{c_v} \text{ at } X = 0 \tag{A-14a}$$

$$\frac{dT}{dx} = 0 \text{ at } X = D_o/2 \tag{A-14b}$$

Nondimensionalizing with

$$\theta_L = \frac{T_{a_L} - T}{T_{a_L} - T_{c_v}} \tag{A-15a}$$

and

$$\xi = \frac{2x}{D_o} \tag{A-15b}$$

Equation (A-9) assumes the classic form

$$\frac{d^2\theta_L}{d\xi^2} = N_L^2 \, \theta_L \tag{A-16}$$

where

$$N_L = \sqrt{\frac{(h_{f_L} + U) \, D_o^2}{4K_T t}} \tag{A-17}$$

and similarly, Equation (A-11) becomes

$$\frac{d^2\theta_v}{d\xi^2} = N_v^2 \, \theta_v \tag{A-18}$$

where

$$\theta_v = \frac{T_{a_v} - T}{T_{a_v} - T_{c_v}} \tag{A-19}$$

and

$$N_v = \sqrt{\frac{(h_{f_v} + U)\, D_o^2}{4K_T t}} \,. \tag{A-20}$$

The solution to Equation (A-16) for the IDU liquid region is

$$\theta_L = \frac{\cosh N_L\ (1 - \xi)}{\cosh N_L} \tag{A-21}$$

or

$$T_L = T_{a_L} - (T_{a_L} - T_{c_L}) \frac{\cosh N_L\ (1 - \xi)}{\cosh N_L} \tag{A-22}$$

The solution to Equation (A-18) for the IDU vapor region is

$$\theta_v = \frac{\cosh N_v\ (1 - \xi)}{\cosh N_v} \tag{A-23}$$

or

$$T_v = T_{a_v} - (T_{a_v} - T_{c_v}) \frac{\cosh N_v\ (1 - \xi)}{\cosh N_v} \,. \tag{A-24}$$

The heat flux at X = 0 is assumed to be transferred to the fluid in the TVS tube. The heat entering the tube from one side is given by, for the liquid region,

$$Q_L\Big|_{x=0} = - K_T \frac{LtH_L}{H_T} \frac{dT}{dx}\Big|_{x=0}$$

Using Equation (A-22),

$$Q_L\Big|_{x=0} = - \frac{LH_L}{H_T} \sqrt{(h_{f_L} + U) K_T t}\,(T_{a_L} - T_{c_L}) \tanh N_L \qquad \text{(A-25)}$$

Similarly, the heat flux entering the tube from one side is given by, for the vapor region, using Equation (A-24),

$$Q_v\Big|_{x=0} = - L \left(1 - \frac{H_L}{H_T}\right)(T_{a_v} - T_{c_v}) \sqrt{(h_{f_v} + U) K_T t}\,\tanh N_v \qquad \text{(A-26)}$$

The total heat transfer removed by the TVS flow, Q, must be equal to twice the heat transfer entering one side of the TVS coil, or

$$Q_T = 2\, Q_L\Big|_{x=0} + 2\, Q_v\Big|_{x=0}, \qquad \text{(A-27)}$$

since heat is transferred to the tube from both sides.

For long-term storage, it may be necessary that steady-state conditions be maintained. In this case, the net heat entering the tank must be zero. If the heat exchanger covers the tank wall, and no extraneous heat flows into the tank, steady-state conditions can be maintained by requiring that the surface integral of heat flux between the wall and the fluid contained in the IDU, $Q_{\text{wall fluid}}$, is zero:

$$Q\Big|_{\substack{\text{wall}\\ \text{fluid}}} = + 2 \int_0^{D_o/2} h_{f_L} L \frac{H_L}{H_T} (T_{H_2} - T_L)\, dx + 2 \int_0^{D_o/2} h_{f_v} \qquad \text{(A-28)}$$

$$L \left(1 - \frac{H_L}{H_T}\right)(T_{H_2} - T_V)\, dx = 0$$

Substituting into Equation (A-28) for T_L and T_V from Equations (A-22) and (A-24), respectively, gives upon integrating,

$$Q\Big|_{\substack{\text{wall}\\\text{fluid}}} = +2\,h_{f_L}\,L\,\frac{H_L}{H_T}\left\{\frac{D_o}{2}\,(T_{H_2}-T_{a_L})+\frac{(T_{a_L}-T_{c_L})}{\cosh N_L}\,\frac{\text{Sinh } N_L}{N_L(-\frac{2}{D_o})}\right.$$
$$\left.(1-\frac{2x}{D_o})\Big|_0^{D_o/2}\right\}+2h_{f_V}\,L\,(1-\frac{H_L}{H_T})\left\{\frac{D_o}{2}\,(T_{H_2}-T_{a_V})\right. \qquad \text{(A-29)}$$
$$\left.+\frac{(T_{a_V}-T_{c_V})}{\cosh N_V}\,\frac{\text{Sinh } N_V}{N_V\,(\frac{2}{D_o})}\right\}=0$$

Simplifying Equation (A-29)

$$Q_{\substack{\text{wall}\\\text{fluid}}} = +2\,h_{f_L}\,L\,\frac{H_L}{H_T}\,\frac{D_o}{2}\left\{(T_{H_2}-T_{a_L})+\frac{(T_{a_L}-T_{c_L})}{N_L}\tanh N_L\right\}$$
$$+2\,h_{f_V}\,L\,(1-\frac{H_L}{H_T})\,\frac{D_o}{2} \qquad \text{(A-30)}$$
$$\left\{(T_{H_2}-T_{a_V})+\frac{(T_{a_V}-T_{c_V})}{N_V}\tanh N_V\right\}=0$$

However, if extraneous sources of heat flux into the tank are present, then the heat exchanger must flow an additional amount of coolant in order to maintain steady state conditions. In this case, the extraneous heat transfer, Q_{ext} into the IDU and the wall heat transfer out of the IDU must be equal, giving,

$$Q\Big|_{\substack{\text{wall}\\\text{fluid}}} - Q_{ext} = 0 \qquad \text{(A-31)}$$

The above Equation (A-31) gives a relationship for T_{c_L} and T_{c_V} which must be satisfied in order to maintain steady-state conditions.

A.2 IDU FILLED WITH LIQUID

For the IDU/TVS test, the IDU will be full of LH_2. Therefore, this case is treated separately, and is the condition programmed. The appropriate steady-state condition for the IDU filled with liquid is solved below:

Since

$$Q_{wall} - Q_{ext} = 0,$$

Equation (A-29) gives

$$+ 2\, h_{f_L} \frac{L\, D_o}{2} \left(T_{H_2} - T_{a_L}\right) + \frac{\left(T_{a_L} - T_{c_L}\right) \tanh N_L}{N_L} - Q_{ext} = 0 \qquad \text{(A-32)}$$

$$\therefore \quad T_{a_L} - T_{c_L} = - \left(T_{H_2} - T_{a_L}\right) \frac{N_L}{\tanh N_L} + \frac{Q_{ext}\, N_L}{2\, h_{f_L} \frac{L\, D_o}{2} \tanh N_L} \qquad \text{(A-33)}$$

The total heat transfer removed by the TVS is given by Equation (A-27) is

$$Q_T = 2Q_L\Big|_{x\,=\,0} \qquad \text{(A-34)}$$

Substituting Equation (A-33) into Equation (A-25) and then into Equation (A-34) gives

$$Q_T = - 2\, L \sqrt{\left(h_{f_L} + U\right) K_T t} \left\{ - \left(T_{H_2} - T_{a_L}\right) N_L + \frac{Q_{ext}}{2\, h_{f_L} \frac{L\, D_o}{2}} N_L \right\}$$

$$Q_T = - 2\, N_L\, L \sqrt{\left(h_{f_L} + U\right) K_T t} \left\{ - \left(T_{H_2} - T_{a_L}\right) + \frac{Q_{ext}}{2\, h_{f_L} \frac{L\, D_o}{2}} \right\}$$

$$Q_T = + 2\, L \left(h_{f_L} + U\right) \frac{D_o}{2} \left\{ \left(T_{H_2} - T_{a_L}\right) - \frac{Q_{ext}}{2\, h_{f_L} \frac{L\, D_o}{2}} \right\} \qquad \text{(A-35)}$$

Since Q_T is the heat removed by the TVS, the minimum mass flow rate of liquid in the TVS is determined by

$$|Q_T| = \dot{m}_L \Delta h_{LV}$$

where $\dot{m}_L$ is the initial fraction of liquid mass flow rate resulting from the expansion through the inlet orifice.

It is assumed that $\dot{m}_L$, the mass flowrate of the liquid in the TVS, is known and that vaporization transforms all liquid in the TVS to vapor but no superheating of the vapor occurs. Knowing $\dot{m}_L$ for the steady state gives Q_T for the experiment, which allows an overall heat transfer coefficient on the inner surface of the IDU to be calculated, if extraneous sources of heat can be determined, by using Equation (A-35).

The heat flux transferred to the fluid in the TVS assuming the IDU is full of liquid is given in terms of the saturation temperature, T_{HEX} of the two-phase fluid in the TVS and the tube internal heat transfer coefficient as:

$$Q_T\Big|_{liquid} = \pi D_{tube} h_i L (T_{c_L} - T_{HEX}) , \qquad (A-37)$$

where it is assumed that T_{HEX} is a constant, no superheat of the TVS vapor is present, there is no significant pressure drop along the TVS line, and h_i is a constant.

For given heat transfer coefficients, the IDU and external temperatures determine Q_T and T_{c_L}; the TVS tube length can be evaluated knowing the heat exchanger temperature, T_{HEX}, or vice versa.

Since L is known for the IDU, the necessary T_{HEX} is determined as

$$T_{HEX} = T_{c_L} - \frac{Q_T}{\pi D_{tube} h_i L} , \text{ where } T_{c_L} \text{ is given by Equation (A-33)} \qquad (A-38)$$

(The saturation temperature of the TVS fluid must be lowered as Q_T increases.)

The above experssion is used to establish the TVS pressure required to obtain the coolant T_{HEX} which corresponds to steady-state conditions in the tube. Or, knowing Q_T, T_{C_L}, and T_{HEX}, the associated average h_f can be determined.

From the standpoint of controlling the TVS so as to maintain steady-state conditions, it is seen that the mass flowrate must be set such that the total heat flux, Q_T, can be removed and such that the TVS fluid temperature, T_{HEX}, determined by the tank and TVS pressures must be low enough to allow Q_T heat to be transferred to the fluid, given h_f and L. However, it should be noted that in practice a greater mass flowrate may be used in the TVS than is required for the IDU, with the remainder of the liquid used for cooling downstream equipment.

As a check, the heat transfer to the tank wall from the surrounding region plus the extraneous heat is determined, since this must be identically equal in magnitude and opposite in size to Q_T, the heat transfer removed from the IDU, as obtained in Equation (A-35). Heat transferred to the tank is given by

$$Q_T\Big|_{ext} = 2\int_0^{D_o/2} UL\,(T_e - T)\,dx + Q_{ext} \tag{A-39}$$

$$= 2\,UL\left\{\frac{D_o}{2}(T_e - T_{a_L}) + \frac{D_o}{2}\,\frac{(T_{a_L} - T_{c_L})}{N_L}\tanh N_L\right\} + Q_{ext} \tag{A-40}$$

Using Equation (A-33),

$$Q_T = 2\,UL\left\{\frac{D_o}{2}(T_e - T_{a_L}) - \frac{D_o}{2}(T_{H_2} - T_{a_L}) + \frac{Q_{ext}}{2\,h_{f_L}\,L}\right\} + Q_{ext} \tag{A-41}$$

$$= UL\,D_o\,(T_e - T_{H_2}) + \left(1 + \frac{U}{h_{f_L}}\right) Q_{ext}$$

From Equation (A-35), using the expression for T_{a_L}

$$Q_T = +2\,L\,(h_{f_L} + U)\,\frac{D_o}{2}\left\{T_{H_2} - \frac{(h_{f_L}\,T_{H_2} + UT_e)}{h_{f_L} + U} - \frac{Q_{ext}}{h_{f_L}\,L\,D_o}\right\} \tag{A-42}$$

which gives, for the heat transfer from the IDU,

$$Q_T = - U L D_o (T_e - T_{H_2}) - (1 + \frac{\dot{U}}{\dot{m}_{f_L}}) Q_{ext} \quad (A-43)$$

Since Q_T determined by the heat transfer from the liquid in the IDU is identical in magnitude and opposite in size with that based on the heat transfer from the surrounding region, the analysis is consistent.

Heat transfer coefficients are given in Table A-1 based on the compilation of Reference A-1. At this point, there is no applicable information on the flow pattern of liquid or gas with a vertical wall subjected to cyclical temperature variations, nor is it known what type of condensate flow occurs. Standard equations for the heat transfer equation are used in the analysis which can be modified where appropriate following additional TVS tests. The assumptions used in selecting the expressions for the heat transfer coefficients are summarized below.

A.2.1 Condensation – Outer

Film condensation is assumed and the Nusselt film theory expression is used. Condensate is assumed to flow down a characteristic distance, D_o, equal to the tube spacing. The outer condensate temperature is equal to the saturation temperature of the surrounding vapor (GH_2) and the wall temperauure is approximated as an average temperature, $(T_c + T_{max})/2$. If $(T_c + T_{max})/2$ is greater than the saturation temperature, condensation is assumed not to occur.

A.2.2 Free Convection – Gas, Outer

The free convection heat transfer outside the IDU is assumed to be due to convection cells such as are shown in Table A-1. The characterisitic length, x, is $D_o/2$ in the heat transfer coefficient expression. The temperature difference between the area of width $D_o/2$ centered on the tube is approximated as $T_e - T_{c_L}$ which is high, since this area has a temperature gradient and the average wall temperature is less than T_{c_L}.

Between the coils the wall temperature is assumed to be high enough such that the temperature difference is $T_{max} - T_e$, corresponding to free convection with a warm wall and cold gas. The direction of rotation of the associated cell

Table A-1
IDU HEAT TRANSFER COEFFICIENTS

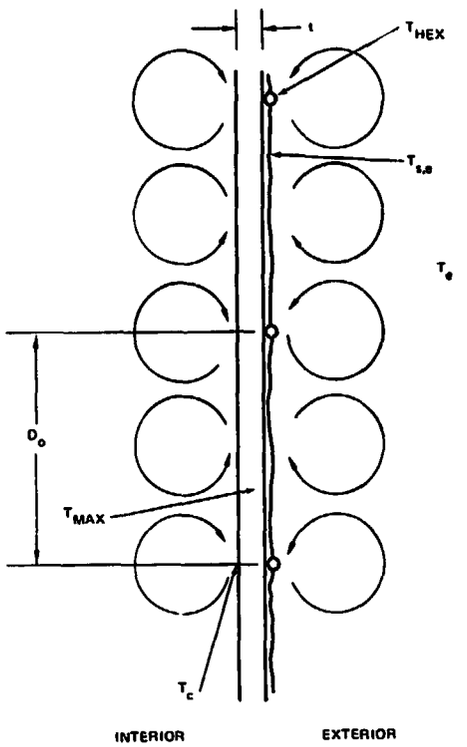

Condensation - Outer

$$h_{e,c} = \frac{K_L}{X}\left[g\rho_L h_{LV} X^3/4\ V_L K_L\ (T_{s,e} - T_w)\right]^{1/4}$$

$$x = D_o\ ;\ T_w = \frac{T_c + T_{max}}{2}$$

Free Convection - Vapor, Outer - Alternating Cells

cold wall, warm vapor: $X = D_o/2$

$$h_{e,wg} = 0.55\ \frac{K_g}{X}\left[\frac{\rho_g^{\,2}\beta_g\ g\left(T_e - T_{c_L}\right) X^3}{\mu_g^{\,2}} \cdot \frac{c_{p_g}\ \mu_g}{K_g}\right]^{1/4}$$

warm wall, cold gas: $X = D_o/2$

$$h_{e,cg} = 0.55\ \frac{K_g}{X}\left[\frac{\rho_g^{\,2}\beta_g\ g\left(T_{max_L} - T_e\right) X^3}{\mu_g^{\,2}} \cdot \frac{c_{p_g}\ \mu_g}{K_g}\right]^{1/4}$$

$$T_{max_L} = T_{a_L} - \frac{\left(T_{a_L} - T_{c_L}\right)}{\cosh N_L}$$

$$h_e = \left(h_{e,wg} + h_{e,cg}\right)/2$$

$$10^3 < [\quad] < 10^9$$

Free Convection - Vapor, Outer

cold wall, warm vapor: $X = H_T$

$$h_{e,wg} = 0.55\ \frac{K_g}{X}\left[\frac{\rho_g^{\,2}\beta_g\ g\left(T_e - T_{avg}\right) X^3}{\mu_g^{\,2}} \cdot \frac{c_{p_g}\ \mu_g}{K_g}\right]^{1/4}$$

$$T_{avg} = \left(T_{c_L} + T_{max_L}\right)/2$$

$$10^3 < [\quad] < 10^9$$

Free Convection - Liquid, Inner - Alternating Cells

cold wall, warm liquid: $X = D_o/2$

$$h_{f_{L,wl}} = 0.55\ \frac{K_L}{X}\left[\frac{\rho_L^{\,2}\beta_L\ g\left(T_{H_2} - T_{c_L}\right) X^3}{\mu_L^{\,2}} \cdot \frac{c_{p_L}\ \mu_L}{K_L}\right]^{1/4}$$

warm wall, cold liquid: $X = D_o/2$

$$h_{f_{L,cl}} = 0.55\ \frac{K_L}{X}\left[\frac{\rho_L^{\,2}\beta_l\ g\left(T_{H_2} - T_{c_L}\right) X^3}{\mu_L^{\,2}} \cdot \frac{c_{p_L}\ \mu_L}{K_L}\right]^{1/4}$$

$$10^3 < [\quad] < 10^9$$

pattern is opposite to that for the cold wall/warm gas combination. The equations for free convection are valid for Rayleigh numbers between 10^3 and 10^9.

The calculated heat transfer coefficients are averaged to obtain an overall heat transfer coefficient. Thus,

$$h_e = \frac{h_{e,wg} + h_{e,cg}}{2} .$$

The temperature differences assumed are not expected to have a major effect on the values of the heat transfer coefficients, since they are taken to the 1/4 power in the equation. Moreover, the most significant approximation is the use of free convection boundary layer expressions for a complicated ablation flow pattern, for which there is no known analysis.

In some cases, T_{max} will be less than T_e, and therefore, the entire IDU wall is cold with respect to the surrounding fluid. In this case, the characteristic length is $x = H_T$, and the temperature difference assumed in determining $h_{e,wg}$ is $(T_{c_L} + T_{max_L})/2$.

A.2.3 Free Convection – Liquid Inner

The alternating cellular flow pattern is assumed to exist inside the IDU with a characteristic length of $X = D_0/2$. The temperature difference between the cold wall and warm liquid is assumed to $T_{H_2} - T_{c_L}$, which is high.

The corresponding temperature difference between the warm wall and cold liquid is $T_{max,L} - T_{H_2}$. Again, these equations are assumed to be valid for Rayleigh numbers between 10^3 and 10^9, and the overall heat transfer coefficient on the inside of the IDU cylindrical wall is the average of the two values calculated:

$$h_{f_L} = (h_{f_{L,wl}} + h_{f_{L,cl}})/2.$$

Table A-2 (Page 1 of 2)

EXTRANEOUS HEAT TRANSFER - TOP OF IDU TANK

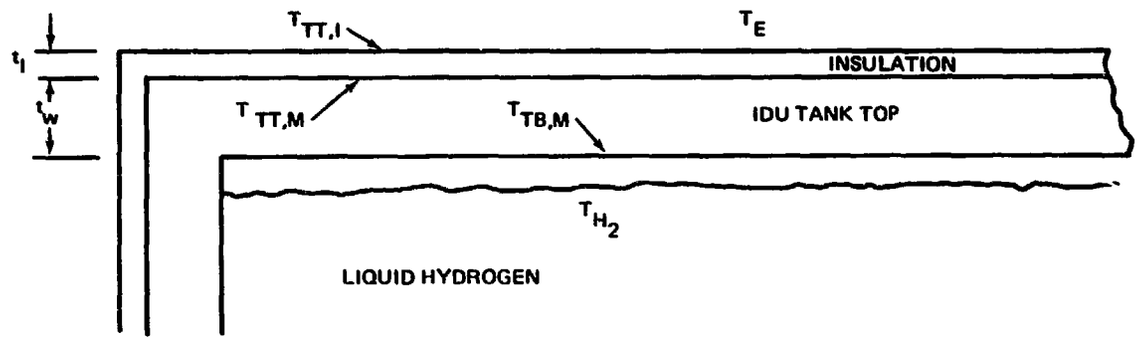

Extraneous Heat Flux Relation Based on Total Thermal Resistance

$$Q_{EXT} = U_{TOP} A_c (T_e - T_{H_2});$$

$$\frac{1}{U_{TOP}} = \frac{1}{h_{T,external}} + \frac{t_I}{K_I} + \frac{t_w}{K_w} + \frac{1}{h_{T,\ internal}};$$

$$A_c = \frac{\pi D^2_{TANK}}{4}$$

Heat Flux Relations for Individual Thermal Resistances

Free convection heat transfer from external gas to insulated top of tank at temperature $T_{TT,I}$:

$$Q_{EXT} = h_{T,external} A_c (T_e - T_{TT,I})$$

Free convection heat transfer from external gas to uninsulated top of tank at temperature $T_{TT,M}$:

$$Q_{EXT} = h_{T,external} A_c (T_e - T_{TT,M})$$

Conductive heat transfer through insulation

$$Q_{EXT} = \frac{K_I A_c}{t_I} (T_{TT,I} - T_{TT,M})$$

Table A-2 (Page 2 of 2)

EXTRANEOUS HEAT TRANSFER - TOP OF IDU TANK

Conductive heat transfer through metal tank top

$$Q_{EXT} = \frac{K_M A_c}{t_M} (T_{TT,M} - T_{TB,M})$$

Free convection heat transfer from bottom wall of metal tank top to IDU hydrogen vapor

$$Q_{EXT} = h_{T,internal} A_c (T_{TB,M} - T_{H_2})$$

$$h_{T,external} = 0.08 K_g \left[\frac{\rho_g^2 \beta_g c_{p,g} g (T_e - T_{TT,M})}{\mu_g K_g} \right]^{1/3}$$

$$h_{T,internal} = 0.08 K_g \left[\frac{\rho_g^2 \beta_g c_{p,g} g (T_{TB,M} - T_{H_2})}{\mu_g K_g} \right]^{1/3}$$

A.2.4 Extraneous Heat Transfer

The extraneous heat transfer is not known nor is it practical with the present IDU instrumentation to determine it. However, an estimate can be made based on the assumption that the major portion of this heat flux enters the IDU through the top of the cover. Free convection heat transfer coefficients are assumed and insulation may be included, as shown in Table A-2. It is assumed that the IDU is not completely full and, therefore, an ullage gas layer exists between the liquid surface and the top of the cover.

A.2.5 Forced Convection – TVS Tube (Mist Flow Regine)

At relatively high heat fluxes, a mist flow regime is possible since liquid droplets no longer "wet" the tube wall, due to the momentum of the rapidly evaporating vapor between the liquid droplet and heat surface supporting droplet. This is referred to as stable film boiling, and occurs at or above the Leidenfrost point. Measurements of heat transfer coefficient for this regime are close to the corresponding values for the vapor alone.

As a first approximation, the Dittus-Boelter equation for forced convection heat transfer coefficient is used, which gives

$$h_i = \frac{.023\ k_v}{L} (Re_V)^{0.8} (P_{r_V})^{0.4}$$

where

$$Re_V = \frac{4\ \dot{m}}{\pi \mu\ D_{TUBE}}$$

$$P_{r_V} = \frac{c_p \mu}{k}$$

$$P_{r_V} = \frac{2.6(.00202)}{.0074} = 0.71 \quad \text{at} \quad T = 31°R$$

However, in normal operations with the IDU/TVS, the heat flux is relatively low. Assuming a maximum value of 600 Btu/hr, distributed over the surface of the 70 feet of 0.25-inch O.D. tube, the heat flux is 130 Btu/ft^{2}hr. The peak nucleate boiling heat flux for liquid hydrogen is reported to be 32,000 Btu/ft^{2}hr in Reference A-2. Since the heat flux for the TVS is far below that required for peak nucleate boiling, it is probable that the heat transfer coefficient will correspond to that of the two-phase flow in the initial region. The heat transfer calculations in this regime are more involved and require that two heat transfer regions be treated. The associated analysis is treated in Appendix B.

IDU/TVS HEAT TRANSFER EFFECTS ON LIQUID FLOWING FROM IDU TO ORIFICE MANIFOLD

When the IDU is completely surrounded by warm ullage gas in the 105" APS tank, heat transfer to the liquid hydrogen coolant flowing from the IDU/TVS feedline outlet to the orifice manifold through the initial inlet section can cause boiling before the liquid reaches the orifices. The severity of this problem and the importance of TVS line insulation is determined below. In most applications, however, the lower portion of the IDU will be submerged in liquid, and therefore, boiling in the initial inlet section will not occur.

The tube leading from the start tank feedline to the orifice manifold is taken to be about 15 inches long (including end fittings). The tube is 1/4 inch stainless steel with a wall thickness of 0.020 inch.

Assume hydrogen properties at 100°R and 50 psi.

Density, $\rho = 0.095$ lb/ft^3 (data range from 0.088 to 0.102)
Specific heat, $C_p = 2.61$ Btu/Lb°R
Viscosity, $\mu = 1.49 \times 10^{-7}$ lb/in-sec
$= 1.79 \times 10^{-6}$ lb/ft-sec
Thermal Conductivity, $k = 0.55 \times 10^{-6}$ Btu/in-sec°R
$= 6.6 \times 10^{-6}$ Btu/ft-sec°R
Thermal Expansion Coefficient, $\beta = 0.022\ (°R)^{-1}$

For a horizontal cylinder in laminar flow, the Nusselt number for free convection is

$$N_{u_L} = \frac{hD}{k} = 0.53\ (R_a)^{1/4},\ 10^4 < R_a < 10^8$$

and in turbulent flow

$$N_{u_T} = 0.13\ (R_a)^{1/3},\ 10^4 < R_a < 10^{12} \tag{A-45}$$

Free convection heat transfer will actually be somewhat lower because of the proximity of the cold IDU bottom; it shall be assumed to be about

$$N_{u_L} = 0.4\ (R_a)^{1/4};\ N_{u_T} = 0.1\ (R_a)^{1/3} \tag{A-46}$$

where

$$R_a = \frac{g\beta\Delta T D^3}{\nu k} = 1.16 \times 10^3\ \Delta T \tag{A-47}$$

Since temperature differences of the order of 100 R are assumed, the flow is laminar and the Nussult number is

$$N_u = 2.34\ (\Delta T)^{1/4} \tag{A-48}$$

The free convection heat transfer rate is

$$\dot{Q} = hA\Delta T = \frac{k}{D} Nu\ (\pi DL\Delta T)$$

$$\dot{Q} = 0.218\ \Delta T^{\,5/4}\ \text{Btu/hr} \tag{A-49}$$

Let the initial state of the liquid hydrogen be saturated at 14.7 psia, but pressurized at 30 psia. The liquid bulk temperature is T = 36.5°i

The initial enthalpy, H_o, is -108 Btu/lb, the saturated liquid enthalpy at 30 psia, $H_{30,\ell}$, is -95 Btu/lb, and the saturated vapor enthalpy at 30 psia, $H_{30,v}$, is +90 Btu/lb. At steady state, the liquid enthalpy reaching the orifices is

$$H = H_o + \dot{Q}/\dot{W}$$

where $\dot{W}$ is the mass flow rate, lbs/hr. The mass flow rate must be $\dot{W} \geq \dot{Q}/13$ in order for pure liquid to reach the orifice for the above case.

The enthalpy of saturated liquid at 14.7 psi is -108 Btu/lb, and the enthalpy of saturated vapor is +82 Btu/lb. The heat of vaporization is, therefore, 190 Btu/lb, and the quality of liquid reaching the orifices is

$$X = \frac{\dot{Q}}{\dot{W}h_v} = 1.09 \times 10^{-3} \frac{\Delta T^{5/4}}{\dot{W}}, \qquad \text{(A-50)}$$

if the liquid is stored in the tank at the saturation pressure of 14.7 psi.

In general, the quality of the liquid reaching the orifice will be, for the tank pressurized to 30 psia,

$$X = \frac{\dot{Q} - \dot{W}\,(H_{30,\ell} - H_o)}{\dot{W}h_v} \qquad \text{(A-51)}$$

where

$$h_v = H_{30,v} - H_{30,\ell}$$

In order for pure liquid to reach the orifices, X must be zero and, therefore, high flowrates and/or high tank pressures must be applied if the heat flux into the line is significant. For example, $\dot{Q}$ = 29 Btu/hr with ΔT - 50°R, which requires a flowrate in excess of 2.2 lb/hr with a tank pressure of 30 psia, if pure liquid is to be supplied to the orifice.

Since it is necessary to be able to supply lower coolant flowrates, the need for insulation on the TVS inlet line up to and including the viscojet flow control orifices is apparent. In addition, condensation heat transfer rates are higher than the free convection rates used in this analysis, further indicating the necessity for insulation in the event the IDU tank bottom is exposed to hydrogen ullage.

A.3 REFERENCES

A-1. B. E. Lauer. Heat Transfer Compilations. The Oil and Gas Company Journal and the Petroleum Publishing Company, Tulsa, Oklahoma, 1953.

A-2. E. G. Brentari, etal. Boiling Heat Transfer for Oxygen, Nitrogen Hydrogen, and Helium. NBS TN No. 317, September 20, 1965.

Appendix B
IDU/TVS ANALYSIS — TWO REGION MODEL

The analysis of the IDU/TVS presented in Appendix A assumes that the heat transfer coefficient between the heat exchanger fluid and the tube wall is uniform over the tube length, which corresponds to the case of oversupplying LH_2 to the TVS, in order to use the liquid remaining at the TVS exit for cooling of components, turbopumps, etc. If the flow rate is such that the fluid quantity exceeds a critical value, X_c, then there will be two regions in this two-phase tube flow with different mechanisms of heat transfer and sigmificantly different transfer coefficients. An analysis of this two-region heat transfer mcdel performed by D. W. Kendle is developed below.

The model is shown in Figure B-1. For the purposes of analysis, the tank surface and the heat exchanger tube length attached to this surface are divided into two regions as shown. Coolant fluid flows first through region 1 and then region 2; mass flow $\dot{m}$ and coolant temperature T_{hex} are the same for both regions. Two-phase fluid enters region 1 with quality X_1 and leaves at X_C (the value of X_C determines the boundary between the two regions). Entering with X_C, the fluid exits region 2 with a quality of X_F. Associated heat transfer coefficients are given in Appendix C.

Since the coolant temperature is the same throughout, the region with the higher heat transfer coefficient, assumed to be region 1, will have the lower tank wall temperature. In order for the net heat input to the tank contents to be zero when there are significant wall temperature differences, heat will pass through the warmer wall area (region 2) into the fluid and be removed from the fluid in the cooler wall area (region 1). The heat transfer rate between the two regions is Q_d. The extraneous heat input, Q_{ext}, enters the tank contents by means other than through the cooled wall; Q_{ext} is removed from the fluid by the cooled wall in region 1.

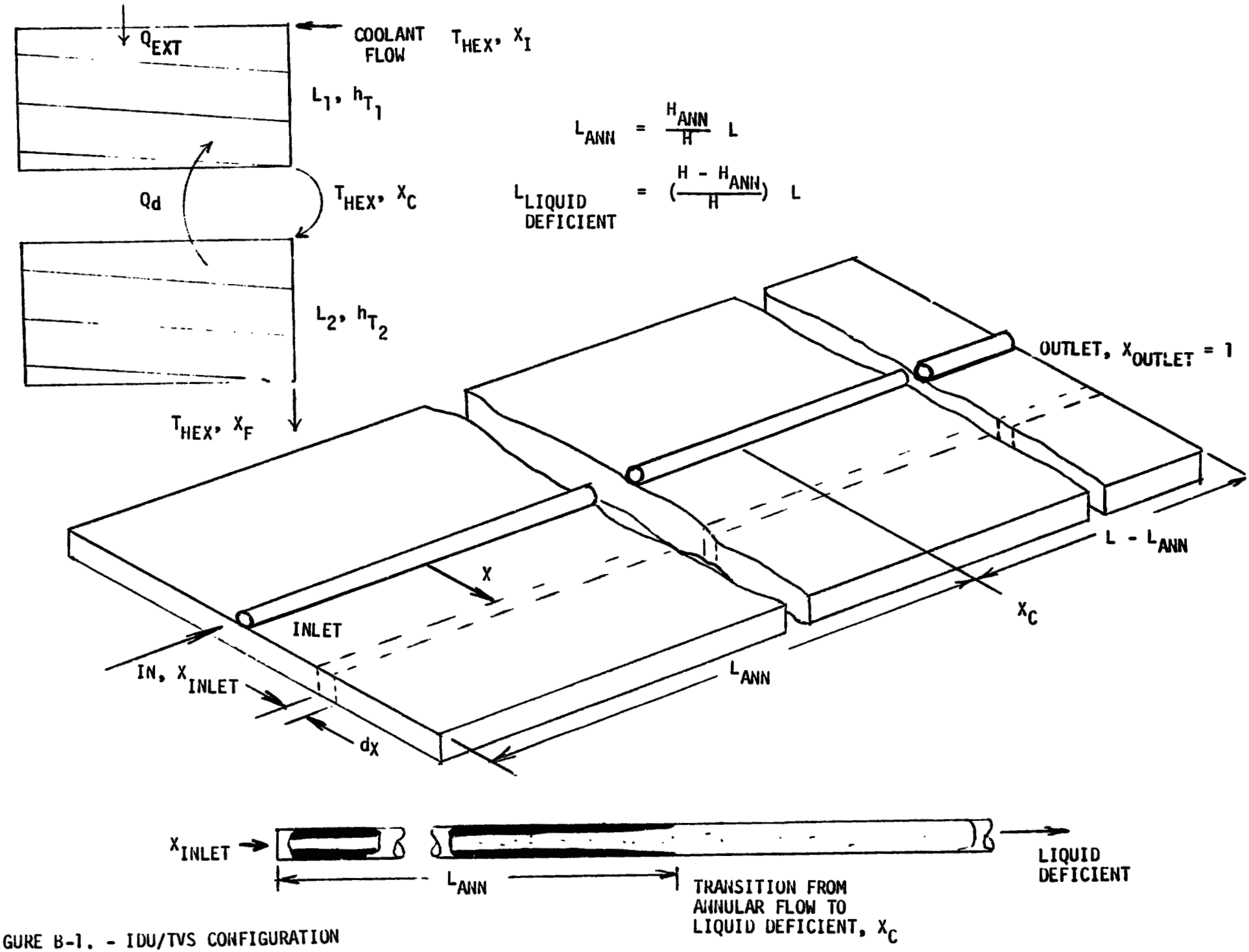

FIGURE B-1. - IDU/TVS CONFIGURATION

With this model, the thermal behavior of each region can be described by the same equations derived in Appendix A for a single region. The additional conditions described above link the two regions and enable a solution for the individual tube lengths, L_1 and L_2, in each region.

The fin root (tube wall) temperatures are given by Equation (A-33) in Appendix A; for the two regions of this model, they are written

$$T_{C_1} = T_{A_1} + (T_H - T_{A_1}) \frac{N_1}{\tanh N_1} - \frac{(Q_{ext} + Q_d) N_1}{L_1 h_{f_1} D_o \tanh N_1} \tag{B-1}$$

$$T_{C_2} = T_{A_2} + (T_H - T_{A_2}) \frac{N_2}{\tanh N_2} + \frac{Q_d \; N_2}{L_2 h_{f_2} D_o \tanh N_2} \tag{B-2}$$

In the above equations,

$$T_{A_i} = \frac{q_{r_i} + h_{f_i} T_H + U_i T_E}{h_{f_i} + U_i} \tag{B-3}$$

from Equation (A-10) of Appendix A and

$$N_i = \sqrt{\frac{\left(h_{f_i} + U_i\right) D_o^2}{4 k_{T_i} t}} \tag{B-4}$$

from Equation (A-17) of Appendix A, where subscript i can be either 1 or 2.

The Q_{ext} term of Appendix A is replaced in Equations (B-1) and (B-2) by $(Q_{ext} + Q_d)$ for region 1 and $(-Q_d)$ for region 2. Making this same substitution in Equation (A-43) of Appendix A gives

$$Q_{T_1} = L_1 U_1 D_o (T_E - T_H) + \left(1 + \frac{U}{h_f}\right)_1 (Q_{ext} + Q_d) \tag{B-5}$$

$$Q_{T_2} = L_2 U_2 D_o (T_E - T_H) - \left(1 + \frac{U}{h_f}\right)_2 Q_d \tag{B-6}$$

The heat wxchanger fluid temperature, given by Equation (A-38) in Appendix A, is the same for both regions:

$$T_{hex} = T_{C_1} - \frac{Q_{T_1}}{\pi D_{tube} L_1 h_{T_1}} = T_{C_2} - \frac{Q_{T_2}}{\pi D_{tube} L_2 h_{T_2}} \tag{B-7}$$

Substituting Equations (B-1), (B-2), (B-5), and (B-6) into Equation (B-7) gives

$$A_1 - B_1\left(\frac{Q_{ext} + Q_d}{L_1}\right) = A_2 + B_2\left(\frac{Q_d}{L_2}\right) \tag{B-8}$$

where

$$A_i = T_{A_i} + \left(T_H - T_{A_i}\right)\frac{N_i}{\tanh N_i} - \frac{U_i D_o (T_E - T_H)}{\pi D_{tube} h_{T_i}} \tag{B-9}$$

$$B_i = \frac{N_i}{h_{f_i} D_o \tanh N_i} + \frac{\left(1 + \frac{U}{h_f}\right)_i}{\pi D_{tube} h_{T_i}} \tag{B-10}$$

where subscript i is again 1 or 2. Solving Equation (B-8) for the rate of heat transfer internally from zone 2 to zone 1 gives

$$Q_d = \frac{A_1 - A_2 - \frac{B_1}{L_1} Q_{ext}}{\left(\frac{B_1}{L_1} + \frac{B_2}{L_2}\right)} \tag{B-11}$$

Adapting Equation (A-36) from Appendix A, the heat capacity of the fluid in each section is related to the heat load by

$$\dot{m} \Delta h_v (X_C - X_I) = Q_{T_1} \tag{B-12}$$

$$\dot{m} \Delta h_v (X_F - X_C) = Q_{T_2} \tag{B-13}$$

where $\dot{m}$ is the mass flowrate of heat exchanger fluid and Δh_v is the heat of vaporization of the fluid. Eliminating $\dot{m} \Delta h_v$ between these two equations and substituting Equations (B-5) and (B-6) gives

$$(L_1 C_1 - L_2 C_2)\left(\frac{B_1}{L_1} + \frac{B_2}{L_2}\right) + \left(\frac{D_2}{L_2} - \frac{D_1}{L_1}\right) + C_3 = 0 \tag{B-14}$$

where

$$C_1 = (X_F - X_C) U_1 D_o (T_E - T_H)$$

$$C_2 = (X_C - X_I) U_2 D_o (T_E - T_H)$$

$$C_3 = \left[(X_F - X_C)\left(1 + \frac{U}{h_f}\right)_1 + (X_C - X_I)\left(1 + \frac{U}{h_f}\right)_2\right](A_1 - A_2)$$

$$D_1 = B_1 (X_c - X_I) \left(1 + \frac{U}{h_f}\right)_2 Q_{ext}$$

$$D_2 = B_2 (X_F - X_C) \left(1 + \frac{U}{h_f}\right)_1 Q_{ext}$$

The total tube length L is

$$L_1 + L_2 = L \tag{B-15}$$

which is substituted into Equation (B-14) to eliminate L_2 giving a quadratic in L_1:

$$AL_1^2 + BL_1 + C = 0 \tag{B-16}$$

$$A = C_3 - (C_1 + C_2)(B_2 - B_1)$$

$$B = C_1 L (B_2 - B_1) - B_1 L (C_1 + C_2) - (D_1 + D_2) - C_3 L$$

$$C = C_1 B_1 L^2 + D_1 L$$

Since the coefficients of this quadratic are dependent on the temperature of the system which are in turn a function of L_1, the solution must be obtained iteratively. Values for the system temperatures are assumed initially and the coefficients are calculated, giving an approximate value of L_1. The system temperatures are calculated based on this L_1 and the iteration is repeated until things settle down.

Appendix C

INTERNAL HEAT TRANSFER EQUATIONS FOR INTERFACE DEMONSTRATION UNIT THERMODYNAMIC VENT SYSTEM

C.1 ANNULAR FLOW

Annular flow in the TVS is assumed from the viscojets to a distance along the tube at which transition to liquid deficient flow occurs. The model is based on the work of Chen (Reference D-1) who used Forster and Zuber's microconvective heat transfer relation for boiling and the Dittus-Boelter macroconvective heat transfer relation for forced convection, and obtains:

$$h = h_{MIC} + h_{MAC} \tag{C-1}$$

or

$$h = S\,(0.00122)\,\frac{K_L^{0.79}\,C_L^{0.45}\,\rho_L^{0.49}\,g_e^{0.25}\,\Delta T^{0.24}\,\Delta P^{0.75}}{\sigma^{0.5}\,\mu_L^{0.29}\,h_{fg}^{0.24}\,\rho_v^{0.24}}$$

$$+\ F\,(0.023)\,(Re)_L^{0.8}\,(Pr)_L^{0.4}\,\frac{K_L}{D} \tag{C-2}$$

where S and F are empirically determined dimensionless functions which allow for variations in the boiling and forced convection components, respectively. The value of S and F are given in Figures C-1 and C-2.

C.2 VAPOR FLOW (LIQUID DEFICIENT REGIME)

At an initial quality, X_c, transition from annular flow to vapor flow occurs, and the Dittus-Boelter equation for forced convection in a tube is used:

$$\frac{hD}{K_v} = 0.023\,\left(\frac{\rho_v\,V_v\,D}{\mu_v}\right)^{0.8}\,(Pr)_v^{0.4} \tag{C-3}$$

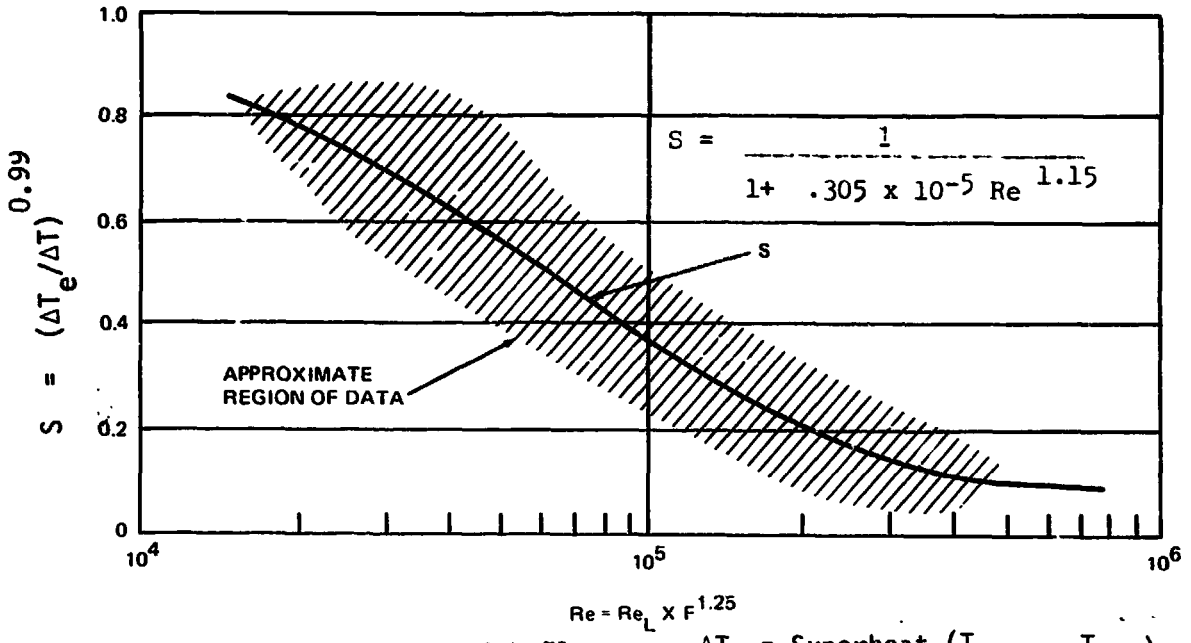

ΔT_e = Effective Superheat With Flow ΔT = Superheat $(T_{wall} - T_{sat})$

Figure C-1. Suppression Factor, S

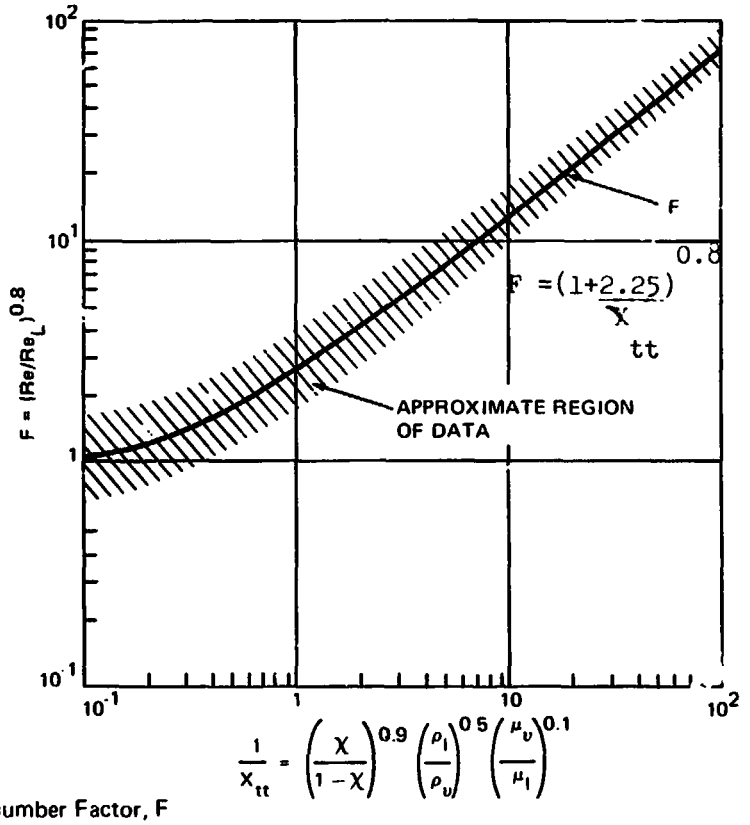

Figure C-2. Reynolds Number Factor, F

Appendix D
IDU/TVS TWO PHASE FLOW PRESSURE DROP

An approximate solution to the pressure drop of the TVS coolant flow is obtained using the homogeneous (Fog Flow) flow model (Reference D-1). The model assumes equal linear velocities of vapor and liquid, thermodynamic equilibrium between the phases, and use of a single-phase friction factor which is applicable to the two-phase flow. The pressure drop through the Viscojets is calculated separately.

D-1. TVS LINE PRESSURE DROP

The total pressure gradient, composed of frictional and dynamic losses, is given by (Reference D-1):

$$\left.\frac{dP}{dZ}\right|_{TOTAL} = \left.\frac{dP}{dZ}\right|_{FRICTION} + \left.\frac{dP}{dZ}\right|_{DYNAMIC} \qquad (D\text{-}1)$$

$$\left.\frac{dP}{dZ}\right|_{FRICTION} = \frac{f_\ell \dot{m}^2}{2 g_c \rho_\ell D\left(\frac{\pi D_i^2}{4}\right)^2} = \left\{\frac{1 + X\left(\frac{\rho_\ell}{\rho_v} - 1\right)}{1 + \frac{X \dot{m}^2}{g_c\left(\frac{\pi D_i^2}{4}\right)^2} \frac{d}{dP}\left(\frac{1}{\rho_v}\right)}\right\} \qquad (D\text{-}2)$$

$$\left.\frac{dP}{dZ}\right|_{DYNAMIC} = \frac{\dot{m}^2}{\left(\frac{\pi D_i^2}{4}\right)^2 \rho_\ell g_c} = \left\{\frac{\left(\frac{\rho_\ell}{\rho_v} - 1\right)\frac{dX}{dZ}}{1 + \frac{X \dot{m}^2}{\left(\frac{\pi D_i^2}{4}\right)^2 g_c} \frac{d}{dP}\left(\frac{1}{\rho_v}\right)}\right\} \qquad (D\text{-}3)$$

(Z = length of tube, D_i is inner diameter, f is friction factor, $\dot{m}$ is total mass flowrate, X is quality, ρ_ℓ is liquid density, ρ_v is vapor density, P is pressure)

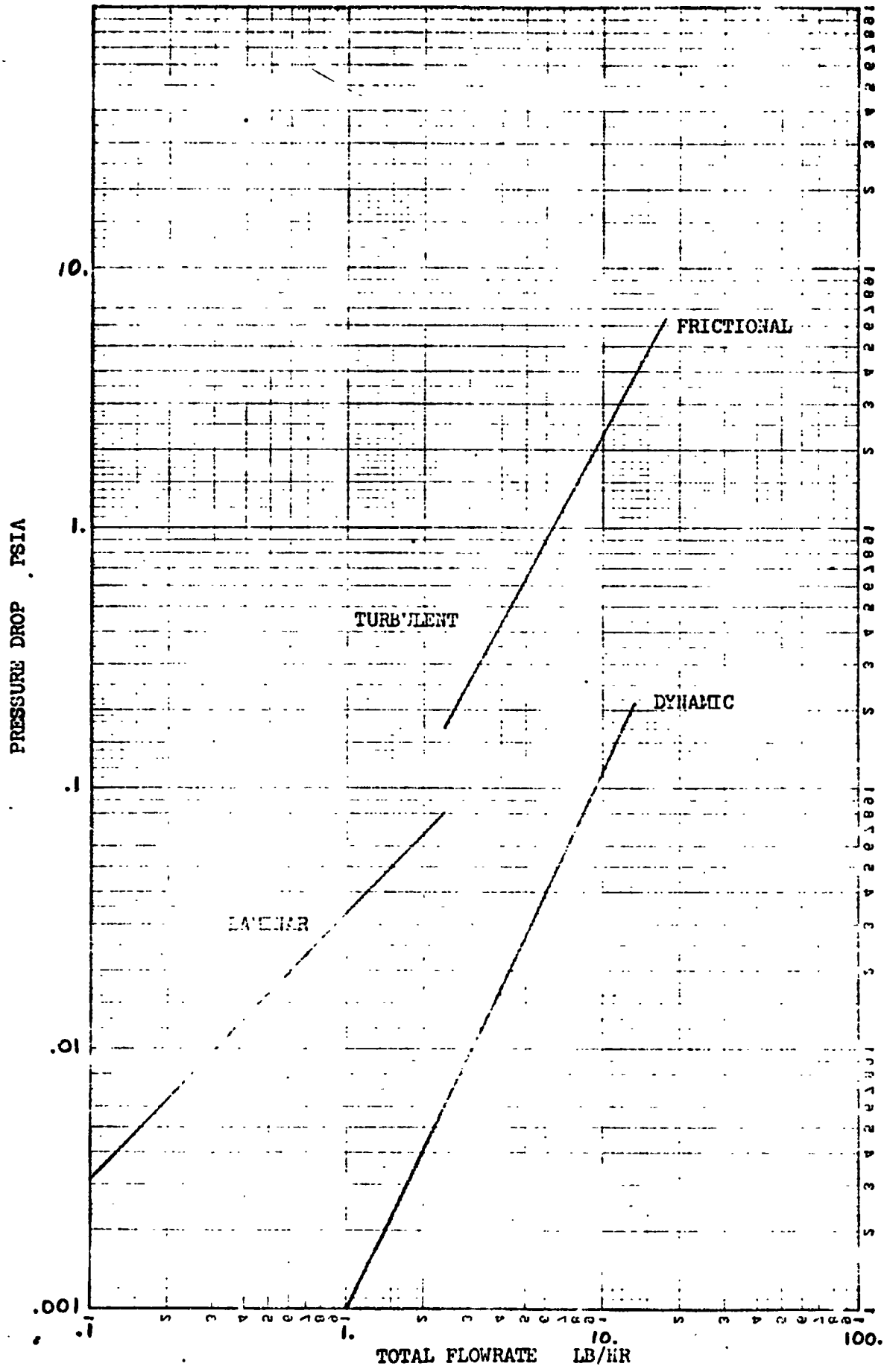

Figure D-1 TWO PHASE FLOW PRESSURE DROP IN TVS D-5

The total pressure drop is obtained by integrating Equations (D-2) and (D-3) with the quality, X, varying with the tube length, Z. Assuming X increases linearly with Z, which implies a constant heat flow, obtain

$$X = X_i + (X_f - X_i)\frac{Z}{L} \qquad \begin{matrix}(X_f \text{ is final quality, } X_i \text{ is} \\ \text{initial quality})\end{matrix} \tag{D-4}$$

Substituting Equation (D-4) into Equation (D-2) gives, for the frictional pressure gradient

$$\left.\frac{dP}{dZ}\right|_{FRICTION} = \frac{f_\ell \dot{m}^2}{\left(\frac{\pi D_i^2}{4}\right)^2 D_i^2 g_c \rho_\ell} \frac{\left[1 + \left(\frac{\rho_\ell}{\rho_v} - 1\right) Y_i + \left(\frac{\rho_\ell}{\rho_v} - 1\right)(X_f - X_i)\frac{Z}{L}\right]}{1 + \frac{X \dot{m}^2}{g_c \left(\frac{\pi D_i^2}{4}\right)^2} \frac{d}{dP}\left(\frac{1}{\rho_v}\right)} \tag{D-5}$$

Integrating Equation (D-5) gives, for the frictional pressure drop,

$$\Delta P_{FRICTION} = \frac{(A + B X_i) L}{C (X_f - X_i)} \ln\left[1 + \frac{C (X_f - X_i)}{1 + C X_i}\right]$$

$$+ \frac{BL}{C^2 (X_f - X_i)} \left\{ C (X_f - X_i) - (1 + C X_i) \ln\left[1 + \frac{C (X_f - X_i)}{1 + C X_i}\right] \right\} \tag{D-6}$$

Similarly, the dynamic pressure gradient is

$$\left.\frac{dP}{dZ}\right|_{DYNAMIC} = \frac{\dot{m}^2}{\left(\frac{\pi D_i^2}{4}\right)^2 \rho_\ell g_c} \frac{\left[\left(\frac{\rho_\ell}{\rho_v} - 1\right)\left(\frac{X_f - X_i}{L}\right)\right]}{1 + \frac{X \dot{m}^2}{g_c \left(\frac{\pi D_i^2}{4}\right)^2} \frac{d}{dP}\left(\frac{1}{\rho_v}\right)} \tag{D-7}$$

Integrating Equation (D-7) gives

$$\Delta P_{DYNAMIC} = \frac{D}{C} \ln \left[1 + \frac{C (X_f - X_i)}{1 + C X_i} \right] \qquad \text{(D-8)}$$

By definition,

$$A = \frac{E f_\ell}{2 \rho_\ell D_i} \qquad D = \frac{E}{\rho_\ell} \left(\frac{\rho_\ell}{\rho_v} - 1 \right)$$

$$B = A \left(\frac{\rho_\ell}{\rho_v} - 1 \right) \qquad E = \left(\frac{4 \dot{m}}{\pi D_i^2} \right)^2 \frac{1}{g_c}$$

$$C = - \frac{E}{\rho_v P}$$

Following Owens, (References D-2), the friction factor of the single-phase liquid flow is used for the two-phase friction factor.

The friction factor is given by:

$$\text{for } Re_{D_i} < 3000 \text{ , } \left(Re_{D_i} = \frac{4 \dot{m}}{\pi D_i \mu} \right) \qquad \text{(D-9)}$$

$$f = \frac{64}{Re_{D_i}} \qquad \text{(D-10)}$$

$$\text{for } Re_{D_i} > 3000$$

$$f = \frac{0.316}{\left(Re_{D_i} \right)^{1/4}} \qquad \text{(D-11)}$$

Since the compressibility factor of vapor is 0.96 and does not vary appreciably with pressure for conditions in the TVS tube, the perfect gas law can be used in the expression C, giving

$$\frac{d}{dP}\left(\frac{1}{\rho_v}\right) = -\frac{1}{\rho_v P} \cong -.004\ \frac{ft^5}{lb^2}$$

assuming $\dot{m} = 5$ lb/hr, $D_i \cong 0.25$ in., the expression for C is found to be of the order of 0.01. It should be noted that since $C \ll 1$, the pressure drop equation containing the log term can be simplified using

$$\lim_{C \to 0} \ln (1 + C) = C$$

This simplification illustrates the appropriate linear dependence of pressure with $\dot{m}^2$, for the dynamic pressure drop and turbulent frictional pressure drop, and the linear dependence of pressure with $\dot{m}$ for laminar flow.

The curves of Figure D-1 for conditions corresponding to those of the IDU/TVS tests show: (1) that the dynamic pressure drop is of the order of 1 percent of the frictional pressure drop; and (2) the total pressure drop is of the order of a few psi.

The heat transfer part of the program gives the required TVS tube pressure, P_{TUBE}. This must equal the average pressure in the tube,

$$P_{\substack{TUBE \\ CALCULATED}} = \frac{P_{INLET_{TVS}} + P_{EXIT_{TVS}}}{2} \qquad (D\text{-}12)$$

The pressure loss is

$$\Delta P_{LOSS} = P_{INLET_{TVS}} - P_{EXIT_{TVS}} \qquad (D\text{-}13)$$

Thus, the inlet pressure, immediately downstream of the viscojet, must be adjusted such that

$$P_{INLET_{TVS}} = P_{\substack{TUBE \\ CALCULATED}} + \frac{\Delta P_{LOSS}}{2} \qquad \text{(D-14)}$$

or

$$P_{EXIT_{TVS}} = P_{\substack{TUBE \\ CALCULATED}} - \frac{\Delta P_{LOSS}}{2} \qquad \text{(D-15)}$$

D.2 PRESSURE DROP THROUGH THE LEE VISCOJETS

Lee viscojets are used as flow control orifices since their design provides a flow area 10 to 25 times that of an equivalent orifice having the same resistance (Reference D-3). Therefore, there is less likelihood of clogging. It is necessary to determine the effective resistance of the various viscojets used in the IDU/TVS, and these resistances vary over a wide range, depending on whether liquid, gas, or a two-phase mixture is flowing.

A previous MDAC study (Reference D-4) obtained data of flowrate vs pressure drop through the viscojets. A reexamination of this data has shown that the effective resistance for two phase flow is essentially the same as for liquid flow alone, for conditions of $X_i < 0.1$. The resistance of the gas flow, even assuming choked flow, is relatively small. Therefore, the analysis given below assumes that the two-phase flow pressure drop/flowrate dependence is given by that for all liquid flow. An improvement in the pressure drop/flowrate correlation is achieved if the two-phase flow density, ρ_{TPF}, is used, rather than the liquid density, as discussed in Section 4.13.

Information received on the Lee viscojets (Reference D-5) indicates that flow resistance is treated in terms of LOHMS, with

$$L\ (\text{LOHMS}) = \frac{1270\ f}{\dot{m}_L}\sqrt{\Delta P\ \rho_L} \qquad \text{(D-16)}$$

ΔP, psi
ρ, lb/ft^3
$\dot{m}$, lb/hr

where LOHM is a flow resistance unit corresponding to the flow of 100 gallons/minute of 80°F water with a pressure drop of 25 psi. The factor f was determined in Reference D-4 from flow tests with subcooled LH_2 (such that vaporization did not occur, and X = 0). The value obtained was f = 0.823, which will be used in our analysis.

The values of L for the visojets used in the IDU/TVS are given in Figure D-5 which shows the expected flowrates versus pressure drop. Note that the correlation of Equation D-16 is improved by using ρ_{TPF} instead of ρ_L, which allows the equation to be extended into the range of low quality two-phase flow.

The actual flowrates versus pressure drop compared well with predicted values. Knowing $\dot{m}$ vs P for the viscojets is necessary for the proper setting of the IDU tank pressure. The pressure at the TVS line inlet is given by Equation (D-14) and the corresponding mass flowrate for given heat transfer conditions is given by a curve such as that of Figure 3-3 of this report. Knowing $\dot{m}$, the IDU tank pressure must be set such that $P_{IDU}-P_{INLET\ TVS}$ supplies the required mass flowrate.

D.3 REFERENCES

D-1. Tong, L. S. Boiling Heat Transfer and Two Phase Flow, 1965, John Wiley & Sons.

D-2. Owens, W. L. Two Phase Pressure Gradient, pp 363-368, International Developments in Heat Transfer, Pt II, ASME, (1961).

D-3. Lee Viscojet Catalog, 1972.

D-4. Castle, J. N. and Cady, E. C. Performance Testing of An Integrated Liquid Hydrogen Storage, Acquisition, and Vent System MDAC Report No. MDC G3092, June, 1972.

D-5. Personal Communication. Walt Reynolds (Lee Company) to E. C. Cady (MDAC), December 31, 1970.

Appendix E
IDU/TVS PERFORMANCE COMPUTER CODE DESCRIPTION

E.1 PROGRAM STRUCTURE

E.1.1 Analysis

The equations included in this program are derived in Appendices A, B, C, and D. Some additional features of this analysis as it is interpreted and incorporated into the code will be briefly described.

E.1.1.1 Multiple Tubes

Appendices A and B apply to a single tube for the vent flow. The program has the capability of parallel flow in multiple, equal-length tubes. This is accomplished by assuming that Equation (B-16) for L_1 is written in terms of a single tube length and then multiplying L_1, L_2 and L by the number of tubes in the heat transfer equations to provide the correct overall heat balance.

E.1.1.2 Condensation Heat Transfer

The condensation heat transfer equation is used to calculate the external wall coefficient when the average wall temperature is less than the saturation temperature at the external pressure. When this occurs, the external temperature T_e in Equations (A-10) and (A-41) is replaced by $T_{s,e}$, the external saturation temperature.

E.1.1.3 Insulation

Throughout the program, options are provided for all computations to be performed with or without external insulation. Insulation may be specified independently for the wall and the tank top.

E.1.1.4 Conductivities

Constant values of tank wall and insulation conductivity are input to the program. Separate variables are used within the code for tank top, region 1 wall and region 2 wall. These conductivity values could be read from a temperature-dependent table or equations, but such temperature-dependent data

were not available with sufficient reliability. This change can be made at a later date if desired.

E.1.1.5 Radiation

The radiation heat transfer analysis was not developed. However, this variable is carried in the code and the subroutine is provided for its evaluation to simplify the task of adding this feature at a later date if desired.

E.1.1.6 Tank Top

The equations given in Table A-2 for the extraneous heat flux through the tank top are solved by direct substitution. Two solution options are included in the code, with and without tank top insulation.

E.1.1.7 Region 1 Tube Length

Equation (B-16) is a quadratic in L_1. However, it is possible for the coefficient of the squared term to be zero so that the solution would not be operable. To circumvent this possibility, this coefficient is checked against a minimum limit, if its magnitude is less than this limit, the equation is solved approximately as a linear equation and corrected iteratively for the small squared term. If the coefficient is zero, the linear solution will be exact.

E.1.1.8 Single Flow Regime Solution

The solution for a single flow regime throughout the tube can be obtained by setting the transition quality X_c equal to the final quality of the flow in the tube to eliminate the mist flow regime. The reverse cannot be done to completely eliminate the annular flow regime; however, the annular flow regime can be made insignificantly small by setting the value at X_c very close to that of the initial flow quality.

E.1.1.9 Curve Fits

The heat transfer coefficient equation in the annular flow regime of the tube flow is discussed in Appendix C. The suppression factor S and the Reynolds

number factor F used in equation (C-2) are shown as curves in Figure C-1 and Figure C-2. These curves are represented by equations in the code as follows:

$$S = \frac{1}{1 + 0.305 \times 10^{-5} Y_1^{1.15}} \qquad (E\text{-}1)$$

$$Y_1 = Re_L F^{1.25}$$

and

$$F = (1. + 2.25 Y_2)^{0.8}$$

$$Y_2 = \left(\frac{X}{1 - X}\right)^{0.9} \left(\frac{\rho_\ell}{\rho_v}\right)^{0.5} \left(\frac{\mu_v}{\mu_\ell}\right)^{0.1} \qquad (E\text{-}2)$$

An average value of the latter quantity is evaluated by integrating the X-term from X_I to X_c.

E.1.1.10 Properties

Tabular data for the fluid properties are grouped in the BLOCK DATA subroutine. Other properties are approximated by linear relationships; these are found in the subroutines which calculate the heat transfer coefficients at the inner wall, outer wall and inside the coolant tube.

E.1.2 Solution Technique

The computer code effects an iterative solution to the quadratic equation derived in the preceding analysis for the region 1 flow regime (annular two-phase flow) tube length. Iteration is necessary because the equation contains many temperature dependent terms and these temperatures cannot be determined until the region 1 tube length is known.

The iteration is initiated by assigning estimates to the unknown temperatures. Based on these values, the coefficients of Equation (B-16) are evaluated and the equation solved for L_1. With this approximate solution, the system temperatures are then calculated and the process repeated. However, a straightforward application of this simple iteration process frequently does not

converge due to extreme fluctuations in some of the variables. To overcome this difficulty, the iteration proceeds in the manner illustrated by the flow chart in Figure E-1.

After the first evaluation of L_1, that value is held constant while the temperatures and heat transfer coefficients are iterated to achieve a moderate degree of convergence. With the temperatures thus stabilized, a new value of L_1 is calculated and the temperature iteration is repeated. In this manner, a well-behaved convergence of L_1 is attained. This two-level iteration is achieved by the two nested DØ-loops shown in Figure E-1. Since tube lengths are evaluated only on the first pass through the inner loop, their calculation is shown logically to be a part of the outer loop.

As L_1 approaches it solution value, the iterative variation of the system temperatures decreases and fewer temperature/properties iterations are required. Unnecessary computation is avoided by decreasing the count limit on the inner loop as the solution proceeds. In the first four passes through the outer DØ-loop, the inner DØ-loop is executed 6, 3, 2 and 1 times; thereafter, the entire iteration is performed as a single loop.

Checks for convergence are initiated on the third pass through the outer loop. The difference between the maximum and minimum values of the three most recent flowrates must be less than a specified limit to exit the iteration loop. If the error check is not satisfied in ten iterations, an error message is printed and the variable values at that point are printed in the normal manner.

A complete program listing, a glossary of principal variable names and a diagram of subroutine relationships (calling sequence) are given in Appendix F. Comment cards are provided in the listing to describe the function of each subroutine and to identify the principal operations within the code.

E.2 PROGRAM UTILIZATION

E.2.1 Capabilities and Limitations

This code calculates the mass flow rate necessary to maintain a zero net heat input into the tank. The capabilities and limitations inherent in the model and analysis are adequately described in the derivation of the equations in

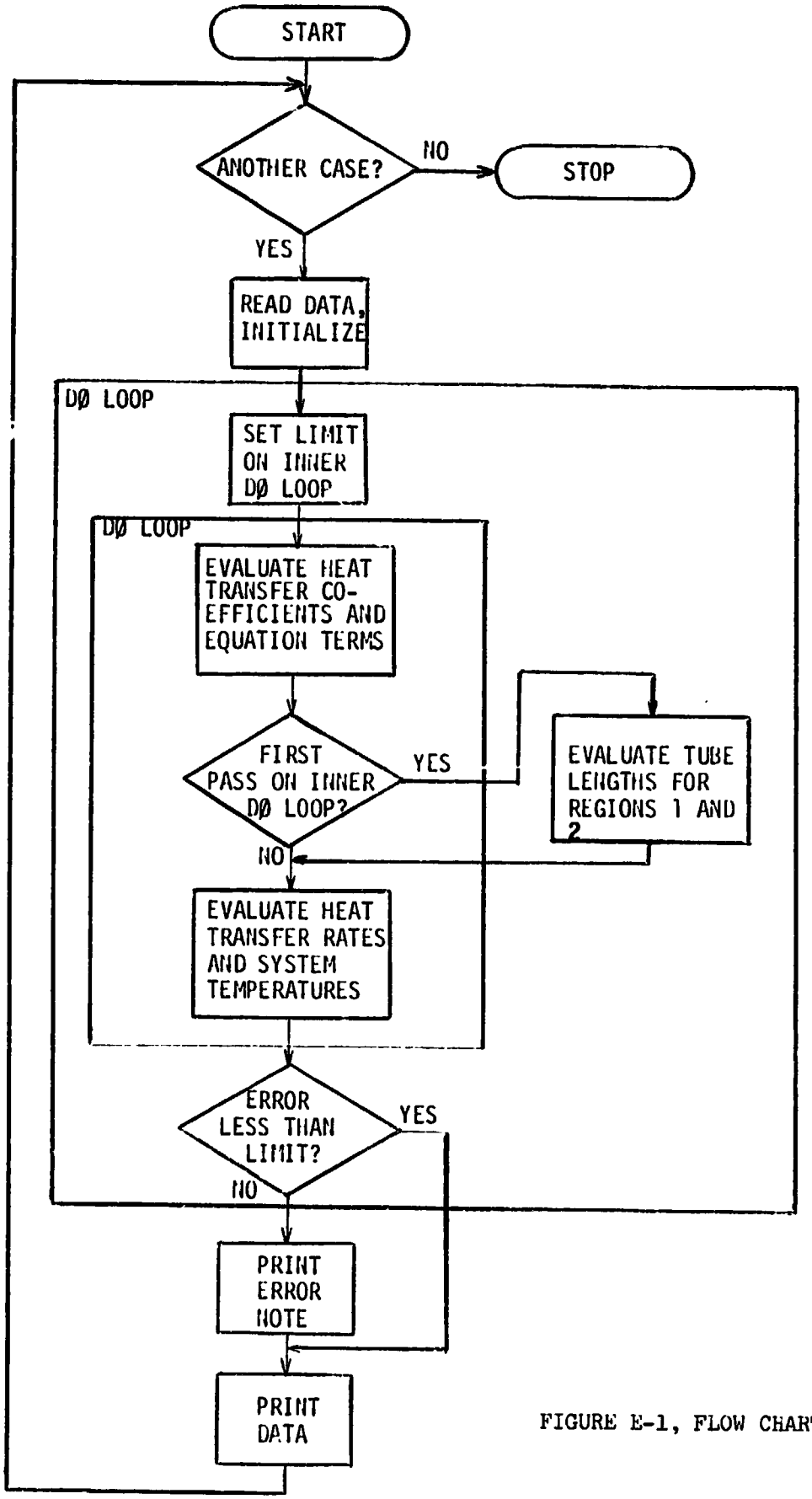

FIGURE E-1, FLOW CHART

C-3

Appendices A and B, and in the preceding section on analysis. The tank configuration is a flat-end cylinder. The product of the number of tubes, single-tube length, and tube spacing must equal the cylindrical wall area. The solution is restricted to the case in which the outer wall of the tank sees gas only (but it may have a film of condensation), the inner wall sees liquid only, and the tank top sees gas on both sides.

Since this code treats the transfer of heat from the external environment to the tank, it will not operate unless the external temperature is greater than the temperature of the tank contents. Also, as mentioned in the preceding section on analysis, the code does not permit the complete elimination of the annular flow regime by setting the transition quality X_C equal to the initial quality X_I. If the input data violate either of these restrictions, the code will skip to the next input case.

E.2.2 Input

The input variables are listed in Table E-1. Each variable is identified by a number which precedes it on the input card. All cards are written in the same format (I3, E12.7). The cards may be arranged in any order within an input case. The end of an input case is designated by a blank card. The end of a run is designated by two blank cards.

Data must be input for all variables in the first case. Exceptions for which default values are supplied are given in Table E-2. In the case of the values read from the vapor pressure table, either the pressure or temperature must be input for the other value to be calculated.

For subsequent cases, only those variables are input for which new data are specified. The remaining variables retain their values from the previous case.

A listing of input cards for a series of test cases is given in Appendix G.

E.2.3 Output

The output format is illustrated in the test case output in Appendix G. The listing is separated into three sections by blank lines. The first section lists the input data, the second lists solution data, and the third lists some of the

Table E-1
INPUT VARIABLES

ID No.	Variable Name	Definition and Units
1	DO	Tube spacing (in.)
2	EL	Single tube length (ft)
3	Y	Number of tubes
4	DTUBE	Outside diameter of tube (in.)
5	TWTH	Tube wall thickness (in.)
6	T	Tank wall thickness (in.)
7	TI	Wall insulation thickness (in.)
8	ATT	Tank top area (ft^2)
9	TTM	Tank top thickness (in.)
10	TTI	Tank top insulation thickness (in.)
11	HTK	Tank height (ft)
12	AKTx	Tank conductivity (Btu/hr-ft-°R)
13	AKIx	Insulation conductivity (Btu/hr-ft-°R)
14	TE	External temperature (°R)
15	TSE	External saturation temperature (°R)
16	P	External pressure (Psia)
17	TH2	Internal temperature (°R)
18	PTT	Internal pressure (Psia)
19	XI	Initial quality in tube (fraction)
20	XC	Transition quality in tube (fraction)
21	XF	Exit quality in tube (fraction)
22	ACC	Acceleration (g)

Notes: Each input card is occupied by a single variable. Format for all inputs is I3,E12.7. Input No. 12 is assigned to AKT1, AKT2, and AKTT; Input No. 13 is assigned to AKI1, AKI2, and AKIT. End-of-case is indicated by a blank card; end-of-run by two blank cards.

Table E-2

INPUT DATA DEFAULT VALUES

Variable Name	Default Value
Y	1.0
AKIx	0.1
TE	TSE
TSE	TSE<P>
P	P<TSE>
TH2	TH2<PTT>
PTT	PTT<TH2>
XI	0.05
XF	1.00
ACC	1.00

Note: The notation A<B> indicates the value of A is read from the vapor pressure table as a function of B by linear interpolation.

quantities calculated in the course of the solution. All data are labeled with units (B/FDH and B/F2DH are Btu/ft^2-°R-hr respectively).

The input data are identified by their variable names which are defined in Table E-1. They are printed in the numerical order of their ID numbers. The initial data, describing the tank configuration, are recessed; the remaining data specify operating conditions. New input data in each case are identified by a leading asterisk.

In the remaining sections, the single-value printouts are identified by their variable names used in the code. The double-value printouts are for regions 1 and 2 respectively and are identified by the common heading of their variable names, with the terminal number removed (i.e., El denotes the variables EL1 and EL2). The last line is an exception, where DPFD labels the frictional and dynamic pressure drop in the tube. These outputs are defined in Table E-3 in their order of appearance.

Table E-3
OUTPUT VARIABLES

Label	Definition
EMD	Total mass flow rate in all tubes
THEX	Temperature of two-phase fluid in heat exchanger tube
PHEX	Pressure in heat exchanger tube
QEXT	Extraneous heat input to tank through top
QR	Radiation heat flux to wall
EL	Flow regime tube length
QT	Heat transfer rate to tube
TS	Insulation surface temperature
TC	Minimum tank wall temperature
TM	Maximum tank wall temperature
HE	Heat transfer coefficient at external wall/insulation surface
HF	Heat transfer coefficient at internal wall surface
HT	Heat transfer coefficient at internal tube wall
U	Combined external heat transfer coefficient
TA	Characteristics temperature
EN	Dimensionless parameter
DP F D	Frictional and dynamic pressure drop in the tube

Note: Labels EL through EN apply to two output data for the two flow regime regions. The variable names in the code for these two data are formed by adding 1 and 2 to the label.

Appendix F
IDU/TVS PERFORMANCE COMPUTER CODE LISTING

A listing of the main program, followed by the subroutines in alphabetical order, is given on the following pages. Preceding the listing is the subroutine calling sequence in Table F-1 and a glossary of major variables (those appearing in CØMMØN) in Table F-2. A printout of main program is shown in Figure F-2.

Table F-1

SUBROUTINE RELATIONSHIPS IN PROGRAM STRUCTURE

```
MAIN
   INPUT
      W
      PTABLE
      EXTHT
         FRECTT
              GENTAB
      RADHT
   HØUTER
      GENTAB
      FRECØN
   HINNER
      GENTAB
      FRECON
   HTUBE
      GENTAB
   OUTPUT
      W
      W12
      PDROP
```

Table F-2 (Page 1 of 3)
GLOSSARY OF COMMON BLOCK VARIABLES

Block Ø1	General Variables
TE	External temperature
TH2	Internal temperature
T	Tank wall thickness
TI	Tank wall insulation thickness
DO	Tube spacing on tank wall
EL	Single tube length
DTUBE	Tube outside diameter
P	External pressure
TSE	Saturation temperature at external pressure
QR	Radiation heat flux at tank wall
QEXT	Extraneous heat transfer rate through tank top
EMD	Total mass flow rate in all tubes
THEX	Fluid temperature inside tube
Y	Number of tubes
TTM	Tank top thickness
TTI	Tank top insulation thickness
ATT	Area of tank top
AKIT	Insulation conductivity at tank top
AKTT	Tank metal conductivity at tank top
PTT	Internal pressure
HTK	Tank height
ACC	Acceleration
XI	Initial quality in tube flow
XC	Transition quality in tube flow
XF	Exit quality in tube flow
DI	Tube inside diameter
PHEX	Pressure inside tube
CHIFAC	Average value of chi-function used to evaluate F in subroutine HTUBE
RETA	Reynold's number in annular flow region of tube

Table F-2 (Page 2 of 3)

GLOSSARY OF COMMON BLOCK VARIABLES

Block Ø2	Region 1 and 2 Variables
Variables for Regions 1 and 2 are denoted by their terminal numbers. These variables are listed below in the form Vx to indicate that V1 and V2 are the variable names for Regions 1 and 2.	
AKIx	Insulation conductivity
AKTx	Tank wall conductivity
HEx	External heat transfer coefficient
Ux	Combined external heat transfer coefficient
HFx	Internal heat transfer coefficient
HTx	Tube flow internal heat transfer coefficient
ENx	Dimensionless variable, N
TAx	Characteristic temperature, T_A
TCx	Minimum wall temperature
TMx	Maximum wall temperature
ELx	Flow regime tube length
QTx	Heat transfer rate
TSx	Insulation surface temperature
Block Ø3	**Properties**
VPR(20)	Vapor pressure
TSAT(20)	Saturation temperatures
NVPR	Number of values in vapor pressure table
THV(20)	Temperature for heat of vaporization
HV(20)	Heat of vaporization
NHV	Number of values in heat of vaporization table
TDN(20)	Temperatures for liquid density
DN(20)	Liquid density
NDN	Number of values in liquid density table
NCC	Number of values in gas conductivity table
CS(10)	Gas conductivity
CT(10)	Temperatures for gas conductivity
NVV	Number of values in gas viscosity table

Table F-2 (Page 3 of 3)
GLOSSARY OF COMMON BLOCK VARIABLES

VS(10)	Gas viscosity
VT(10)	Temperatures for gas viscosity
CP(120)	Gas specific heat, function of pressure and temperature
TCP(20)	Temperatures for gas specific heat
PCP(6)	Pressures for gas specific heat
NCPP	Number of pressures in gas specific heat table
NCPT	Number of temperatures in gas specific heat table
CP1(20)	Specific heat table at P, function of temperature
CP2(20)	Specific heat table at PTT, function of temperature

```
      PROGRAM MAIN (INPUT,OUTPUT,TAPE5=INPUT,TAPE6=OUTPUT)
      COMMON / 01 / TE,TH2,T,TI,DO,EL,DTUBE,P,TSE,QR,QEXT,EMD,THEX,Y
     $  ,TTM,TTI,ATT,AKIT,AKTT,PTT,HTK,ACC,X1,XC,XF,DI,PHEX,CHIFAC,RETA
      COMMON / 02 / AKI1,AKT1,HE1,U1,HF1,HT1,EN1,TA1,TC1,TM1,EL1,QT1,TS1
     $             ,AKI2,AKT2,HE2,U2,HF2,HT2,EN2,TA2,TC2,TM2,EL2,QT2,TS2
      COMMON / 03 / VPR(20),TSAT(20),NVPR,THV(20),HV(20),NHV,
     $  TLN(20),DN(20),NDN,NCC,CS(10),CT(10),NVV,VS(10),VT(10)
     $  ,CP(120),TCP(20),PCP(6),NCPP,NCPT,CP1(20),CP2(20)
   10 FORMAT ( 35HOITERATION LOOP COMPLETED - ERROR =,E9,2 )
  101 FORMAT ( 1H1 )
      DIMENSION V(3)
      WRITE ( 6,101 )
  100 CONTINUE
      CALL INPUT
      EC = 3,14159 * DTUBE/12,
      DO 102 I = 1,10
C**** FLOW REGIME TUBE LENGTHS AND ERROR CHECK ARE CALCULATED ON EACH
C     PASS THROUGH THE OUTER LOOP (ERROR CHECK STARTS ON THIRD PASS)
      KL = MAXO ( 6/I, 1 )
      DO 108 K = 1,KL
C**** TEMPERATURES, PROPERTIES, HEAT TRANSFER COEFFICIENTS AND RATES
C     ARE CALCULATED ON EACH PASS THROUGH THE INNER LOOP
C **  EVALUATE HEAT TRANSFER COEFFICIENTS AND EQUATION TERMS
      IF ( TI .LE. 0, ) GO TO 110
      CALL BOILER ( HE1, TS1, TS1, HF1 )
      CALL BOILER ( HE2, TS2, TS2, HF2 )
      GO TO 111
  110 CONTINUE
      CALL BOILER ( HE1, TC1, TM1, HF1 )
      CALL BOILER ( HE2, TC2, TM2, HF2 )
  111 CONTINUE
      U1 = HE1*AKI1 / ( AKI1 + HE1 * TI/12, )
      U2 = HE2*AKI2 / ( AKI2 + HE2 * TI/12, )
      CALL HINNER ( HF1, TC1, TM1 )
      CALL HINNER ( HF2, TC2, TM2 )
      TT1 = TE
      IF ( KF1 .EQ. 1 ) TT1 = TSE
      TA1 = ( QR + HF1*TH2* U1*TT1) / ( HF1 + U1 )
      TT2 = TE
      IF ( KF2 .EQ. 1 ) TT2 = TSE
      TA2 = ( QR + HF2*TH2* U2*TT2) / ( HF2 + U2 )
      EN1 = SQRT ( ( HF1 + U1 ) / ( AKT1 * T/12, ) ) * DO/24,
      EN2 = SQRT ( ( HF2 + U2 ) / ( AKT2 * T/12, ) ) * DO/24,
      TANHN1 = TANH(EN1)
      TANHN2 = TANH(EN2)
      E1 = DO/12, * ( TT1- TH2 )
      E2 = DO/12, * ( TT2- TH2 )
      E3 = 1, + U1 / HF1
      E4 = 1, + U2 / HF2
      IF ( EMD .EQ. 0, ) QT1 = Y*EL1*U1*E1 + EJ*QEXT
      CALL HTUBE ( HT1, TC1, 1 )
      CALL HTUBE ( HT2, TC2, 2 )
      A1 = TA1+(TH2-TA1)*EN1/TANHN1-U1*E1 / (EO*HT1)
      A2 = TA2+(TH2-TA2)*EN2/TANHN2-U2*E2 / (EO*HT2)
      B1 = EN1 / (TANHN1*HF1*DO/12,) + E3 / (EO*HT1)
      B2 = EN2 / (TANHN2*HF2*DO/12,) + E4 / (EO*HT2)
      IF ( K .GT. 1 ) GO TO 107
```


Figure F-1 IDU/TVS PROGRAM LISTING

```
C *** BEGIN CALCULATION OF FLOW REGIME TUBE LENGTHS
      E5 = ((XC-XI)*E4 + (XF-XC)*E3) * ( A1 - A2 )
      C1 = (XC-XI) * U2 * E1 / E5
      C2 = (XF-XC) * U1 * E2 / E5
      D1 = QEXT * B1 / E5 * (XC-XI) * E4 / ( Y * EL )
      D2 = QEXT * B2 / E5 * (XF-XC) * E3 / ( Y * EL )
      AA = 1. - (C1+C2)*(B2-B1)
      BB = C1*(B2-B1) - B1*(C1+C2) - (D1+D2) + 1.
      CC = C1 * B1 + D1
      RADIC = BB**2 + 4.*AA*CC
      IF ( ABS(AA) .LT. ABS(BB**2/(4.*CC)) * 0.001 ) GO TO 103
      ELX = ( -BB - SQRT( RADIC ) ) / ( 2.*AA )
      GO TO 104
  103 ELX = 0.
      DO 105 J = 1,5
  105 ELX = ( -CC - ELX**2*AA ) / BB
  104 IF ( ELX .LT. .9999 ) GO TO 106
      EL1 = EL
      EL2 = 0.
      GO TO 107
  106 EL1 = ELX * EL
      EL2 = EL - EL1
C *** END   CALCULATION OF FLOW REGIME TUBE LENGTHS
  107 CONTINUE
C **  EVALUATE HEAT TRANSFER RATES AND SYSTEM TEMPERATURES
      QI = ((A1-A2)*Y - B1/EL1*QEXT) * EL2 / (B1*EL2/EL1 + B2)
      THEX = A1 - B1 * (QI+QEXT) / (EL1*Y)
      GT1 = Y*EL1*U1*E1 + E3*(QI+QEXT)
      GT2 = Y*EL2*U2*E2 - E4*QI
      TC1 = THEX + GT1/(ED*EL1*HT1*Y)
      TC2 = TC1
      IF ( EL2 .GT. 0. ) TC2 = THEX + GT2/(ED*EL2*HT2*Y)
      TM1 = TA1 - ( TA1 - TC1 ) / COSH(EN1)
      TM2 = TA2 - ( TA2 - TC2 ) / COSH(EN2)
      IF ( TI .LE. 0. ) GO TO 108
      TW1 = ( TC1 + TM1 ) * 0.5
      TS1 = TW1 + TI/12.*U1/AKI1 * ( TE - TW1 )
      TW2 = ( TC2 + TM2 ) * 0.5
      TS2 = TW2 + TI/12.*U2/AKI2 * ( TE - TW2 )
  108 CONTINUE
C **  ERROR CHECK
      L = I - ((I-1)/3)*3
      V(L) = ERR
      IF ( I .LT. 3 ) GO TO 102
      AVV = ( V(1) + V(2) + V(3) ) / 3.
      ER = (AMAX1(V(1),V(2),V(3))-AMIN1(V(1),V(2),V(3))) / AVV
      IF ( ER .LT. 0.0001 ) GO TO 109
  102 CONTINUE
      WRITE ( 6, 10 ) ER
  109 CALL OUTPUT
      GO TO 100
      END
```

```
      BLOCK DATA
      COMMON / C3 / VPR(20),TSAT(20),NVPR,THV(20),HV(20),NHV,
     $  TLN(20),DN(20),NDN,NCC,CS(10),CT(10),NVV,VS(10),VT(10)
     $  ,CP(120),TCP(20),PCP(6),NCPP,NCPT,CP1(20),CP2(20)
C *** VAPOR PRESSURE  ( DR - PSIA )
      DATA  NVPR / 14 /, ( TSAT(I), I = 1,14 )
     $ /25.,27.5,30.,32.5,35.,37.5,40.,42.5,45.,47.5,50.,52.5,55.,57.5/,
     $       ( VPR(I), I = 1,14 )
     $ /1.1,2.1,4.,6.7,11.,17.,25.,34.,46.5,62.,82.,104.,130.,160./
C *** HEAT OF VAPORIZATION  ( DR - BTU/LB )
      DATA  NHV / 13 /, ( THV(I), I = 1,13 )
     $ / 25., 28., 30., 32., 37., 40., 45., 50., 53., 56., 58., 59., 59.4/,
     $       ( HV(I), I = 1,13 )
     $ /193.,195.,196.,195.,191.,187.,175.,153.,134.,105.,70.,40.,0.   /
C *** LIQUID DENSITY  ( DR - LB/FT3 )
      DATA  NDN / 20 /, ( TDN(I), I = 1,20 )
     $ / 25. , 31. , 36. , 40. , 44. , 45. , 46. , 47. , 48. , 49. ,
     $   50. , 51. , 52. , 53. , 54. , 55. , 56. , 57. , 58. , 59.   /,
     $       ( DN(I), I = 1,20 )
     $ / 4.60, 4.62, 4.44, 4.29, 4.16, 4.02, 3.97, 3.91, 3.85, 3.78,
     $   3.71, 3.64, 3.56, 3.48, 3.39, 3.29, 3.17, 3.02, 2.85, 2.5   /
C *** GAS CONDUCTIVITY  ( DR - BTU/FT-HR-DR )
      DATA (CT(I),I=1,3) / 35.,140.,240. /, NCC / 3 /,
     $  (CS(I),I=1,3) / .0062,.0337,.0644 /
C *** GAS VISCOSITY  ( DR - LB/FT-HR )
      DATA (VT(I),I=1,10) / 33.,40.,45.,52.,60.,71.,85.,101.,130.,200. /
     $ , (VS(I),I=1,10) / .00216,.00270,.00306,.00360,.00411,.00485,
     $  .00575,.00647,.00791,.0110 /, NVV / 10 /
C *** GAS SPECIFIC HEAT  ( DR,PSIA - BTU/LB-DR )
      DATA CP / 2.55,2.51,2.50,2.49,6*2.48,2.49,2.51,2.55,2.60,2.77,2.97
     1 ,3.21,0.,2*2.80,2.67,2.60,2.56,2.54,2.53,2.52,2.51,3*2.50,2.51,
     2  2.53,2.56,2.61,2.77,2.99,3.21,0.,3*2.96,2.79,2.68,2.62,2.58,2.56
     3 ,2.55,2.54,2.53,2*2.52,2.55,2.56,2.62,2.78,2.99,3.22,0.,4*3.28,
     4  2.98,2.82,2.73,2.68,2.64,2.61,2.59,2.57,2.56,2.57,2.59,2.64,2.79
     5 ,3.00,3.23,0.,4*4.20,3.49,3.10,2.92,2.82,2.75,2.69,2.65,2.63,2.60
     6 ,2.60,2.62,2.66,2.81,3.01,3.24,0.,5*4.50,3.56,3.16,2.95,2.84,2.77
     7 ,2.72,2.68,2.64,2.63,2.65,2.68,2.82,3.02,3.05,0, /, TCP / 25.,30.
     8 ,35.,40.,45.,50.,55.,60.,65.,70.,75.,80.,90.,100.,110.,120.,140.,
     9  160.,180.,0. /, PCP / 1.47,7.35,14.7,29.4,44.1,58.8 /
      DATA NCPP, NCPT / 6, 19 /
      END
```

```
      SUBROUTINE EXTHT
C**** CALCULATE EXTRANEOUS HEAT TRANSFER THROUGH TANK TOP
      COMMON / 01 / TE,TH2,T,TI,DO,EL,DTUBE,P,TSE,QR,QEXT,EMD,THEX,Y
     $  ,TTM,TTI,ATT,AKIT,AKTT,PTT,RTK,ACC,XI,XC,XF,DI,PHEX,CHIFAC,RETA
      T1 = TE
      T5 = TH2
      T2 = T3 = T4 = (T1+T5)*.5
      DO 101 I =1,5
      CALL FRECTT ( A1, (T1+T2)*.5, ABS(T1-T2), P )
      A3 = AKTT / TTM * 12.
      CALL FRECTT ( A4, (T4+T5)*.5, ABS(T4-T5), PTT )
      IF ( TTI .GT. 0. ) GO TO 102
      T2 = (A3*A4*T5+A1*(A3+A4)*T1) / (A1*A3+A1*A4+A3*A4)
      T3 = T2
      GO TO 103
  102 CONTINUE
      A2 = AKIT / TTI * 12.
      T2 = (A2*A3*A4*T5+A1*(A2*A3+A2*A4+A3*A4)*T1) /
     $  ((A1+A2)*(A2*A3+A2*A4+A3*A4)+A2**2*(A3+A4))
      T3 = (A3*A4*T5+A2*(A3+A4)*T2) / (A2*A3+A2*A4+A3*A4)
  103 CONTINUE
      T4 = (A4*T5+A3*T3) / (A3+A4)
      QEXT = A3 * ( T3 - T4 ) * ATT
  101 CONTINUE
      RETURN
      END
```

```
      SUBROUTINE FRECON ( HH,DT,X,RHO,BET,CP,CON,VIS )
C**** CALCULATE FREE CONVECTION COEFFICIENT AT TANK WALL
      COMMON / 01 / TE,TH2,T,TI,DO,EL,DTUBE,P,TSE,QR,QEXT,EMD,THEX,Y
     $  ,TTM,TTI,ATT,AKIT,AKTT,PTT,RTK,ACC,XI,XC,XF,DI,PHEX,CHIFAC,RETA
      GR = RHO**2 * BET * ACC*1.296E+07 * DT * X**3 / VIS**2
      PR = CP * VIS / CON
      HH = 0.55*CON/X * ( GR * PR ) ** .25
      RETURN
      END
```

```
      SUBROUTINE FREETT ( HH, TF, DT, PG )
C**** CALCULATE FREE CONVECTION COEFFICIENT AT TANK TOP
      COMMON / 01 / TE,TH2,T,TI,DO,EL,DTUBE,P,TSE,QR,DEXT,EMD,THEX,Y
     $  ,TTM,TTI,ATT,AKIT,AKTT,PTT,PTK,ACC,XI,XC,XF,DI,PHEX,CHIFAC,RETA
      COMMON / C3 / VPR(20),TSAT(20),NVPR,TMV(20),HV(20),NHV,
     $  TEM(20),DM(20),IDM,NCC,CS(10),CT(10),NVV,VS(10),VT(10)
     $  ,CP(120),TCP(20),PCP(6),NCPF,NCPT,CP1(20),CP2(20)
      DATA  IK,IV,IC / 3*1 /
      DATA  BCR / 0.188 /
      RHO = BCR * PG / TF
      BETG = 1. / TF
      CALL GENTAB ( TF, CPG, 3, IK, TCP, CP2, NCPT )
      CALL GENTAB ( TF, CONG, 3, IC, CT, CS, NCC )
      CALL GENTAB ( TF, VISG, 3, IV, VT, VS, NVV )
      HH = .0e*CONG*(RHO**2*BETG*CPG*ACC*1.296E+07/(VISG*CONG)*DT)**.333
      RETURN
      END
```

```
      SUBROUTINE GENTAB ( T, F, L, I, X, Y, N )
C**** GENERAL TABLE READER (LINEAR INTERPOLATION OR STEP FUNCTION)
      DIMENSION  X(1), Y(1)
      IF ( T - X(I) ) 100, 104, 101
  100 IF ( I .EQ. 1 ) GO TO ( 104, 104, 106, 104, 106 ), L
      I = I - 1
      IF ( T - X(I) ) 100, 104, 103
  101 IF ( I .EQ. N ) GO TO ( 104, 104, 105, 105, 104 ), L
      I = I + 1
      IF ( T - X(I) ) 102, 104, 101
  102 I = I - 1
  103 GO TO ( 104, 106, 106, 105, 106 ), L
  104 F = Y(I)
      RETURN
  105 I = I - 1
  106 F = Y(I) + (T-X(I)) / (X(I+1)-X(I)) * (Y(I+1)-Y(I))
      RETURN
      END
```

```
      SUBROUTINE FINNER ( HF, TC, TI )
C***** HEAT TRANSFER COEFFICIENT ON INNER WALL (LIQUID ONLY)
      COMMON / C1 / TI,TW2,T,TI,DP,CL,LTUBE,P,TSF,QR,QEXT,END,THEX,Y
     *  ,TTM,TTI,ATT,ACIT,AITT,FTT,TK,ACC,VI,XC,XF,PI,PHEX,CHIFAC,BETA
      COMMON / C3 / VPR(20),TSAT(20),NVPR,TW(20),HV(20),NHV,
     *  TLA(20),DM(20),NOT,NCC,CS(10),CT(10),NVT,VS(10),VT(10)
     *  ,CP(120),TCF(20),PCP(6),NCPF,NCFT,CF1(20),CP2(20)
      DATA ID,IC / 1,1 /
      HFTL = 0.01
      DXT = 10/24.
C *** HIGHER TEMPERATURE REGION
      TLF = (TM + TW2) * .5
      CALL GENTAB ( TLF, DLF, 3, ID, TDA, DT, NDN )
      CPL = 1.2 + 0.07 * ( TLF - 20. )
      VISL = 3.00E-2 - 1.11E-3 * ( TLF - 40. )
      CONL = 6.37E-2 + 7.39E-4 * ( TLF - 30. )
      CALL FNECON ( H1,ABS(TM-TW2),DXT,DLF,HFTL,CPL,CONL,VISL )
C *** LOWER TEMPERATURE REGION
      TLF = (TW2+TC) * .5
      CALL GENTAB ( TLF, DLF, 3, ID, TDA, DT, NDN )
      CPL = 1.2 + 0.07 * ( TLF - 20. )
      CONL = 6.37E-2 + 7.39E-4 * ( TLF - 30. )
      VISL = 3.00E-2 - 1.11E-3 * ( TLF - 40. )
      CALL FNECON ( H2,ABS(TW2-TC),DXT,DLF,HFTL,CPL,CONL,VISL )
C **  AVERAGE HEAT TRANSFER COEFFICIENT
      HF = ( H1 + H2 ) * .5
      RETURN
      END
```

```
      SUBROUTINE HOUTER ( HE, TC, TM, KF )
C**** HEAT TRANSFER COEFFICIENT ON OUTER WALL (GAS ONLY)
      COMMON / 01 / TE,TH2,T,TI,CO,EL,DTUBE,P,TSE,OR,QEXT,FMD,THEX,Y
     $  ,TTM,TTI,ATT,AKIT,AKTT,PTT,HTK,ACC,XI,XC,XF,DI,PFEX,CHIFAC,RETA
      COMMON / 03 / VPR(20),TSAT(20),NVPR,THV(20),HV(20),NHV,
     $  TDN(20),DN(20),NDN,NCC,CS(10),CT(10),NVV,VS(10),VT(10)
     $  ,CP(120),TCP(20),PCP(6),NCPP,NCPT,CP1(20),CP2(20)
      DATA  WOR / 0.1880 /
      DATA  IH,ID,IC,IV,IK  / 5 * 1 /
      KF = 0
      TW = ( TM + TC ) * .5
      IF ( TW .GE. TSE ) GO TO 101
C *** CONDENSATION HEAT TRANSFER
      KF = 1
      XLF = DO/12.
      TLF = ( TW + TSE ) * .5
      CALL GENTAB ( TLF, DLF, 3, ID, TDN, DN, NDN )
      CALL GENTAB ( TLF, H, 3, IH, THV, HV, NHV )
      CONL = 0.177E-4 + 0.205E-6 * ( TLF - 30. )
      VISL = 8.34E-6 + 3.075E-7 * ( TLF - 40. )
      HE = 3600.*( ACC*DLF**2*H*CONL**3 / (4.*XLF*VISL*(TSE-TW)) )**0.25
      RETURN
C *** FREE CONVECTION HEAT TRANSFER
  101 CONTINUE
      IF ( (TM-TE) .LT. 0. ) GO TO 102
C **  FOR WALL REGION WHICH IS ABOVE EXTERNAL TEMPERATURE
      DXT = DO/24.
      TF = (TM+TE)*.5
      CALL GENTAB ( TF, CPG, 3, IK, TCP, CP1, NCPT )
      CALL GENTAB ( TF, CONG, 3, IC, CT, CS, NCC )
      CALL GENTAB ( TF, VISG, 3, IV, VT, VS, NVV )
      BETG = 1./TF
      RHOG = WOR * P / TF
      CALL FRECON ( H1,(TM-TE),DXT,RHOG,BETG,CPG,CONG,VISG )
C **  FOR WALL REGION WHICH IS BELOW EXTERNAL TEMPERATURE
      TF = (TE+TC)*.5
      DT = ABS(TE-TC)
      FF = 1.
      GO TO 103
  102 CONTINUE
C **  ENTIRE WALL COLDER THAN EXTERNAL TEMPERATURE
      DXT = HTK
      H1 = 0.
      FF = 2.
      TF = ( TE + TW ) * .5
      DT = TE - TW
  103 CONTINUE
      CALL GENTAB ( TF, CPG, 3, IK, TCP, CP1, NCPT )
      CALL GENTAB ( TF, CONG, 3, IC, CT, CS, NCC )
      CALL GENTAB ( TF, VISG, 3, IV, VT, VS, NVV )
      BETG = 1./TF
      RHOG = WOR * P / TF
      CALL FRECON ( H2,DT,DXT,RHOG,BETG,CPG,CONG,VISG )
C **  AVERAGE HEAT TRANSFER COEFFICIENT
      HE = ( H1 + FF*H2 ) * .5
      RETURN
      END
```

```
      SUBROUTINE HTUBE ( HT, TC, K )
C**** HEAT TRANSFER COEFFICIENT INSIDE TUBE
      COMMON / 01 / TE,TH2,T,TI,CO,EL,DTUBE,P,TSE,QR,QFXT,EMD,THEX,Y
     $  ,TTM,TTI,ATT,AKIT,AKTT,PTT,HTK,ACC,XI,XC,XF,DI,PFEX,CHIFAC,RETA
      COMMON / 02 / AKI1,AKT1,HE1,U1,HF1,HT1,EN1,TA1,TC1,TM1,EL1,QT1,TS1
     $             ,AKI2,AKT2,HE2,U2,HF2,HT2,EN2,TA2,TC2,TM2,EL2,QT2,TS2
      COMMON / 03 / VPR(20),TSAT(20),NVPR,THV(20),HV(20),NHV,
     $  TDN(20),DN(20),NDN,NCC,CS(10),CT(10),NVV,VS(10),VT(10)
     $  ,CP(120),TCP(20),PCP(6),NCPP,NCPT,CP1(20),CP2(20)
      DATA  IP,IW,IR,IH,IC,IV / 6 * 1 /, WOR / 0.1880 /, PI / 3.14159 /
      CALL GENTAB ( THEX, HTVT, 3, IH, THV, HV, NHV )
      EMD = ABS(QT1) / ((XC-XI)*HTVT)
      CALL GENTAB ( THEX, VISG, 3, IV, VT, VS, NVV )
      IF ( K .EQ. 2 ) GO TO 101
C *** REGION 1 = ANNULAR FLOW
C **  FORCED CONVECTION COMPONENT
      CPL = 1.2 + 0.07 * ( THEX - 20. )
      CONL = 6.37E-2 + 7.39E-4 * ( THEX - 30. )
      VISL = 3.00E-2 - 1.11E-3 * ( THEX - 40. )
      PR = CPL * VISL / CONL
      RETA = 48. * EMD / ( PI * VISL * DI * Y )
      HC = 0.276 * CONL / DI * RETA**0.8 * PR**0.4
C **  BOILING COMPONENT
      CALL GENTAB ( THEX, PHEX, 3, IP, TSAT, VPR, NVPR )
      RHOV = WOR * PHEX / THEX
      CALL GENTAB ( TC , PSW, 3, IW, TSAT, VPR, NVPR )
      DP = ABS( PSW - PHEX ) * 144.
      CALL GENTAB ( THEX, RHOL, 3, IR, TDN, DN, NDN )
      DT = ABS( TC  - THEX )
      GE = ACC * 1.296E+07
      SIG = 1.6E-04 - 0.06E-04 * ( THEX - 32. )
      PRCOEF = ( RHOL/(WOR*PHEX/THEX) )**0.5 * (VISG/VISL)**0.1
      F = ( 1. + 2.25*CHIFAC*PRCOEF )**0.8
      S = 1. / ( 1. + .305E-05 * ( F**1.25 * RETA )**1.13 )
      HB = S*.00122*CONL**.79*CPL**.45*RHOL**.49/VISL**.29*(GE*DP**3/
     $  SIG**2)**.25*(DT/HTVT/RHOV)**.24
C **  COMBINED HEAT TRANSFER COEFFICIENT FOR REGION 1
      HT = HB + F * HC
      GO TO 102
  101 CONTINUE
C *** REGION 2 = DROPLET FLOW
      CPG = 2.0 + 0.0556 * ( THEX - 20. )
      CALL GENTAB ( THEX, CONG, 3, IC, CT, CS, NCC )
      PR = CPG * VISG / CONG
      RE = 48. * EMD / ( PI * VISG * DI * Y )
      HT = 0.276 * CONG / DI * RE**0.8 * PR**0.4
  102 CONTINUE
      HT = AMAX1 ( HT, 0.1 )
      RETURN
      END
```

```
      SUBROUTINE INPUT
C**** INPUT, INITIALIZE AND PRINT DATA
      COMMON / 01 / TE,TH2,T,TI,DO,EL,DTUBE,P,TSE,QR,QEXT,EMD,THEX,Y
     $  ,TTM,TTI,ATT,AKIT,AKTT,PTT,HTK,ACC,XI,XC,XF,DI,PREX,CHIFAC,RETA
      COMMON / 02 / AKI1,AKT1,HE1,U1,HF1,HT1,EN1,TA1,TC1,TM1,EL1,QT1,TS1
     $            ,AKI2,AKT2,HE2,U2,HF2,HT2,EN2,TA2,TC2,TM2,EL2,QT2,TS2
      COMMON / 03 / VPR(20),TSAT(20),NVFR,THV(20),HV(20),NHV,
     $  TDN(20),DN(20),NDN,NCC,CS(10),CT(10),NVV,VB(10),VT(10)
     $  ,CP(120),TCP(20),PCP(6),NCPP,NCPT,CP1(20),CP2(20)
      DIMENSION  V(25), O(25)
      DATA  AST, BLA / 1H*, 1H  /, V / 25*0 /, IS / 1 /
  101 FORMAT ( I3,E12,7 )
  115 FORMAT ( 43H0* * * * THE ABOVE CASE DID NOT RUN * * * * / )
      CHIFUN(A) = ( A / (1.-A) )**0.9
  100 CONTINUE
      KSF = 1
      ICHI = 0
      EMD = 0.
      DO 110 I = 1,10
  110 O(I) = 0.
C *** READ DATA
  104 CONTINUE
      READ ( 5,101 ) II,VV
      IF ( II .EQ. 0 .AND. KSF .EQ. 1 ) STOP
      IF ( II .EQ. 0 ) GO TO 103
      IF ( II .EQ. 20 .OR. II .EQ. 21 ) ICHI = 1
      V(II) = VV
      O(II) = 1.
      KSF = 0
      GO TO 104
  114 CONTINUE
      WRITE ( 6,115 )
      GO TO 100
  103 CONTINUE
C *** ASSIGN VARIABLE VALUES
      DO   = V(1)
      EL   = V(2)
      Y    = V(3)
      DTUBE = V(4)
      TWTH = V(5)
      DI = DTUBE - 2.*TWTH
      T    = V(6)
      TI   = V(7)
      ATT  = V(8)
      TTM  = V(9)
      TTI  = V(10)
      HTK  = V(11)
      AKTT = V(12)
      AKT1 = AKTT
      AKT2 = AKTT
      AKIT = V(13)
      AKI1 = AKIT
      AKI2 = AKIT
      TE   = V(14)
      TSE  = V(15)
      P    = V(16)
      TH2  = V(17)
```

```
      PTT = V(18)
      XI  = V(19)
      XC  = V(20)
      XF  = V(21)
      ACC = V(22) * 32.16
C **  CALCULATE OR ASSIGN DEFAULT VALUES
      IF ( Y .LE. 0. ) Y = 1.
      IF ( TSE .GT. 0. ) GO TO 102
      IF ( O(16) .GT. 0. ) O(15) = 1.
      CALL GENTAB ( P, TSE, 3, IS, VPR, TSAT, NVPR )
  102 CONTINUE
      IF ( TE .LE. 0. ) TE = TSE
      IF ( O(15) .GT. 0. ) O(14) = 1.
      IF ( P .GT. 0. ) GO TO 107
      IF ( O(15) .GT. 0. ) O(16) = 1.
      CALL GENTAB ( TSE, P, 3, IS, TSAT, VPR, NVPR )
  107 CONTINUE
      IF ( TH2 .GT. 0. ) GO TO 106
      IF ( O(18) .GT. 0. ) O(17) = 1.
      CALL GENTAB ( PTT, TH2, 3, IS, VPR, TSAT, NVPR )
  106 CONTINUE
      IF ( PTT .GT. 0. ) GO TO 108
      IF ( O(17) .GT. 0. ) O(18) = 1.
      CALL GENTAB ( TH2, PTT, 3, IS, TSAT, VPR, NVPR )
  108 CONTINUE
      IF ( XI .LE. 0. ) XI = 0.05
      IF ( XF .LE. 0. ) XF = 1.
      IF ( ACC .LE. 0. ) ACC = 32.16
C **  MARK NEW INPUT VALUES
      DO 111 I = 1,22
      IF (O(I)) 112,112,113
  112 O(I) = BLA
      GO TO 111
  113 O(I) = AST
  111 CONTINUE
C *** PRINT INPUT DATA
      CALL W ( 6H DO    , DO     , 6HIN     , O(1) )
      CALL W ( 6H EL    , EL     , 6HFT     , O(2) )
      CALL W ( 6H Y     , Y      , 6H       , O(3) )
      CALL W ( 6H DTUBE , DTUBE  , 6HIN     , O(4) )
      CALL W ( 6H TWTH  , TWTH   , 6HIN     , O(5) )
      CALL W ( 6H T     , T      , 6HIN     , O(6) )
      CALL W ( 6H TI    , TI     , 6HIN     , O(7) )
      CALL W ( 6H ATT   , ATT    , 6HSQ FT  , O(8) )
      CALL W ( 6H TTM   , TTM    , 6HIN     , O(9) )
      CALL W ( 6H TTI   , TTI    , 6HIN     , O(10) )
      CALL W ( 6H HTK   , HTK    , 6HFT     , O(11) )
      CALL W ( 6H AKT   , AKT1   , 6HB/FDH  , O(12) )
      CALL W ( 6H AKI   , AKI1   , 6HB/FDH  , O(13) )
      CALL W ( 6HTE     , TE     , 6HDEG R  , O(14) )
      CALL W ( 6HTSE    , TSE    , 6HDEG R  , O(15) )
      CALL W ( 6HP      , P      , 6HPSIA   , O(16) )
      CALL W ( 6HTH2    , TH2    , 6HDEG R  , O(17) )
      CALL W ( 6HPTT    , PTT    , 6HPSIA   , O(18) )
      CALL W ( 6HXI     , XI     , 6H       , O(19) )
      CALL W ( 6HXC     , XC     , 6H       , O(20) )
      CALL W ( 6HXF     , XF     , 6H       , O(21) )
      CALL W ( 3HACC, ACC/32.16, 6HG      , O(22) )
```

```
      IF ( TE .LE. TH2 ) GO TO 114
      IF ( XC .LE. XI ) GO TO 114
C *** ASSIGN INITIAL VALUES TO START ITERATION
      TM1 = 1.01 * TH2
      TM2 = TM1
      TC1 = 0.99 * TH2
      TC2 = TC1
      THEX = TC1 - 1.0
      TS1 = 0.
      TS2 = 0.
      IF ( TI .LE. 0. ) GO TO 109
      TS1 = ( TSE + TE ) * 0.5
      TS2 = TS1
  109 CONTINUE
      EL1 = AMAX1( XC**3, 0.1 )
      EL2 = EL - EL1
C *** CALCULATE OTHER QUANTITIES USED IN SOLUTION
      CALL PTABLE ( P, CP1 )
      CALL PTABLE ( PTT, CP2 )
      CALL EXTHT
      CALL RADHT
      IF ( ICHI .EQ. 0 ) RETURN
      H = ( XC - XI ) / 100.
      X = XI
      YSUM = 0.5 * CHIFUN(X)
      DO 105 I = 1,99
      X = X + H
  105 YSUM = YSUM + CHIFUN(X)
      IF ( XC .LT. 1.) YSUM = YSUM + CHIFUN(XC)*0.5
      CHIFAC = YSUM / 100.
      RETURN
      END
```

```
      SUBROUTINE OUTPUT
C**** PRINT SOLUTION DATA
      COMMON / D1 / TE,TH2,T,T1,DD,FL,CTUBE,P,TSE,QR,QEXT,EMD,THEX,Y
     $  ,TTM,TTI,ATT,AKIT,AKTT,PTT,PTK,ACC,YI,XC,XF,DI,PHEX,CHIFAC,BETA
      COMMON / D2 / AK11,AKT1,HF1,U1,HF1,HT1,EN1,TA1,TC1,TM1,EL1,QT1,TS1
     $             ,AK12,AKT2,HE2,U2,HF2,HT2,EN2,TA2,TC2,TM2,EL2,QT2,TS2
   90 FORMAT ( 1H  )
   99 FORMAT ( 3H --,7(4H-------)/ )
      WRITE ( 6, 99 )
      CALL W ( 6HEMD   , EMD   , 6HLBF/HR , 1H  )
      CALL W ( 6HTHEX  , THEX  , 6HDEG R , 1H  )
      CALL W ( 6HPHEX  , PHEX  , 6HPSIA  , 1H  )
      CALL W ( 6HQEXT  , QEXT  , 6HBTU/HR, 1H  )
      CALL W ( 6HQR    , QR    , 6HBTU/HR, 1H  )
      CALL W12 ( 3HEL , EL1, EL2, 6HFT     )
      CALL W12 ( 2HQT, QT1, QT2, 6HBTU/HR )
      CALL W12 ( 2HTS, TS1, TS2, 6HDEG R )
      CALL W12 ( 3HTC , TC1, TC2, 6HDEG R  )
      CALL W12 ( 3HTM , TM1, TM2, 6HDEG R  )
      WRITE ( 6, 99 )
      CALL W12 ( 3HHE , HE1, HE2, 6HB/F2DH )
      CALL W12 ( 3HHF , HF1, HF2, 6HB/F2DH )
      CALL W12 ( 3HHT , HT1, HT2, 6HB/F2DH )
      CALL W12 ( 3HU  , U1, U2, 6HB/F2DH )
      CALL W12 ( 3HTA , TA1, TA2, 6HDEG R  )
      CALL W12 ( 3HEN , EN1, EN2, 6H       )
      CALL ENDUP
      WRITE ( 6, 90 )
      RETURN
      END
```

```
      SUBROUTINE PDROP
C**** CALCULATES PRESSURE DROP IN THE TUBE (FOR OUTPUT ONLY)
      COMMON / 01 / TE,TH2,T,TI,DO,EL,DTUBE,P,TSE,QR,QEXT,EMD,THEX,Y
     $  ,TTM,TTI,ATT,AKTT,AKTT,PTT,HTK,ACC,XI,XC,XF,DI,PHEX,CHIFAC,RETA
      COMMON / 02 / AKI1,AKT1,HE1,U1,HF1,HT1,EN1,TA1,TC1,TM1,EL1,QT1,TS1
     $             ,AKI2,AKT2,HE2,U2,HF2,HT2,EN2,TA2,TC2,TM2,EL2,QT2,TS2
      COMMON / 03 / VPR(20),TSAT(20),NVPR,THV(20),HV(20),NHV,
     $  TDN(20),DN(20),NDN,NCC,CS(10),CT(10),NVV,VS(10),VT(10)
     $  ,CP(120),TCP(20),PCP(6),NCPP,NCPT,CP1(20),CP2(20)
      DATA  ID / 1 /
      RHOV = 0.1880 * PHEX / THEX
      CALL GENTAB ( THEX, RHOL, 3, ID, TDN, DN, NDN )
      FL = 64. / RETA
      IF ( RETA .GT. 3000. ) FL = 0.316 / RETA**0.25
      E = (4.*EMD/Y/(3.14159*(DI/12.)**2) )**2 / ( ACC*1.296E+07 )
      A = E * FL / ( 2. * RHOL * DI/12. )
      B = A * ( RHOL/RHOV - 1. )
      C = -E / ( RHOV * PHEX*144. )
      D = ALOG ( 1. + C * (XC-XI) / (1.+C*XI) )
      DELPF = EL/(C*(XC-XI)) * ((A+B*XI)*D+E/C*(C*(XC-XI)-(1.+C*XI)*D))
      DELPD = PHEX*(RHOV/RHOL-1.) * D
      CALL W12 ( 6HDP F D, DELPF/144., DELPD, 4HPSIA )
      RETURN
      END
```

```
      SUBROUTINE PTABLE ( P, CPX )
C**** GENERATE A TABLE OF SPECIFIC HEAT AS A FUNCTION OF TEMPERATURE AT
C     INPUT PRESSURE P FROM A TWO-VARIABLE (TEMPERATURE,PRESSURE) TABLE
      COMMON / 03 / VPR(20),TSAT(20),NVPR,THV(20),HV(20),NHV,
     $  TDN(20),DN(20),NDN,NCC,CS(10),CT(10),NVV,VS(10),VT(10)
     $  ,CP(120),TCP(20),PCP(6),NCPP,NCPT,CP1(20),CP2(20)
      DIMENSION  CX(20,6),CPX(1)
      EQUIVALENCE  ( CP, CX )
      PIF = 1.
      DO 105 I = 2, NCPP
      II = I
      IF ( PCP(I) .LT. P ) GO TO 105
      PIF = ( P - PCP(I-1) ) / ( PCP(I) - PCP(I-1) )
      IF ( PCP(1) .GE. P ) PIF = 0.
      GO TO 106
  105 CONTINUE
  106 CONTINUE
      DO 107 I = 1,NCPT
  107 CPX(I) = CX(I,II-1) + PIF * ( CX(I,II) - CX(I,II-1) )
      RETURN
      END
```

```
      SUBROUTINE RADHT
C**** CALCULATE RADIATION HEAT TRANSFER
      COMMON / C1 / TE,TH2,T,TI,DD,L,CTUBE,P,TSE,QR,QEXT,EMD,THEX,Y
     *  ,TTM,TTI,ATT,AKIT,AKTT,CTT,HTK,ACC,YI,XC,XF,DI,PHEX,CHIFAC,BETA
      A = 0.
      RETURN
      END
```

```
      SUBROUTINE P ( T, D, U, C )
C**** WRITE SINGLE OUTPUT NUMBER
  1 0 FORMAT ( 4X,A1,A6,3H = ,E9.4,7X,A6 )
  1 1 FORMAT ( 4X,A1,A6,3H = ,E9.2,2X,A6 )
      A = ABS ( C )
      IF ( A .LT. 0.01 .OR. A .GE. 1000. ) GO TO 102
      WRITE ( 6,100 ) D, T, C, U
      RETURN
  102 CONTINUE
      WRITE ( 6,101 ) D, T, C, U
      RETURN
      END
```

```
      SUBROUTINE W12 ( T, D1, D2, U )
C**** WRITE TWO OUTPUT NUMBERS (USUALLY REGION 1 AND 2)
  101 FORMAT ( 5X,A6,3H = ,F9.4,2X,F9.4,2X,A6 )
  102 FORMAT ( 5X,A6,3H = ,E9.2,2X,F9.4,2X,A6 )
  103 FORMAT ( 5X,A6,3H = ,F9.4,2X,E9.2,2X,A6 )
  104 FORMAT ( 5X,A6,3H = ,E9.2,2X,E9.2,2X,A6 )
      N = 1
      A = ABS ( D1 )
      IF ( A .LT. 0.01 .OR. A .GE. 1000. ) N = N + 1
      B = ABS ( D2 )
      IF ( B .LT. 0.01 .OR. B .GE. 1000. ) N = N + 2
      GO TO ( 105, 106, 107, 108 ), N
  105 WRITE ( 6,101) T,D1,D2, U
      RETURN
  106 WRITE ( 6,102) T,D1,D2, U
      RETURN
  107 WRITE ( 6,103) T,D1,D2, U
      RETURN
  108 WRITE ( 6,104) T,D1,D2, U
      RETURN
      END
```

Appendix G
IDU/TVS PERFORMANCE COMPUTER CODE TEST CASES

A listing of the input deck for the test cases is given in Table G-1. Definitions are given in Table E-1. A complete set of input data is given in the first case; each subsequent case includes only the data to be changed from the previous case. Each case is terminated by a blank card; an additional blank card ends the run. The end-of-file note on the listing is for clarification only and is not a part of the deck.

In these cases, the external temperature is varied over the values 40, 45, 50, 60, 80, 100 °R for two internal pressures, 20 and 25 psia. For the conditions of the last case of this series (100 °R external and 25 psia internal), the transition quality in the tube flow is given values of 1.0 (no mist flow regime), 0.05 (no annular flow regime), and 0.0501 (negligible annular flow regime).

The tank configuration consists of two wall-mounted tubes, each 35 feet in length and spaced 2.5 inches apart on the tank. The tube outside diameter is 0.25 inch and wall thickness is 0.032 inch. The tank height is 2.8 feet and the area of the top is 4.4 square feet. The wall thickness is 0.5 inch and the top thickness is 1.0 inch. Insulation thicknesses are 0.25 and 0.5 inch on both wall and top. Conductivities of the wall and insulation are 90 and 0.01 Btu/ft-°R-hr, respectively.

For all cases, the external pressure is 15 psia; the external saturation temperature is taken from the vapor pressure table. The internal LH_2 temperature is also taken from the vapor pressure table, at the internal pressure. The transition quality in the two-phase tube flow is 0.85 for the first 12 cases. Default values were used for the initial and final quality in the tube and the acceleration level.

The output from the above cases is given in Table 2; cases 1 through 13 are for the 0.25 inch insulation, and cases 14 through 28 are for the 0.5 inch insulation.

Table G-1

TEST CASE INPUT DATA LISTING

1	3.5	14	40.0
2	35.0	14	45.0
3	2.0	14	50.0
4	0.25	14	60.0
5	0.032	14	80.0
6	0.5	14	100.0
7	0.25	18	25.0
8	4.4	14	40.0
9	1.0	14	45.0
10	0.25	14	50.0
11	2.8	14	60.0
12	90.0	14	80.0
13	0.01	14	100.0
16	15.0	20	1.0
20	0.85	20	0.05
18	20.0	20	0.0501

END OF FILE

Table G-2

IDU/TVS PERFORMANCE COMPUTER CODE RESULTS

	CASE 1		CASE 2		CASE 3	
DO	3.5000 IN		3.5000 IN		3.5000 IN	
EL	35.0000 FT		35.0000 FT		35.0000 FT	
Y	2.0000		2.0000		2.0000	
DTUBE	.2500 IN		.2500 IN		.2500 IN	
TWTH	.0320 IN		.0320 IN		.0320 IN	
T	.5000 IN		.5000 IN		.5000 IN	
TI	.2500 IN		.2500 IN		.2500 IN	
ATT	4.4000 SQ FT		4.4000 SQ FT		4.4000 SQ FT	
TTM	1.0000 IN		1.0000 IN		1.0000 IN	
TTI	.2500 IN		.2500 IN		.2500 IN	
HTK	2.5000 FT		2.5000 FT		2.5000 FT	
AKT	90.0000 B/F2H		90.0000 B/F2H		90.0000 B/F2H	
AKI	.0100 B/F2H		.0100 B/F2H		.0100 B/F2H	
*TE	40.0000 DEG R		45.0000 DEG R		50.0000 DEG R	
*TSE	36.6667 DEG R		36.6667 DEG R		36.6667 DEG R	
*P	15.0000 PSIA		15.0000 PSIA		15.0000 PSIA	
*TH2	38.4375 DEG R		38.4375 DEG R		38.4375 DEG R	
*PTT	20.0000 PSIA		20.0000 PSIA		20.0000 PSIA	
XI	.0500		.0500		.0500	
*XC	.8500		.8500		.8500	
XF	1.0000		1.0000		1.0000	
ACC	1.0000 G		1.0000 G		1.0000 G	
EMD	.0662 LB/HR		.0661 LB/HR		.0547 LB/HR	
THEX	38.2889 DEG R		38.1964 DEG R		37.1855 DEG R	
PHEX	19.5242 PSIA		19.5240 PSIA		19.0466 PSIA	
QEXT	1.7574 BTU/HR		8.6049 BTU/HR		15.6361 BTU/HR	
QR	0. BTU/HR		0. BTU/HR		0. BTU/HR	
EL	10.1304 24.8696 FT		10.4925 18.5075 FT		16.9134 18.0866 FT	
QT	16.1225 1.8792 BTU/HR		46.3869 6.6979 BTU/HR		84.0903 15.7669 BTU/HR	
TS	39.4521 39.4795 DEG R		43.1353 43.1867 DEG R		46.6566 47.0123 DEG R	
TC	38.3665 38.4635 DEG R		36.3444 36.5156 DEG R		38.2626 38.5536 DEG R	
TM	38.3713 38.4668 DEG R		38.3180 38.5179 DEG R		38.2642 38.5583 DEG R	
HE	.9489 .9367 B/F2DH		1.2446 1.2362 B/F2DH		1.3656 1.3564 B/F2DH	
HF	17.3493 13.6536 B/F2DH		20.2241 18.0271 B/F2DH		21.5573 19.9395 B/F2DH	
HT	97.3661 3.3065 B/F2DH		196.8704 11.2463 B/F2DH		275.9626 18.8261 B/F2DH	
U	.3188 .3174 B/F2DH		.3464 .3454 B/F2DH		.3552 .3547 B/F2DH	
TA	38.4657 38.4736 DEG R		38.5481 38.5615 DEG R		38.6249 38.6396 DEG R	
EN	.3165 .2615		.3414 .3229		.3525 .3393	
DP F D	2.61E-03 4.16E-04 PSIA		9.85E-03 9.07E-05 PSIA		.0180 3.00E-04 PSIA	

Table G-2 (continued)

IDU/TVS PERFORMANCE COMPUTER CODE RESULTS

CASE 4

DO	3.5000	IN	
EL	35.0000	FT	
Y	2.0000		
DTUBE	.2500	IN	
TWTH	.0320	IN	
T	.5000	IN	
TI	.2500	IN	
ATT	4.4000	SQ FT	
TTH	1.0000	IN	
TTI	.2500	IN	
HTK	2.5000	FT	
AKT	90.0000	B/FDH	
AKI	.0100	B/FDH	
*TE	60.0000	DEG R	
TSE	36.6667	DEG R	
P	14.6700	PSIA	
TH2	34.4375	DEG R	
PTT	20.0000	PSIA	
XI	.0500		
XC	.8500		
XF	1.0000		
ACC	1.0000	G	
EMD	1.8684	LB/HR	
THEX	38.6550	DEG R	
PHEX	18.7782	PSIA	
QEXT	30.6463	BTU/HR	
QR	0.	BTU/HR	
EL	21.3283	13.6717	FT
QT	100.6824	33.1588	BTU/HR
TS	54.7182	54.7879	DEG R
TC	38.1674	36.6105	DEG R
TH	38.2337	38.6212	DEG R
HE	1.4952	1.4892	B/F2DH
HF	23.2528	22.0267	B/F2DH
HT	454.5395	35.3347	B/F2DH
L	.3634	.3633	B/F2DH
TA	38.7695	38.7663	DEG R
EN	.3658	.3569	
DP F D	.0349	1.11E-03	PSIA

CASE 5

DO	3.5000	IN	
EL	35.0000	FT	
Y	2.0000		
DTUBE	.2500	IN	
TWTH	.0320	IN	
T	.5000	IN	
TI	.2500	IN	
ATT	4.4000	SQ FT	
TTH	1.0000	IN	
TTI	.2500	IN	
HTK	2.5000	FT	
AKT	90.0000	B/FDH	
AKI	.0100	B/FDH	
*TE	80.0000	DEG R	
TSE	36.6667	DEG R	
P	19.0000	PSIA	
TH2	36.4375	DEG R	
PTT	20.0000	PSIA	
XI	.0500		
XC	.8500		
XF	1.0000		
ACC	1.0000	G	
EMD	2.0851	LB/HR	
THEX	37.9288	DEG R	
PHEX	16.3723	PSIA	
QEXT	60.6710	BTU/HR	
QR	0.	BTU/HR	
EL	23.4926	11.5074	FT
QT	316.5340	59.5501	BTU/HR
TS	72.4500	72.5585	DEG R
TC	38.0938	38.6861	DEG R
TH	38.1585	38.7109	DEG R
HE	1.6247	1.6197	B/F2DH
HF	25.2525	24.3207	B/F2DH
HT	623.7472	52.0252	B/F2DH
U	.3705	.3705	B/F2DH
TA	39.0385	39.0403	DEG R
EN	.3812	.3747	
DP F D	.0763	4.38E-04	PSIA

CASE 6

DO	3.5000	IN	
EL	35.0000	FT	
Y	2.0000		
DTUBE	.2500	IN	
TWTH	.0320	IN	
T	.5000	IN	
TI	.2500	IN	
ATT	4.4000	SQ FT	
TTH	1.0000	IN	
TTI	.2500	IN	
HTK	2.5000	FT	
AKT	90.0000	B/FDH	
AKI	.0100	B/FDH	
*TE	100.0000	DEG R	
TSE	36.6667	DEG R	
P	15.6000	PSIA	
TH2	36.4375	DEG R	
PTT	20.0000	PSIA	
XI	.0500		
XC	.8500		
XF	1.0000		
ACC	1.0000	G	
EMD	3.1187	LB/HR	
THEX	37.8263	DEG R	
PHEX	16.0443	PSIA	
QEXT	90.9376	BTU/HR	
QR	0.	BTU/HR	
EL	24.5829	10.4171	FT
QT	473.7932	88.8362	BTU/HR
TS	86.3790	86.5334	DEG R
TC	38.0055	38.7346	DEG R
TH	38.0921	38.7757	DEG R
HE	1.7024	1.6962	B/F2DH
HF	26.4138	25.5550	B/F2DH
HT	821.4947	71.7101	B/F2DH
U	.3744	.3747	B/F2DH
TA	39.2916	39.3269	DEG R
EN	.3912	.3836	
DP F D	.2635	9.95E-03	PSIA

Table G-2 (continued)

IDU/TVS PERFORMANCE COMPUTER CODE RESULTS

CASE 7

DO	3.5000		IN
EL	35.0000		FT
Y	2.0000		
DTUBE	.2500		IN
TWTM	.0320		IN
T	.5000		IN
TI	.2500		IN
ATT	4.4000		SQ FT
TTM	1.0000		IN
TTI	.2500		IN
HTK	2.6900		FT
AKT	90.0000		B/FDH
AKI	.0100		B/FDH
*TE	45.0000		DEG R
TSE	36.6667		DEG R
P	15.0000		PSIA
TH2	40.0000		DEG R
PTT	25.0000		PSIA
XI	.1500		
XC	.4500		
XF	1.0000		
ACC	1.0000		G
EMD	.2322		LB/HR
THEX	39.7657		DEG R
PHEX	24.3142		PSIA
QEXT	6.5127		BTU/HR
QR	0.		BTU/HR
EL	15.3619	19.6381	FT
CT	34.7962	6.5243	BTU/HR
TS	43.5174	43.5597	DEG R
TC	39.4059	40.0422	DEG R
TM	39.8966	40.0638	DEG R
HE	1.1748	1.1653	B/F2DH
HF	20.0620	17.5354	B/F2DH
HT	172.7414	9.1809	B/F2DH
U	.2467	.3496	B/F2DH
TA	40.0635	40.0951	DEG R
EN	.2402	.3164	
DP F D	5.65E-03	4.26E-05	PSIA

CASE 8

DO	3.5000		IN
EL	35.0000		FT
Y	2.0000		
DTUBE	.2500		IN
TWTM	.0320		IN
T	.5000		IN
TI	.2500		IN
ATT	4.4000		SQ FT
TTM	1.0000		IN
TTI	.2500		IN
HTK	2.8300		FT
AKT	90.0000		B/FDH
AKI	.0100		B/FDH
*TE	5[illegible].0000		DEG R
TSE	36.6667		DEG R
P	15.0000		PSIA
TH2	40.0000		DEG R
PTT	25.0000		PSIA
XI	.0300		
XC	.8500		
XF	1.0000		
ACC	1.0000		G
EMD	.4821		LB/HR
THEX	39.7234		DEG R
PHEX	24.1150		PSIA
QEXT	13.7500		BTU/HR
QR	0.		BTU/HR
EL	18.3883	16.6117	FT
CT	72.2599	13.5487	BTU/HR
TS	47.2686	47.3553	DEG R
TC	39.6416	40.1021	DEG R
TM	39.8805	40.1060	DEG R
HE	1.3233	1.3161	B/F2DH
HF	21.6954	19.8902	B/F2DH
HT	294.0487	16.4558	B/F2DH
U	.3522	.3517	B/F2DH
TA	40.1598	40.1736	DEG R
EN	.3536	.3486	
DP F D	.0122	1.66E-04	PSIA

CASE 9

DO	3.5000		IN
EL	35.0000		FT
DTUBE	.2500		IN
TWTM	.0320		IN
Y	2.0000		
T	.5000		IN
TI	.2500		IN
ATT	4.4000		SQ FT
TTM	1.0000		IN
TTI	.2500		IN
HTK	2.8100		FT
AKT	90.0000		B/FDH
AKI	.0100		B/FDH
*TE	60.0000		DEG R
TSE	36.6667		DEG R
P	15.0000		PSIA
TH2	40.0000		DEG R
PTT	25.0000		PSIA
XI	.1500		
XC	.6500		
XF	1.0000		
ACC	1.0000		G
EMD	.5927		LB/HR
THEX	39.6355		DEG R
PHEX	23.8335		PSIA
QEXT	28.6749		BTU/HR
QR	0.		BTU/HR
EL	21.1269	13.8731	FT
CT	148.8911	27.9371	BTU/HR
TS	55.0283	55.1049	DEG R
TC	39.7750	40.1632	DEG R
TM	39.8365	40.1698	DEG R
HE	1.4739	1.4650	B/F2DH
HF	23.5678	22.3315	B/F2DH
HT	305.9546	29.2984	B/F2DH
U	.3619	.3615	B/F2DH
TA	40.3125	40.3166	DEG R
EN	.3684	.3597	
DP F D	.0255	7.94E-04	PSIA

Table G-2 (continued)

IDU/TVS PERFORMANCE COMPUTER CODE RESULTS

CASE 10

DO	=	3.5000		IN
EL	=	35.0000		FT
Y	=	2.0000		
DTUBE	=	.2500		IN
TWTH	=	.0320		IN
T	=	.5000		IN
TI	=	.2500		IN
ATT	=	4.4000		SQ FT
TTM	=	1.0000		IN
TTI	=	.2500		IN
HTK	=	2.6[illegible]		FT
AKT	=	90.0000		B/FDH
AKI	=	[illegible]		B/FDH
*TE	=	[illegible]		DEG R
TSC	=	36.6667		DEG R
P	=	15.0000		PSIA
TH2	=	4[illegible]		DEG R
PTT	=	25.0000		PSIA
XI	=	[illegible]		
XC	=	.6500		
XF	=	1.0000		
ACC	=	1.0000		G
FMD	=	2.0292		LB/HR
THEX	=	39.5[illegible]74		DEG R
PHEX	=	23.4137		PSIA
QEXT	=	56.9794		BTU/HR
QH	=	0.		BTU/HR
EL	=	26.4405	11.5595	FT
QT	=	324.6304	57.1182	BTU/HR
TS	=	7[illegible].7495	75.6535	DEG R
TC	=	39.6715	40.2356	DEG R
TM	=	39.7239	40.2594	DEG R
HE	=	1.6115	1.6062	B/F2DH
HF	=	25.7337	24.7260	B/F2DH
HT	=	234.9440	51.8355	B/F2DH
U	=	.3654	.3494	B/F2DH
TA	=	40.5667	40.5390	DEG R
EN	=	.3548	.3775	
DP F D	=	[illegible]	[illegible]	PSIA

CASE 11

DO	=	3.5000		IN
EL	=	35.0000		FT
Y	=	2.0000		
DTUBE	=	.2500		IN
TWTH	=	.0320		IN
T	=	.5000		IN
TI	=	.2500		IN
ATT	=	4.4000		SQ FT
TTM	=	1.0000		IN
TTI	=	.2500		IN
HTK	=	2.6000		FT
AKT	=	90.0000		B/FDH
AKI	=	.0100		B/FDH
*TE	=	100.0000		DEG R
TSF	=	36.6667		DEG R
P	=	15.0000		PSIA
TH2	=	40.0000		DEG R
PTT	=	25.0000		PSIA
XI	=	.0500		
XC	=	.6500		
XF	=	1.0000		
ACC	=	1.0000		G
EMD	=	3.0753		LB/HR
THEX	=	39.4145		DEG R
PHEX	=	23.0944		PSIA
QEXT	=	69.4347		BTU/HR
QH	=	0.		BTU/HR
EL	=	24.5719	10.4281	FT
QT	=	462.0419	96.6328	BTU/HR
TS	=	86.6641	86.7881	DEG R
TC	=	39.5542	40.2834	DEG R
TM	=	39.6742	40.3233	DEG R
HE	=	1.6929	1.6835	B/F2DH
HF	=	27.1662	26.0259	B/F2DH
HT	=	130.1765	72.2095	B/F2DH
U	=	.3740	.3738	B/F2DH
TA	=	40.8147	40.8495	DEG R
EN	=	.3952	.3849	
DP F D	=	.2176	7.83E-03	PSIA

CASE 12

DO	=	3.5000		IN
EL	=	35.0000		FT
Y	=	2.0000		
DTUBE	=	.2500		IN
TWTH	=	.0320		IN
T	=	.5000		IN
TI	=	.2500		IN
ATT	=	4.4000		SQ FT
TTM	=	1.0000		IN
TTI	=	.2500		IN
HTK	=	2.6000		FT
AKT	=	90.0000		B/FDH
AKI	=	.0100		B/FDH
TE	=	100.0000		DEG R
TSF	=	36.6667		DEG R
P	=	15.0000		PSIA
TH2	=	40.0000		DEG R
PTT	=	25.0000		PSIA
XI	=	.6500		
*XC	=	1.0000		
XF	=	1.0000		
ACC	=	1.0000		G
FMD	=	3.0530		LB/HR
THEX	=	39.6365		DEG R
PHEX	=	23.9963		PSIA
QEXT	=	69.4347		BTU/HR
QH	=	0.		BTU/HR
EL	=	35.0000	0.	FT
QT	=	548.9200	0.	BTU/HR
TS	=	86.6954	86.6954	DEG R
TC	=	39.7616	39.7616	DEG R
TM	=	39.8270	39.8470	DEG R
HE	=	1.6915	1.6919	B/F2DH
HF	=	63.2950	63.295	B/F2DH
HT	=	1.00E+03	72.57[illegible]	B/F2DH
U	=	.3739	.3[illegible]39	B/F2DH
TA	=	40.9479	40.9479	DEG R
EN	=	.3664	.3664	
DP F D		.2335	9.05E-03	PSIA

Table G-2 (continued)
IDU/TVS PERFORMANCE COMPUTER CODE RESULTS

CASE 13

~~DO~~	~~=~~	~~3.5000~~	~~IN~~	
EL	=	35.0000	FT	
Y	=	2.0000		
DTUBE	=	.2500	IN	
TNTH	=	.0320	IN	
T	=	.5000	IN	
~~T1~~	~~=~~	~~.2500~~	~~IN~~	
ATT	=	4.4000	SQ FT	
TTM	=	1.0000	IN	
TTI	=	.2500	IN	
HTK	=	2.0000	FT	
AKT	=	90.1000	B/FTF	
~~AKI~~	~~=~~	~~[illegible]~~	~~[illegible]~~	
TE	=	100.0000	DEG R	
TSE	=	36.4667	DEG R	
P	=	15.0000	PSIA	
TH2	=	40.0000	DEG R	
PTT	=	25.0000	PSIA	
~~XI~~	~~=~~	~~.0500~~		
*XC	=	.0501		
XF	=	1.0000		
ACC	=	1.0000	G	
GHD	=	3.0676	LB/HR	
THEX	=	38.0046	DEG R	
PHEX	=	16.8069	PSIA	
QEXT	=	69.4349	BTU/HR	
QH	=	[illegible]	BTU/HR	
FL	=	1.44E-03	34.9966	FT
CT	=	.0576	548.6026	BTU/HR
~~TS~~	~~=~~	~~[illegible]~~	~~[illegible]~~	~~DEG R~~
TC	=	38.6193	39.7619	DEG R
TM	=	38.8112	36.6371	DEG R
HL	=	1.6956	1.6919	B/F2DR
HF	=	38.6659	23.2936	B/F2DR
~~HT~~	~~=~~	~~556.2431~~	~~76.5964~~	~~B/F2DR~~
U	=	.3742	.3739	B/F2DR
TA	=	40.6159	40.9479	DEG R
EA	=	.4585	.3664	
PRES D	=	.0272	1.15E-05	PSIA

Table C-2 (continued)

IDU/TVS PERFORMANCE COMPUTER CODE RESULTS

CASE 14

• DO	=	3,9000	IN		
• EL	=	35,0000	FT		
• Y	=	2,0000			
• DTUBE	=	,4500	IN		
• TWTH	=	,0320	IN		
• T	=	,5000	IN		
• TI	=	,5000	IN		
• ATT	=	4,4000	SQ FT		
• TTH	=	1,0000	IN		
• TTI	=	,5000	IN		
• HTK	=	2,5000	FT		
• AKT	=	90,0000	B/F2DH		
• AKI	=	,0100	B/F2DH		
•TE	=	40,0000	DEG R		
•TSE	=	36,6667	DEG R		
•P	=	15,0000	PSIA		
•TH2	=	38,4375	DEG R		
•PTT	=	20,0000	PSIA		
XI	=	,6500			
•XC	=	,6500			
XF	=	1,0000			
ACC	=	1,0000	G		
EMD	=	,0393	LB/HR		
THEX	=	38,3669	DEG R		
PHEX	=	19,5863	PSIA		
QEXI	=	1,1093	BTU/HR		
QR	=	0,	BTU/HR		
EL	=	8,2127	29,7873	FT	
QT	=	5,9548	1,1105	BTU/HR	
TS	=	39,6438	39,9576	DEG R	
TC	=	38,3785	38,4549	DEG R	
TM	=	38,3820	38,4551	DEG R	
HE	=	,6513	,8429	B/F2DH	
HF	=	16,5795	12,3542	B/F2DH	
HT	=	79,6441	2,1808	B/F2DH	
U	=	,1872	,1888	B/F2DH	
TA	=	38,4549	38,4888	DEG R	
EN	=	,3084	,2867		
DP F D	=	1,95E-03	1,47E-06	PSIA	

CASE 15

DO	=	3,9000	IN		
EL	=	35,0000	FT		
Y	=	2,0000			
DTUBE	=	,4500	IN		
TWTH	=	,0320	IN		
T	=	,5000	IN		
TI	=	,5000	IN		
ATT	=	4,4000	SQ FT		
TTH	=	1,0000	IN		
TTI	=	,5000	IN		
HTK	=	2,5000	FT		
AKT	=	90,0000	B/F2DH		
AKI	=	,0100	B/F2DH		
•TE	=	45,0000	DEG R		
TSE	=	36,6667	DEG R		
P	=	15,0000	PSIA		
TH2	=	38,4375	DEG R		
PTT	=	20,0000	PSIA		
XI	=	,6500			
XC	=	,6500			
XF	=	1,0000			
ACC	=	1,0000	G		
EMD	=	,1758	LB/HR		
THEX	=	38,2363	DEG R		
PHEX	=	19,3582	PSIA		
QEXI	=	5,1625	BTU/HR		
QR	=	0,	BTU/HR		
EL	=	14,1838	20,8162	FT	
QT	=	26,6205	4,9924	BTU/HR	
TS	=	43,6144	43,8372	DEG R	
TC	=	38,3319	38,4902	DEG R	
TM	=	38,3469	38,4913	DEG R	
HE	=	1,1069	1,1035	B/F2DH	
HF	=	19,1171	16,3138	B/F2DH	
HT	=	150,1367	7,2161	B/F2DH	
U	=	,1973	,1971	B/F2DH	
TA	=	38,3945	38,5159	DEG R	
EN	=	,3315	,3060		
DP F D	=	5,63E-03	2,97E-09	PSIA	

CASE 16

DO	=	3,9000	IN		
EL	=	35,0000	FT		
Y	=	2,0000			
DTUBE	=	,4500	IN		
TWTH	=	,0320	IN		
T	=	,5000	IN		
TI	=	,5000	IN		
ATT	=	4,4000	SQ FT		
TTH	=	1,0000	IN		
TTI	=	,5000	IN		
HTK	=	2,5000	FT		
AKT	=	90,0000	B/F2DH		
AKI	=	,0100	B/F2DH		
•TE	=	50,0000	DEG R		
TSE	=	36,6667	DEG R		
P	=	15,0000	PSIA		
TH2	=	38,4375	DEG R		
PTT	=	20,0000	PSIA		
XI	=	,6500			
XC	=	,6500			
XF	=	1,0000			
ACC	=	1,0000	G		
EMD	=	,3152	LB/HR		
THEX	=	38,1969	DEG R		
PHEX	=	19,2174	PSIA		
QEXI	=	9,2561	BTU/HR		
QR	=	0,	BTU/HR		
EL	=	16,6487	18,3513	FT	
QT	=	47,7624	6,3554	BTU/HR	
TS	=	48,6696	48,9962	DEG R	
TC	=	38,3815	38,5108	DEG R	
TM	=	38,3953	38,5141	DEG R	
HE	=	1,2136	1,2090	B/F2DH	
HF	=	20,3153	19,0987	B/F2DH	
HT	=	201,8361	11,9116	B/F2DH	
U	=	,2004	,2002	B/F2DH	
TA	=	38,3504	38,5041	DEG R	
EN	=	,3411	,3221		
DP F D	=	,0101	9,62E-09	PSIA	

Table G-2 (continued)

IDU/TVS PERFORMANCE COMPUTER CODE RESULTS

CASE 17

DD	=	3,9000	IN	
EL	=	35,0000	FT	
Y	=	2,0000		
DTUBE	=	,2500	IN	
TWTH	=	,0320	IN	
T	=	,5000	IN	
TI	=	,5000	IN	
ATT	=	4,4000	SQ FT	
TTH	=	1,0000	IN	
TTI	=	,5000	IN	
HTK	=	2,5000	FT	
AKT	=	90,0000	B/F2DH	
AKI	=	,0100	B/F2DH	
*TE	=	80,0000	DEG R	
TSE	=	36,6667	DEG R	
P	=	15,0000	PSIA	
TH2	=	38,4375	DEG R	
PTT	=	20,0000	PSIA	
XI	=	,0500		
XC	=	,6500		
XF	=	1,0000		
ACC	=	1,0000	G	
EMD	=	,2970	LB/HR	
THEX	=	38,1297	DEG R	
PHEX	=	19,0193	PSIA	
QEXT	=	17,6745	BTU/HR	
QR	=	0.	BTU/HR	
EL	=	19,2334	35,7666	FT
QT	=	90,5009	16,9989	BTU/HR
TS	=	56,6692	56,7064	DEG R
TC	=	38,4549	33,5560	DEG R
TP	=	38,2775	33,5037	DEG R
HE	=	1,3263	1,3222	B/F2DH
HF	=	21,7317	23,1540	B/F2DH
HT	=	207,2985	19,1736	B/F2DH
U	=	,2092	,2091	B/F2DH
TA	=	38,6367	38,6527	DEG R
EN	=	,3292	,3398	
DP F D	=	,0194	3,48E-04	PSIA

CASE 18

DD	=	3,9000	IN	
EL	=	35,0000	FT	
Y	=	2,0000		
DTUBE	=	,2500	IN	
TWTH	=	,0320	IN	
T	=	,5000	IN	
TI	=	,5000	IN	
ATT	=	4,4000	SQ FT	
TTH	=	1,0000	IN	
TTI	=	,5000	IN	
HTK	=	2,5000	FT	
AKT	=	90,0000	B/F2DH	
AKI	=	,0100	B/F2DH	
*TE	=	80,0000	DEG R	
TSE	=	36,6667	DEG R	
P	=	15,0000	PSIA	
TH2	=	38,4375	DEG R	
PTT	=	20,0000	PSIA	
XI	=	,0500		
XC	=	,6500		
XF	=	1,0000		
ACC	=	1,0000	G	
EMD	=	1,1649	LB/HR	
THEX	=	36,6378	DEG R	
PHEX	=	18,7212	PSIA	
QEXT	=	35,6486	BTU/HR	
QR	=	0.	BTU/HR	
EL	=	21,6809	13,3191	FT
QT	=	176,7014	33,1315	BTU/HR
TS	=	74,0193	74,0085	DEG R
TC	=	38,1831	36,6191	DEG R
TP	=	38,2243	38,6310	DEG R
HE	=	1,4372	1,4341	B/F2DH
HF	=	23,3592	22,3777	B/F2DH
HT	=	428,6486	32,6953	B/F2DH
U	=	,2057	,2056	B/F2DH
TA	=	38,7972	38,8159	DEG R
EN	=	,3671	,3579	
DP F D	=	,0385	1,34E-03	PSIA

CASE 19

DD	=	3,9000	IN	
EL	=	35,0000	FT	
Y	=	2,0000		
DTUBE	=	,2500	IN	
TWTH	=	,0320	IN	
T	=	,5000	IN	
TI	=	,5000	IN	
ATT	=	4,4000	SQ FT	
TTH	=	1,0000	IN	
TTI	=	,5000	IN	
HTK	=	2,5000	FT	
AKT	=	90,0000	B/F2DH	
AKI	=	,0100	B/F2DH	
*TE	=	100,0000	DEG R	
TSE	=	36,6667	DEG R	
P	=	15,0000	PSIA	
TH2	=	38,4375	DEG R	
PTT	=	20,0000	PSIA	
XI	=	,0500		
XC	=	,6500		
XF	=	1,0000		
ACC	=	1,0000	G	
EMD	=	1,7362	LB/HR	
THEX	=	37,9649	DEG R	
PHEX	=	18,4676	PSIA	
QEXT	=	52,2819	BTU/HR	
QR	=	0.	BTU/HR	
EL	=	22,9716	12,0284	FT
QT	=	263,4961	49,4059	BTU/HR
TS	=	91,5045	91,5066	DEG R
TC	=	38,1234	38,6629	DEG R
TP	=	38,1765	38,6529	DEG R
HE	=	1,5073	1,5040	B/F2DH
HF	=	24,7449	23,6911	B/F2DH
HT	=	592,7258	44,9541	B/F2DH
U	=	,2070	,2070	B/F2DH
TA	=	38,9463	38,9707	DEG R
EN	=	,3762	,3681	
DP F D	=	,0581	3,02E-03	PSIA

Table G-2 (continued)

IDU/TVS PERFORMANCE COMPUTER CODE RESULTS

CASE 20

▼ D0	=	3,9000	IN
EL	=	35,0000	FT
V	=	2,0000	
DTUBE	=	,2900	IN
TWTM	=	,0320	IN
T	=	,5000	IN
TI	=	,5000	IN
ATT	=	4,4000	SQ FT
TTM	=	1,0000	IN
TTI	=	,5000	IN
HTK	=	2,5000	FT
AKT	=	90,0000	B/F2DH
AKI	=	,0100	B/F2DH
*TE	=	40,0000	DEG R
TSE	=	36,6667	DEG R
P	=	15,0000	PSIA
*TH2	=	40,0000	DEG R
*PTT	=	25,0000	PSIA
XI	=	,0500	
XC	=	,0500	
XF	=	1,0000	
ACC	=	1,0000	G

• • • • THE ABOVE CASE DID NOT RUN • • • •

CASE 21

D0	=	3,9000	IN	
EL	=	35,0000	FT	
V	=	2,0000		
DTUBE	=	,2900	IN	
TWTM	=	,0320	IN	
T	=	,5000	IN	
TI	=	,5000	IN	
ATT	=	4,4000	SQ FT	
TTM	=	1,0000	IN	
TTI	=	,5000	IN	
HTK	=	2,5000	FT	
AKT	=	90,0000	B/F2DH	
AKI	=	,0100	B/F2DH	
*TE	=	45,0000	DEG R	
TSE	=	36,6667	DEG R	
P	=	15,0000	PSIA	
TH2	=	40,0000	DEG R	
PTT	=	25,0000	PSIA	
XI	=	,0500		
XC	=	,0500		
XF	=	1,0000		
ACC	=	1,0000	G	
EPD	=	,1241	LB/HR	
THEX	=	39,6602	DEG R	
PHEX	=	24,9284	PSIA	
QEXI	=	3,9161	BTU/HR	
QH	=	0.	BTU/HR	
EL	=	13,0659	21,9301	FT
QT	=	60,0943	3,7007	BTU/HR
TS	=	44,0518	44,0719	DEG R
TC	=	39,9987	43,0418	DEG R
TM	=	39,9161	43,0427	DEG R
HE	=	1,0477	1,0421	B/F2DH
HF	=	19,6165	15,6077	B/F2DH
HT	=	132,8327	5,9199	B/F2DH
U	=	,1953	,1951	B/F2DH
TA	=	40,0508	43,0037	DEG R
EN	=	,3350	,3018	
DP F D	=	3,46E-03	1,42E-02	PSIA

CASE 22

D0	=	3,9000	IN	
EL	=	35,0000	FT	
V	=	2,0000		
DTUBE	=	,2900	IN	
TWTM	=	,0320	IN	
T	=	,5000	IN	
TI	=	,5000	IN	
ATT	=	4,4000	SQ FT	
TTM	=	1,0000	IN	
TTI	=	,5000	IN	
HTK	=	2,5000	FT	
AKT	=	90,0000	B/F2DH	
AKI	=	,0100	B/F2DH	
*TE	=	90,0000	DEG R	
TSE	=	36,6667	DEG R	
P	=	15,0000	PSIA	
TH2	=	40,0000	DEG R	
PTT	=	25,0000	PSIA	
XI	=	,0500		
XC	=	,0500		
XF	=	1,0000		
ACC	=	1,0000	G	
EPD	=	,2748	LB/HR	
THEX	=	39,7764	DEG R	
PHEX	=	24,2717	PSIA	
QEXI	=	8,1137	BTU/HR	
QH	=	0.	BTU/HR	
EL	=	10,1029	16,8971	FT
QT	=	41,1464	7,7156	BTU/HR
TS	=	48,2865	48,3129	DEG R
TC	=	39,8783	42,0699	DEG R
TM	=	39,8666	40,0719	DEG R
HE	=	1,1772	1,1729	B/F2DH
HF	=	20,4800	18,0439	B/F2DH
HT	=	107,9243	10,4903	B/F2DH
U	=	,1994	,1992	B/F2DH
TA	=	40,0963	42,1342	DEG R
EN	=	,3623	,3217	
DP F D	=	9,93E-03	5,29E-02	PSIA

Table G-2 (continued)

IDU/IVS PERFORMANCE COMPUTER CODE RESULTS

CASE 23

DB	=	3,9000	IN	
EL	=	35,0000	FT	
Y	=	2,0000		
DTUBE	=	,2500	IN	
THTH	=	,0320	IN	
T	=	,5000	IN	
TI	=	,5000	IN	
ATT	=	4,4000	SQ FT	
TTH	=	1,0000	IN	
TTI	=	,5000	IN	
HTK	=	2,0000	FT	
AKT	=	90,0000	B/F2DH	
AKI	=	,0100	B/F2DH	
*TE	=	60,0000	DEG R	
TSE	=	36,6667	DEG R	
P	=	15,0000	PSIA	
TH2	=	40,0000	DEG R	
PTT	=	25,0000	PSIA	
XI	=	,0500		
XC	=	,8500		
XF	=	1,0000		
▼ACC	=	1,0000	G	
END	=	,9593	LB/HR	
THEX	=	39,7006	DEG R	
PHEX	=	24,0611	PSIA	
QEXT	=	16,8714	BTU/HR	
QR	=	0.	BTU/HR	
EL	=	19,0104	15,9896	FT
QT	=	83,8473	15,7213	BTU/HR
TS	=	96,8689	96,9037	DEG R
TC	=	39,8287	40,1119	DEG R
TP	=	39,8499	40,1107	DEG R
HE	=	1,3052	1,3014	B/F2DH
HF	=	22,1186	20,3693	B/F2DH
HT	=	275,9933	18,5298	B/F2DH
U	=	,2027	,2026	B/F2DH
TA	=	40,1817	40,1979	DEG R
EN	=	,3557	,3415	
DP F D	=	,0142	2,50E-04	PSIA

CASE 24

DB	=	3,9000	IN	
EL	=	35,0000	FT	
Y	=	2,0000		
DTUBE	=	,2500	IN	
THTH	=	,0320	IN	
T	=	,5000	IN	
TI	=	,5000	IN	
ATT	=	4,4000	SQ FT	
TTH	=	1,0000	IN	
TTI	=	,5000	IN	
HTK	=	2,0000	FT	
AKT	=	90,0000	B/F2DH	
AKI	=	,0100	B/F2DH	
*TE	=	80,0000	DEG R	
TSE	=	36,6667	DEG R	
P	=	15,0000	PSIA	
TH2	=	40,0000	DEG R	
PTT	=	25,0000	PSIA	
XI	=	,0500		
XC	=	,8500		
XF	=	1,0000		
ACC	=	1,0000	G	
END	=	1,1337	LB/HR	
THEX	=	39,6134	DEG R	
PHEX	=	23,7628	PSIA	
QEXT	=	33,9431	BTU/HR	
QR	=	0.	BTU/HR	
EL	=	21,0177	13,9823	FT
QT	=	170,0684	31,8878	BTU/HR
TS	=	74,2539	74,2513	DEG R
TC	=	39,7573	40,1722	DEG R
TP	=	39,7949	40,1659	DEG R
HE	=	1,4256	1,4229	B/F2DH
HF	=	24,6024	22,7580	B/F2DH
HT	=	418,2541	32,5755	B/F2DH
U	=	,2054	,2054	B/F2DH
TA	=	40,1954	40,3977	DEG R
EN	=	,3705	,3609	
DP F D	=	,0252	1,04E-03	PSIA

CASE 25

DB	=	3,9000	IN	
▼EL	=	35,0000	FT	
Y	=	?,0000		
DTUBE	=	,2500	IN	
THTH	=	,0320	IN	
T	=	,5000	IN	
TI	=	,5000	IN	
ATT	=	4,4000	SQ FT	
TTH	=	1,0000	IN	
TTI	=	,5000	IN	
HTK	=	2,0000	FT	
AKT	=	90,0000	B/F2DH	
AKI	=	,0100	B/F2DH	
*TE	=	100,0000	DEG R	
TSE	=	36,6667	DEG R	
P	=	15,0000	PSIA	
TH2	=	40,0000	DEG R	
PTT	=	25,0000	PSIA	
XI	=	,0500		
XC	=	,8500		
XF	=	1,0000		
ACC	=	1,0000	G	
END	=	1,7117	LB/HR	
THEX	=	39,5401	DEG R	
PHEX	=	23,5285	PSIA	
QEXT	=	51,2763	BTU/HR	
QR	=	0.	BTU/HR	
EL	=	22,5556	12,0444	FT
QT	=	256,5169	48,1719	BTU/HR
TS	=	91,6820	91,7386	DEG R
TC	=	39,6983	40,2154	DEG R
TH	=	39,7518	40,2345	DEG R
HE	=	1,4991	1,4965	B/F2DH
HF	=	25,2469	24,1393	B/F2DH
HT	=	541,6337	45,2569	B/F2DH
U	=	,2069	,2066	B/F2DH
TA	=	40,4876	40,5097	DEG R
EN	=	,3800	,3716	
DP F D	=	,0446	2,36E-03	PSIA

Table G-2 (continued)

IDU/TVS PERFORMANCE COMPUTER CODE RESULTS

CASE 26

DD	=	3,2000	IN	
EL	=	35,0000	FT	
V	=	2,0000		
DTUBE	=	,2500	IN	
TWTM	=	,0325	IN	
T	=	,2000	IN	
TI	=	,2000	IN	
ATT	=	4,4000	SQ FT	
TTM	=	1,0000	IN	
TTI	=	,2000	IN	
HTK	=	2,5000	FT	
AKT	=	90,0000	B/F2H	
AKI	=	,0100	B/F2H	
TE	=	100,0000	DEG R	
TSE	=	36,6667	DEG R	
P	=	15,0000	PSIA	
TM2	=	40,0000	DEG R	
PTT	=	25,0000	PSIA	
XI	=	,0500		
*XC	=	1,0000		
XF	=	1,0000		
ACC	=	1,0000	G	
EPD	=	1,7193	LB/HR	
TTHEX	=	39,7854	DEG R	
PHEX	=	24,5134	PSIA	
QEXT	=	91,6783	BTU/HR	
QR	=	0.	BTU/HR	
EL	=	35,0000	0.	FT
QT	=	305,1955	0.	BTU/HR
TS	=	91,6987	91,6987	DEG R
TC	=	39,8514	39,8514	DEG R
TM	=	39,8934	39,8934	DEG R
HE	=	1,4984	1,4984	B/F2DH
HF	=	20,8324	20,8324	B/F2DH
HT	=	1,0116-03	45,4982	B/F2DH
U	=	,2069	,2069	B/F2DH
TA	=	40,5899	40,5899	DEG R
EA	=	,3454	,3454	
DP F D	=	,0500	2,77E-03	PSIA

CASE 27

DD	=	3,2000	IN	
EL	=	35,0000	FT	
V	=	2,0000		
DTUBE	=	,2500	IN	
TWTM	=	,0325	IN	
T	=	,2000	IN	
TI	=	,2000	IN	
ATT	=	4,4000	SQ FT	
TTM	=	1,0000	IN	
TTI	=	,2000	IN	
HTK	=	2,5000	FT	
AKT	=	90,0000	B/F2H	
AKI	=	,0100	B/F2H	
TE	=	100,0000	DEG R	
TSE	=	36,6667	DEG R	
P	=	15,0000	PSIA	
TM2	=	40,0000	DEG R	
PTT	=	25,0000	PSIA	
XI	=	,0500		
*XC	=	,0500		
XF	=	1,0000		
ACC	=	1,0000	G	

• • • • THE ABOVE CASE DID NOT RUN • • • •

CASE 28

DD	=	3,2000	IN	
EL	=	35,0000	FT	
V	=	2,0000		
DTUBE	=	,2500	IN	
TWTM	=	,1325	IN	
T	=	,2000	IN	
TI	=	,2000	IN	
ATT	=	4,4000	SQ FT	
TTM	=	1,0000	IN	
TTI	=	,2000	IN	
HTK	=	2,5000	FT	
AKT	=	90,0000	B/F2H	
AKI	=	,0100	B/F2H	
TE	=	100,0000	DEG R	
TSE	=	36,6667	DEG R	
P	=	15,0000	PSIA	
TM2	=	40,0000	DEG R	
PTT	=	25,0000	PSIA	
XI	=	,0500		
*XC	=	,0501		
XF	=	1,0000		
ACC	=	1,0000	G	
EPD	=	1,6982	LB/HR	
THEX	=	38,2459	DEG R	
PHEX	=	19,7195	PSIA	
QEXT	=	91,2703	BTU/HR	
QR	=	0.	BTU/HR	
EL	=	1,09E-03	34,9989	FT
QT	=	,0341	305,1633	BTU/HR
TS	=	91,2881	91,6987	DEG R
TC	=	38,8285	39,8513	DEG R
TM	=	38,8697	39,8934	DEG R
HE	=	1,5033	1,4984	B/F2DH
HF	=	35,2816	20,8327	B/F2DH
HT	=	471,4862	44,3588	B/F2DH
U	=	,2072	,2069	B/F2DH
TA	=	40,2469	40,5930	DEG R
EA	=	,4486	,3454	
DP F D	=	8,32E-03	3,41E-07	PSIA

Appendix H
IDU BREAKDOWN LEVEL AND FLOW LOSS PROGRAM

H.1 Breakdown Level

Sample oscillograph data obtained on liquid hydrogen breakdown is given in Figures H-1 to H-10; the figures are annotated to illustrate liquid levels, the breakdown points, flowrate, valve actuation, pressure difference between the main tank and IDU, and temperature T4. Additional temperature data for test J-39 are shown in Figure H-9. It is interesting to note that breakdown in Test J-39 is closely correlated with the temperature increase in the ullage due to the warm, incoming GH_2, and occurs approximately five seconds after the top of the LHAD is exposed to the warm ullage gas. However, a more precise correlation between the ullage gas temperature increases and the breakdown point could not be obtained since the Dymec system sampled 33 data channels in approximately 35 seconds. Therefore, a given data point would be sampled every 35 seconds; within this time gap, more accurate curves of ullage temperature could not be obtained. Further, the actual maximum temperatures may not have been recorded.

Breakdown in all cases was determined by examining the continuous level sensor voltage vs. time, and then determining the height vs. time by use of Figure 4-1. Flowrates were determined by calculating the corresponding flow area in the IDU, using the equations given in Appendix I. It should be reiterated that due to the strong possibility of leakage out of the IDU through PV2, the actual flowrate through the LHAD and out through PV1 may have been less than measured. Thus, the discrepancy in agreement between actual and predicted breakdown heights vs. flowrates shown by Tests J-11, J-19, J-25A, J-27B, and N-11, may have been partially due to failure of PV1 to open properly and PV2 to close properly.

H.2 Flow Loss Program

The flow loss program used to design the IDU LHAD, select the screen mesh, and correlate breakdown data is given in Tables H-1 and H-2.

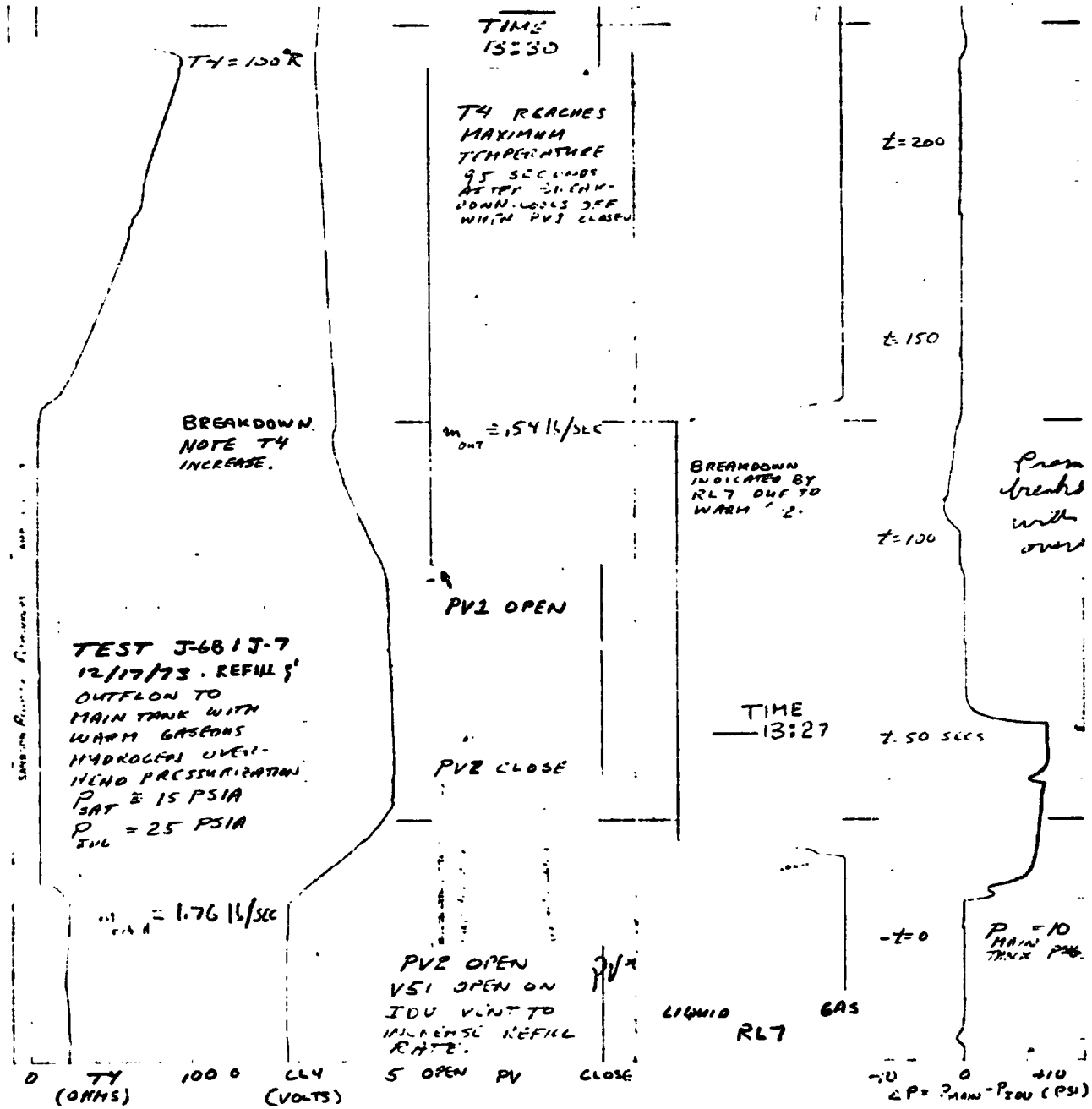
TIME
13:30
T4 = 100°R
T4 REACHES MAXIMUM TEMPERATURE 95 SECONDS AFTER SHUTDOWN. LOSS OF WARM PV1 CLOSED
t = 200
t = 150
t = 100
BREAKDOWN. NOTE T4 INCREASE.
$\dot{m}_{OUT}$ = 1.54 lb/sec
BREAKDOWN INDICATED BY RL7 OUT TO WARM 2.
PV1 OPEN
TEST J-68 J-7 12/17/73. REFILL 5' OUTFLOW TO MAIN TANK WITH WARM GASEOUS HYDROGEN OVER-HEAD PRESSURIZATION
P_{SAT} = 15 PSIA
P_{INL} = 25 PSIA
TIME
13:27
t. 50 secs
PV2 CLOSE
$\dot{m}_{FILL}$ = 1.76 lb/sec
PV2 OPEN
VS1 OPEN ON IDU VENT TO INCREASE REFILL RATE.
PV4
LIQUID
GAS
RL7
-t = 0
$P_{MAIN\ TANK}$ = 10 PSIA
0 TY (OHMS) 100 0 CL4 (VOLTS)
5 OPEN PV CLOSE
-10 0 +10
$\Delta P = P_{MAIN} - P_{IDU}$ (PSI)

Figure II-1

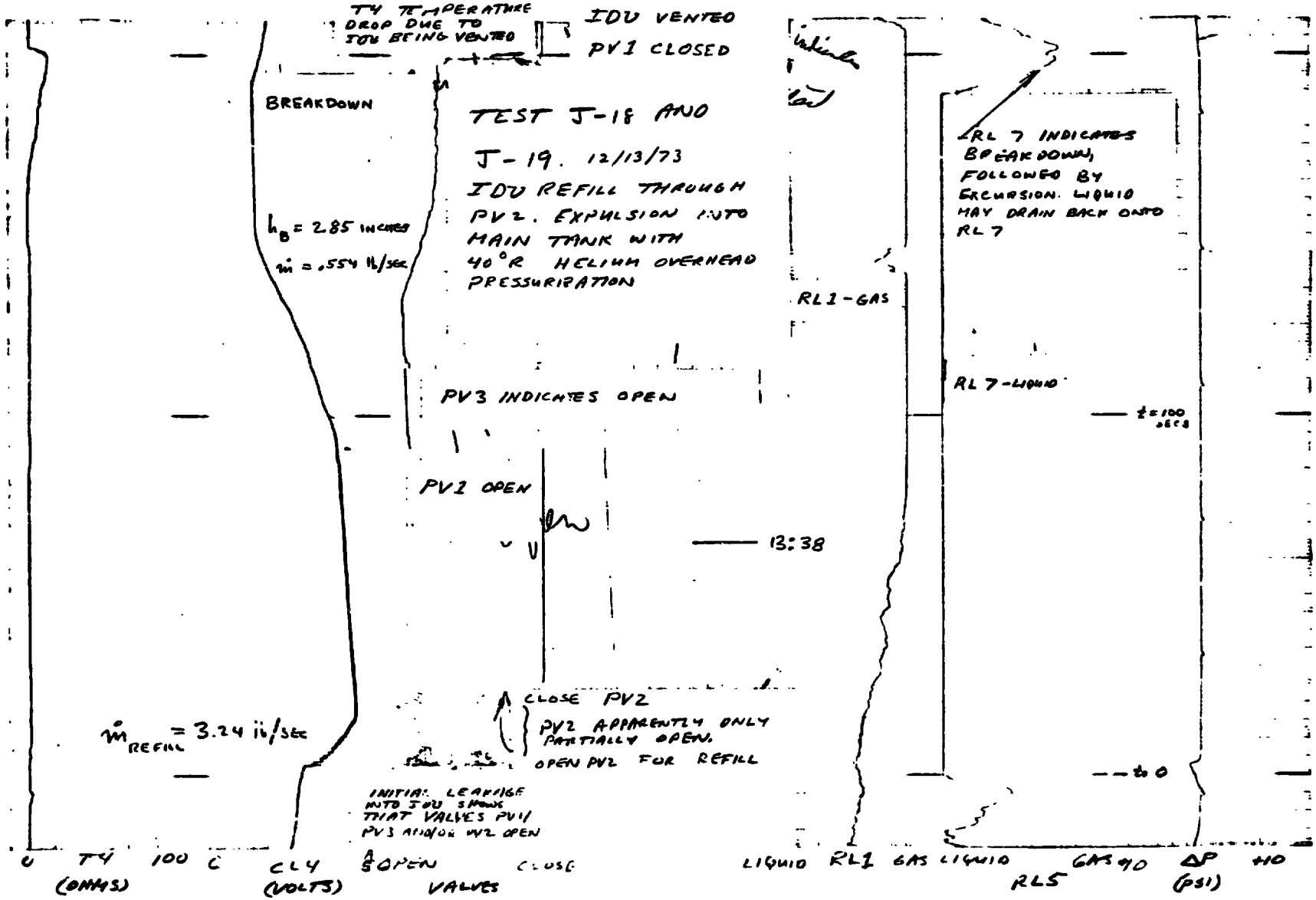

Figure II-2

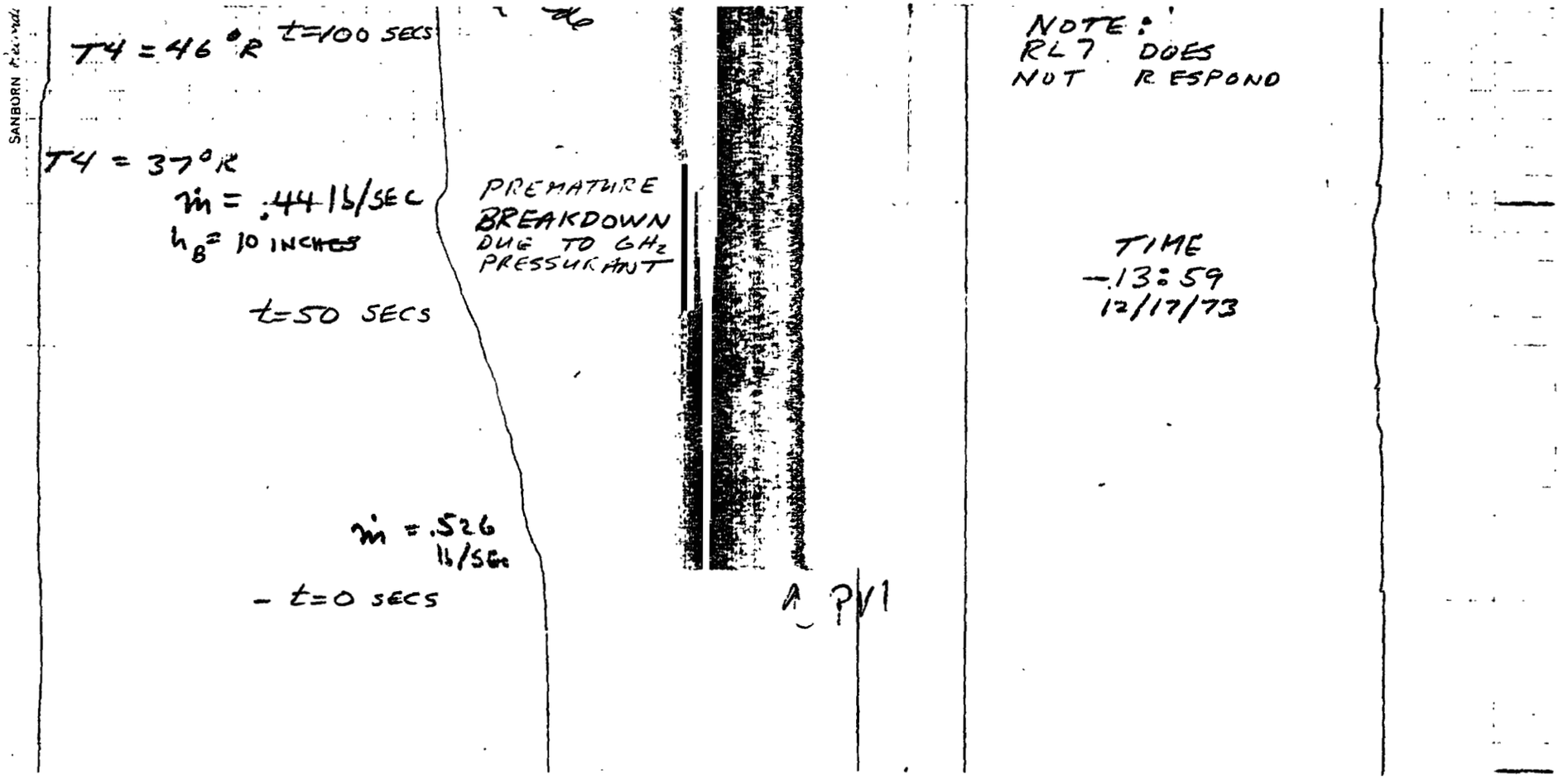

TEST J-21 12/17/73 OUTFLOW TO MAIN TANK WITH COLD GASEOUS HYDROGEN OVERHEAD PRESSURIZATION

$P_{IOV} = 16$ PSIA, $P_{SAT\ LH_2} \cong 15$ PSIA

Figure H-3

ORIGINAL PAGE IS POOR

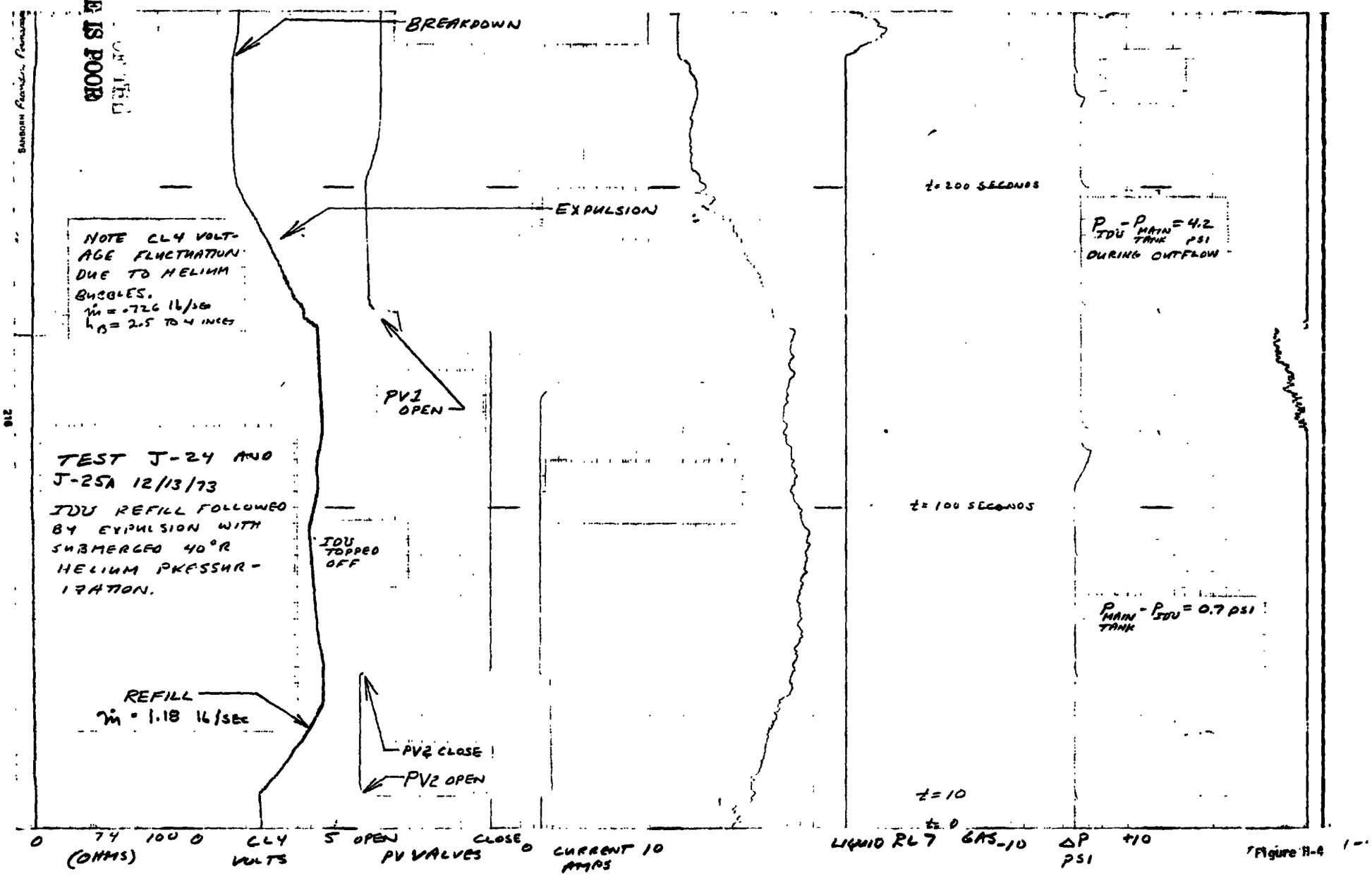

Figure II-4

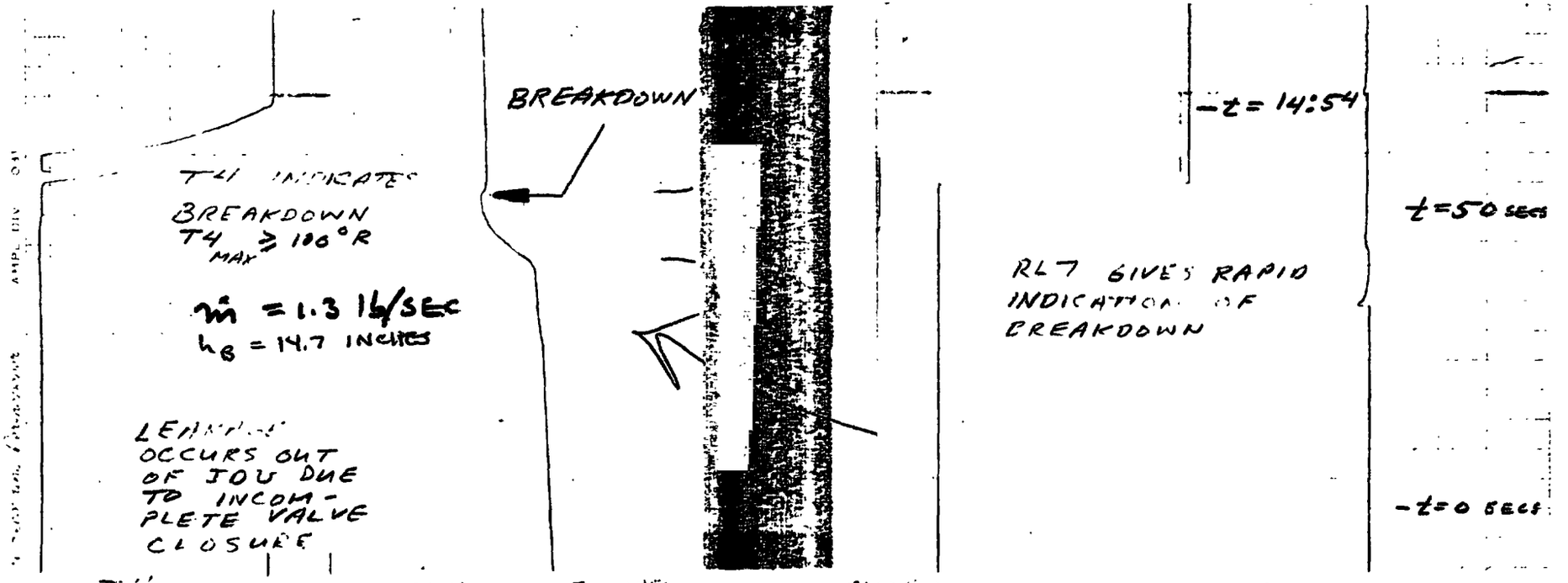

TEST J-31 12/17/73

OUTFLOW TO MAIN TANK WITH WARM GASEOUS HYDROGEN OVERHEAD PRESSURIZATION. $P_{IDU} = 35$ PSIA ; $P_{SAT} = 15$ PSIA

PREMATURE BREAKDOWN OCCURS

Figure H-5

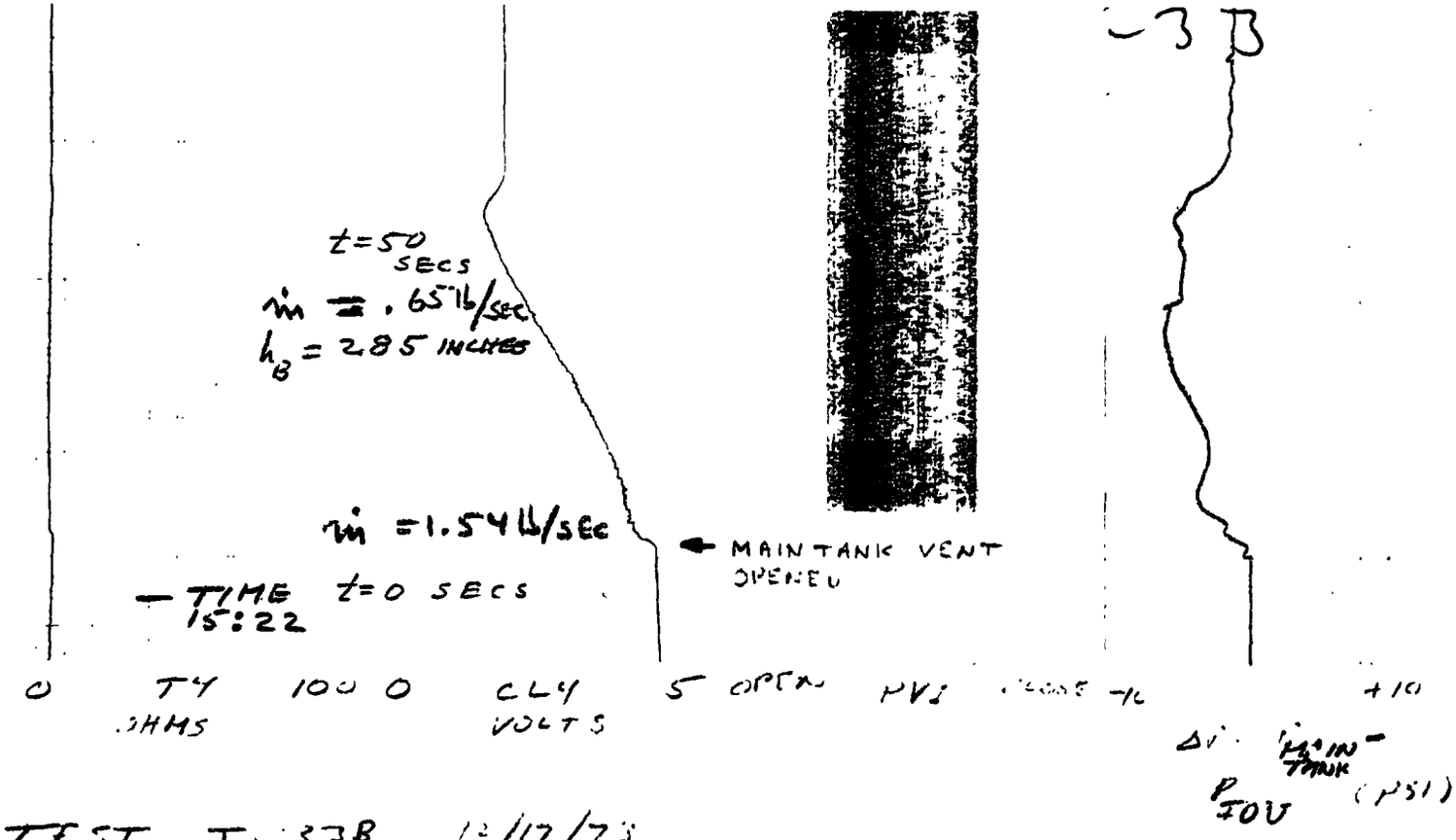

TEST J-33B 12/17/73

OUTFLOW TO MAIN TANK WITH COLD (40°R) SUBMERGED HELIUM PRESSURIZATION

P_{IOU} = 37 PSIG, $P_{MAIN\ TK.}$ = 33 PSIG

Figure H-6

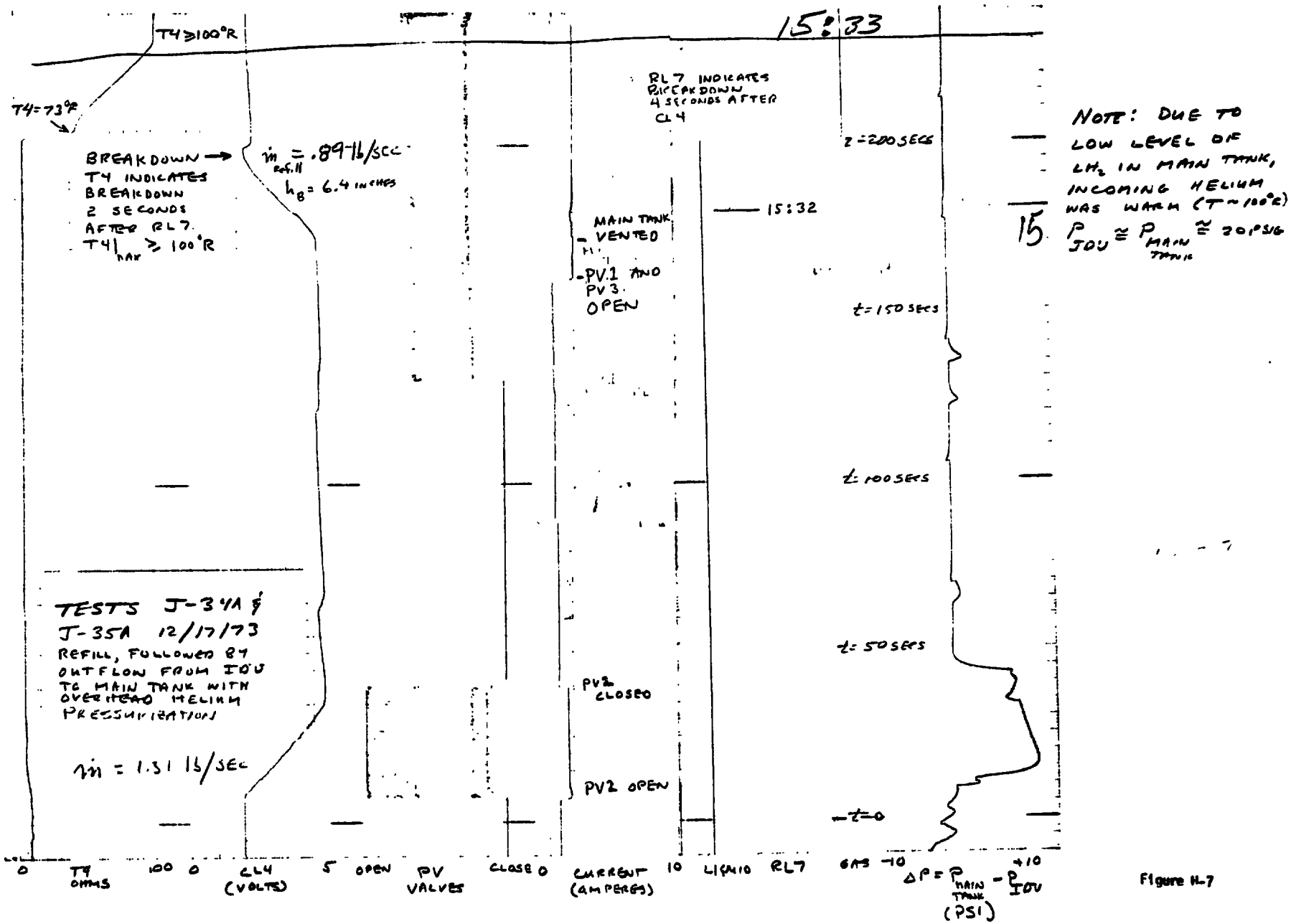
15:33
T4 ≥ 100°R
T4 = 73°F
BREAKDOWN → T4 INDICATES BREAKDOWN 2 SECONDS AFTER RL7. T4|MAX ≥ 100°R
ṁ ref.11 = .89 lb/sec
h_B = 6.4 INCHES
RL7 INDICATES BREAKDOWN 4 SECONDS AFTER CL4
MAIN TANK VENTED
PV1 AND PV3 OPEN
15:32
PV2 CLOSED
PV2 OPEN
TESTS J-34A & J-35A 12/17/73
REFILL, FOLLOWED BY OUTFLOW FROM IOU TO MAIN TANK WITH OVERHEAD HELIUM PRESSURIZATION
ṁ = 1.31 lb/sec
t = 200 SECS
t = 150 SECS
t = 100 SECS
t = 50 SECS
t = 0
15
NOTE: DUE TO LOW LEVEL OF LH2 IN MAIN TANK, INCOMING HELIUM WAS WARM (T ~ 100°R)
P_IOU ≅ P_MAIN TANK ≅ 20 PSIG
0 T4 OHMS 100
0 CL4 (VOLTS) 5
OPEN PV VALVES CLOSE 0
CURRENT (AMPERES) 10
LIQUID RL7 GAS
-10 ΔP = P_MAIN TANK - P_IOU +10
(PSI)

Figure H-7

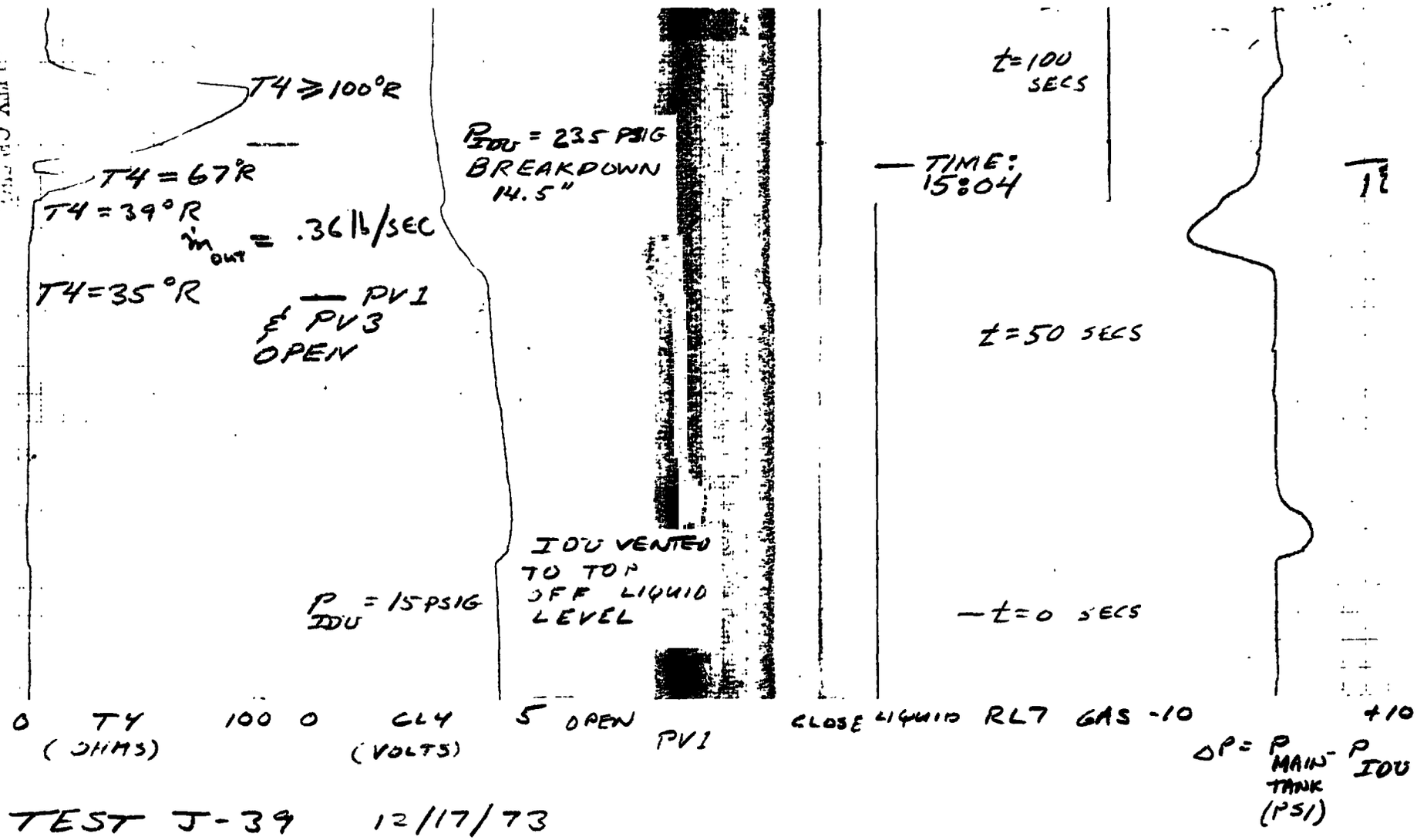

TEST J-39 12/17/73

OUTFLOW TO MAIN TANK WITH WARM GASEOUS HYDROGEN OVERHEAD PRESSURIZATION PREMATURE BREAKDOWN OCCURS

Figure II-8

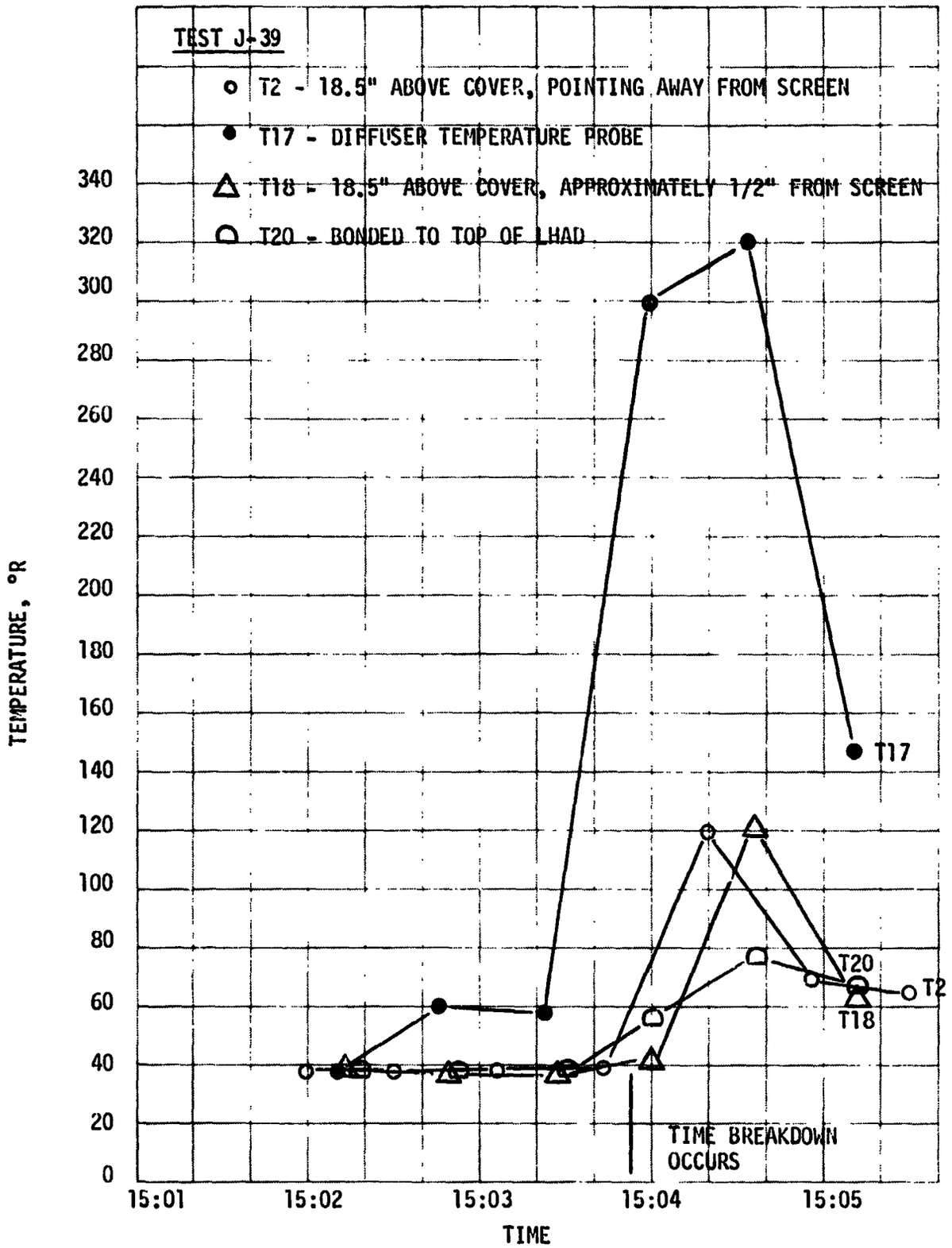

Figure H-9 TEST J-39 TEMPERATURES

REDUCE TO 8½x11

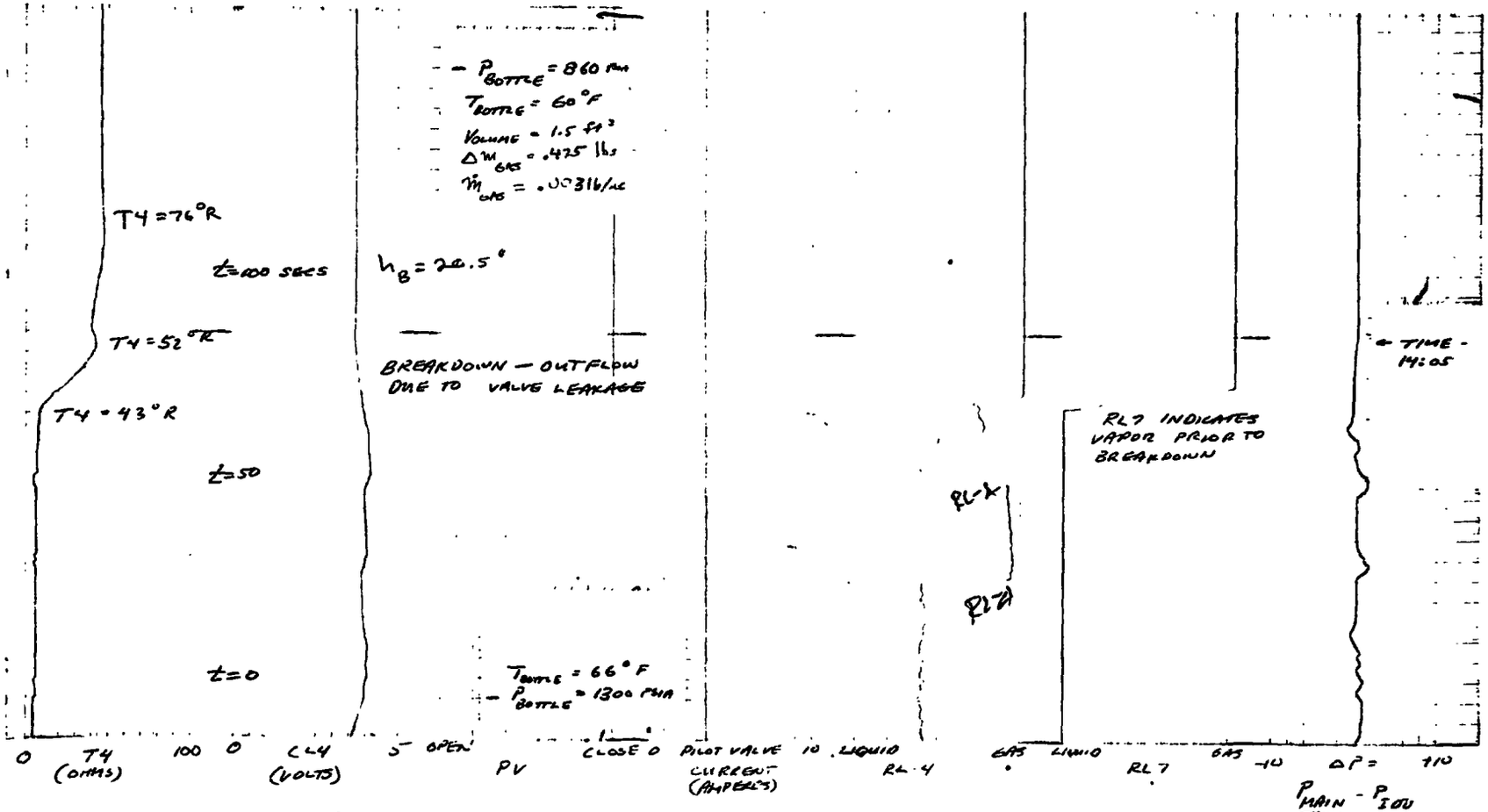

TEST S-1B 12/16/73
AUTOGENOUS PRESSURIZATION
MAIN TANK LIQUID LEVEL
AT BOTTOM OF IGU
NOTE: HEAT FLUX GAUGES NOT MONITORED

Figure II-10

Table II-1

IDU BREAKDOWN LEVEL AND FLOW LOSS PROGRAM

NOMENCLATURE

D3 = Outer Screen Diameter (Inches)
T = Annulus Width (Inches)
L1 = Screen Height (Inches)
F = Friction Factor For Flow Within Annulus
Q = Flowrate (Lbm/Sec)
D2 = Liquid Density (Lbm/Ft^3)
D = Screen Pore Diameter (Ft)
B = Screen Thickness (Ft)
A = Surface Area to Unit Volume Ratio of Screen Wire (Ft^{-1})
E = Screen Volume Void Fraction
N1 = Multiplying Factor For Pleating
N2 = Number of Screen Layers
U = Viscosity (Lb/Ft-Sec)

PROGRAM

```
10 INPUT D3, T, L1
20 F = .025
30 INPUT Q, D2
40 INPUT D, B, A, E
50 INPUT N1, N2
60 Q=Q/D2
70 U=.000008
80 A4 = 3.14 * ( D3 * T - T * T ) / 144
90 R1 = A4 / ( 6.28 * D3 - 6.28 * T ) * 12
100 D1 = 4 * R1
110 FØR G =  .3 TØ .95STEP .05
120 X = L1 * ( 1-G )
130 A3 = 6.28 * X * ( D3 - T ) / 144 * N2
140 V = Q / A3
150 N = V * D2 /U/A/A/D
160 F1 = 8.6 / N + .52
170 P1 = N1 * 1.3 * F1 *D2 *B * V * V / E /E/ D / 32.2
180 V1 = Q / A4
190 P3 = D2 * V1 *D1 / U
200 P2 = F * ( L1 -X / 2) /12 / D1 * D2 * V1 * V1 / 2 / 32.2
210 P3 = D2 * V1 * V1 / 2 / 32.2
220 P4 = D2 * ( L1 - X ) / 12
230 P5 = P1+P2+P3+P4
240 PRINT X; P1; P2; P3; P4; P5; P3
250  NEXT G
260 END
```

Table H-2

PROGRAM OUTPUT

CONDITIONS

250 X 1370 Screen

D3 = 24"; T = 1.5"; L1 = 18.37"; Q = 2 Lb/Sec; D2 = 4.37 Lb/Ft^3;

D = .000026 Ft; B = .0004 Ft; A = 22773 Ft^{-1}; E = .2409; N1 = 1; N2 = 1

SUBMERGED SCREEN DEPTH (INCHES)	P1-FLOW LOSS THROUGH SCREEN (LB/FT^2)	P2-ANNULUS FLOW LOSS (LB/FT^2)	P3-DYNAMIC LOSS (LB/FT^2)	P4-HYDROSTATIC HEAD (LB/FT^2)	P1+P2+P3+P4	REYNOLD'S NO. IN ANNULUS
12.8590	.13[illegible]	[illegible]-04	3.62040E-03	2.00[illegible]	2.15953	31347.1
11.9405	.150455	3.31334E-04	3.62040E-03	2.34141	2.49614	31347.1
11.0220	.16[illegible]	[illegible]E-04	3.62040E-03	2.67[illegible]	2.84367	31347.1
10.1035	.173171	4.02531E-04	3.62040E-03	3.01077	3.12365	31347.1
9.18500	.197700	4.22734E-04	3.62040E-03	3.34437	3.54637	31347.1
8.26650	.220946	4.27307E-04	3.62040E-03	3.67931	3.90445	31347.1
7.34800	.250113	4.51251E-04	3.62040E-03	4.01284	4.26311	31347.1
6.42950	.287092	4.66074E-04	3.62040E-03	4.34330	4.64059	31347.1
5.51100	.337415	4.80133E-04	3.62040E-03	4.68[illegible]	5.09660	31347.1
4.59250	.410417	4.94001E-04	3.62040E-03	5.01731	5.43491	31347.1
3.67400	.527721	5.03445E-04	3.62040E-03	5.35179	5.33379	31347.1
2.75550	.723226	5.22563E-04	3.62040E-03	5.63623	6.41372	31347.1
1.83700	1.16533	5.33592E-04	3.62040E-03	6.02077	7.19[illegible]	31347.1
.918500	2.77262	5.50315E-04	3.62040E-03	6.35525	9.13212	31347.1

Appendix I

INTERFACE DEMONSTRATION UNIT AND MDAC 260-GALLON LH_2 TANK GEOMETRIES AND INSTALLATION CONFIGURATIONS

Tne rate of outflow from, or inflow to, the IDU is derived from the liquid level rise rate as measured by the capacitance liquid level sensor. The IDU internal hardware and condition of the annular screen device (full or empty) determines the effective free surface area of the liquid, which must be known in order to determine volume flowrates of liquid hydrogen. The net free surface area as a function of height measured from the inside bottom of the IDU is given in Table I-1. A_1 corresponds to outflow with the liquid retained in the LHAD annular region. A_2 and A_3 correspond to specific regions for which the area is determined by the presence of hardware alone. A_4 corresponds to refill or outflow when the LHAD does not retain liquid above the nominal liquid level.

Figure I-1 depicts the layout geometry and associated volumes of the IDU and the MDAC 260-gallon tank.

Table I-1

FREE INTERFACE AREA OF IDU

1. $0 \leq Z \leq 23$ in. (prior to breakdown)

$$A_1 = \frac{\pi}{4}\left[D_T^2 - (D_{SO}^2 - D_{SI}^2) - D_{CC}^2 - D_{PL}^2 - D_{PSL}^2 - D_W^2\right] - A_{CP}$$

$$A_1 = 498 \text{ in.}^2 = 3.458 \text{ ft}^2$$

2. $23 \leq Z \leq 24$ in.

$$A_2 = \frac{\pi}{4}\left[D_T^2 - D_{CC}^2 - D_{PL}^2 - D_{PSL} - D_{TCC}^2\right] - A_{CP}$$

$$A_2 = 584.8 \text{ in.}^2 = 3.811 \text{ ft}^2$$

3. $Z \geq 24$ in.

$$A_3 = \frac{\pi}{4}\left[D_T^2 - D_{CC}^2 - D_{PL}^2 - D_{PSL}^2\right] - A_{CP}$$

$$A_3 = 611.8 \text{ in.}^2 = 4.25 \text{ ft}^2$$

4. $0 \leq Z \leq 23$ in. (refill with gas venting from top of LHAD)

$$A_4 = A_1 + \frac{\pi}{4}(D_{SO}^2 - D_{SI}^2) = 604.4 \text{ in.}^2 = 4.197 \text{ ft}^2$$

Nomenclature:

D_T = Internal diameter of IDU tank = 28 in.

D_{SO} = External diameter of screen device = 24 in.

D_{SI} = Internal diameter of screen device = 21 in.

D_{CC} = Diameter of central column = 3 in.

D_{PL} = Diameter of pressurization line (with Teflon insulation) = 1.5 in.

D_{PSL} = Diameter of pressure sensing line - 1.25 in.

D_W = Effective diameter of instrumentation wiring bundles = 0.75 in.

A_{CP} = Cross-sectional area of capacitance probe = 1.25 in.^{2}

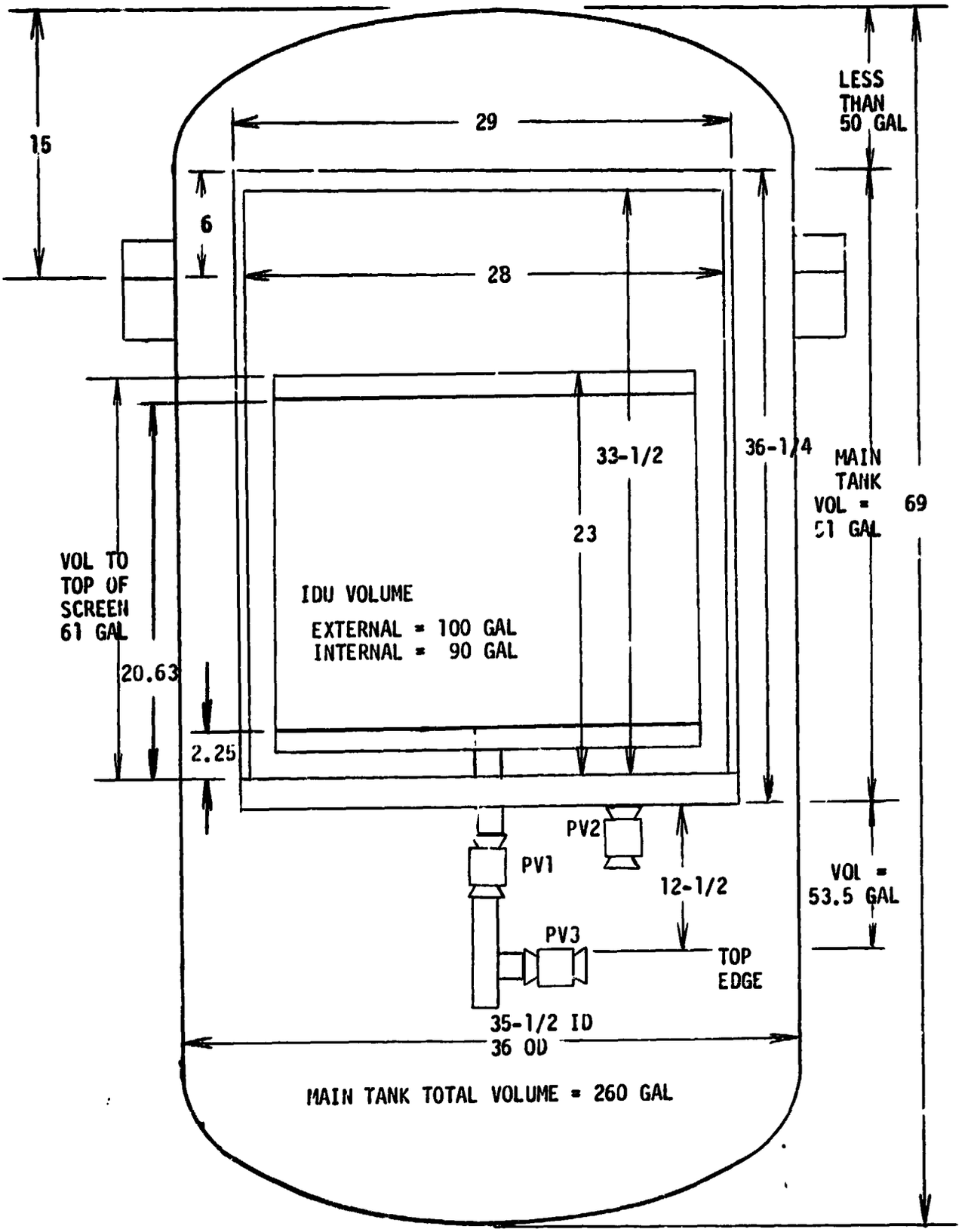

Figure I-1 LAYOUT GEOMETRY OF IDU AND MAIN TANK

Appendix J

PARKER 5640027 SUBMERGED LIQUID HYDROGEN SHUTOFF VALVE OPERATIONAL ANALYSIS

J.1 INTRODUCTION

The Parker Submerged LH_2 Shutoff Valve, shown in Figure J-1, is a 2-inch diameter, pressure actuated, ball type shutoff valve. The valve was designed for use inside a liquid hydrogen aircraft propellant tank. The following description is based on Parker Company Report SPD-132.

Its features include:

1. The design configuration which allows valve operation while completely submerged in liquid hydrogen, which lessens the LH_2 boil off due to external lines.
2. The valve may easily be converted from a normally open to a normally closed configuration.
3. Internal sealing is provided in either flow direction by a specially designed double ball seal.
4. The valve can be pressure actuated for both opening and closing.

The unit meets the following requirements (P/N 5640027)

Fluids	Liquid or gaseous hydrogen
Inlet Pressure	0-50 psig
Flow Capacity	2.8 psi pressure drop at 30 lb/sec LH_2
Temperature	-423 to +165°F
Actuation Fluid	Helium
Actuation Fluid Pressure	500 to 750 psig
Leakage	10 scim typical at -420°F

J.2 OPERATION

The valve consists of a main valve mechanism, an actuator, and a position switch assembly. Figure J-1 shows two of these three elements for the valve in its normally closed position. The position switches, not shwon, monitor

OPERATION

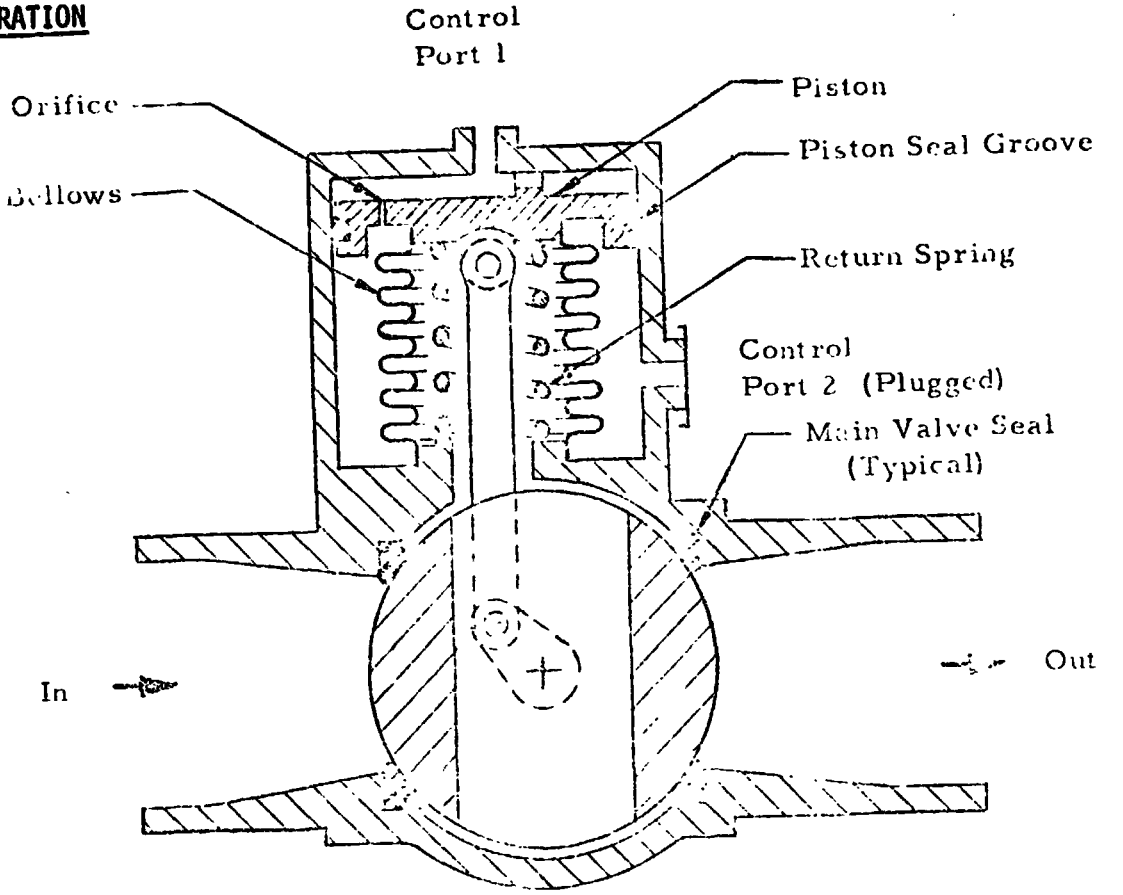

Figure J-1. VALVE SCHEMATIC

valve positions by means of a cam located on the ball shaft. To open the main valve, GHe pressure is applied to the control port. The resulting pressure difference across the piston opens the valve against the force supplied by the return spring. The force supplied by the actuator is transmitted to the main valve by means of a linkage which converts the linear piston motion to rotational motion of the ball. As the control port is pressurized, the small bleed orifice through the piston allows the pressure in the cavity to the outside diameter of the bellows to increase. To close the valve again, control port one is vented and the spring, along with the residual pressure acting on the bottom of the piston, closes the valve.

The following analysis was performed to determine the operating factors of safety of the Parker Submerged Liquid Hydrogen Ball valves. This analysis is based on a preliminary informal analysis obtained from Parker Aircraft Co.; operating pressures of 500 and 750 psig are considered. The operating factor of safety, FS, is defined as the ratio of applied actuation pressure to

minimum actuation pressure required to (1) start acceleration, (2) complete actuation, (3) start deactuation, and (4) complete deactuation.

A summary of the analysis is presented below. The valve schematic and appropriate dimensions are shown in Figure J-2.

J.2.1 Pressure to Start Actuation

A. With pressure drop across piston

$$P_1 = \frac{f + F_{b_1} + F_{s_1} + P_2 A_b}{A_p}$$

$$= \frac{670 + (-50) + 130 + 50\ (2.32)}{4.92} = 176 \text{ psig}$$

$$FS = \frac{500}{176} = 2.8$$

$$FS = \frac{750}{176} = 4.3$$

B. No ΔP across piston

$$P_1 = \frac{f + F_{b_1} + F_{s_1} + P_2 A_b}{A_b}$$

$$= \frac{670 + (-50) + 130 + 50\ (2.32)}{2.32} = 373 \text{ psig}$$

$$FS = \frac{500}{373} = 1.3$$

$$FS = \frac{750}{373} = 2.0$$

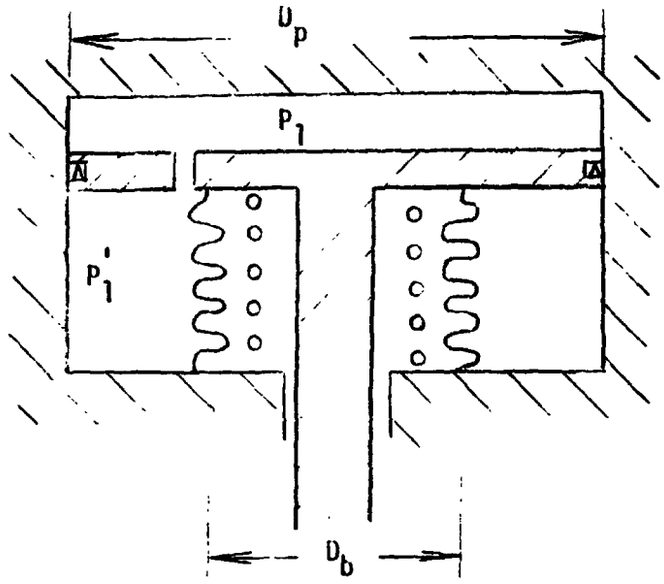

D_p = Piston Diameter = 2.50 In

D_b = Effective Bellows Diameter = 1.72 In

A_p = Piston Area = 4.92 In^2

A_b = Effective Bellows Area = 2.32 In^2

f = Seal Friction Force = 670 Lbs

F_b = Bellows Force = 50 to 75 Lbs

F_s = Spring Force = 130 to 305 Lbs

P_1 = Pneumatic Pressure = 500/750 Psig

P_2 = Line Pressure = 50 Psig

Figure J-2 PARKER VALVE SCHEMATIC - ACTUATION CYLINDER

J.2.2 Pressure to Complete Actuation

A. With ΔP across piston

$$P_1 = \frac{f + F_{b_2} + F_{s_2} + P_2 A_b}{A_p}$$

$$= \frac{670 + 75 + 305 + 50\ (2.32)}{4.92} = 237 \text{ psig}$$

$$FS = \frac{500}{237} = 2.1$$

$$FS = \frac{750}{237} = 3.2$$

B. No ΔP across piston

$$P_1 = \frac{f + F_{b_2} + F_{s_2} + P_2 A_b}{A_b}$$

$$= \frac{670 + 75 + 305 + 50\ (2.32)}{2.32} = 502 \text{ psig}$$

$$FS = \frac{500}{502} = 1.0$$

$$FS = \frac{750}{502} = 1.5$$

J.2.3 Pressure to Start Deactuation

A. Line pressure 50 psig; $P_1 = 0$

$$P_1' = \frac{f - F_{b_2} - F_{s_2} - P_2(A_b)}{A_p - A_b}$$

$$= \frac{670 - 75 - 305 - 50\ (2.32)}{(4.92 - 2.32)} = 67 \text{ psig}$$

B. Line pressure - psig; $P_1 = 0$

$$P_1' = \frac{670 - 75 - 305 - 0\ (2.32)}{4.92 - 2.32} = 111.5 \text{ psig}$$

Note that calculated pressure P_1' is required to start valve to deactuate. Hence, valve will not move unless P_1' is greater than P_1 by the values noted above. Also valve will not fully deactuate unless P_1' is greater than:

A. Line pressure 50 psig; $P_1 = 0$

$$P_1' = \frac{670 + 50 - 130 - 50\ (2.32)}{4.92 - 2.32} = 182 \text{ psig}$$

B. Line pressure 0 psig; $P_1 = 0$

$$P_1' = \frac{670 + 50 - 130 - 0\ (2.32)}{4.92 - 2.32} = 227 \text{ psig}$$

J.3 CONCLUSIONS

A. Successful deactuation of valve is dependent upon venting actuation pressure (P_1) quickly enough such that deactuation pressure (P_1') exceeds P_1 by 227 psid.

B. The following conditions may prevent this ΔP from developing:

1. Restriction in pneumatic vent, i.e., obstruction in orifice or screen located in actuation pneumatic port, slow acting or sluggish solenoid.

2. Ineffective seal on actuator i.e., damaged seal, damaged cylinder surface, contamination, tapered cylinder.

C. The following conditions may require a higher ΔP to accomplish complete deactuation:

1. Binding, i.e., contamination, incomplete temperature stabilization, excessive seal drag on ball.

J.4 RECOMMENDATIONS

A. Provide a separate pneumatic "close" system for each valve. Reasons:

1. Full pneumatic pressure will be available for deactuation, i.e.,

$$F.S.' = \frac{500}{227} = 2.2.$$

2. Leakage past damaged piston seal is not critical.
3. Operation of actuator is not time dependent.
4. Reliability of actuation increased greatly.

B. Add second seal to actuator piston to reduce piston leakage when actuation (open) pressure is applied.

C. Plug orifice in actuator piston to reduce piston leakage.

D. Purging of the volume external to the valve ball should be accomplished either by partially opening of the valve during the vacuum/purge cycle, or by installing a separate purge system attached to the ball shaft boss. Partial opening of valves may be accomplished by applying a reduced pneumatic pressure to the open port.

E. All pneumatic helium vents should be protected from breathing air by trapping and holding exhausted helium at vent opening. An inverted chamber (opening on the bottom) over a vent opening may be suitable, and/or a check valve should be used.